ZooKeys 929: 1–17 (2020)
doi: 10.3897/zookeys.929.49987
http://zookeys.pensoft.net

RESEARCH ARTICLE

A peer-reviewed open-access journal
ZooKeys
Launched to accelerate biodiversity research

The genera *Erhaia* and *Tricula* (Gastropoda, Rissooidea, Amnicolidae and Pomatiopsidae) in Bhutan and elsewhere in the eastern Himalaya

Edmund Gittenberger[1], Pema Leda[2], Jigme Wangchuk[3], Choki Gyeltshen[2],
Björn Stelbrink[4,5]

1 *Naturalis Biodiversity Center, P.O. Box 9517, NL-2300 RA Leiden, The Netherlands* **2** *National Biodiversity Centre, Serbithang, Thimphu, Bhutan* **3** *Ugyen Wangchuck Institute for Conservation and Environmental Research, Bumthang, Bhutan* **4** *Department of Animal Ecology & Systematics, Justus Liebig University, Heinrich-Buff-Ring 26-32 IFZ, D-35392 Giessen, Germany* **5** *Zoological Institute, Department of Environmental Sciences, University of Basel, Vesalgasse 1, 4051 Basel, Switzerland*

Corresponding author: Edmund Gittenberger (egittenberger@yahoo.com)

Academic editor: Thierry Backeljau | Received 8 January 2020 | Accepted 8 March 2020 | Published 22 April 2020

http://zoobank.org/4FCA3A27-973C-49F7-8264-6A34D279EC5C

Citation: Gittenberger E, Leda P, Wangchuk J, Gyeltshen C, Stelbrink B (2020) The genera *Erhaia* and *Tricula* (Gastropoda, Rissooidea, Amnicolidae and Pomatiopsidae) in Bhutan and elsewhere in the eastern Himalaya. ZooKeys 929: 1–17. https://doi.org/10.3897/zookeys.929.49987

Abstract

Shells of the Rissooidea species that are known from Bhutan are characterized. *Tricula montana* is reported from that country for the first time. Two *Erhaia* species from Bhutan are described as new to science, viz. *E. jannei* **sp. nov.**, and *E. pelkiae* **sp. nov.**, The holotypes of the *Erhaia* species that were described from Nepal are figured with photographs for the first time and compared with the congeneric taxa from Bhutan and India. *Erhaia nainitalensis* is considered a senior synonym of *E. chandeshwariensis*. An identification key is presented for the *Erhaia* species of the Himalayan foothills.

Keywords

Erhaia, *Tricula*, 16S rRNA, taxonomy, distribution, Nepal, India, Bhutan

Introduction

The rissooidean gastropods that are widespread over the globe have a confusing history of taxonomic rearrangements that follow the increasing amount of morphological and molecular data, the ongoing methodological refinements in cladistics and the wealth of more or less conflicting speculations in the phylogeography of the taxa. The species of the Rissooidea Gray, 1847 from Bhutan, Nepal and northern India that are dealt with here, are classified in two genera that belong to different families, viz. the family Amnicolidae Tryon, 1863, with the genus *Erhaia* Davis & Kuo, 1985 and the family Pomatiopsidae Stimpson, 1865, with the genus *Tricula* Benson, 1843. Some species of these two genera are intermediate hosts for Platyhelminthes that are medically significant since they may transmit the human lung fluke *Paragonimus* Braun, 1899 or human *Schistosoma* Weinland, 1858 (Liu et al. 2014).

These species are characterized by minute shells that cannot always be recognized easily from descriptions and identified because of the limited number of diagnostic characters and the fact that many conchological character states that are used in the literature cannot be strictly quantified. The general shape of the shell and the form of the aperture may be described as ovoid, conical, subcylindrical, squat, or with another term of that kind. The convexity of the whorls and the depth of the suture are equally difficult to describe unequivocally. The surface of the shells is often heavily encrusted, so that the microsculpture of the proto- and teleoconch cannot always be recognized. Despite all this, an attempt is made here to characterize the genus conchologically.

The anatomy of these micro-snails cannot easily be investigated, so that DNA sequencing has become a promising tool to investigate the systematics of the Rissooidea. The classification of two *Erhaia* species from Bhutan is based now on DNA data, whereas a third species from that country is considered congeneric by reason of conchological and ecological similarity. Three nominal species of *Erhaia* from Nepal and one species from nearby northern India are compared with the Bhutanese taxa in more detail because of their joint occurrence in springs and brooklets of the southern foothills of the Himalaya. Photographs of *Tricula montana* from Bhutan, of the holotypes of the two new Bhutanese *Erhaia* species, and of a specimen of the third Bhutanese *Erhaia* species from its type locality, are provided together with photographs of the three Nepalese nominal species of *Erhaia*, that are published here for the first time.

Material and methods

Four species of minute snails were collected in spring areas and in a brooklet in Bhutan (Fig. 1). *Tricula montana*, *Erhaia wangchuki* and two undescribed *Erhaia* species could be recognized conchologically. Representative shells of these four species were photographed by Björn Stelbrink (Figs 16, 17) with a digital microscope system (KEYENCE VHX-2000; KEYENCE Corp., Itasca, IL, USA) and Mr Jeroen Goud (Figs 2–7) with

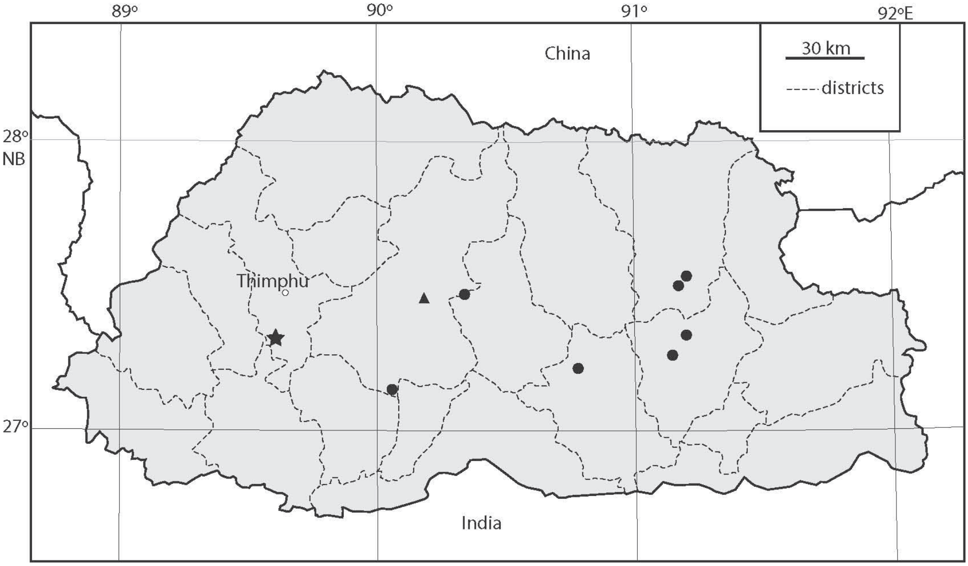

Figure 1. Records of the sympatric *Erhaia jannei* and *E. pelkiae* (star), *E. wangchuki* (triangle), and *Tricula montana* (dots) in Bhutan.

a ZEISS SteREO Discovery.V20. Specimens of *T. montana* and of one of the two new *Erhaia* species were used for DNA analysis. Only two specimens of the third Bhutanese *Erhaia* species were available and these were kept as dry shells.

Photographs of the holotypes of the three *Erhaia* species that were described from Nepal and illustrated with drawings only were made with a Nikon SMZ25 stereomicroscope by Ms Sara Schnedl and provided for study by Ms Anita Eschner (both Museum of Natural History, Vienna, Austria). The only *Erhaia* species that is known from the Himalayan foothills in India is compared with the species from Bhutan and Nepal on the basis of its detailed description and photographs that are available in the literature. An identification key for the *Erhaia* species in the study area, using shell characters, is provided.

The standard CTAB protocol for molluscs was used for the DNA lab isolation (Winnepenninckx et al. 1993). In addition to the 16S rRNA fragment (c. 535 bp; using standard primers by Palumbi et al. 1991), the mitochondrial COI gene was also amplified (658 bp; standard primers by Folmer et al. 1994). The final genetic dataset mainly comprised sequences from the study by Liu et al. (2014) and additional sequences for *Tricula* that were obtained from Guan et al. (2008). Uncorrected genetic p-distances for 16S rRNA and COI were calculated using MEGA 7.0.20 (Kumar et al. 2016).

The following abbreviations are used: B = shell breadth; H = shell height; NBCB = National Biodiversity Centre, Serbithang, Thimphu, Bhutan; NHMW = Naturhistorisches Museum, Wien, Austria.

Systematics

Superfamily Rissooidea Gray, 1847

Key to the *Erhaia* and *Tricula* species from Bhutan

1 Aperture ovoid; palatal side curved and gradually passing into the basal side .... ***Erhaia***

– Aperture triangular with broadly rounded edges; palatal side straight..... ***Tricula***

Family Amnicolidae Tryon, 1863

Genus *Erhaia* Davis & Kuo, 1985

Type species by original designation. *Erhaia daliensis* Davis & Kuo, in Davis et al. 1985.

Shells. The shells vary from conical to more or less ovoid, rarely with a flaring final part of the body whorl. The apex is flattened as in the European amnicolid genus Bythinella Moquin-Tandon, 1856, because of the very low spiral of the protoconch. The peristome is continuous and may be more or less protruding. The parietal and the columellar side of the aperture are about equally long and the regularly curved palatal side of the aperture gradually passes into the basal side, forming a single, regularly curved border. Bythinella cannot be distinguished from Erhaia conchologically, but in some Erhaia species from China the columella has one or two spiral lamellae, that are not known from Bythinella. In Erhaia the protoconch may have spiral striae, which have not been described for any of the Bythinella species.

Distribution. The genus Erhaia is mainly known from China, where it has been recorded with various species from the province of Yunnan in the west to the provinces of Hunan, Hubei and Fujian in the east (Davis et al. 1985; Davis and Kang 1995; Davis and Rao 1997; Wilke et al. 2000, 2001; Liu et al. 2014). One species was described from northern India (Davis and Rao 1997), three from Nepal (Nesemann et al. 2007) and one from Bhutan (Gittenberger et al. 2017a). Here we deal with the systematics of only the species occurring in the southern Himalayan foothills in Bhutan, India, and Nepal.

Key to the *Erhaia* species from Bhutan, Nepal and northern India

1 Final half of the body whorl conspicuously flaring; whorls of the spire flattened.. ***E. sugurensis*** (Fig. 10)

– Final half of the body whorl not flaring; whorls convex.............................. **2**

2 Aperture measuring half the total shell height or more............................... **3**

– Aperture measuring less than half the total shell height.............................. **4**

3 Shell conical, umbilical chink wide .... ***E. wangchuki***
– Shell ovoid, umbilical chink narrow.................................. ***E. jannei* sp. nov.**
4 Parietal border of the aperture attached to the body whorl.......................... **5**
– Parietal border of the aperture touching the body whorl or free .... ***E. nainitalensis***
5 Spire turreted; shell base straight in side view........................ ***E. banepaensis***
– Spire ovoid; peristome widened basally and shell base concave in side view .... ***E. pelkiae* sp. nov.**

Erhaia in Bhutan

Erhaia jannei Gittenberger & Stelbrink, sp. nov.

http://zoobank.org/3CEAF442-E7C8-4699-B291-882EE902D7D7
Figs 2, 3, 11

Erhaia sp. Gittenberger et al. 2017a: 25, fig. 3; 2017c: 900, 903, fig. 8.

Material examined. *Holotype.* (Fig. 2) Bhutan • District Thimphu, c. 5 km E of Chhuzom, W of Geneykha; in brooklet with a prayer wheel along the road; 2750 m a.s.l.; 27°18'43"N, 89°36'10"E; E. Gittenberger, Choki Gyeltshen & Pema Leda leg. 25.X.2018; NBCB 1057. ***Paratypes.*** (Fig. 3) 6 shells and 2 animals in ethanol 70%; same data as for holotype; NBCB 1058.

Diagnosis. Shell large for the genus (H > 2mm), ovoid, with a relatively large aperture.

Shell. Shell obliquely ovoid, with 3½-4 convex, shouldered whorls that are separated by a deep suture; clearly higher than broad; yellowish brown with fine irregular growth lines and some blackish brown periostracal ridges, one of which runs from the apertural columellar border into the umbilicus. Peristome not reflected. Parietal, columellar and a short part of the adjoining basal apertural border thickened by a whitish callus. Most specimens with a continuous peristome and a narrow umbilical chink. Protoconch encrusted in all specimens; teleoconch without spiral sculpture.

Measurements. ($N = 9$): H 2.2–2.4 mm, B 1.5–1.6 mm. Holotype 2.2×1.6 mm.

Ecology (Fig. 11). The species is uncommon on the rocks in the shaded streamlet uphill of the prayer wheel, where it occurs with *Galba truncatula* (Müller, 1774), *Physa* sp. (new for Bhutan), and *Erhaia pelkiae* sp. nov.

DNA data (Fig. 18). The three individuals shared the same haplotype for both 16S rRNA (GenBank acc. no. MT239078) and COI (GenBank acc. no. MT237716). The uncorrected genetic p-distances between this species and *E. wangchuki* were 0.84% for 16S rRNA and 4.87% for COI. The distances were considerably higher when compared to *Erhaia* sp. from China, Guangxi, viz. 2.74% for 16S rRNA and 10.25% for COI (GenBank acc. nos. KC832722 and KC832701, respectively).

Notes. This species was discovered in 2012, but since only a single shell was collected then, a description was considered premature.

Etymology. The epithet *jannei* refers to Mr Janne Clewing, the son of the last author.

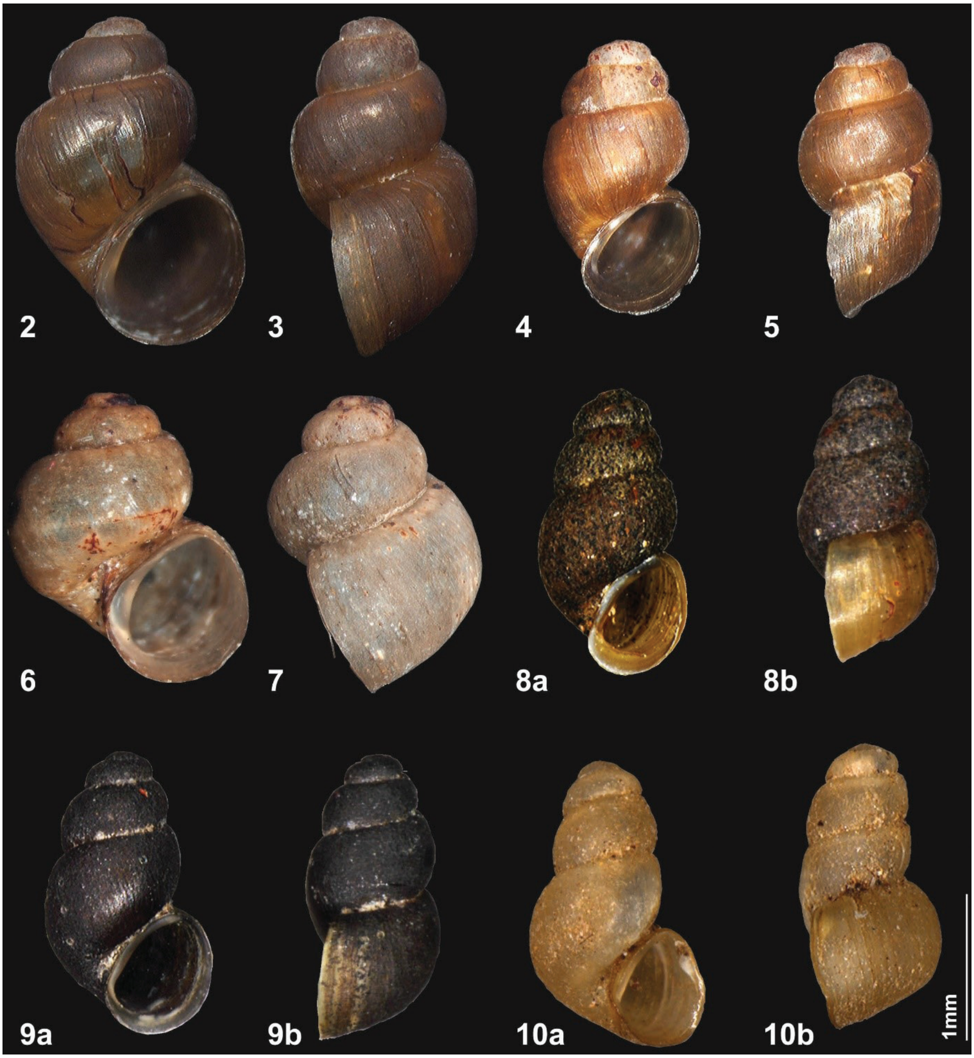

Figures 2–10. *Erhaia jannei* sp. nov., holotype (**2** H 2.25 mm) and paratype (**3** H 2.02 mm). Bhutan, district Thimphu, W of Geneykha, brooklet with water powered prayer wheel, 2750 m a.s.l. Photos by J. Goud *Erhaia pelkiae* sp. nov., holotype (**4** H 1.86 mm) and paratype (**5** H 1.86 mm). Bhutan, district Thimphu, W of Geneykha, brooklet with water powered prayer wheel, 2750 m a.s.l. Photos by J. Goud *Erhaia wangchuki* Gittenberger, Sherub & Stelbrink, 2017. Shells from the type locality (**6** H 1.98 mm) (**7** H 2.03 mm); NBCB 1072. Bhutan, district Wangdue Phodrang, Gangchhu, Gangzetem brooklet, 2883 m a.s.l. Photos by J. Goud **8** *Erhaia banepaensis* Nesemann & S. Sharma, 2007, holotype (H 1.95 mm); NHMW 103319. Nepal, Central Zone, Kavre district, small forest stream, left tributary of the Chandeswari Khola upstream from Chandeshwari at Banepa. NHMW **9** *Erhaia nainitalensis* Davis & Rao, 1997, holotype of *E. chandeshwariensis* Nesemann & S. Sharma, 2007 (H 1.94 mm); NHMW 103315. Nepal, Central Zone, Kavre district, small forest stream, left tributary of the Chandeswari Khola upstream from Chandeshwari at Banepa. NHMW **10** *Erhaia sugurensis* Nesemann, Shah & Tachamo, 2007, holotype (H 1.95 mm); NHMW 104172. Nepal, Central Zone, Lalitpur district, Godawari, upper reaches of Sugure Khola forest stream, 1700 m a.s.l. NHMW.

Figure 11. Type locality of both *Erhaia jannei* and *E. pelkiae*; Bhutan, district Thimphu, W of Geneykha, brooklet with water powered prayer wheel, 2750 m a.s.l. Photo by EG.

Erhaia pelkiae Gittenberger & Gyeltshen, sp. nov.

http://zoobank.org/8548A11B-5AAC-4D3E-9064-6321DF57677C
Figs 4, 5, 11

Material examined. ***Holotype.*** (Fig. 4) Bhutan • District Thimphu, c. 5 km E of Chhuzom, W of Geneykha; in brooklet with a prayer wheel along the road; 2750 m a.s.l.; 27°18'43"N, 89°36'10"E; E. Gittenberger, Choki Gyeltshen & Pema Leda leg. 25.X.2018; NBCB 1059. ***Paratype.*** (Fig. 5) 1 shell; same data as for holotype; NBCB 1060.

Diagnosis. Shell with a partly reflected peristome, teleoconch with spiral lirae.

Shell. Shell elongated ovoid, with 3½ convex, shouldered whorls that are separated by a deep suture; clearly higher than broad; light yellowish brown with fine growth lines and some brown periostracal ridges. Peristome reflected at the columellar and the basal side. Parietal and columellar side of the aperture thickened by a whitish callus. An irregular umbilical chink only in the paratype might be represent a malformation resulting from repair of the shell wall. Protoconch encrustated; teleoconch with fine spiral lines.

Measurements. ($N = 2$): holotype and paratype H 1.9 mm, B 1.1 mm.

Ecology (Fig. 11). The snails are rare on the rocks in the shaded streamlet uphill the prayer wheel. See also the data for *E. jannei*.

Notes. The differences between the sympatric *E. pelkiae* and *E. jannei* are too large to regard as sexual dimorphism.

Etymology. The epithet *pelkiae* refers to Ms. Pelki Yangdon, the daughter of the fourth author.

Erhaia wangchuki Gittenberger, Sherub & Stelbrink, 2017

Figs 6, 7, 12

Erhaia wangchuki Gittenberger, Sherub & Stelbrink, 2017a: 23 ("district Wangdue Phodrang, Gangchhu, 2883 m a.s.l.; 27°26'N, 90°11'E"). Gittenberger et al. 2017b: 43, fig. 28. Gittenberger et al. 2017c: 900, 903, figs 9, 10.

Material examined. ***Holotype.*** Bhutan • District Wangdue Phodrang, Gangchhu, 2883 m a.s.l.; 27°26'N, 90°11'E; Jigme Wangchuk leg. 21.III.2015; shell; NBCB1013. ***Paratypes.*** 2 shells; same data as for holotype; NBCB1014. Additional specimens from the type locality: 23 shells and 88 specimens in ethanol 70%, 10 specimens in ethanol 97%, E. Gittenberger, Choki Gyeltshen & Pema Leda leg. 22.X.2018; NBCB 1072.

Shell. Shell conical, with 3–3½ convex, broadly shouldered whorls, that are separated by a deep suture; a little higher than broad; pale yellowish grey with fine irregular growth lines and some dark brown periostracal ridges, one of which sometimes running from a slightly angled site of the apertural columellar border into the umbilicus. Peristome not reflected. Parietal, columellar and about half the adjoining basal apertural border strongly thickened by a whitish callus. Most specimens with a continuous peristome and a broad umbilical chink. Protoconch with faint spiral lirae; teleoconch without spiral sculpture.

Measurements. ($N = 124$): H 1.6–2.1 mm, B 1.3–1.7 mm.

Ecology (Fig. 12). See Gittenberger et al. (2017a) for data about the Gangzetem brooklet and its surroundings. The snails are very common on the pebbles and rocks in the open area near the road, next to the water powered prayer wheel.

DNA data (Fig. 18). A single individual (GenBank acc. nos. KY798003 and MT237715, for 16S rRNA and COI, respectively) is genetically distinct from *E. jannei* (see data for that species) and showed genetic distances of 2.74% for 16S rRNA and 11.43% for COI compared to *Erhaia* sp. from China, Guangxi (GenBank acc. nos. KC832722 and KC832701).

Notes. Only three relatively large shells form the type series of this species. Many more specimens, none of which exceed 1.7 mm in breadth and over 2.0 mm in height, were collected recently. This necessitated some adaptations in the description of the shells. Contrary to the original description, the shell should be described as higher than broad.

Figure 12. Type locality of *E. wangchuki*; Bhutan, district Wangdue Phodrang, Gangchhu, Gangzetem brooklet, 2883 m a.s.l. Photo by A.C. Gittenberger-de Groot.

***Erhaia* in Nepal and northern India.** In their monograph on the aquatic molluscs of the Ganga River system Nesemann et al. (2007: 64–65) published short descriptions with drawings only of three *Erhaia* species from Nepal. We acquired photos of the holotypes of these nominal species, which are compared with the congeneric species from Bhutan and northern India.

Erhaia sugurensis Nesemann, Shah & Tachamo, 2007

Fig. 10

Erhaia sugurensis Nesemann, Shah & Tachamo, 2007, in Nesemann et al. 2007: 65 ("Nepal, Central Zone, Lalitpur District, Godawari, upper reaches of Sugure Khola forrest stream, elevation of 1700 m a.s.l.").

Shell. According to Nesemann et al. (2007: 65) the shells are 1.6–1.9 mm high, with 3½ whorls that are "not convex", the aperture is "rounded, widened and enlarged, the inner and outer lip is thickened". The species is said to differ most conspicuously by "the separation of the last half whorl from the shell".

Figure 13. Habitat of *Tricula montana*; Bhutan, district Mongar, Chhuburee, 818 m a.s.l. Photo by JW.

Material examined (photo only). ***Holotype.*** (NHMW 104172).

Discussion. A flaring final half of the body whorl, though not as extreme as in the holotype of *E. sugurensis*, may also occur as an individual variation in *E. nainitalensis* and the width of the umbilical chink may vary, as is shown by Davis and Rao (1997: 277, figs 2A–F).

Notes. *Erhaia sugurensis* occurs sympatrically with *E. banepaensis* at the type locality.

Erhaia banepaensis Nesemann & S. Sharma, 2007

Fig. 8

Erhaia banepaensis Nesemann & S. Sharma, in Nesemann et al. 2007: 64 ("Nepal, Central Zone, Kavre District, small forest stream, left tributary of the Chandeswari Khola upstream from Chandeshwari at Banepa"; the altitude is not indicated).

Shell. The shells are described by Nesemann and Sharma (2007: 64) as 1.6–2.0 mm high, with 4–4½ "convex" whorls, an aperture that is "ovate but not widened and not enlarged", with an inner lip that is "thin and fused to the body whorl"; it can be distinguished from the other Nepalese *Erhaia* species by the "conical and compact shape" and "convex" whorls (2007: 65).

Material examined (photo only). ***Holotype.*** (NHMW 1033159).

Figure 14. Habitat of *Tricula montana*; Bhutan, district Lhuentse, Jarkangchhu, 1333 m a.s.l. Photo by JW

Notes. Nesemann and S. Sharma are mentioned as authors for this species, without specifying for what part of the text in Nesemann et al (2007) they have responsibility.

According to Nesemann et al. (2007: 64) *E. banepaensis* occurs sympatrically with *E. chandeshwariensis* at the shared type locality of these species. *Erhaia banepaensis* is supposed to be more widely distributed in Nepal between 1400 and 2085 m a.s.l., but the type series is restricted to the holotype (NHMW 103319 [not 1033159]) and a paratype (NHMW 103320). The location of the additional material is not indicated.

Erhaia nainitalensis Davis & Rao, 1997

Fig. 9

Erhaia nainitalensis Davis & Rao, 1997: 276 ("India, Uttar Pradesh, Nainital District, Padampuiri"; "29°23'N, 79°30'E")

Erhaia chandeshwariensis Nesemann and S. Sharma, in Nesemann et al. 2007: 64, 78 fig. 4 ("Nepal, Central Zone, Kavre District, small forest stream, left tributary of the Chandeswari Khola upstream from Chandeshwari at Banepa"; the altitude is not indicated).

Material examined (photos only). Holotype and 4 paratypes of *Erhaia chandeshwariensis* (NHMW 103315 and 103316).

Figure 15. Habitat of *Tricula montana*; Bhutan, district Lhuentse, Khardungchhu, 1634 m a.s.l. Photo by JW.

Discussion. According to Davis and Rao (1997: 277, legends to figure 2) the holotype of *E. nainitalensis* is 2.28 mm high. However, elsewhere in the same article (Davis and Rao 1997: 279, table 1) the shell height of a single male animal is reported as 1.62 mm whereas 1.88–1.95–2.14 mm (minimum-mean-maximum) is indicated for five female snails. The difference in measurements between the single male and the five females might be indicative of sexual dimorphism. Shells of the species are also supposed to be "minute", what is defined as 2.0 mm high or smaller (Davis and Rao 1997: 275, 289, table 5). We suppose that the dimensions of the holotype of *E. chandeshwariensis* , i.e. H 1.94 mm, fall within the range of the measurements of *E. nainitalensis*. Three of the four paratypes of *E. chandeshwariensis* (NHMW 103316/4) are c. 1.9 mm high, whereas the fourth shell is damaged, missing the apical whorls. Davis and Rao (1997: 278, fig. 3) figure a smooth columella for *E. nainitalensis*, but mention (p. 289) a "discernable glassy thickening of the columella".

Judging the nominal taxa on the basis of photographs of shells and additional data in the literature, we conclude that in general shape and apertural characters, i.e. a narrow umbilical chink, a virtually smooth columella, and a thickened outer and inner lip, the holotype of *E. chandeshwariensis* cannot be distinguished from the shells of *E. nainitalensis* that are figured by Davis and Rao (1997: 277, figs 2A–F, 280, figs 4A–D). The fact that Davis and Rao (1997: 276) indicate 3¾-4 whorls for *E. nainitalensis*, whereas Nesemann and Sharma (2007: 64) mention 3½ whorls for *E. chandeshwariensis*, might be due to different counting methods.

Family Pomatiopsidae Stimpson, 1865

Genus *Tricula* Benson, 1843

Type species by monotypy. *Melania* (*Tricula*) *montana* Benson, 1843

Tricula montana (Benson, 1843)

Figs 1, 16–17

Melania (*Tricula*) *montana* Benson, 1843: 467 ("Bhimtal", Nainital District, Uttarakhand, India; 1370 m a.s.l.). Lectotype in The Natural History Museum, London no. 1964426 (design. Davis et al. 1986: 428, fig. 3A).

Tricula montana; Preston 1915: 68. Davis et al. 1986: 428–433, figs 3–4 (shell), 4 (operculum), 5–8 (anatomy), 9–10 (radula). Nesemann et al. 2007: 62, 78 pl. 15, fig. 1.

Material examined. Bhutan • District Lhuentse: Khardungchhu; 27°31'56"N, 91°12'19"E; 1634 m a.s.l.; J. Wangchuk leg. 28.IV.2017; 3 shells; NBCB 1061. Same data except for 27.III.2019; 8 specimens in ethanol 70%; NBCB 1064.

District Lhuentse: Jarkangchhu; 27°32'27"N, 91°12'25"E; 1333 m a.s.l.; J. Wangchuk leg. 28.IV.2017; 2 shells; NBCB 1063. Same data except for 27.III.2019; 7 specimens in ethanol 70%; NBCB 1066.

District Lhuentse: Songkhangchhu; 27°31'54"N, 91°11'17"E; 1152 m a.s.l.; J. Wangchuk leg. 27.III.2019; 3 specimens in ethanol 70%; NBCB 1068.

District Lhuentse: Fawan; 27°29'22"N, 91°10'57"E; 940 m a.s.l.; J. Wangchuk leg. 27.III.2019; 3 specimens in ethanol 70%; NBCB 1069.

District Mongar: Chhuburee; 27°15'41"N, 91°09 02"E; 818 m a.s.l.; J. Wangchuk leg. 3.V.2017; 2 shells; NBCB 1062. Same data except for 26.III.2019; 5 specimens in ethanol 70%; NBCB 1065.

District Mongar: Rekpalung; 27°19'34"N, 91°13'28"E; 885 m a.s.l.; J. Wangchuk leg. 27.III.2019; 3 specimens in ethanol 70%; NBCB 1070.

District Trongsa: Chendebji; 27°29'24"N, 90°20'18"E; 2631 m a.s.l., J. Wangchuk photographed 12.I.2018 .

District Wangdue Phodrang: 40 km SSE of Wangdue Phodrang; 27°09'25"N, 90°04'05"E; 527 m a.s.l.; E. Gittenberger, Choki Gyeltshen & Kezang Tobgay leg. 24.IX.2019; 23 shells; 23 specimens in ethanol 70%; 10 specimens in ethanol 97%; NBCB 1084.

District Zhemgang, Kekhar, 27°12'37"N, 90°46'28"E; 1540 m a.s.l., J. Wangchuk leg. photographed 17.I.2018.

Shell. Shell slender conical, with up to c. 5 shouldered, moderately convex whorls, separated by an incised suture; with obsolete growth lines and poorly discernible dense spiral lirae. Pale yellowish grey, with a light brown apertural border when fully grown. Apex not flattened, often decollate. Aperture triangular with broadly rounded edges, its parietal side about double the length of the columellar side; palatal side straight,

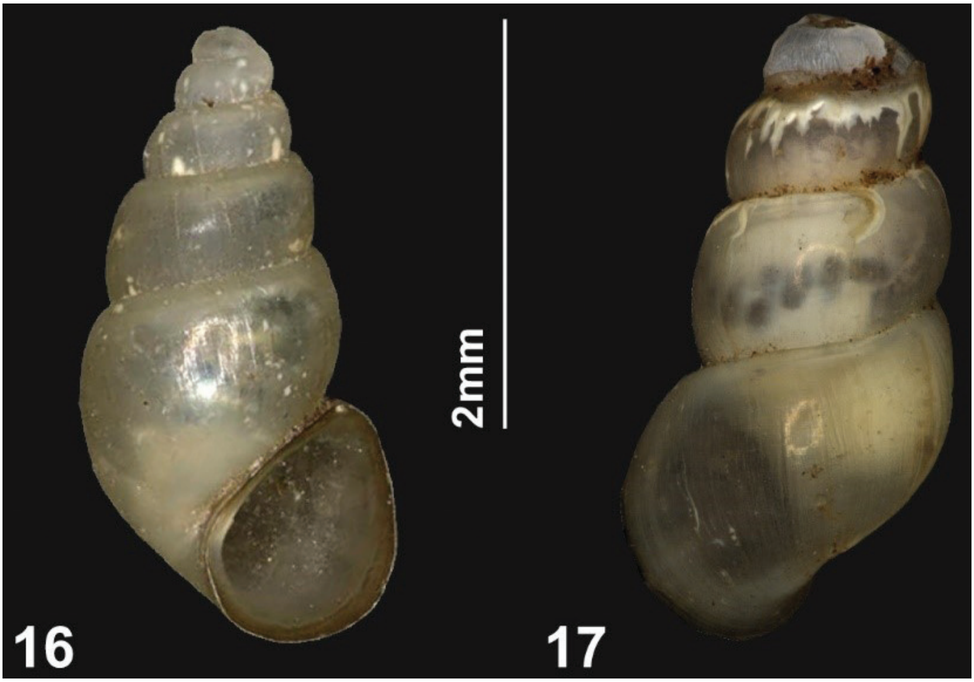

Figures 16, 17. *Tricula montana* (Benson, 1843), Bhutan **16** District Lhuentse, Khardungchhu, 1634 m a.s.l. (H 3.1 mm) **17** Bhutan, district Mongar, Chhuburee, 818 m a.s.l. (decollate specimen, H 3.0 mm). Photos by J. Goud.

passing into the slightly curved basal border with a more strongly curved transitional part. Parietal border of the aperture attached, at least in the middle and not or only slightly protruding. Umbilicus closed or nearly so.

Measurements. According to Davis et al. (1986: 431) the shell height of males and females combined ($N = 10$) is 3.32–3.72 mm. However, for the lectotype a larger shell height is indicated, i.e. 3.92 mm (Davis et al. 1986: 429, fig. 3A, 430). That shell is not even a relatively large specimen. Additional shells figured by Davis et al. (1986: 429, 430, fig. 3F, G, H, K, L) and printed at the same scale, are larger.

The shells that are known from Bhutan ($N = 73$) are relatively small, with 5–5½ whorls measuring H 2.8–3.6 mm, B 1.3–1.7 mm.

Distribution. (Fig. 1). According to Subba Rao (1989: 68) this species occurs in the Indian states of Himachal Pradesh (“Jhiri valley”) and Uttarakhand (= Uttaranchal). Nesemann et al. (2007: 62) refers to it as widely distributed in the western and central Himalaya, in Nepal mainly at 1300–2100 m a.s.l. The records for Bhutan, at altitudes of 527–2631 m a.s.l., extend its range eastwards.

Habitat. This species was found in Bhutan without accompanying *Erhaia* species mostly in densely vegetated, shaded areas with more or less overgrown springs and streamlets (Figs 1, 13–15). Davis et al. (1986: 427) describe a similar habitat for the Nainital District near the type locality of *T. montana*. The locality in the district of Wangdue Phodrang is an overgrown, dripping wet, vertical, rocky wall along the road.

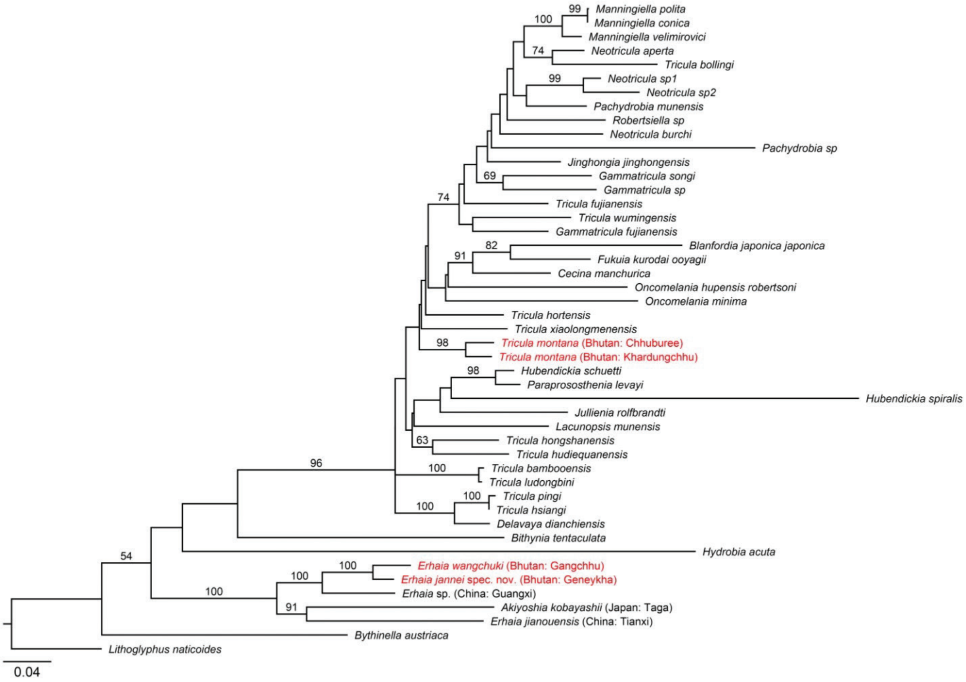

Figure 18. Maximum likelihood tree reconstructed with RAxML BlackBox (Stamatakis et al. 2008; GTR+G substitution model for each partition and 100 bootstrap replicates) based on the 16S rRNA and COI dataset of Liu et al. (2014) and Guan et al. (2008), with new data in red. Numbers on branches denote bootstrap values >50.

The shells from Mongar, Chhuburee, and from Lhuentse, Jarkangchhu, are all decollate (Fig. 17), whereas shells from the other localities still have their apical whorls present (Fig. 16). This might be a consequence of unknown differences in water quality at those different localities.

DNA data. Two snails from Chhuburee and two snails from Khardungchhu were sequenced. These specimens shared the same haplotype per population for both 16S rRNA (GenBank acc. nos. MT239080 and MT239079, for Chhuburee and Khardungchhu,) and COI (GenBank acc. nos. MT237718 and MT237717, for Chhuburee and Khardungchhu). The two populations differed genetically by 1.0% and 4.9% for 16S rRNA and COI, respectively. Because the monophyly of *Tricula* remains uncertain (see e.g., Liu et al. 2014), we compared these sequences with additional data available from GenBank. For 16S rRNA, the lowest genetic distances, i.e., 3.1% and 3.3%, were identified between snails from Chhuburee and Khardungchhu, respectively, and *Tricula* sp. from China, Hunan, Xiangxi, Fenghuang (GenBank acc. no. EU311736), and 3.3% and 3.5% between snails from Chhuburee and Khardungchhu, respectively, and *T. ludongbini* Davis & Y.-H. Guo, 1986 from China, Yunnan, Panlong River, Hei Long Tan (GenBank acc. no. KC832717).

The genetic distances between *T. montana* from Chhuburee and Khardungchhu were considerably higher for COI, with 8.9% and 9.3%, respectively, between snails from Chhuburee and Khardungchhu and *Tricula* sp. from China, Sichuan, Dayi, Tian Gong Mia, Huang Ba (GenBank acc. no. AF253070), and *Tricula hortensis* Attwood & Brown, 2003 from China (GenBank acc. no. JQ082621).

Notes. The species was identified conchologically by using the data provided by Benson (1843), Davis et al. (1986) and Nesemann et al. (2007), taking also the distributional data (Nesemann et al. 2007: 62) into account.

Some species of *Tricula* may transmit schistosomes that could in principle infect humans and other mammals. No data in respect of this are known for *T. montana*.

See Davis et al. (1986) for a detailed account on this species, with data on shell morphology, anatomy of males and females, biogeography, and systematic relationships.

Acknowledgements

We would like to thank Dr Tashi Y. Dorji, Program Director of the NBC and Ms Sangay Dema (NBC) for their support and guidance to carry out this research. We also thank Mr J. Goud (Naturalis, Leiden), who made the photographs for Figures 2–7, Ms Sara Schnedl (Naturhistorisches Museum, Vienna) who photographed the shells for Figures 8–10, Mr E.-J. Bosch (Naturalis, Leiden), who composed the distribution map, Mr H. Caspers (Naturalis, Leiden), who mounted the illustrations, and Mr Kezang Tobgay (NBC Serbithang, Thimphu), who assisted during collecting. Ms Anita Eschner is gratefully acknowledged for the assistance in the Naturhistorisches Museum, Vienna, Austria. We also gratefully acknowledge the Department of Forests and Park Services for providing the permits to collect specimens. We owe a debt of gratitude to the National Geographic Society (grants GEFNE 131-14 and NGS-61618R-19) and the Bhutan Trust Fund for Environmental Conservation (grant MB0149Y15) for supporting our work in Bhutan.

References

Benson WH (1843) Description of Camptoceras, a new genus of the Lymnaeadae, allied to Ancylus, and of Tricula, a new type of form allied to Melania. Calcutta Journal of Natural History: and Miscellany of the Arts and Sciences in India 3(12): 465–468.

Davis GM, Kuo Y-H, Hoagland KE, Chen P-L, Yang H-M, Chen D-J (1985) Erhaia, a new genus and new species of Pomatiopsidae from China (Gastropoda: Rissoacea). Proceedings of the Academy of Natural Sciences of Philadelphia 137: 48–78. http://www.jstor.org/stable/4064860

Davis GM, Rao NVS, Hoagland KE (1986) In search of Tricula (Gastropoda: Prosobranchia): Tricula defined, and a new genus described. Proceedings of the Academy of Natural Sciences of Philadelphia 138: 426–442. http://www.jstor.org/stable/4064915

Davis GM, Kang ZB (1995) Advances in the Systematics of Erhaia (Gastropoda: Pomatiopsidae) from the People's Republic of China. Proceedings of the Academy of Natural Sciences of Philadelphia 146: 391–427. http://www.jstor.org/stable/4065020

Davis GM, Rao S (1997) Discovery of *Erhaia* (Gastropoda: Pomatiopsidae) in northern India with description of a new genus of Erhaiini from China. Proceedings of the Academy of Natural Sciences of Philadelphia 148: 273–299. http://www.jstor.org/stable/4065055

Folmer O, Black M, Hoeh W, Lutz R, Vrijenhoek R (1994) DNA primers for amplification of mitochondrial cytochrome c oxidase subunit I from diverse metazoan invertebrates. Molecular Marine Biology and Biotechnology 3: 294–299.

Gittenberger E, Sherub S, Stelbrink B (2017a) Erhaia Davis & Kuo (Gastropoda, Rissooidea, Amnicolidae) also in Bhutan. ZooKeys 679: 21–28. https://doi.org/10.3897/zookeys.679.13326

Gittenberger E, Leda P, Gyeltshen C, Sherub S, Dema S (2017b) A field guide to the common molluscs of Bhutan: i–v, 1–111. National Biodiversity Centre, Thimphu, Bhutan.

Gittenberger E, Leda P, Wangdi K, Sherub S (2017c) Bhutan freshwater gastropods and trematodes, with a warning. Biodiversity Journal 8(4): 895–906. http://www.biodiversityjournal.com/pdf/8(4)_895-906.pdf

Guan F, Niu AO, Attwood SW, Zhu YH (2008) Molecular phylogenetics of triculine snails (Gastropoda: Pomatiopsidae) from southern China. Molecular Phylogenetics and Evolution 48: 702–707. https://doi.org/10.1016/j.ympev.2008.04.021

Kumar S, Stecher G, Tamura K (2016) MEGA7: Molecular Evolutionary Genetics Analysis version 7.0 for bigger datasets. Molecular Biology and Evolution 33: 1870–1874. https://doi.org/10.1093/molbev/msw054

Liu L, Huo G-N, He H-B, Zhou B, Attwood SW (2014) A phylogeny for the Pomatiopsidae (Gastropoda: Rissooidea): a resource for taxonomic, parasitological and biodiversity studies. BMC Evolutionary Biology 14: 29. https://doi.org/10.1186/1471-2148-14-29

Nesemann H, Sharma S, Sharma G, Khanal SN, Pradhan B, Shah DN, Tachamo RD (2007) Class Gastropoda. In: Nesemann H, Sharma S, Sharma G, Khanal SN, Pradhan B, Shah DN, Tachamo RD (Eds) Aquatic Invertebrates of the Ganga River System, Volume 1: Mollusca, Annelida, Crustacea (in part). 57–102.

Palumbi SR, Martin A, Romano S, McMillan WO, Stice L, Grabowski G (1991) The simple fool's guide to PCR. University of Hawaii, Honolulu.

Preston HB (1915) Mollusca. (Freshwater Gastropoda & Pelecypoda). – The fauna of British India, including Ceylon and Burma: i–xix, 1–244. Taylor and Francis, London.

Subba Rao NV (1989) Handbook, Freshwater Molluscs of India: 1–289. Zoological Survey of India, Kolkata.

Stamatakis A, Hoover P, Rougemont J (2008) A rapid bootstrap algorithm for the RAxML web servers. Systematic Biology 57: 758–771. https://doi.org/10.1080/10635150802429642

Wilke T, Davis GM, Falniowski A, Giusti F, Bodon M, Szarowska M (2001) Molecular systematics of Hydrobiidae (Mollusca: Gastropoda: Rissooidea): testing monophyly and phylogenetic relationships. Proceedings of the Academy of Natural Sciences of Philadelphia 151: 1–21. https://doi.org/10.1635/0097-3157(2001)151[0001:MSOHMG]2.0.CO;2

Wilke T, Davis GM, Gong X, Liu H-X (2000) Erhaia (Gastropoda: Rissooidea): phylogenetic relationships and the question of Paragonimus coevolution in Asia. The American Journal of Tropical Medicine and Hygiene 62: 453–459. https://doi.org/10.4269/ajtmh.2000.62.453

Winnepenninckx B, Backeljau T, De Wachter R (1993) Extraction of high molecular weight DNA from molluscs. Trends in Genetics 9: 407. https://doi.org/10.1016/0168-9525(93)90102-N

ZooKeys 929: 19–51 (2020)
doi: 10.3897/zookeys.929.37666
http://zookeys.pensoft.net

RESEARCH ARTICLE

A peer-reviewed open-access journal
ZooKeys
Launched to accelerate biodiversity research

Description of six new large species of *Argentinomyia* Lynch-Arribálzaga, 1891 and redescription of *Talahua fervida* (Fluke, 1945) (Diptera, Syrphidae, Syrphinae)

Augusto L. Montoya[1], Marta Wolff[1]

[1] *Grupo de Entomología, Universidad de Antioquia, Calle 67 # 53-108, Medellín, Colombia*

Corresponding author: *Augusto León Montoya* (aleon.montoya@udea.edu.co; guto.spider@gmail.com)

Academic editor: *Ximo Mengual* | Received 25 June 2019 | Accepted 9 January 2020 | Published 22 April 2020

http://zoobank.org/33EAB957-6453-425A-BE3D-D382B8F155D0

Citation: Montoya AL, Wolff M (2020) Description of six new large species of *Argentinomyia* Lynch-Arribálzaga, 1891 and redescription of *Talahua fervida* (Fluke, 1945) (Diptera, Syrphidae, Syrphinae). ZooKeys 929: 19–51. https://doi.org/10.3897/zookeys.929.37666

Abstract

The morphological similarities between five new large *Argentinomyia* species and *Talahua fervida* Fluke are characterized and presented. Six new species of *Argentinomyia* (10–12 mm long) are described: *Argentinomyia andina* Montoya & Wolff, **sp. nov.** (Colombia), *Argentinomyia choachi* Montoya, **sp. nov.** (Colombia), *Argentinomyia quimbaya* Montoya & Wolff, **sp. nov.** (Colombia), *Argentinomyia huitepecensis* Montoya, **sp. nov.** (México), *Argentinomyia puntarena* Montoya, **sp. nov.** (Costa Rica), and *Argentinomyia talamanca* Thompson, **sp. nov.** (Costa Rica). The genus *Talahua* Fluke is re-diagnosed and, *Talahua fervida* redescribed. A taxonomic key and a comparison of diagnostic characters are presented. Photographs of head, abdominal and wing maculae patterns, as well as illustrations of male genitalia are provided for species identification.

Keywords

Endemism, flower flies, hover flies, Neotropical diversity, Mesoamerica, Tropical Andes

Introduction

Flower flies or hoverflies (Syrphidae) are one of the most diverse families of Diptera with more than 6100 described species worldwide, and ca. 1560 species distributed in the Neotropical region (Thompson et al. 2010; Pape and Evenhuis 2018). Currently, the family is subdivided into four subfamilies: Syrphinae, Pipizinae, Eristalinae, and

Microdontinae (Mengual 2015). Syrphinae comprises more than 30% of worldwide diversity of the family and contains mostly species with larvae that feed on soft-body arthropods (Rojo et al. 2003). Within Syrphinae, the tribe Bacchini comprises 332 species worldwide (13 genera) and more than 83 Neotropical species classified into seven genera: *Melanostoma* Schiner, 1860 is present in all biogeographic regions (Haarto and Ståhls 2014); in the Neotropics, only *Melanostoma bellum* Giglio-Tos, 1892 is found in Chiapas, México, but may also occur in the adjacent highlands of Guatemala (Thompson et al. 2010). *Platycheirus* Lepeletier & Serville, 1828 and *Xanthandrus* Verrall, 1901 are widely distributed in the Neotropics and other biogeographic regions (Vockeroth 1990; Borges and Pamplona 2003; Mengual et al. 2008). Genera *Argentinomyia* Lynch-Arribálzaga, 1891, *Leucopodella* Hull, 1949, *Tuberculanostoma* Fluke, 1943, and *Talahua* Fluke, 1945 are Neotropical endemics and reach the highest diversity in the highlands of the Tropical Andes (Fluke 1943, 1945, 1957; Thompson 1981, 1999), with some species of *Argentinomyia* and *Leucopodella* extending to Central America.

Argentinomyia contains 27 valid species distributed from the cloud forests in Northern Central America to low and middle elevations in the Caribbean and Galápagos Islands. The genus is also found in cold Andean forests and Páramo ecosystems in the Tropical Andes, and in lowlands in southeastern of South America. Even though extensive sampling has been done, the genus is apparently absent in the Chilean subregion and, has not been registered in Surinam (Thompson 1999; Thompson et al. 2010; Reemer 2010). Adults of *Argentinomyia* are common flower visitors in pristine ecosystems, whilst immature stages are unknown.

Argentinomyia is distinguished from other genera of Bacchini by the combination of: 1) long antenna, with scape much longer than broad; 2) basoflagellomere oval or slightly elongate; 3) face straight in profile, not produced anteriorly, generally with pollinosity broadly punctuate, tubercle low, usually with transverse grooves dorsally or pollinosity broadly punctuate; 4) metacoxa without posteromedial pile on apical angle; 5) abdomen dark colored, often with variously shaped light-colored yellow, orange to silvery-grey pollinose paired maculae; triangular to quadrate or oval markings on 2nd to 4th abdominal tergite, sometimes including a small macula on 5th tergite, and 6) male genitalia normal size, superior lobes triangular to rectangular, irregular in shape and cercus short (Fluke 1945, 1957; Thompson 1999; Huo 2014; Thompson and Skevington 2014).

Talahua is a small Neotropical genus that inhabits the highlands of Colombia and Ecuador (Fluke 1945; Montoya et al. 2012; Montoya 2016; Marín-Armijos et al. 2017). The genus was originally established by Fluke (1945) as subgenus of *Melanostoma*, including the only species *Melanostoma* (*Talahua*) *fervida* Fluke, 1945. In a subsequent study, Fluke (1957) gave *Talahua* full generic status based on the study of male genitalia. Later, Thompson et al. (1976) also considered *Talahua* a valid genus. In 1999, Thompson proposed to transfer the aberrant species, *Melanostoma palliatum* Fluke, 1945 to *Talahua*, despite the species being previously considered part of *Xanthandrus* (Thompson et al. 1976). In the revision of the Neotropical *Xanthandrus*, Borges and Pamplona (2003) considered *M. palliatum* as part of *Xanthandrus*, and consequently, *Talahua* was again recognized as monotypic (Borges and Pamplona 2003; Marín-Armijos et al. 2017; Thompson and Skevington 2014).

Talahua can be distinguished from other genera of Bacchini largely by the following combination of characters: 1) antennae relatively short, scape broader than long, nearly equal to pedicel; 2) basoflagellomere large, slightly oval and apically rounded; 3) face slightly receding to perpendicular with a well-rounded tubercle, never with transverse grooves dorsally along tubercle or broadly punctuate; 4) metacoxa with a tuft of pile at posteromedial apical angle; 5) abdomen elongated or with parallel sides, with four to five pairs of large rounded to triangular markings on the terga, always with small macula on 5th tergum; and 6) male genitalia greatly enlarged, with superior lobes, and cerci elongated, surstyli three to four times longer than broad (Fluke 1945, 1957; Thompson 1999; Thompson and Skevington 2014).

Extensive sampling in the cloud forest, high-Andean and Páramo ecosystems in Mesoamerica (México and Costa Rica) and Tropical Andes (Colombia and Ecuador) in the last twenty-five years resulted in the discovery of several new *Argentinomyia* species including six species, large in body size, that are similar in appearance to *Talahua fervida*. Therefore, we take the opportunity to describe the new species and provide a full redescription for *T. fervida*, as well as a taxonomic key, photographs, illustrations, and a comparison of morphological diagnostic characters, including distributional maps to all species.

Material and methods

Syrphidae-specific characters used in the key, descriptions, and drawings largely follows the terminology established by Thompson (1999), Thompson et al. (2010), and Cumming and Wood (2017). Figures of some characters employed in the key correspond to those treated in the chapter of Syrphidae in the Manual of Central America Diptera (Thompson et al. 2010) and are indicated by the abbreviation "MCAD". The specimens were determined to genus level using the keys of Thompson et al. (2010), Huo (2014) and Thompson and Skevington (2014). Our new species were compared with type specimens of twenty-seven *Argentinomyia* species and one of *Talahua* deposited in the AMNH, BMNH, USNM, and WIRC collections (Suppl. material 1), including the study of the original descriptions (Fluke 1945). A complete revision of the genus is in preparation and will be published soon. Recognition of the new species was facilitated by examination and comparison of the reference material of *Argentinomyia* identified by F. C. Thompson in the USNM (Smithsonian Institution). The acronyms used for the collections examined are as follows (curators' names in parentheses):

AMNH	American Museum of Natural History, New York, USA (David Grimaldi)
CEUA	Colección de Entomología Universidad de Antioquia, Medellín, Colombia (Marta Wolff)

ECO-TAP-E	Colección Entomológica de la Unidad San Cristóbal de las Casas de El Colegio de la Frontera Sur, México (Philippe Sagot and Rémy Vandame)
IAvH	Instituto de Investigación de Recursos Biológicos Alexander von Humboldt, Villa de Leyva, Colombia (John César Neita-Moreno)
INBio	Instituto Nacional de Biodiversidad, Heredia, Costa Rica (Manuel Zumbado)
QCAZ	Departamento de Biología, Pontifica Universidad Católica del Ecuador, Quito, Ecuador (Álvaro Barragán)
UNAB	Museo Entomológico de la Facultad de Agronomía, Universidad Nacional de Colombia, Bogotá, Colombia (Francisco Serna and Erika Vergara)
USNM	National Museum of Natural History, Washington, D.C., USA (Torsten Dikow)
WIRC	Wisconsin Insect Research Collection, Department of Entomology, University of Wisconsin, Madison, USA (Steven Krauth)

The type series of the new species is comprised of dry pinned material deposited in the CEUA, USNM, INBio, and ECO-TAP-E.

To illustrate the morphological variation of the herein described species, habitus photographs were created from a series of images taken at different focal depths with a digital camera Olympus OM-D (Olympus Raw Image file in .ORF) using the facilities of the Diptera Collection, Department of Entomology (https://naturalhistory.si.edu/research/entomology/collections-overview/diptera-collection) at the USNM. Additional photos were taken using a Moticam 3.0 megapixel DFC500 digital camera attached to an Olympus SZX7 stereomicroscope. Final images were combined using the HeliconFocus Pro (version 6.7.1) stacking software. The scale bar was added in Photoshop according to the camera focal aperture used when the photo was taken. Editing was conducted in Adobe Photoshop CC, and the final image plates were prepared in Illustrator CC.

Body length was measured from frons to the posterior end of the abdomen; wing length was measured from wing insertion to the apex of the wing. Measurements were made using a Zeiss Stemi 2000-C stereomicroscope (magnification 6.5–115×) equipped with a stereoscope grid. Measurements of antennal segments are approximations based on the mid-line of the inner surface and are presented in the ratio format scape:pedicel:flagellomere.

For the study of the male genitalia, the structure was dissected. The genitalia were cleared in a KOH solution (approximately 10%) boiling at 37 °C for 10 to 15 minutes. Schema of internal structures were illustrated from digital images taken through the stereomicroscopes. Additional, sketches were produced with a camera Lucida attached to the stereomicroscope. Final drawings were prepared by tracing and vectorizing in Adobe Illustrator CC, and pile was omitted.

The new species are described from males and females collected together in at least one locality, and sexual dimorphic variation reported. Only *Argentinomyia choachi* Montoya sp. nov. is described from a single female because it markedly differs in the morphological characters from the other species.

With the aim of spanning the entire known distribution of included species, original label information was compiled in a Darwin Core standard-compliant data. Distributional maps were generated using the software QGIS desktop 2.2.0 and an excel .csv file (comma delimited) to plot presence. A digital file with an elevation model (SRTM30 CGIAR-SRTM with 30 seconds resolution) was used in addition to a shapefile with the biogeographic provinces proposed by Morrone (2014) and digitalized by Löwenberg-Neto (2015) for the Neotropics.

Description of new species

The new *Argentinomyia* species described here are characterized by the scutellum with a deep groove next to the rim (emarginate), face with a well-rounded tubercle, never with transversal grooves dorsally along tubercle or broadly punctuate, metacoxa with a tuft of pile at posteromedial apical angle, wing generally with a brownish macula extensively covering the apex of cells r and m or hyaline, and abdomen with large markings on the terga. The new species are superficially similar to *Talahua fervida*, differing in the male genitalia.

Identification key to the large (10–12 mm long) species of *Argentinomyia*

The new key was modified based on characters provided by Thompson (1999), Thompson et al. (2010), Huo (2014), Thompson and Skevington (2014) and Ramage et al. (2018).

1 Postpronotum pilose (MCAD fig. 30); male abdomen with four unmodified pregenital segments; tergum 5 usually not visible in dorsal view (MCAD figs 1, 4) (subfamilies Eristalinae, Microdontinae and Pipizinae) .... **other flower flies**

– Postpronotum bare; male abdomen with five unmodified pregenital segments; tergum 5 visible in dorsal view (MCAD figs 53-61) (subfamily Syrphinae) **2**

2 Face and/or scutellum partially yellow or yellowish-brown in background color, aedeagus two-segmented .... **other Syrphinae genera**

– Face and scutellum entirely black in background color (some species with partly pale face or scutellum), aedeagus unsegmented (Bacchini) **3**

3 Abdomen petiolate, distinctly narrower than thorax (MCAD figs 59, 60); face usually without tubercle, flat, straight or convex .... ***Leucopodella* Hull**

– Abdomen parallel-sided or narrowly oval (MCAD figs 55, 58); face with tubercle **4**

4 Antennal cavity broadly confluent (MCAD fig. 24); metathoracic pleuron with several fine subappressed pile ventral to spiracle; katepisternum with pile patches broadly separated posteriorly, joined anteriorly.................. ***Xanthandrus* Verrall**

– Antennal cavity broadly separated (MCAD fig. 23); metathoracic pleuron bare; katepisternum with pile patches usually broadly separated throughout.............. **5**

5 Metasternum greatly reduced to a small diamond (MCAD fig. 34; Haarto and Ståhls 2014: 95, fig. 1A); face not produced below, with small tubercle, facial pruinosity neither punctate nor rippled (MCAD fig. 28) .... ***Melanostoma* Schiner**

– Metasternum entire, not reduced (MCAD fig. 35; Haarto and Ståhls 2014: 95, fig. 1B); face variable, almost straight in profile with weak tubercle or moderately to strongly produced forward ventrally, sometimes with pruinescence forming punctuate or rippled pattern **6**

6 Antennae shorter, scape broader than long, scape nearly equal to pedicel, basoflagellomere large, slightly oval and apically rounded (Fig. 12 A, B); face perpendicular with a well-rounded tubercle (Figs 12A, 13A, D); mesocoxa pilose posteriorly; male genitalia enlarged (Fluke 1957: 278, fig. 123) .... ***Talahua* Fluke**

– Antenna elongate, scape longer than broad; basoflagellomere oval or elongate (MCAD fig. 22); face straight in profile, tubercle low (MCAD fig. 22); mesocoxa bare posteriorly; male genitalia normal size (*Argentinomyia* Lynch-Arribálzaga *sensu lato*) 7

7 Basoflagellomere oval or slightly elongate (MCAD fig. 22); face usually with transversal grooves dorsally along tubercle (MCAD fig. 23) and shine (bare) punctuate maculae laterally; scutellum without a deep groove next to the rim; metacoxa without a pile tuft at posteromedial apical angle; abdomen slightly spatulate, oval or with parallel sides, with triangular to quadrate or oval markings .... **other species of *Argentinomyia*** (not treated here)

– Basoflagellomere large, slightly oval and apically rounded (Fig. 1C, F); face with a well-rounded tubercle, never with transversal grooves dorsally along tubercle or broadly punctuate (Fig. 1A, D); scutellum with a deep groove next to the rim (emarginate) (Figs 1B, 1E, 12D); metacoxa with pile posteromedial on apical angle (Fig. 12C); abdomen elongated, with large markings on the terga, sometimes with a transverse fascia on the third or with a pair of small maculae in the basal corners of fifth tergum (Fig. 1B, E) **8**

8 Antenna brown (Fig. 10A, C, D, F); alula and costal cell extensively microtrichose (Fig. 10B, C, D); femur extensively brown (Fig. 10C, F); second tergum with a pair of small maculae on basal 1/5 (Fig. 10B–E); male genitalia as Fig. 11A–C [Costa Rica]................ ***Argentinomyia talamanca* Thompson, sp. nov.**

– Antenna orange ventrally; alula and costal cell bare; femur yellow on apical 1/3 or more; second tergum with broad macula.. **9**

9 Legs extensively yellow (Fig. 8A–E); male genitalia as Fig. 9A–C [Colombia] .... ***Argentinomyia quimbaya* Montoya & Wolff, sp. nov.**

– Legs black on basal 1/3 or more (Figs 1, 3, 4, and 6)...................................... **10**

10 Abdomen with a transverse fascia on the third tergum (Fig. 4B, E); metacoxa black pilose (Fig. 4C, F); male genitalia as Fig. 5A–C [México] ....***Argentinomyia huitepecensis*** **Montoya, sp. nov.**

– Abdomen with a pair of large maculae on the third tergum, slightly touching each other toward the middle; metacoxa yellowish pilose (Figs 1, 3, 6) **11**

11 Metafemur brown basally; coxa black; third and fourth tergum with a pair of quadrangular maculae (Fig. 3A–D) (male unknown) [Colombia] ....***Argentinomyia choachi*** **Montoya, sp. nov.**

– Metafemur yellow basally; coxa orange-brown; third and fourth tergum with a pair of triangular maculae (Figs 1, 6)..**12**

12 Face white pollinose and pilose (Fig. 6A, D); metafemur orange on basal 1/5 and apical 3/5, metatibia extensively brown, only orange brownish on basal 2/3 (Fig. 6C, F); fifth tergum without maculae (Fig. 6B, E); male genitalia as Fig. 7A, C [Costa Rica] ....***Argentinomyia puntarena*** **Montoya, sp. nov.**

– Face yellow pollinose and pilose (Fig. 1A, D); metafemur brown, only slightly orange on apical 1/6, tibiae yellow with a dark ring near the middle, more prominent on the metalegs (Fig. 1C, F); fifth tergum with a pair of small maculae in the basal corners (Fig. 1B, E); male genitalia as Fig. 2A–C [Colombia] ....***Argentinomyia andina*** **Montoya & Wolff, sp. nov.**

Argentinomyia andina **Montoya & Wolff, sp. nov.**

http://zoobank.org/72FC4AEB-1E3D-4529-8DE2-E541D25207EB
Figures 1, 2, 15

Differential diagnosis. Face yellow pollinose and pilose. Metafemur extensively brown, only slightly orange on apical 1/6. Tibiae yellow with a dark ring near the middle, more prominent on the metalegs. Third and fourth tergum with a pair of broad subquadrate maculae, reaching the lateral margin in their full width, fifth tergum with a pair of small maculae in the basal corners. *Argentinomyia puntarena* sp. nov. is similar to *A. andina* sp. nov., but differs in having the face white pollinose and pilose; metafemur orange on basal 1/5 and apical 3/5, metatibia extensively brown, only orange brownish on basal 2/3; fifth tergum without maculae.

Type locality. Colombia, department of Antioquia, Sonsón municipality, Vereda Norí municipal rural settlement, Norí Mountain hill, forest, 05°48.580'N, 75°16.142'E, alt. 2896 m a.s.l.

Description. Male. Head (Fig. 1A, C): Black metallic, covered with yellow pollinosity, oral tips, ocellar triangle, and a large triangular macula on the frons, yellow pilose, pile on front black, on gena and face golden yellow, on the occiput yellow except the dorsal pile black, frontal triangle coppery metallic. Antennae brown, orange-red ventrally, rounded, as long as wide, the lower basal corner of basoflagellomere, ratio 1.0:1.2:2.3, arista orange, dark brown toward the tip. **Thorax** (Fig. 1C). Black, the

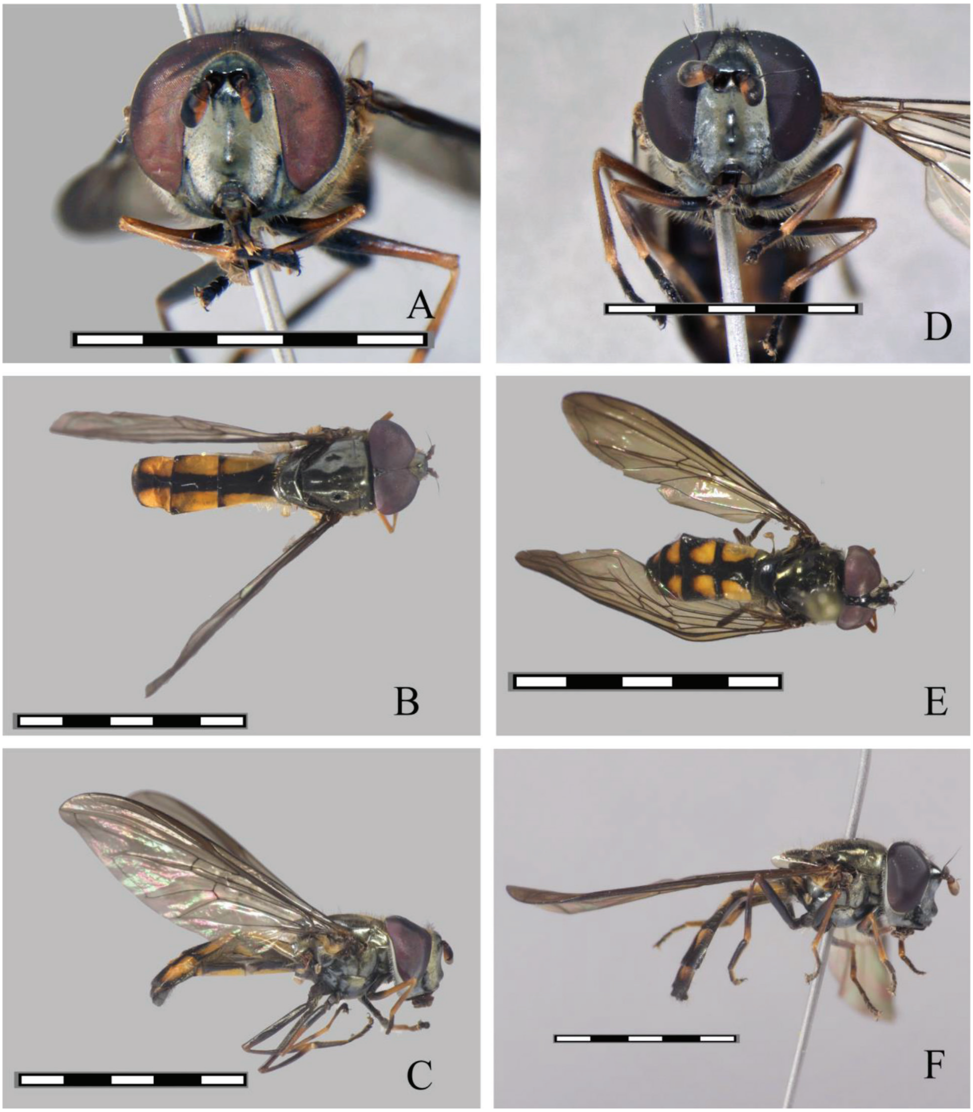

Figure 1. *Argentinomyia andina* sp. nov., male (CEUA 103551): **A** head, frontal, male **B** dorsal view **C** lateral view. Female (CEAU 69016): **D** head, frontal view **E** dorsal view **F** lateral view. Scale bars: 5 mm.

scutum shining, with iridescent to coppery yellow reflections, with two median brownish pollinose vittae on anterior half, pile mostly yellow, with long black pile before the scutellum. *Wing* (Fig. 1C). Slightly smoky, the stigma brown yellowish, marginal maculae slightly brownish at apex of cells r and m; membrane microtrichose, except for extensive bare areas on basal half (cells c, sc, r1, dm and bm); tegula and basicosta black pilose, alula extensively bare medially, calypter whitish yellow, border whitish tawny, fringe yellow tawny, plumula yellow, halter white, knob white. *Legs* (Fig. 1C). Yellow to brown, pro and mesofemora brown, only slightly yellow on apical 1/3, respectively, metafemora brown, only slightly orange on apical 1/6, tibiae yellow with a dark ring near the middle, more prominent on the metalegs, tarsi brown, yellow pilose below, black pilose above. **Abdomen** (Fig. 1B). Elongate, black, with five pairs of lateral orange maculae reaching the apical 5/6 of the tergum, first tergum shining black, second to fourth tergum with a pair of broad subquadrate maculae, reaching the lateral margin in their full width; fifth tergum with a pair of small maculae in the basal corners. Pile orange on the sides basally, black down the middle and on the apical terga, as well as in the maculae; male genitalia as Fig. 2.

Female. (Fig. 1D–F). Similar to male except for normal sexual dimorphism. Abdominal maculae triangular and comparatively shorter than in the male, apically rounded, second to fifth tergum with maculae only reaching the apical 3/4, but not reaching the lateral margin in their full width. Frons shining above with a white pollinose transversal macula below. The female of *Argentinomyia andina* sp. nov. is similar in appearance to *Talahua fervida*, but *T. fervida* has a pair of small basolateral maculae on the sixth tergum and maculae on second to third tergum are longer than in *A. andina* sp. nov.

Length (*N* = 2). Body 11.2–11.5 mm; wing 10.8–11.1 mm.

Etymology. The specific epithet *andina* (nominative, adjective feminine) is derived from the Andes South American mountain chain system where the type specimens were collected.

Distribution. *Argentinomyia andina* sp. nov. (*N* = 8) is distributed on the west slope of the Central Cordillera in Northern Colombian Andes (Antioquia) at elevations between 1800–2700 m. a.s.l., in the provinces of Cauca (Fig. 15).

Type material. Holotype. COLOMBIA ♂, Antioquia, Sonsón, Norí. Original label: "Colombia, Antioquia, Sonsón, vereda Norí / Norí mountain hill, Forest; 5°48.580'N, 75°16.142'E, 2896 m / 1-12.iv.2018, Malaise trap, Leg. A.L. Montoya and J.P. Carmona / CEUA 103430". "HOLOTYPE / *Argentinomyia andina* / Montoya & Wolff 2020" [red, handwritten except first line]". The holotype is in good condition and deposited at the CEUA, Medellín, Colombia. **Paratypes.** COLOMBIA • 1 ♂ same data as for holotype (CEUA) but differs on: Net, 2.vii.2018, Leg. J.P. Carmona, J. Sauceda, J. Vallejo (CEUA 103385); 2♂, same, except; 24.v-4.vi.2019, Leg. A.L. Montoya; J. Sauceda; M. Posada (CEUA 103552-53); 1♂, Antioquia, Santa Elena, Vereda El Placer, El Robledal, 6°13.717'N, 75°30.267'E, 2480 m a.s.l., Van Sommeren-Rydon trap baited with fish, 1–5.iii.2007, Leg A. Vélez (CEUA 103551); 1♀, Antioquia, San José de la Montaña, Vereda El Congo, Sector La Laguna, 6°45.827'N, 75°42.104'E, 3100-3200 m a.s.l., Páramo, Van Sommeren-Rydon trap baited with fish, 10-11.ix.2011, Leg. L. Rios (CEUA 69016); 1♀, same, except; 46.013'N, 75°41.979'E, 3100–3183 m a.s.l., Malaise, 4–14.ii.2017, Leg. C. Henao; A. F. Sepúlveda (CEUA 103635); 1♂, Sonsón, Vereda San Francisco, Las Palomas A Mountain hill, 5°43.606'N, 75°15.371'E, 2749 m a.s.l., Forest, Net, 1-12.iv.2018, Leg. A.L. Montoya, J. Carmona (CEUA 103434).

Comments. *Argentinomyia andina* sp. nov. inhabits pristine Andean forest and Páramo ecosystems in Colombia, being particularly abundant in forest.

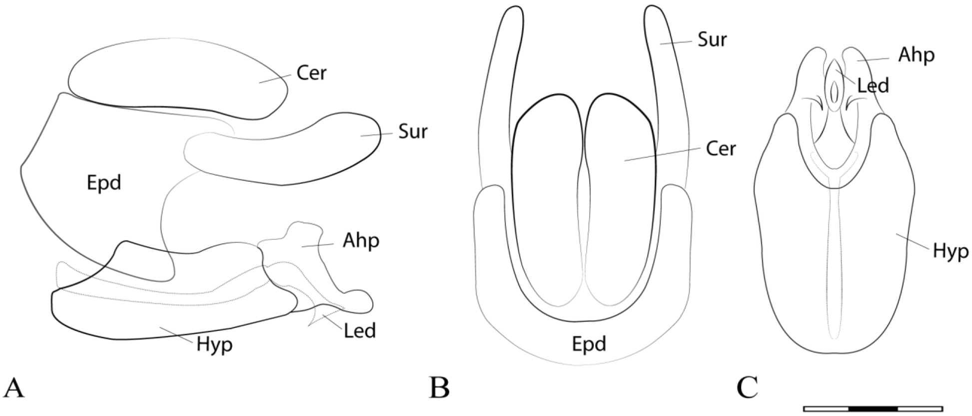

Figure 2. *Argentinomyia andina* sp. nov., male genitalia: **A** whole genitalia including epandrium, cercus, and surstylus, lateral view **B** epandrium, dorsal view **C** hypandrium, ventral view. Abbreviations used in male genitalia structures are as follows: **Ahp** = apex of hypandrium (superior lobes; **Cer** = cercus; **Epd** = epandrium; **Hyp** = hypandrium; **Led** = aedeagal lobe; **Sur** = surstyle. Scale bar: 0.05 mm.

Argentinomyia choachi Montoya, sp. nov.

http://zoobank.org/AACD240E-CB96-4DEF-A2A5-BB5AB779EF79
Figure 3, 15

Differential diagnosis. Abdomen with a pair of large quadrangular maculae on the third and fourth tergum, sometimes slightly touching toward the middle. Legs black, metafemur only slightly yellow in the extreme apex. Coxae black. Metacoxa yellowish pilose. *Argentinomyia choachi* sp. nov. is similar in appearance to the female of *Argentinomyia andina* sp. nov. but in *A. andina* sp. nov. the third and fourth tergum have a pair of short rounded basal maculae; metafemur is extensively brown, only slightly orange on apical 1/6; all coxae yellow.

Type locality. Colombia, department of Cundinamarca, Choachí municipality, La Victoria. 4°32.721'N, 73°55.884'E, 2450 m a.s.l.

Description. Female. Head (Fig. 3A, C). Black, covered with white pollinosity, oral tips, ocellar triangle, and a large triangular macula on the front, white pilose, pile on front black, on gena and face white, on ocellar triangle black, on the occiput white except for the dorsal pile, which are black. Antennae brown, orange-red ventrally, oval, longer than wide pedicel and the lower basal corner of basoflagellomere, ratio 1.0:1.3:3.1, arista orange, brown toward the tip. **Thorax** (Fig. 3C). Black cyaneous, the scutum shining, with iridescent to coppery reflections in the notopleura, with two median yellowish pollinose vittae on anterior half. *Wing* (Fig. 3C). Smoky apically, the stigma yellow-brown, membrane microtrichose, except for extensive bare areas on basal half (cells c, sc, r1, dm and bm); tegula black pilose, basicosta yellow pilose, alula bare, calypter whitish tawny, border whitish brown, fringe tawny, plumula yellow, halter white, knob white. *Legs* (Fig. 3C, D). Black, pro and mesofemora yellow on the apical two-thirds; metafemora only slightly yellow in the extreme apex, pro and mesotibia with lateral maculae on posterior medial edge, metatibia extensively brown, only yellow

Figure 3. *Argentinomyia choachi* sp. nov., female (UNAB 5156): **A** head, frontal, female **B** posterior view **C** dorsal view **D** lateral view. Scale bars: 5 mm.

on basal 2/7 and apical 1/7; protarsi black, meso- and metabasitarsus yellow, the pile yellow, black on the metatibia and above on the tarsi; coxa black, metacoxa yellowish pilose. **Abdomen** (Fig. 3B). Elongate, black, with two pairs of lateral yellow pale maculae, first tergum shining black, second with broad lateral yellow maculae and only the apex black, third with rounded lateral maculae. Pile yellow-white on the maculae and only a few black down the middle and on the apical terga. Sterna black, black pilose.

Male. Unknown.

Length (*N* = 1). Body, 11.5–12.3 mm, wing, 10.2–10.4 mm.

Etymology. The specific epithet "*choachi*" is a noun in apposition and refers to the name of the town where the type specimen was collected. *Coachí* is a Muiscas word derived from "*Ch-igua-chía*", which means the window where the moon peeked, received the poetic name of "Window of the moon" (according to Miguel Triana). The Muiscas were indigenous people who inhabit the "Altiplano Cundiboyacense" formed by high plains on the eastern Cordillera in Colombian Andes between the departments of Cundinamarca and Boyacá, where the species was collected.

Distribution. *Argentinomyia choachi* sp. nov. (*N* = 1) is present on the western slope of Oriental Cordillera in Colombia (Cundinamarca) at 2240 m. a.s.l., inhabiting cloud forest in the provinces of North Andean Páramo (Fig. 15).

Type material. Holotype. COLOMBIA ♀, Cundinamarca, Choachí, La Victoria. Original label: "Colombia, Cundinamarca, Choachí, Vereda La Victoria / 4°32.721'N, 73°55.884'E, 2450 m a.s.l., Net / 18.iv.2011, Leg. J. Pérez (UNAB 5156)". "HOLOTYPE / *Argentinomyia choachi* / Montoya 2020" [red, handwritten except first line]". The holotype is in good condition and deposited at the UNAB.

Comments. Only type specimen is known.

Argentinomyia huitepecensis Montoya, sp. nov.

http://zoobank.org/0C676DC1-EE48-49D1-A770-A0778E4FAD40
Figures 4, 5, 16

Differential diagnosis. Second tergum with a broad macula reaching apical 1/2. Third tergum with a short rounded basal fascia. Metacoxa black pilose. *Argentinomyia huitepecensis* sp. nov. is similar to *A. puntarena* sp. nov., but differs from it by having the antenna oval, longer than wide, orange ventrally; alula and costal cell bare; pro- and mesofemur yellow; metafemur orange on basal 1/5 and apical 3/5; pro, meso- and metabasitarsomere I–II yellow. *Argentinomyia huitepecensis* sp. nov. is also similar to *A. talamanca* sp. nov. a species with the antenna brown; alula and costal cell extensively microtrichose; femur extensively brown; the second tergum with a pair of small maculae on basal 1/5 (see 'diagnostic features' under each species or key).

Type locality. México, department of Chiapas, San Cristóbal municipality, L.C. Huitepec 16°41.252'N, 92°35.979'E, 2520 m a.s.l.

Description. Male. Head (Fig. 4A, C). Black, covered with white pollinosity, oral tips, ocellar triangle, and a large triangular macula on the front, brown pilose, pile on front black, on gena and face white pilose, on ocellar triangle black pilose, on the occiput white except the dorsal pile, which are black, frontal triangle golden metallic. Antennae brown, orange-red ventrally, oval, longer than wide pedicel and the lower basal corner of basoflagellomere, long, ratio 1.0:1.2:3.0, arista orange, dark brown toward the tip. **Thorax** (Fig. 4C). Black, the scutum opaque, shining, with iridescent to opaque reflections, with two median brownish pollinose vittae on anterior half. *Wing* (Fig. 4C). Slightly smoky, the stigma brown, membrane microtrichose, except for extensive bare areas on basal half (cells, c, sc, r1, dm and bm); tegula black pilose, basicosta yellow pilose, alula bare, calypter whitish, border whitish, fringe yellow, plumula yellow, halter yellow, knob white. *Legs* (Fig. 4C). Yellow, pro- and mesofemur yellow; metafemur orange on basal 1/5 and apical 3/5; pro- and mesotibia orange with a brown macula on posterior medial edge, metatibia extensively brown, only orange brownish on basal 2/3; metacoxa black pilose; pro, meso- and metabasitarsomere I-II yellow, the pile yellow, black on the metatibia and above on the tarsi. **Abdomen** (Fig. 4B). Elongate, black, first tergum shining black, second tergum with a pair of broad maculae, reaching apical 1/2, third tergum with a short rounded basomedial fascia. Pile orange on the sides basally, black down the middle and on the apical terga, as well as in the maculae. Male genitalia as Fig. 5.

Female. (Fig. 4D–F). Similar to male except for normal sexual dimorphism. Abdominal maculae on tergum third comparatively shorter than in the male and re-

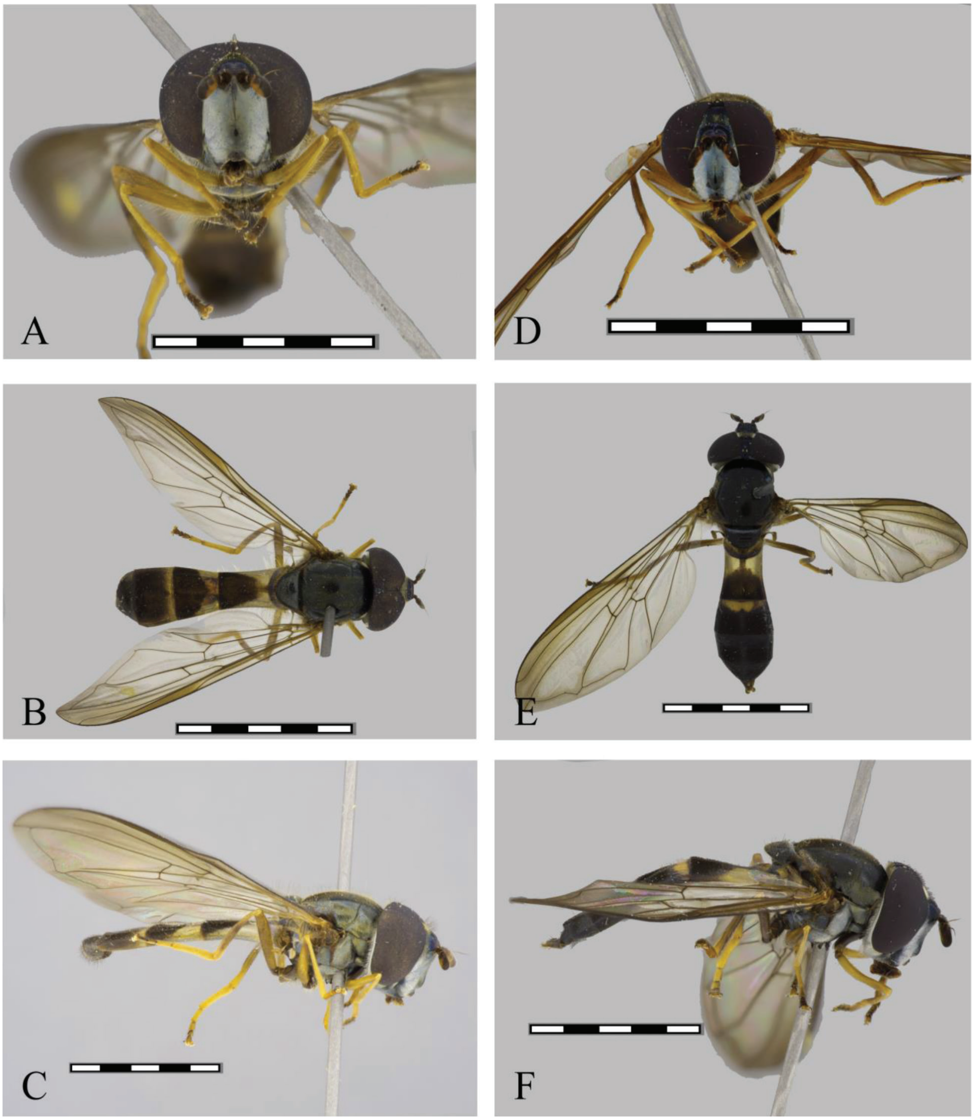

Figure 4. *Argentinomyia huitepecensis* sp. nov., male (ECOSCE 4925): **A** head, frontal, male **B** dorsal view **C** lateral view. Female (ECOSCE 24472): **D** head, frontal view **E** dorsal view **F** lateral view. Scale bars: 5 mm.

stricted to the center of the tergum, no reaching the lateral margin, maculae on fourth and fifth tergum absent.

Length (*N* = 5). Body 12.5–12.8 mm; wing 11.4–11.7 mm.

Etymology. The specific epithet *huitepecensis* (noun in the genitive case) is derived from the Mixtec (native language spoken in México) word "*Huitztli*" which means: thorns, "*Tépeltque*" means: hill, combined with the Latin suffix -*ensis*, meaning from a place. The name is given in reference to the Huitepec Ecological Reserve where the species was collected.

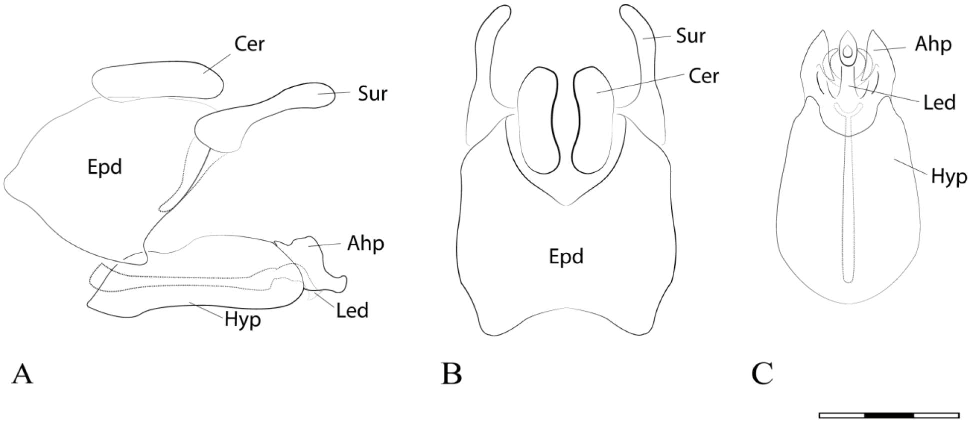

Figure 5. *Argentinomyia huitepecensis* sp. nov., male genitalia: **A** whole genitalia including epandrium, cercus, and surstylus, lateral view **B** epandrium, dorsal view **C** hypandrium, ventral view. Scale bar: 0.05 mm.

Distribution. *Argentinomyia huitepecensis* sp. nov. (*N* = 7) is the northernmost distributed species of the larger *Argentinomyia*, recorded on the western slope of the Chiapas-Guatemalan Highlands, and inhabiting cloud forest at an elevation between 1800 to 2400 m. a.s.l. The species is exclusively known from the province of Chiapas Highlands (Fig. 16).

Type material. Holotype. MÉXICO ♂, Chiapas, San Cristóbal, L.C. Huitepec. Original label: "Mexico, Chiapas, San Cristóbal, L.C. Huitepec / 16°41.252'N, 92°35.979'E, 2520 m a.s.l., 5.x.2010 / wpt 12, P. Sagot, no 6, collect #4301, ECO-SC-E 4925". "HOLOTYPE / *Argentinomyia huitepecensis* / Montoya 2020" [red, handwritten except the first line]". The holotype is in good condition and deposited at the ECO-SC-E, Chiapas, México. "Identified as *Argentinomyia* sp. 16 by P. Sagot". **Paratypes.** MÉXICO • 1 ♂ same data as for holotype (ECO-SC-E) but differs on: 16°41.255'N, 92°35.979'E, 2450 m a.s.l., 20.xi.2009, wpt 30, P. Sagot, no 16, collect #2504 (ECO-SC-E 24471), sp. 16; 1♂, 2450 m a.s.l., 13.i.2010, wpt 25, P. Sagot, no 8, collect #2950. 1♀, 2400 m a.s.l., 20.xi.2009. wpt 30, no 16, collect #2504 (ECO-SC-E 24472); 1♂, 12.x.2010, wpt 13, P. Sagot, no 48, collect #2504 (ECO-SC-E 24471), sp. 16; 1♂, 2560 m a.s.l., 12.x.2010, wpt 13, P. Sagot, no 48, collect #4413 (ECO-SC-E), sp. 16; 1♂, 2310 m a.s.l., 4.i.2011, wpt 34, P. Sagot, collect #4925 (ECO-SC-E), sp. 10; 1♀, 2390 m a.s.l., 31.x.2010, wpt 9, P. Sagot, no 6, collect #4539 (ECO-SC-E) sp. 10.

Argentinomyia puntarena Montoya, sp. nov.

http://zoobank.org/67E5B850-AC47-4027-B412-B1CDDA2785AB
Figures 6, 7, 16

Differential diagnosis. Antenna orange ventrally, oval, longer than wide. Costal cell hyaline, bare basally. Alula bare medially. Pro- and mesofemur yellow. Metafemur or-

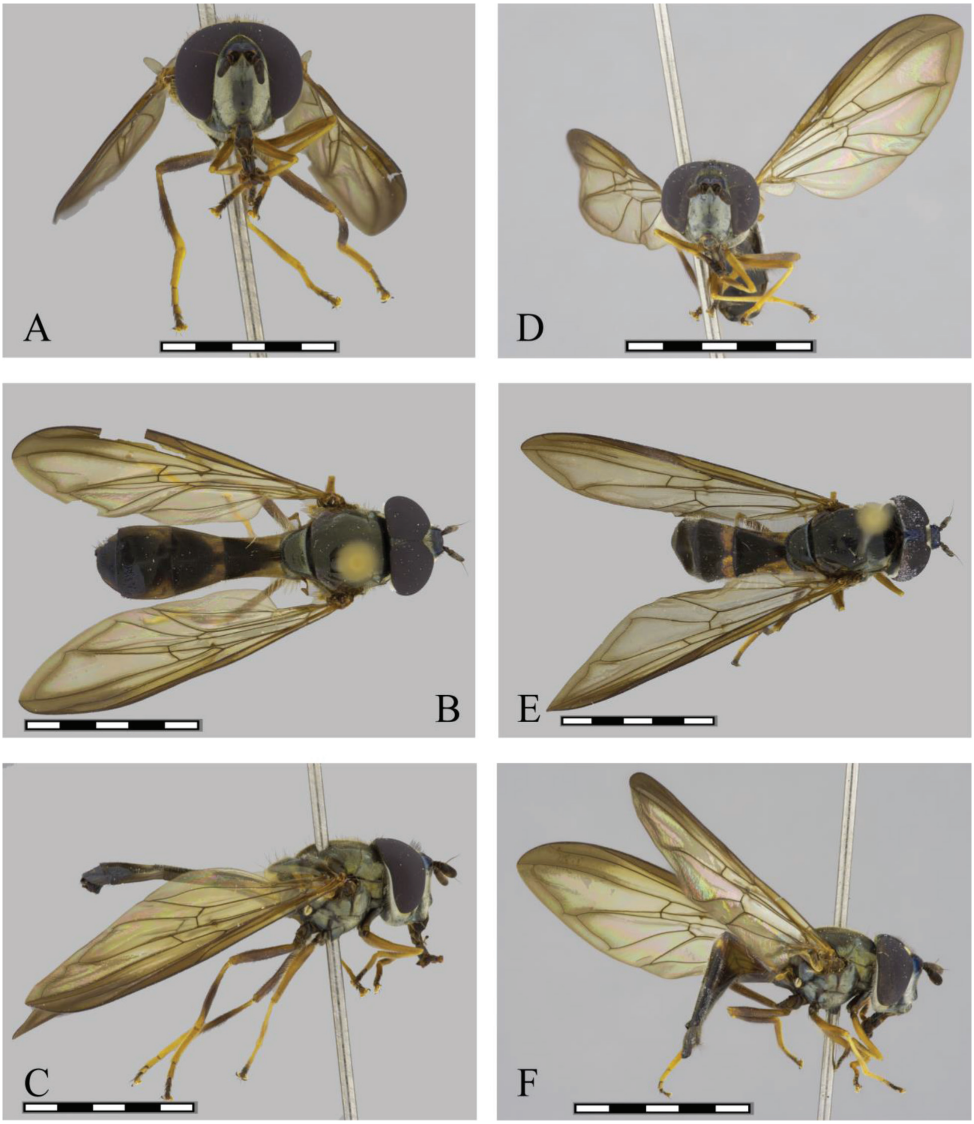

Figure 6. *Argentinomyia puntarena* sp. nov., male (InBio CRI000311623): **A** head, frontal, male **B** dorsal view **C** lateral view. Female (InBio CRI002427774): **D** head, frontal view **E** dorsal view **F** lateral view. Scale bars: 5 mm.

ange on basal 1/5 and apical 3/5. Probasitarsomere, meso- and metabasitarsomere I–II yellow. Second tergum with a broad macula reaching apical 1/3. Third tergum with a broad macula, short in fourth. Sternite fourth to fifth black pilose. *Argentinomyia puntarena* sp. nov. is similar in appearance to *Argentinomyia talamanca* sp. nov., but in *A. talamanca* sp. nov. the antenna is brown; alula and costal cell are extensively microtrichose; femur is extensively brown; the second tergum has a pair of small maculae on basal 1/5 (see 'diagnostic features' under each species or key).

Type locality. Costa Rica, department of Puntarenas, Coto Brus municipality, Sendero entre Estación Tres Colinas y Laguna Seca, 9°1.279'N, 82°, 50.337'E, 2100–2550 m a.s.l.

Description. Male. Head (Fig. 6A, C). Black, covered with white pollinosity, ocellar triangle, and a large triangular macula on the front, brown pilose, pile on front black, on gena and face white pilose, on ocellar triangle black pilose, on the occiput white except for the dorsal pile, which are black, frontal triangle golden metallic. Antennae brown, orange-red ventrally, oval, longer than wide pedicel and the lower basal corner of basoflagellomere, ratio 1.0:1.1:2.9, arista orange, dark brown toward the tip. **Thorax** (Fig. 6C). Black, scutum shining, with iridescent to opaque reflections, with two median brownish pollinose vittae on anterior half. *Wing* (Fig. 6C). Slightly smoky, the stigma brownish, membrane microtrichose, except for extensive bare areas on basal half (cells, sc, r1, dm and bm); costal cell hyaline, bare on basal 1/2; marginal maculae restricted to surrounding areas of veins R1, R4+5 and M1 apically; tegula black pilose, basicosta yellow pilose, alula bare medially, calypter whitish, border whitish, fringe yellow, plumula yellow, halter yellow, knob white. *Legs* (Fig. 6C). Yellow, pro- and mesofemur yellow; metafemur brown, except orange on basal 1/5 and apical 1/5; pro and mesotibia orange, metatibia extensively brown, only orange brownish on basal 2/3; probasitarsomere, meso- and metabasitarsomere I–II yellow, the pile yellow, black on the metatibia and above on the tarsi. **Abdomen** (Fig. 6B). Elongate, black, the first tergum shining black, orange laterally, the second tergum with a broad macula reaching apical 1/3 laterally; third tergum with a broad triangular macula, which is short in the fourth tergum; fourth and fifth sterna black pilose. Pile orange on the sides basally, as well as in the maculae, black down the middle and on the terga apex. Male genitalia as Fig. 7.

Female. (Fig. 6D–F). Similar to male except for normal sexual dimorphism. Frons with pollinose transversal maculae below. Abdominal maculae are comparatively shorter than in the male and indistinguishable in the fourth tergum.

Length (*N* = 4). Body 12.4–12.6 mm; wing 11.3–11.5 mm.

Etymology. The specific epithet *puntarena* is a noun in apposition and refers to the province where the type series was collected.

Distribution. *Argentinomyia puntarena* sp. nov. (*N* = 5) is distributed through the west slope of the Talamanca Cordillera in Costa Rica (Puntarenas, San José) at an elevation between 1000 to 2550 m. a.s.l., in the province of Puntarena-Chiriquí (Fig. 16). *Argentinomyia puntarena* sp. nov. occurs in sympatry with *A. talamanca* sp. nov. in the Puntarena-Chiriquí province.

Type material. Holotype. COSTA RICA ♂, Puntarenas, Coto Brus, Sendero entre Estación Tres Colinas y Laguna Seca. "Original label: "Costa Rica: Puntarenas, Coto Brus, Sendero entre / Estación Tres Colinas y Laguna Seca / 9°1.279'N, 82°50.337'E (L.S. 344300_565800), 2100–2550 m a.s.l. /24.vii.2000, Manual, A. Picado Leg., #59166 (INBio 000311623)". "HOLOTYPE / *Argentinomyia huitepecensis* / Montoya 2020" [red, handwritten except the first line]". The holotype is in good condition and deposited at the INBio museum, in Costa Rica. "identified as *Argentinomyia* sp. 16 by Thompson". **Paratypes.** COSTA RICA • 1 ♂, Puntarenas, Monteverde, San Luis,

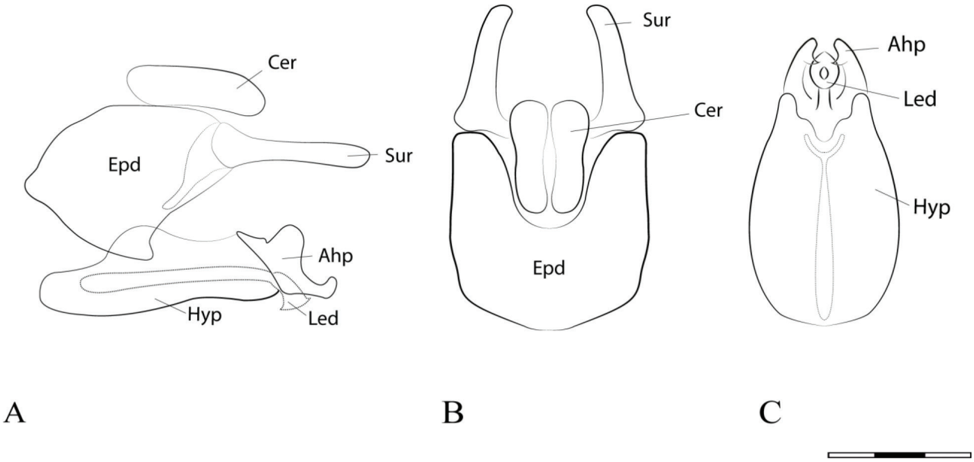

Figure 7. *Argentinomyia puntarena* sp. nov., male genitalia: **A** whole genitalia including epandrium, cercus, and surstylus, lateral view **B** epandrium, dorsal view **C** hypandrium, ventral view. Scale bar: 0.05 mm.

10°16.644'N, 84°47.271'E (L.S. 250850_449250), 1000-1350 m a.s.l., 7.iv.1995, Fuentes #4801 (INBio CRI002202643); 1♀, San José, San Gerardo de Dota, Sevegre Lodge near Rio Sevegre, 9°33.000'N, 83°48.000'E (L.S. 387400_482700), 2200 m a.s.l., 18–21.viii.1995, A.L. Norrbom (USNM ENT 00036925); 1♀, same data as for preceding, 2000–2500 m a.s.l., 22.ii.1992, Tachinidae and Syrphidae course (INBio CRI000406820); 1♀, Farm Zacatales, 2100 m a.s.l., 8–10.viii.1995, M.A. Zumbado, #6280 (INBio CRI002427774).

Comments. *Argentinomyia puntarena* sp. nov. and *Argentinomyia talamanca* sp. nov. can be confused or mistakenly identified as *Xanthandrus mexicanus* Curran, 1930 due to the superficial similarity of these species. However, *X. mexicanus* can be distinguished by the presence of the antennal cavity broadly confluent (synapomorphy for *Xanthandrus*); the central portion of epistoma moderately prominent; the face entirely white pollinose and pilose; the pleura black with white pollinosity; metaepisternum with some fine subappressed long pile (distinctive of *Xanthandrus*); the abdomen oval, wide and flat, opaque, with yellow-orange triangular maculae on second to the fourth tergum, and the male genitalia with surstylus elongated, apically widened (Borges and Pamplona 2003:162, figs 33–37).

Argentinomyia quimbaya Montoya & Wolff, sp. nov.

http://zoobank.org/242B50C6-57FD-4B8E-AA43-65337E1A3D7D
Figures 8, 9, 15

Differential diagnosis. Legs extensively yellow. Tegula yellow pilose and the halter entirely yellow. Abdomen with four pairs of lateral broad yellow maculae. *Argentinomyia quimbaya* sp. nov. is similar in appearance to *Argentinomyia andina* sp. nov., but

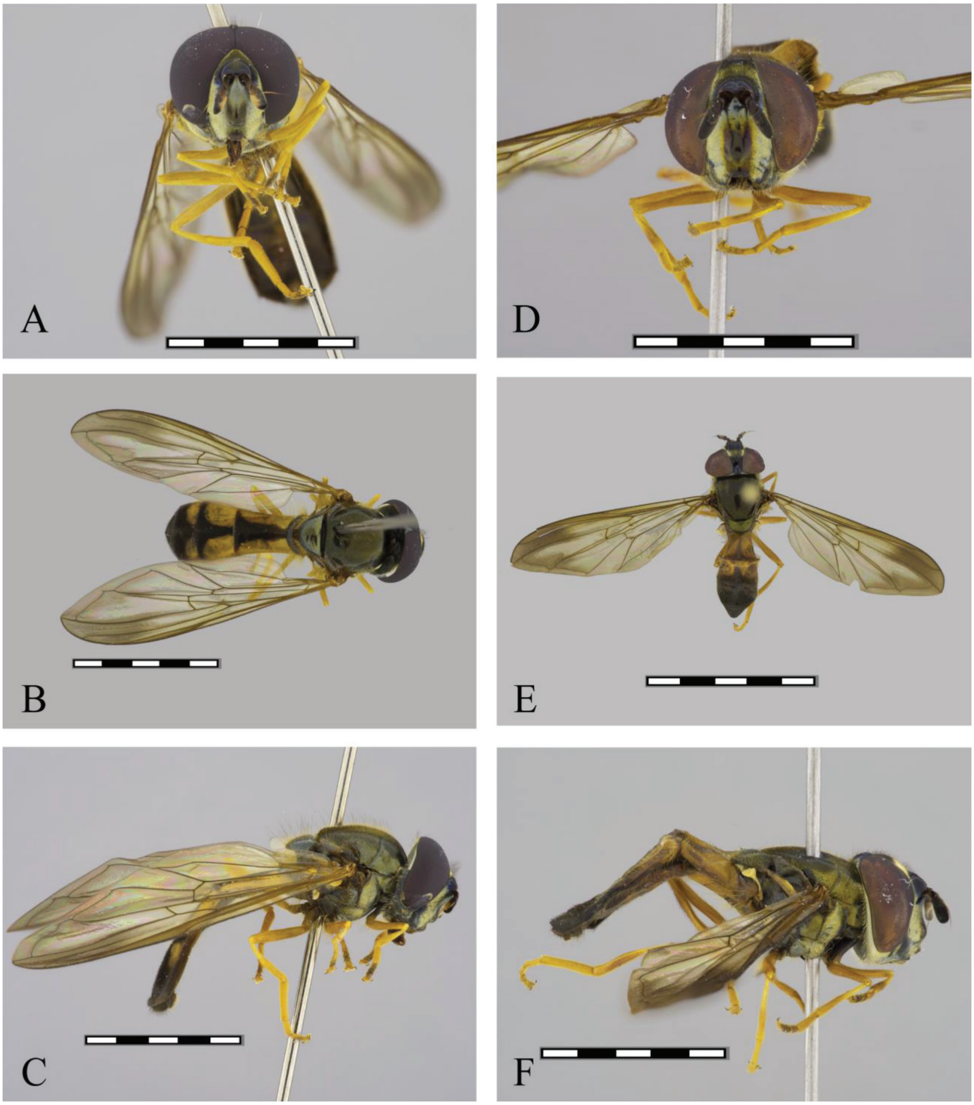

Figure 8. *Argentinomyia quimbaya* sp. nov., male (USMN ENT 000035733): **A** head, frontal, male **B** dorsal view **C** lateral view. Female, Paratype (CEUA 87109): **D** head, frontal view **E** dorsal view **F** lateral view. Scale bars: 5 mm.

in *A. andina* sp. nov. the legs are extensively brown, metafemur only slightly orange on apical 1/6. Tibiae yellow with a dark ring near the middle. Fifth tergum with a pair of small maculae in the basal corners (see 'diagnostic features' under each species or key).

Type locality. Colombia, department of Caldas, Manizales municipality, Corregimiento Las Palmas, Parque Rio Blanco, 5°5.017'N, 75°25.133'E, 2782 m a.s.l.

Description. Male. Head (Fig. 8A, C). Black, covered with yellowish gray pollinosity, shining black on the prominent round tubercle, oral tips, ocellar triangle, and

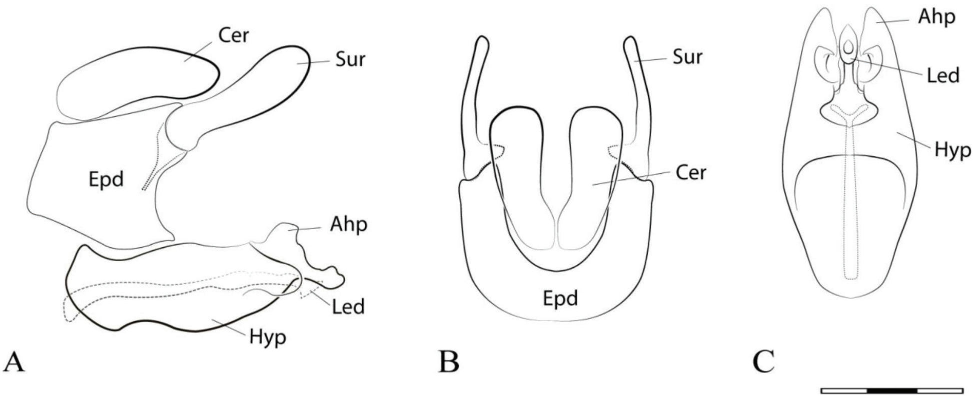

Figure 9. *Argentinomyia quimbaya* sp. nov., male genitalia: **A** whole genitalia including epandrium, cercus, and surstylus, lateral view **B** epandrium, dorsal view **C** hypandrium, ventral view. Scale bar: 0.05 mm.

a large triangular macula on the front; pile on front black, on gena and face yellow, on ocellar triangle black, on the occiput yellow except the dorsal pile, which are black. Antennae brown, orange-red ventrally, oval, longer than wide pedicel and the lower basal corner of basoflagellomere, long, ratio 1.0:1.2:3.1, arista orange, dark brown toward the tip. **Thorax** (Fig. 8C). Black, the scutum shining, covered with coppery pollen and short golden pile with many long black hairs that appear yellowish at the base; these hairs become longer posteriorly and longer on the scutellum, fringe of scutellum yellow; pleura yellow pollinose and pilose. *Wing* (Fig. 8C). Smoky; the stigma brown yellowish; membrane microtrichose, except for extensive bare areas on basal half (cells c, sc, r1, dm, and bm); tegula yellow pilose, basicosta yellow pilose, alula extensively bare, calypter and plumule yellow; halter entirely yellow. *Legs* (Fig. 8B). Yellow, protarsi 1 yellow, 2–4 brown, 5 yellow, mesotarsi 1–2 yellow, 3–4 black, 5 yellow, metatarsi yellow. **Abdomen** (Fig. 8B). Elongate, black, with four pairs of lateral yellow maculae; first tergum shining, laterally yellow, second tergum with the broad lateral yellow maculae reaching the segment apex, third tergum with wide rectangular lateral maculae, which are apically rounded and reach the apical 6/7 of the segment, fourth tergum with still wider but less elongate maculae, reaching only ½ of the segment length. Pile yellow on the sides basally, black down the middle and on the apical terga. Male genitalia as Fig. 9.

Female. (Fig. 8D–F). Similar to male except for normal sexual dimorphism. Abdominal maculae are comparatively wider than in the male. Front narrow above, not the much wider than the ocellar triangle, shining above with pollinose transversal maculae below; legs extensively yellow.

Length (*N* = 2). Body 11.8–12.3 mm; wing 11.5–11.9 mm.

Etymology. The specific epithet *quimbaya* (noun in the genitive case) refers to the indigenous people who inhabit the Central Cordillera of the Colombian Andes in pre-Colombian times, between the departments of Caldas and Risaralda. The name also refers to the Flora and Fauna Sanctuary (SFF, acronym in Spanish) Otún Quimbaya, where part of the type series was collected.

Distribution. *Argentinomyia quimbaya* sp. nov. (*N* = 2) is distributed on the western slope of the Central Cordillera of Colombia (in two very neighbouring Andean states, Caldas and Risaralda) at an elevation between 2700 to 2782 m. a.s.l. in the provinces of Cauca (Fig. 15).

Type material. Holotype. COLOMBIA ♂, Colombia, Caldas, Manizales, Corregimiento Las Palmas, Parque Rio Blanco. Original label: "Colombia, Caldas, Manizales, Corregimiento Las Palmas / Parque Rio Blanco, 5°5.017'N, 75°25.133'E, 2782 m a.s.l. / Net, 18.ii.2006, Leg. B.J. and F.C. Thompson (USMN ENT 000035733)". "HOLOTYPE / *Argentinomyia quimbaya* / Montoya & Wolff 2019 [red, handwritten except first line]". The holotype is in good condition and deposited at the USMN in Washington D.C., USA. **Paratype.** COLOMBIA • 1 ♀, Risaralda, Otún Quimbaya, Peña Bonita, El Jordán 4°44.617'N, 75°31.494'E, 2640–2800 m a.s.l., Van Sommeren-Rydon- Chicken entrails, 13–14.iv.2011, N. Uribe (CEUA 87109).

Argentinomyia talamanca Thompson, sp. nov.

http://zoobank.org/68AFF494-F5E9-4A1F-8C0D-54E523778B2B

Figure 10, 11, 16

Differential diagnosis. Antenna brown, rounded, as long as wide; face opaque, white pollinose and pilose. Wing, alula and, costa cell extensively microtrichose, except for extensive bare areas on basal half (cells, sc, r1, dm, and bm); costal cell brownish, calypter and border whitish, fringe plumula and, halter yellow, knob white. Femora and tarsi extensively brown. Abdomen, second tergum with a pair of small narrow maculae reaching basal 1/5; third and fourth tergum with basomedial maculae, reaching 2/5 and 1/5, respectively; fifth sternite black pilose. *Argentinomyia talamanca* sp. nov. is similar in appearance to *Argentinomyia puntarena* sp. nov., but in *A. puntarena* sp. nov. the antenna is orange ventrally, oval, longer than broad; costal cell hyaline, bare basally; alula bare medially; pro- and mesofemur yellow; metafemur orange on basal 1/5 and apical 3/5; pro-, meso- and metabasitarsomere I–II yellow; second tergum with a broad maculae reaching the apical 1/3; third tergum with a broad macula, short in the fourth; sternite fourth to fifth black pilose (see 'diagnostic features' under each species or key).

Type locality. Costa Rica, department of Cartago, Rio Macho muncipality, Estación Ojo de Agua, 9°36'2.23"N, 83°45'43.31"E, 3000 m a.s.l.

Description. Male. Head (Fig. 10A, C). Black, covered with white pollinosity, oral tips, ocellar triangle, and a large triangular macula on the front, brown pilose, pile on front black, on gena and face white pilose, on ocellar triangle black pilose, on the occiput white except the dorsal pile, which are black, frontal triangle golden metallic; face with a carina above the tubercle. Antennae brown, rounded, as long as wide, ratio 1.1:1.2:2; arista orange, dark brown toward the tip. **Thorax** (Fig. 10B, C). Black, the scutum shining, with iridescent to opaque reflections, with two median brownish pollinose vittae on anterior half. **Wing** (Fig. 10D). Slightly smoky, the stigma brown, membrane extensively microtrichose, except for extensive bare areas on basal half (cells,

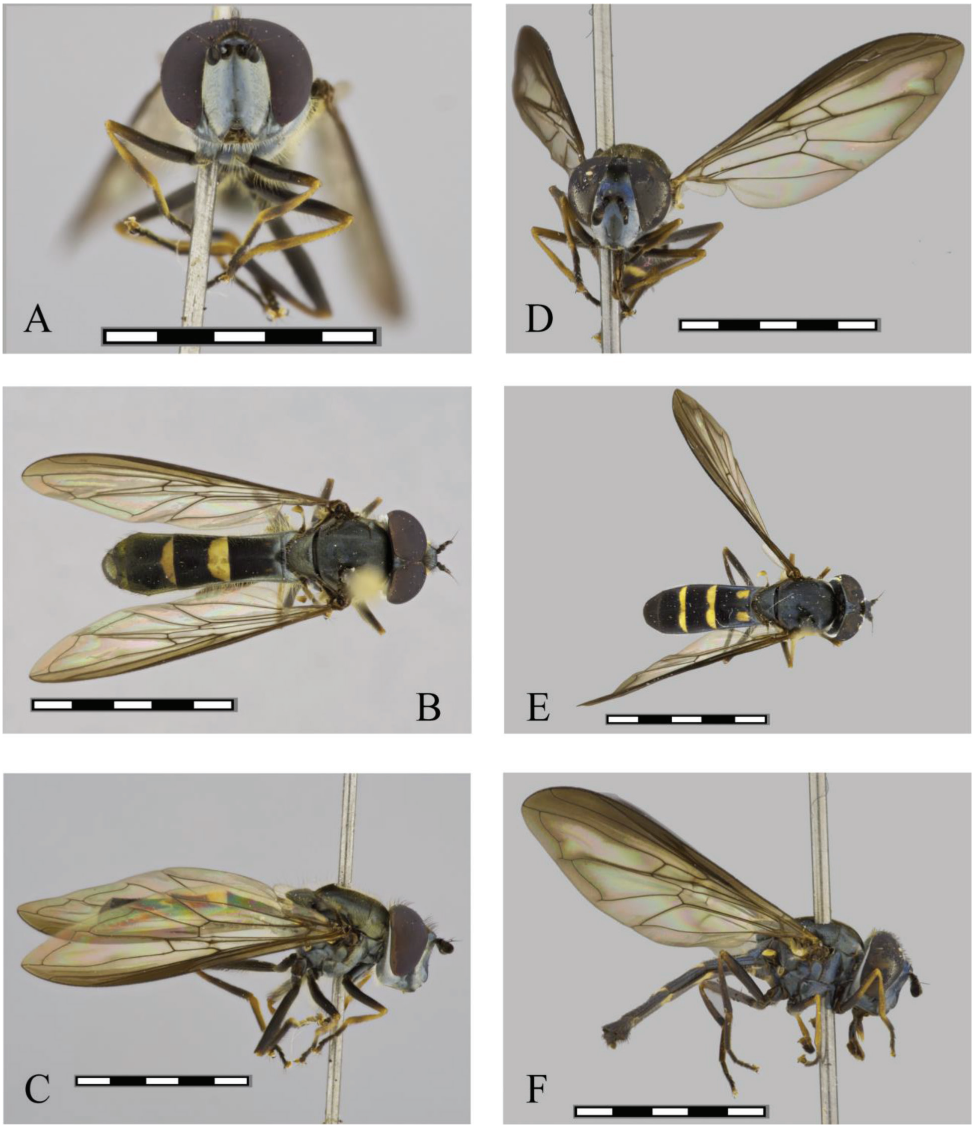

Figure 10. *Argentinomyia talamanca* sp. nov., male (USNM ENT 00036926): **A** head, frontal, male **B** dorsal view **C** lateral view. Female (INBio CRI002462383): **D** head, frontal view **E** dorsal view **F** lateral view. Scale bars: 5 mm.

sc, r1, dm, and bm); costal cell brownish, extensively microtrichose; tegula black pilose, basicosta yellow pilose, alula extensively microtrichose; calypter whitish, border whitish, fringe yellow, plumula yellow, halter yellow, knob white. **Legs** (Fig. 10C). Dark brown, pro- and mesofemur brown, orange on apical 1/8; metafemur extensively brown; pro and mesotibiae orange with a brown macula on posterior medial edge, metatibia extensively brown, only orange brownish on basal 2/3; tarsi brown, only meso-basitarsi orange basally, the pile yellow, black on the metatibia and above on the tarsi. **Abdomen** (Fig. 10B). Elongate, black, first tergum shining black, second with a pair of small narrow maculae, occupying 2/5 of segment length, third and fourth with basomedial maculae, reaching 2/5 and 1/5, respectively. Pile orange on the sides basally, black down the middle and on the apical terga, as well as in the maculae; sternite IV black pilose. Male genitalia as Fig. 11.

Female. (Fig. 10D–F). As male, except for usual sexual dimorphism and following differences: frons with a pollinose transversal macula below. Abdomen with a pair of square-like and apically rounded maculae on the second tergum, which occupies the anterior half of the tergum and comparatively larger than in the male. Profemur extensively yellow on anterior half. Female of *Argentinomyia talamanca* is similar in appearance to *Argentinomyia puntarena* sp. nov. but in *A. puntarena* the antenna is orange ventrally; alula and costal cell bare; pro, meso- and metabasitarsomere I–II yellow; second tergum with a lateral macula reaching the 5/6 of tergum length.

Length (*N* = 4). Body 10.5–11.4 mm; wing 9.2–9.8 mm.

Etymology. The noun in apposition '*Talamanca*' refers to the cordillera where the species was collected in Costa Rica.

Distribution. *Argentinomyia talamanca* sp. nov. (*N* = 21) is distributed through the Talamanca Cordillera in Costa Rica (Cartago, Limón, Puntarenas, San José) at an elevation between 2400 to 3600 m. a.s.l. in the province of Puntarena-Chiriquí (Fig. 16).

Type material. Holotype. COSTA RICA ♂, Cartago, Rio Macho, Estación Ojo de Agua. Original label: "Costa Rica, Cartago, Rio Macho, Estación Ojo de Agua, 9°36'2.23"N, 83°45'43.31"E, (L.S. 396700_482200), 3000 m a.s.l., 25.vii.1999, A. Pinto Leg., #62964 (INBio 003321800)". "HOLOTYPE / *Argentinomyia talamanca* / Thompson 2020" [red, handwritten except first line]". The holotype is in good condition and deposited at the INBio museum, in Costa Rica. "Identified as *Xanthandrus* 75-10 by Thompson 1971". **Paratypes.** COSTA RICA• 1♂, Cartago, Rio Macho, Estación Ojo de Agua, A orillas de la carretera Interamericana, 9°36'2.23"N, 83°45'43.31"E, (L.S. 396700_482200), 3000 m a.s.l., 25.vi.1999, A. Pinto. Libre, #46825 (INBio 0003321799); same data except: 1♂, 26.vi.1997, B. Gamboa #62964, (INBio 0002566220); 1♀, #46825 (INBio 0002566223); 1♀, 9°35'5.48"N, 83°44'14.01"E, 2850 m a.s.l., 11.xii.1997, E. Alfaro, #48829 (INBio CRI002525323); 1♀, Sendero a Torre 47, 9°35'44.84"N, 83°44'37.94"E, 2960 m a.s.l., 26.iii.1997, A. Picado, #45541 (INBio CRI002537729); 1♂, Sendero a Torre 46, 2760 m a.s.l., 9°33'4.23"N, 83°43'45.13"E, 12.iv.1997, B. Gamboa, #46759 (INBio CRI002565331); 1♂, Cartago, Estación Cuericí, El mirador, 4km al E. Villa Mills, Subparamo, 9°31'6.97"N, 83°33'12.55"E, 2900 m a.s.l., 7.xii.1996, A. Picado, #45170 (Collector # 489, 900-093) (INBio CRI002462385); , 1♀, #45170 (INBio CRI002462383); 1♀, sendero Cerro Cuericí, Limite P.N. Chiripo, 9°31'24.05"N, 83°30'15.03"E (L.S. 396700_482200), 3050 m a.s.l., 5.i.1996, A. Picado, #6799 (INBio CRI002367564); 1♂, camino la Auxiliadora, 3.5km E de Villa Mills, 9°32'47.29"N, 83°42'31.97"E, 2700 m a.s.l., 8.vii.1996, A. Picado, #7721 (INBio CRI002467120); 1♂, Cartago, Cerro Urán, 9°30'5.70"N, 83°30'56.31"E, 3600 m a.s.l., 1.v.1997, A. Picado, #46214 (INBio CRI002504307); 1♂, Limón, La Amistad, Bratsi, Cerrito en Fila Dudu-Apri, 9°16'12.31"N, 83°2'53.69"E (L.S. 356400_566000), 3100 m a.s.l., 23.vi.2000, Manual, A. Picado, #59164 (INBio 000311588); 1♂, sendero Circular, 9°17'44.79"N,

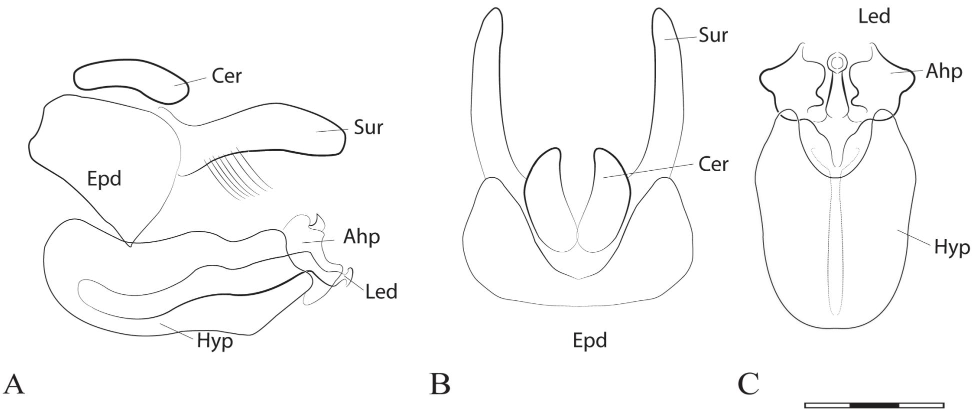

Figure 11. *Argentinomyia talamanca* sp. nov., male genitalia: **A** whole genitalia including epandrium, cercus, and surstylus, lateral view **B** epandrium, dorsal view **C** hypandrium, ventral view. Scale bar: 0.05 mm.

83°2'35.59"E (L.S. 340258_577465), 2406 m a.s.l., 20.vi-5.vii.2003, Libre, D. Rubi, #74159 (INBio 0003724228); 1♂, #74159 (INBio 0003724233). Puntarenas, 5 km, S. Rincón, 15.iii.1973, E.W. Barrows (1♀); 1♀, San José, Barva, i.1997, FCT group (USNM ENT 00036927); 1♂, San José, Estación Cerro de la Muerte, Km 92, Carretera Interamericana, 9°34'22.79"N, 83°44'45.87"E (L.S. 390300_491700 #57449), 3140 m a.s.l., 24.iii.2000, M.A. Zumbado (INBio 0003168749); 1♂, San José, Cerro de la Muerte, 6 km, W. Villa Mills, Inter-Am. Hwy., 9°34'30.93"N, 83°37'47.69"E, 3340 m a.s.l., on flower of Compositae, 2.v.1972, E. R. Heithaus (Collector # 489, 900-093) (INBio 15810, dissected); on flower of Rosaceae, 25.viii.1971, E. R. Heithaus (Collector # 830) (1♀, INBio 4788, identified as *Xanthandrus* 75-10 Thompson); 1♂, San José, Los Santos, Camino a Providencia de Dota, 9°37'0.44"N, 83°50'19.14"E, 2900 m a.s.l., 18.i.1997, M. Segura, #45294 (INBio CRI002535232); 1♂, San José, PamAn Hwy, Km 89, Cerro de la Muerte, Las Torres, 9°34'N, 83°45'E, 3367 m a.s.l., 18-19.viii.1995, A.L. Norrbom (USNM ENT 00036926).

Comments. *Argentinomyia talamanca* sp. nov. is only known from the Talamanca Cordillera in Costa Rica.

Genus *Talahua* Fluke

Talahua Fluke, 1945: 22. Type species, *Melanostoma fervidum* Fluke, 1945 by original designation. Described as subgenus of *Melanostoma*.

Referens. Fluke 1945: 23 (description, key), figs 34 (head), 35 (male genitalia), 53 (abdomen), Fluke 1957: 279, fig. 123 (male genitalia), Thompson et al. 1976: 45 (cat.), Thompson 1999: 325–338 (key and taxonomic notes), Montoya et al. 2012 (distributional records), Huo 2014 (diagnosis), Thompson and Skevington 2014 (key and review of melanostomine genera groups), Montoya 2016: 463 (cat.), Marín-Armijos et al. 2017: 184 (distributional records).

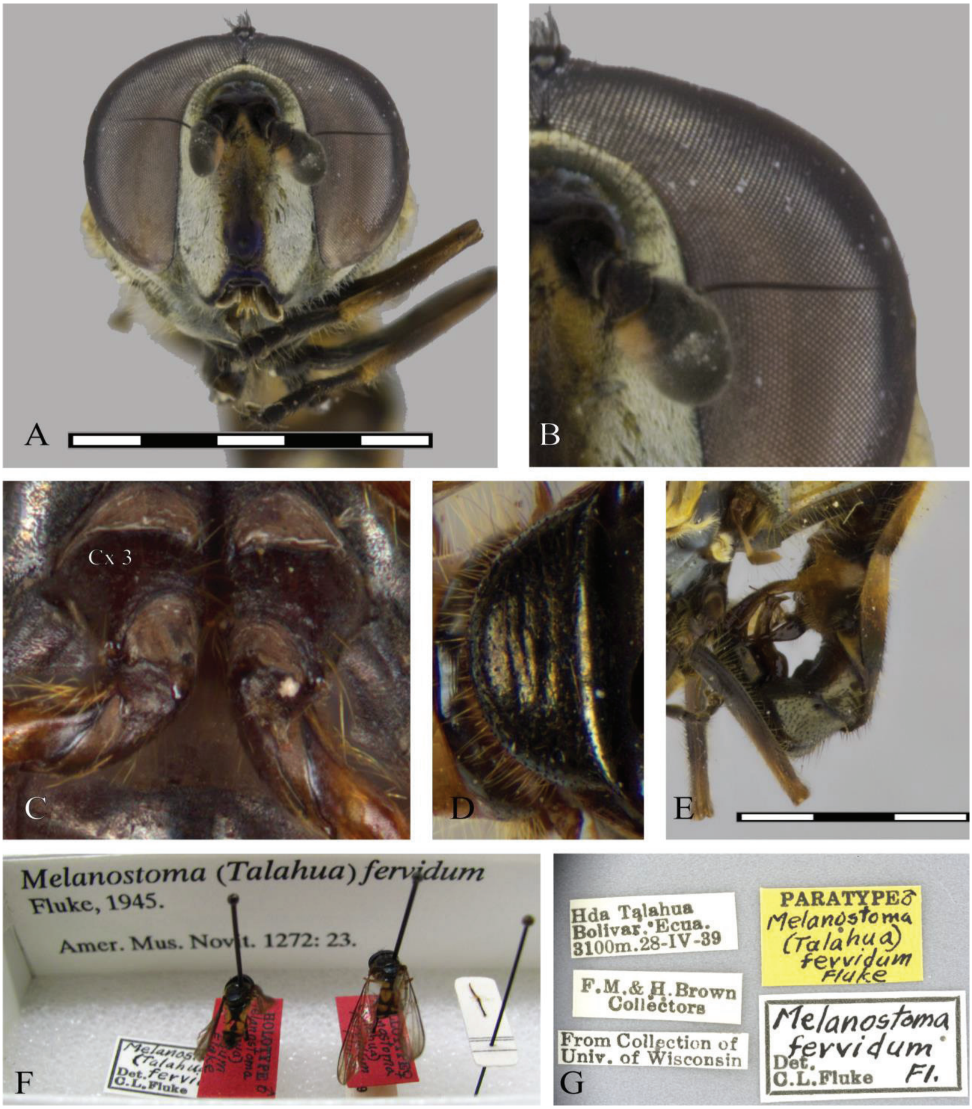

Figure 12. Genus *Talahua* Fluke: **A** head, frontal, male **B** basoflagellomere, frontal view **C** metacoxa pile tuft, ventral view **D** scutellum emarginated, dorsal view **E** male genitalia, lateral view **F** holotype, AMNH **G** paratype label, USNM. Scale bars: 5 mm.

Talahua fervida Fluke, 1945

Figures 12, 13, 14, 17

Melanostoma fervidum: Fluke (1945: 22).

Talahua fervidum: Fluke (1957: 262).

Talahua fervida: Thompson et al. 1976: 45 (catalog citation); Thompson 1999: 338 (catalog and taxonomic notes); Mengual et al. 2008: 545 (taxonomic list); Montoya 2016: 462 (catalog citation); Marín-Armijos et al. 2017: 184 (catalog citation).

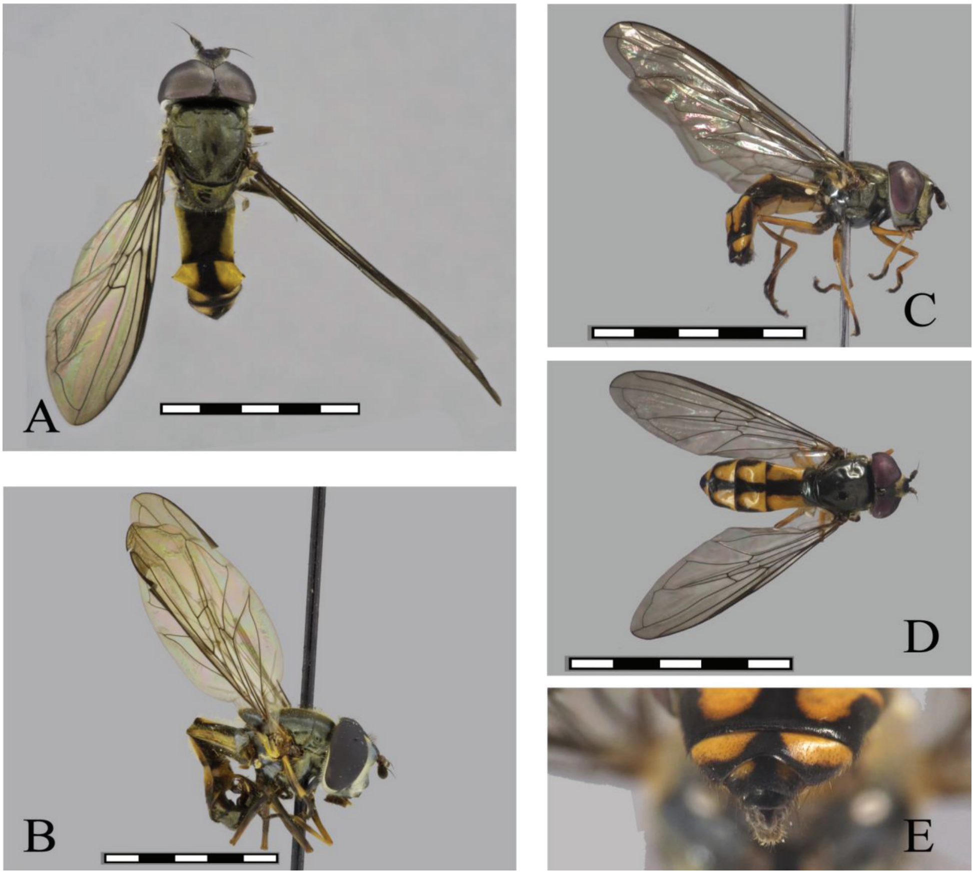

Figure 13. *Talahua fervida*, male (CEUA 95345): **A** dorsal view, male **B** lateral view (Paratype USNM). Female (CEUA 93328): **C** lateral view **D** dorsal view **E** posterior view, detail of maculae on sixth tergum. Scale bars: 5 mm.

Type specimen of *Talahua fervida* Fluke 1945. Holotype. ♂, ECUADOR, Bolívar, Hda. Talahua. Original label: “ECUADOR, Bolivar, Hda. [Hacienda] Talahua, 3100 m a.s.l., 28.iv.1939, F.M. Brown & H. Brown collectors, AMNH”. / *Melanostoma* / (*Talahua*) / *fervidum* / Fluke” [red, handwritten except first line]”. The holotype is deposited at the AMNH in New York, USA. **Paratype** 3 ♂, same information as holotype, deposited in the AMNH, USNM, and WIRC (http://research.amnh.org/iz/types_db/details.php?specimen_id=2724, http://syrphidae.myspecies.info/taxonomy/term/140).

Genus differential diagnosis (modified from Fluke 1945, Thompson and Skevington 2014). Male dichoptic. Both sexes with face slightly receding to perpendicular with a well-rounded tubercle, facial pollinosity yellowish (broadly punctuate in the *Platycheirus stegnus* species group or *Carposcalis* subgenus as well as some *Argentinomyia* species), never with transversal grooves dorsally along tubercle (present in some *Argentinomyia*); antennal pits distinctly separated (confluent in *Xanthandrus*); basoflagellomere large, slightly oval and apically rounded, scape broader than long, nearly equal to pedicel; metespisternum bare (with several fine subappressed hairs in *Xanthandrus*); katepis-

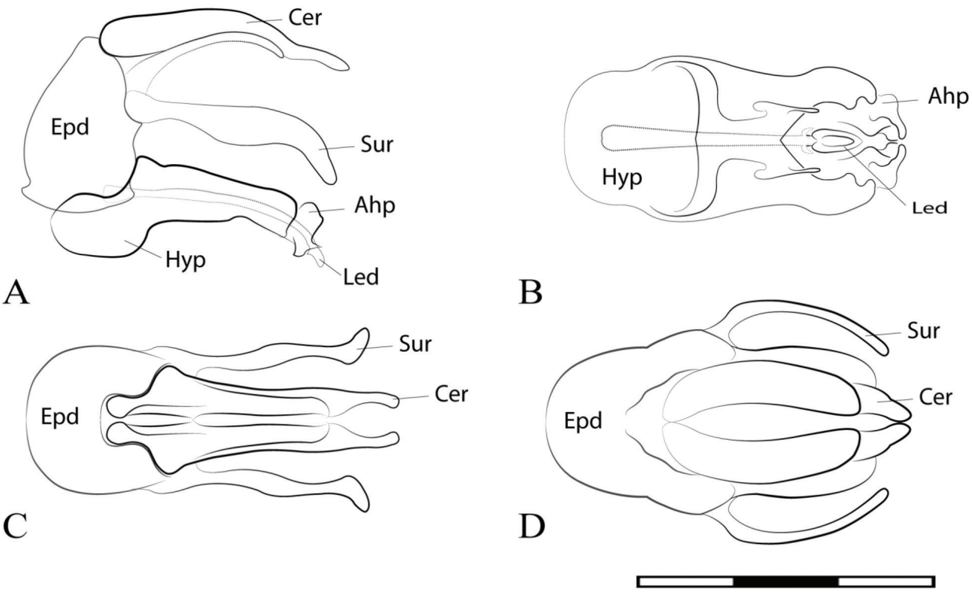

Figure 14. *Talahua fervida*, male genitalia: **A** whole genitalia including epandrium, cercus and surstylus, lateral view **B** hypandrium, dorsal view **C** cerci, and surstyli, ventral view **D** cerci and surstyli, dorsal view. Scale bar: 0.05 mm.

ternal pile patches broadly separated throughout (broadly separated posteriorly, joined anteriorly in *Xanthandrus*); metasternum entire (greatly reduced in *Melanostoma*), bare; mesocoxa pilose posteriorly (bare in *Argentinomyia* and *Melanostoma*); metacoxa with a tuft of pile at posteromedial apical angle (bare in *Argentinomyia*); scutellum with a deep groove next to the rim (present in the new large *Argentinomyia* species described here); wing without maculae along the anterior edge of apical marginal cells; male legs, simple, slender, without bristles, pile tufts or modified hairs (modified, either broadened, or with special bristles, pile tufts or modified hairs as in *Platycheirus* and some *Tuberculanostoma*); tibiae usually yellow with a dark ring near the middle, more prominent on the metalegs; abdomen elongated or with parallel sides, with 4 to 5 pairs of large rounded to triangular maculae; male genitalia large, surstyli elongated, three to four times longer than broad and not forked, black; superior lobes elongate, no sickle-shaped; cerci elongate and yellow, "chitinous box" (= apex of hypandrium= superior lobes) elongated; lingula absent; aedeagus simple, no segmented, without apicomedial teeth.

Redescription (modified from Fluke 1945: 22, and Mengual 2014). **Body size.** Large-sized flies, 9–12 mm. MALE. **Head** (Fig. 13A–C, E). Face large, shining black, wider than the thorax and abdomen, straight to perpendicular, not produced, with a large well-rounded tubercle (low dorsally, not distinct in some *Argentinomyia*), densely pollinose, sides of face usually with coppery reflections and a faint, slightly rugose area; front not swollen; gena large; oral tips, ocellar triangle, and the large triangular macula on the front shining black; pile on front generally black, on gena and face yellow to white, on ocellar triangle black, on the occiput yellow except the dorsal pile black; eyes bare, holoptic in male, with eyes contiguity as long as ocellar triangle; antennae black, pedicel and the lower basal corner of basoflagellomere red, short, scape broader than long, nearly equal to pedicel, basoflagelomere large, rounded or oval, ratio 1.1:1.5:2.5, arista black, dorsobasal, as long as the basoflagellomere or more, bare. **Thorax** (Fig. 13A–F): Black; postpronotum (humerus) bare; notopleuron with distinctive tubercle; scutum shining, covered with yellow pollen and short golden pile with many longer black pile that appear yellowish at the base, these pile become longer posteriorly; pleura yellow pollinose and pilose; scutellum black and with transversal rugose area on the disc, generally with longer yellowish and black setae on the posterior margin; subscutellar fringe complete, with multiple rows yellow pile; postmetacoxal bridge incomplete; pleura black to orange, whitish pollinose and pilose. *Legs* (Fig. 13C). Black; profemora yellow on the apical 1/3, mesofemora yellow on the apical 1/3, metafemora yellow on the apical 1/3; all the tibiae yellow with a dark ring near the middle, more prominent on the metatibia; tarsi brown, the pile yellow, black on the metatibia and above on the tarsi. *Wing* (Fig. 13A–F). Smoky; membrane entirely microtrichose, except for extensive bare areas on basal half (cells c, sc, r_1, dm, and bm); the stigma and costal cell brownish; vein R_{4+5} straight; vein M_1 (apical crossvein) oblique, slightly sinuous; alula broad, broader than cell cup, extensively bare,; calypter yellow, plumule simple, yellow; halter yellow, with a darkened capitulum. **Abdomen** (Fig. 13B–F). Elongated, black, with parallel sides, as broad as or broader than thorax, segments more or less quadrate, as long as broad, without premarginal sulcus, markings on tergites variable, with four pairs of lateral rounded to triangular prominent yellow maculae or with a complete basomedial black maculae; the first tergum shining, second with broad lateral yellow and only the apex black, third tergum with similar but wider maculae, fourth tergum with still wider but less elongate maculae, fifth tergum with a pair of small maculae in the basal corners. Pile yellow on the sides basally, black down the middle and on the apical terga. *Male genitalia* as Figs 12E, 14.

Female. (Fig. 13C–E). Similar to male except for normal sexual dimorphism. Abdominal maculae are comparatively shorter than in the male. Front narrow above, not the much wider than the ocellar triangle, shining above with a pollinose transversal macula below. Sixth tergum with a pair of small basolateral maculae. Sterna extensively yellow, yellow pilose, only brownish pilose in the apical corners of sterna four to sixth.

Distribution. *Talahua fervida* is exclusively restricted to the Tropical Andes of Central and Occidental Cordillera in Colombia (Antioquia, Boyacá, Cundinamarca, Tolima) to Central Cordillera in Ecuador (Bolívar, Sucumbios). The species has a mountainous distribution in the biogeographical provinces of Cauca, Magdalena and North Andean Páramo (Fig. 17).

Additional material examined. COLOMBIA: Antioquia, Bello, San Félix, Las Baldías, 6°20.029'N, 75°39.263'E, 2950–3150 m a.s.l., Net, 22.ii.2015; A. L. Montoya Leg. (1 ♀, CEUA 92108); Belmira, Páramo Santa Inés, Cabaña Cabildo Verde, El Morro-Alto de La Gallina, 6°40.167'N, 75°40.136'E, 3247 m a.s.l., Net in *Clusia* cf. *brachycarpa* Cuatrec., 4–14.ii.2017, A. L. Montoya; J. Sanchez; E. Orozco-G Leg. (1 ♂, CEUA 95345); Medellín, Corregimiento San Sebastián de Palmitas, Vereda La Volca-

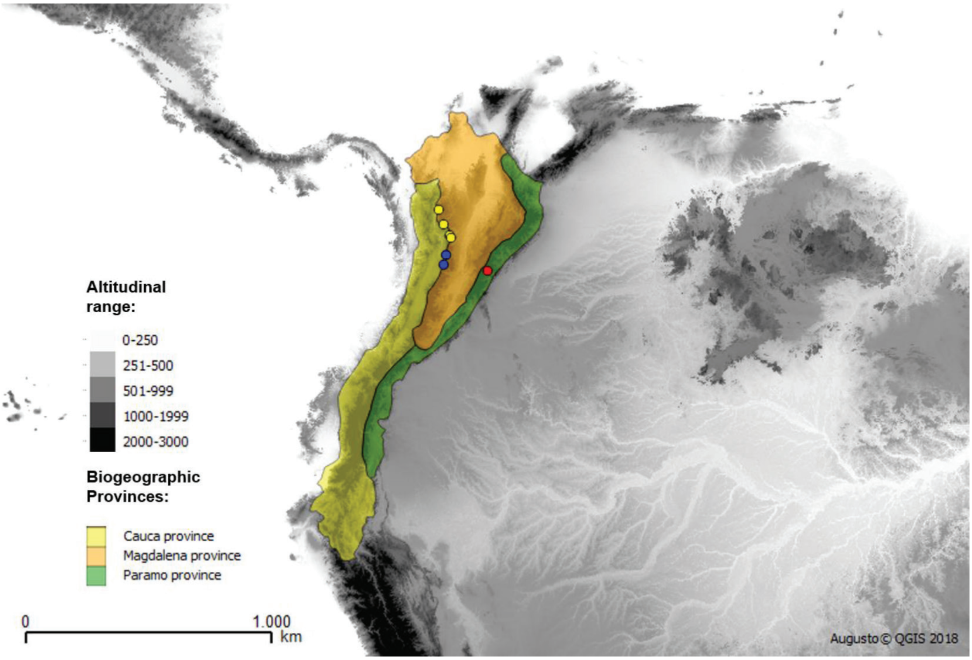

Figure 15. Biogeographical distribution of *Argentinomyia andina* sp. nov. (yellow), *A. quimbaya* sp. nov. (blue) and *A. choachi* sp. nov. (red).

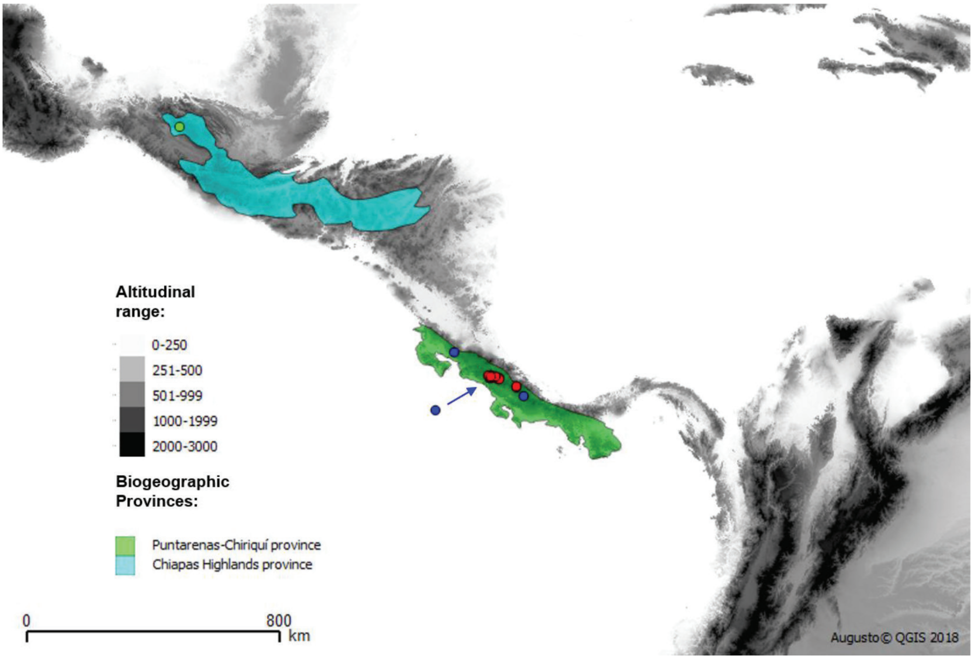

Figure 16. Biogeographical distribution of *Argentinomyia huitepecensis* sp. nov. (green), *A. talamanca* sp. nov. (red) and *A. puntarenas* sp. nov. (blue).

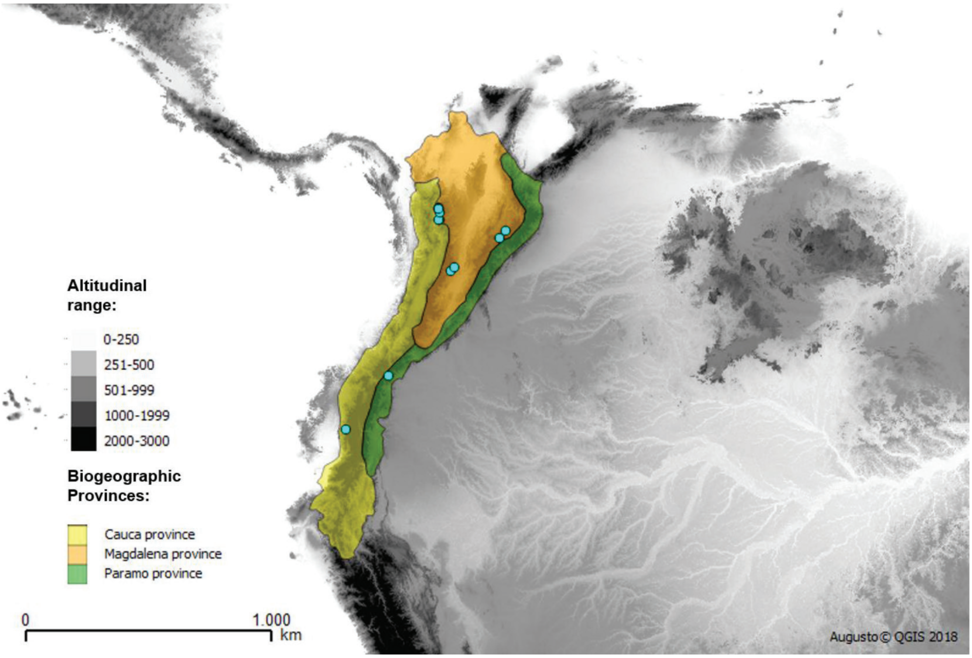

Figure 17. Biogeographical distribution of *Talahua fervida* (light blue).

na, High part, 6°21.232'N, 75°40.883'E, 2569–2650 m a.s.l., Van Sommeren-Rydon trap baited with fish, 22.ix.2011, L. Ríos-M Leg (1 ♀, CEUA 93328); San José de la Montaña, Vereda El Congo, Sector La Laguna, 6°46.013'N, 75°41.979'E, 3100–3183 m a.s.l., Net, 21–30.vi.2017, C. Henao; A. F. Sepúlveda Leg (1 ♀, CEUA 98074); Sonsón, San Francisco, Las Palomas A Mountain hill, 5°43.924'N, 75°15.444'E, 2749 m a.s.l., Forest, Net, 1-12.ix.2018, A.M. Echeverry, J. Vallejo Leg. (1 ♀, CEUA 103636); Boyacá, Flora and Fauna Sanctuary Iguaque, Ravien Carrizal, Cabaña Mamarramos, Lagunillas, 5°41.783'N, 73°26.516'E, 2850–3380 m a.s.l. (IAvH, in Gutiérrez et al. 2006). ECUADOR: Sucumbios, Santa Barbara, 0°37.868'N, 77°31.207'E, 3023 m a.s.l., 14.iii.1994, Gonorre Leg (1 ♂, QCAZ 103712).

Ecology. Adults of *Talahua fervida* are found in highland ecosystems including cloud forests of the Andesand Páramo from 1800 to 3350 m a.s.l. The species has been associated with flowers of *Clusia* cf. *brachycarpa* Cuatrec (Clusiaceae Lindl.), but the immature stages are unknown.

Discussion

The new *Argentinomyia* species described here can be distinguished from its congeners by the combination of the following characters: the basoflagellomere large, slightly oval and apically rounded; face with a well-rounded tubercle, never with transversal grooves dorsally along tubercle or broadly punctuate laterally; scutellum with a deep groove next to the rim (emarginate); metacoxa with pile posteromedial on apical angle; abdomen elongated or parallel sides with large markings. *Talahua fervida* differs from the new species by having the male genitalia large, including the surstyle, superior lobes, and cerci elongated, character recognized by Fluke (1957) and Thompson (1999) as exclusive for *Talahua*.

The new *Argentinomyia* species described here as well as *Talahua fervida* inhabit the Andean cloud forests and Páramo in Mesoamerica (México and Costa Rica) and Tropical Andes (Colombia and Ecuador) including five biogeographical provinces, which have been commonly referred to as hotspots of biodiversity (Maps 1, 2 and 3) (Myers et al. 2000). The distribution patterns suggest the existence of new endemic species in the highlands of neighboring countries.

Their restricted distribution, the local abundance and the fact that most species inhabit Protected and Conserved Areas suggest their vulnerability as proposed for several syrphid groups (see Montoya et al. 2012, Morales et al. 2013). This, besides the fact that many of these areas are facing anthropogenic pressures such as deforestation by mining, and wood extraction, indiscriminate and constant application of herbicides and pesticides, as well as the loss of biological corridors derived from the construction of hydroelectric and roads, highlight the risk for the survival of these species, as well as the maintenance of ecosystem services they provide.

In consequence and given that only one Neotropical species has been assessed in the IUCN Red List (Alaniz et al. 2018, López-García et al. 2019), there are compelling reasons to propose the new species as well as *Talahua fervida* as flagship entities for the conservation of the areas where they occur, been critical as environmental quality bioindicators. We considered that the information provided will constitute a baseline to assess their conservation status following the guidelines of the International Union for Conservation of Nature (IUCN).

Acknowledgments

Thanks are due to F. Christian Thompson (Department of Entomology, National Museum of Natural History, Smithsonian Institution, Washington D.C., USA) for his continuous support to my formation and for allowing me to study the flower flies housed in the USNM collection. I'm very thankful to the collection curators and researchers, in particular to Philippe Sagot for facilitating access to the material to his cure. I sincerely thank Torsten Dikow for all the valuable help during my internship at the Smithsonian Institution. Thank are due to everyone who collects this invaluable material, especially to the members of the Entomology Group, University of Antioquia (GEUA). This study was supported by funding provided by the FONDO NACIONAL DE FINANCIAMIENTO PARA LA CIENCIA LA TECNOLOGÍA Y LA INNOVACIÓN "FRANCISCO JOSÉ DE CALDAS" and COLCIENCIAS (Convocatorias 712–2015, 745–2016) to the project "Las moscas de las flores (Diptera, Syrphidae) como bioindicadoras de la calidad del ambiente en los ecosistemas altoandinos del noroccidente de Colombia" and COLFUTURO Ph.D. Grant (Becas Colciencias Doctorados Nacionales, convocatoria 647 de 2014). The project was partially financed by a grand of the GLOBAL GENOME INITIATIVE, Grant Number: 801-0000-302357-332002-6100-XXXX-4120-33GGI2018GRANTE-BUENAVENTURAE. Thanks are also due to the Samuel Wendell Williston Diptera Research Foundation for financial assistance to attend the 8th International Congress of Dipterology in Potsdam, Germany, where the first advance of this work was presented. Thanks are due to Ximo Mengual and the reviewers Andrew Young and Menno Reemer for helpful comments and suggestions that enriched the manuscript. Thanks to Elizabeth Orozco García for all her support, dedication and for teaching me to fly to achieve my dreams, you are unique. Special thanks to Paula Rozo, who contacted me with Juanita Roca and Álvaro Espinel, who kindly welcomed me at their home during the internship in Washington D.C. and made this experience productive and unforgettable.

References

Alaniz AJ, Carvajal MA, Smith-Ramírez C, Barahona-Segovia RM, Vieli L (2018) Habitat loss of a rainforest specialist pollinator fly as an indicator of conservation status of the South American Temperate Rainforests. Journal of Insect Conservation 22(5–6): 745–755. https://doi.org/10.1007/s10841-018-0098-0

Borges ZM, Pamplona DM (2003) Revision of the Neotropical *Xanthandrus* Verral (Diptera, Syrphidae). Revista Brasileira de Entomologia 47: 155–167. https://doi.org/10.1590/S0085-56262003000200002

Cumming J, Wood DM (2017) Adult morphology and terminology. In: Kirk-Spriggs A, Sinclair B (Eds) Manual of Afrotropical Diptera. 1. South African National Biodiversity Institute, Pretoria, 89–133.

Fluke Jr CL (1943) A new genus and new species of Syrphidae (Diptera) from Ecuador. Annals of the Entomological Society of America 36: 425–431. https://doi.org/10.1093/aesa/36.3.425

Fluke CL (1945) The Melanostomatini of the Neotropical Region (Diptera, Syrphidae). American Museum Novitates 1272: 1–29.

Fluke CL (1957) A study of the male genitalia of the Melanostomatini (Diptera: Syrphidae). Wisconsin Academy of Sciences Arts and Letters 46: 261–279.

Gutiérrez C, Carrejo NS, Ruiz C (2005) Listado de los géneros de Syrphidae (Diptera: Syrphoidea) de Colombia. Biota Colombiana 6: 173–180. https://doi.org/10.21068/bc.v6i2.157

Haarto A, Ståhls G (2014) When mtDNA COI is misleading: congruent signal of ITS2 molecular marker and morphology for North European *Melanostoma* Schiner, 1860 (Diptera, Syrphidae). ZooKeys 431: 93–134. https://doi.org/10.3897/zookeys.431.7207

Henao-Sepúlveda C, Wolff M, Amorin DS (2019) Revision of the Neotropical *Neuratelia* Rondani (Diptera, Mycetophilidae, Sciophilinae): two new species, a new combination, and a new synonym. ZooKeys 861: 63–79. https://doi.org/10.3897/zookeys.861.32835

Huo KK (2014) *Spazigasteroides* a new genus from China with a black face and scutellum in the Syrphini (Diptera: Syrphidae). Zootaxa 3755: 230–40. https://doi.org/10.11646/zootaxa.3755.3.2

López-García G, Barahona-Segovia RM, Maza N, Domínguez MC, Mengual X (2019) Filling gaps in flower fly distributions: first record of *Aneriophora aureorufa* (Philippi, 1865) (Diptera, Syrphidae) from Argentina. Check List 15(3): 349–355. https://doi.org/10.15560/15.3.349

Löwenberg-Neto P (2015) Andean region: a shapefile of Morrone's (2015) biogeographical regionalization. Zootaxa 3985: 600–600. https://doi.org/10.11646/zootaxa.3985.4.9

Marín-Armijos D, Quezada-Ríos N, Soto-Armijos C, Mengual X (2017) Checklist of the flower flies of Ecuador (Diptera, Syrphidae). Zookeys 691: 163–199. https://doi.org/10.3897/zookeys.691.13328

Mengual X, Stahls G, Rojo S (2008) First phylogeny of predatory flower flies (Diptera, Syrphidae, Syrphinae) using mitochondrial COI and nuclear 28S rRNA genes: conflict and congruence with the current tribal classification. Cladistics 23: 1–20. https://doi.org/10.1111/j.1096-0031.2008.00200.x

Mengual X, Stahls G, Rojo S (2015) Phylogenetic relationships and taxonomic ranking of pipizine flower flies (Diptera: Syrphidae) with implications for the evolution of aphidophagy. Cladistics 31: 31: 491–508. https://doi.org/10.1111/cla.12105

Montoya AL (2016) Family Syrphidae. Zootaxa 4122: 457–537. https://doi.org/10.11646/zootaxa.4122.1.39

Montoya AL, Ricarte A, Wolff M (2017) Two new species of *Quichuana* Knab (Diptera: Syrphidae) from the paramo ecosystems in Colombia. Zootaxa 4244: 390–402. https://doi.org/10.11646/zootaxa.4244.3.7

Montoya AL, Pérez SP, Wolff M (2012) The diversity of flower flies (Diptera: Syrphidae) in Colombia and their Neotropical distribution. Neotropical Entomology 41: 46–56. https://doi.org/10.1007/s13744-012-0018-z

Morales MN, Ståhls G, Hippa H (2013) Two new species of *Meropidia* Hippa & Thompson, 1983 (Diptera, Syrphidae) from the Andes Mountains. ZooKey 338: 55–65. https://doi.org/10.3897/zookeys.338.6093

Morrone JJ (2014) Biogeographical regionalisation of the Neotropical region. Zootaxa 3782: 1–110. https://doi.org/10.11646/zootaxa.3782.1.1

Myers N, Mittermeier RA, Mittermeier CG, Fonseca GAB da, Kent J (2000) Biodiversity hotspots for conservation priorities. Nature 403: 853–858. https://doi.org/10.1038/35002501

Pape T, Evenhuis NL (2018) Systema Dipterorum, Version [2.0]. 37 records. https://diptera.dk/ [accessed 15 May 2019]

Reemer M (2010) A second survey of Surinam Syrphidae (Diptera): introduction and Syrphinae. Tijdschrift voor Entomologie 53: 163–196. https://doi.org/10.1163/22119434-900000295

Rojo S, Gilbert F, Marcos-García MA, Nieto JM, Mier PM (2003) A world review of predatory hoverflies (Diptera, Syrphidae: Syrphinae) and their prey. CIBIO Ediciones, Alicante, 319 pp.

Ramage T, Charlat S, Mengual X (2018) Flower flies (Diptera, Syrphidae) of French Polynesia, with the description of two new species. European Journal of Taxonomy 448: 1–37. https://doi.org/10.5852/ejt.2018.448

Thompson FC (1981) The flower flies of the West Indies (Diptera: Syrphidae). Memoirs of the Entomological Society of Washington 9: 1–200.

Thompson FC (1999) A key to the genera of the flower flies of the Neotropical Region including the descriptions of genera and species and a glossary of taxonomic terms. Contributions on Entomology International 3: 319–378.

Thompson FC, Vockeroth JR, Sedman YS, Papavero N (1976) A catalogue of the Diptera of Americas South of the United States: Family Syrphidae, 1–195. https://doi.org/10.5962/bhl.title.49898

Thompson FC, Rotheray GE, Zumbado MA (2010) Syrphidae (Flower flies). In: Brown BV, Borkent A, Cumming JM, Wood DM, Woodley NE, Zumbado MA (Eds) Manual of Central American Diptera, Volume 2. NRC Research Press, Ottawa, 763–792.

Thompson FC, Skevington JH (2014) Afrotropical flower flies (Diptera: Syrphidae). A new genus and species from Kenya, with a review of the melanostomine group of genera. Zootaxa 3847: 97–114. https://doi.org/10.11646/zootaxa.3847.1.5

Vockeroth JR (1990) Revision of the Nearctic species of *Platycheirus* (Diptera, Syrphidae). Canadian Entomologist 122: 659–766. https://doi.org/10.4039/Ent122659-7

Supplementary material 1

Table S1

Authors: Augusto L. Montoya, Marta Wolff

Data type: occurrence

Link: https://doi.org/10.3897/zookeys.929.37666.suppl1

ZooKeys 929: 53–77 (2020)
doi: 10.3897/zookeys.929.50391
https://zookeys.pensoft.net

RESEARCH ARTICLE

A peer-reviewed open-access journal
ZooKeys
Launched to accelerate biodiversity research

Revision of the *Orbamia* Herbulot, 1966 group of genera with description of two new genera, ten new species, and two new subspecies (Lepidoptera, Geometridae, Ennominae, Cassymini)

Tesfu Fekensa Tujuba[1,3], Axel Hausmann[2], Andrea Sciarretta[3]

1 *Ethiopian Biodiversity Institute, Comoros street, Addis Ababa, Ethiopia* **2** *SNSB-Zoologische Staatssammlung München, Münchhausenstr, 21, Munich, Germany* **3** *Department of Agriculture, Environment and Food Sciences, University of Molise, Via Francesco De Sanctis Campobasso, Italy*

Corresponding author: Axel Hausmann (hausmann.a@snsb.de)

Academic editor: E.J. van Nieukerken | Received 22 January 2020 | Accepted 16 March 2020 | Published 22 April 2020

http://zoobank.org/D5E1D8E5-7DF3-4408-93ED-94CDE2C59FEA

Citation: Tujuba TF, Hausmann A, Sciarretta A (2020) Revision of the *Orbamia* Herbulot, 1966 group of genera with description of two new genera, ten new species, and two new subspecies (Lepidoptera, Geometridae, Ennominae, Cassymini). ZooKeys 929: 53–77. https://doi.org/10.3897/zookeys.929.50391

Abstract

The genus *Orbamia* Herbulot, 1966 is revised. Two new genera are described: *Rabomia* Hausmann & Tujuba, **gen. nov.** (type species: *Ectropis*? *subaurata* Warren, 1899), and *Morabia* Hausmann & Tujuba, **gen. nov.** (type species: *Morabia politzari* Hausmann & Tujuba, **sp. nov.**). Ten new species and two new subspecies are described: *Rabomia obscurior* Hausmann & Tujuba, **sp. nov.**, from western Africa, *Morabia politzari* Hausmann & Tujuba, **sp. nov.**, from Kenya, *Morabia brunnea* Hausmann & Tujuba, **sp. nov.**, from Zambia, *Orbamia marginata* Hausmann & Tujuba, **sp. nov.**, from Tanzania, *Orbamia clarissima* Hausmann & Tujuba, **sp. nov.**, from Kenya, *Orbamia clarior* Hausmann & Tujuba, **sp. nov.**, from Kenya, *Orbamia obliqua* Hausmann & Tujuba, **sp. nov.**, from Zambia, *Orbamia obliqua parva* Hausmann & Tujuba, **subsp. nov.**, from South Africa, *Orbamia abiyi* Hausmann & Tujuba, **sp. nov.**, from Zambia, Tanzania, Ethiopia, *Orbamia emanai* Hausmann & Tujuba, **sp. nov.**, from Ethiopia, *Orbamia emanai lenzi* Hausmann & Tujuba, **subsp. nov.**, from Zambia and Malawi, and *Orbamia balensis* Hausmann & Tujuba, **sp. nov.** from Ethiopia. The taxon *Lepiodes ocellata* Warren, 1897 is raised from synonymy of *O. octomaculata* (Wallengren, 1872) to species rank (Zambia, Tanzania, Rwanda). The taxonomical analysis is based on both morphological and genetic cytochrome oxidase I (COI) data. Adults and male and female genitalia of all species are illustrated.

Keywords
Africa, DNA Barcoding, geometrid moths, integrative taxonomy, Lepidoptera, *Morabia*, *Rabomia*, species description

Introduction

After 260 years of intensive work, taxonomists worldwide have together achieved the formal descriptions of approximately 160,000 lepidopteran species (Van Nieukerken et al. 2011), of which some 24,000 are geometrid moths (cf. Scoble 1999; Scoble and Hausmann 2007; Van Nieukerken et al. 2011). Many more are likely to be described and some recent revisions of many genera revealed high percentages of undescribed species (e.g., Brehm 2015, 2018; Hausmann 2003; Hausmann et al. 2016). This probably covers less than half the number of actual extant geometrid species on earth, an estimate which can be inferred from apparently undescribed species in natural history museums and in molecular databases like the Barcode of Life Data Systems (BOLD: Ratnasingham and Hebert 2007). We conclude that conventional taxonomy with an actual description rate of 80–100 species per year works too slowly for addressing the biodiversity of our Earth (taxonomic impediment: de Carvalho et al. 2007; Wheeler 2008). In these times where we are facing a serious extinction rate we cannot afford to wait for another 250–600 years for the taxonomic assessment of our biodiversity. In the recent literature, several pleas for an accelerated taxonomy have been made (Riedel et al. 2013a; Forum Herbulot 2014) and some taxonomists already published exemplary revisions with shortened descriptions (Riedel et al. 2013b; Meierotto et al. 2019).

In this taxonomic revision we follow such a model of accelerated taxonomy (cf. Riedel et al. 2013a, 2013b; Forum Herbulot 2014; Meierotto et al. 2019), which should lead in future to an automated, easy and rapid transfer of genetic data, images and metadata directly from BOLD into manuscripts and which will allow for continuous updates. Similarly, all nomenclatorial information (valid names, synonyms, original descriptions with authorship and year, type localities, type specimens and their deposition) may in future be transferred in an automated way either from BOLD, from the Global Lepidoptera checklist (Banki et al. 2019) and/or from the Geometridae Mundi database once it will be completed by the Forum Herbulot initiative (cf. Löbel and Hausmann 2019). Similar to the approach of Meierotto et al. (2019) we believe that DNA barcodes in most cases are an excellent tool for species diagnosis but that all descriptions should be linked with a brief description of characters in words, supplemented with photographs. In future, such revisions may also be organised in a flexible way, i.e., with the possibility to subsequently publish updated versions (keeping the previous versions visible) with more data, newly added species, and revised taxonomic concepts. In the framework of the ongoing research project "GBOL III - Dark Taxa" (SNSB – Bavarian State Collection of Zoology, Munich) similar workflows are planned to be tested and established.

The genus *Orbamia* Herbulot, 1966 is restricted to the Ethiopian region, where it was so far represented by five species (Scoble 1999; Hausmann 2006): *Orbamia* *octomaculata* (Wallengren 1872), *Orbamia pauperata* Herbulot, 1966, *Orbamia renimacula* (Prout, 1926), *Orbamia subaurata* (Warren, 1899) and *Orbamia becki* Hausmann, 2006. Although the external appearance of *Orbamia* is somewhat reminiscent of that of the tribe Boarmiini, Hausmann (2006) placed *Orbamia* in the tribe Cassymini, due to the long process extending from the base of the dorsal margin of the male genital valvae, similar to the equivalent present in *Zamarada*. Molecular evidence for this tribal assignment was given by Murillo-Ramos et al. (2019) and Brehm et al. (2019). Species of *Orbamia* are recognised by the following characters: wings with conspicuous, contrasting discal spots on all wings, antennae bipectinate in males and filiform in females, dorsal process in male genitalia strongly curved.

Materials and methods

In the present paper, the material housed in the Zoologische Staatssammlung München (**ZSM**), Munich, Germany, collected from 22 different African and Arabian countries, has been studied. Two relevant type specimens available in the ZSM and two from the Natural History Museum in London (**NHMUK**) were examined. Altogether, 298 specimens of the genera *Orbamia*, *Rabomia* gen. nov., and *Morabia* gen. nov. have been examined.

Comparative morphological methods and COI sequence divergences were used to delimit the taxa and to estimate their taxonomic status. We studied morphological characters of adults (including genitalia and wing venation). The abdomens and genitalia were prepared using the method of Hardwick (1950). The analysis is furthermore based on 58 genitalia slides and 72 DNA barcodes.

For DNA analyses, one or two legs were removed from dried specimens and stored in an individual tube, in absolute ethanol. DNA extraction, amplification and sequencing of the “barcode” region of the mitochondrial cytochrome c oxidase I (COI) gene region (658 base pairs) were carried out in the Canadian Centre for DNA Barcoding, Ontario, Canada, using standard high through-put protocols (Ivanova et al. 2006). Sequence divergences within and between species were calculated using the Kimura 2-parameter model (Kimura 1980), using the analytical tools provided by BOLD Systems v4 platform (Ratnasingham and Hebert 2007; http://www.boldsystems.org/). Intra-specific and inter-specific genetic distances are reported as maximum and minimum distances, respectively. The Barcode Index Number (BIN) of each species is reported which was obtained from the BOLD Systems v4 database. BINs represent a species-level taxonomic registry of the animal kingdom based on the analysis of nucleotide variation patterns in the barcode region of the cytochrome c oxidase I (COI) gene (Ratnasingham and Hebert 2013). This genetic information facilitates the species delimitation and constitutes the basis of future phylogenetic works at the genus level and below (Brehm 2015, 2018).

Label data and photographs of types and other barcoded specimens are accessible on BOLD, dataset DS-ORBAMIA (https://dx.doi.org/10.5883/DS-ORBAMIA). All new names are registered in ZooBank. Geo-references were taken from specimen labels.

Systematic accounts

Orbamia Herbulot, 1966

Herbulot (1966): 221. Type species: *Orbamia octomaculata* Wallengren, 1872

Differential features (COI sequences, photographs of adults and their genitalia see https://dx.doi.org/10.5883/DS-ORBAMIA). Adult: Male antennae bipectinate. Upperside of wings with conspicuous, contrasting discal spots on all wings. Underside with yellowish scales, with darker pattern towards termen. Male genitalia: Differing from those of the other two genera by longer uncus, naked dorsal process of valva, long and narrow cornutus. Female genitalia: Apophyses anteriores usually half-length of apophyses posteriores, lamellae ante- and post-vaginalis sclerotised (often oval), ductus bursae membranous, signum a small sclerite with transverse ridge.

Genetic data and phylogeny. Multigene analyses of Geometridae revealed evidence for assignation of the genus *Orbamia* to Cassymini and for sister group relationship with the African genus *Pycnostega* (Murillo-Ramos et al. 2019; Brehm et al. 2019). The maximum likelihood analysis of COI barcode data underpins the monophyly of the genus *Orbamia* as conceived and circumscribed here (cf. Table 1, Fig. 85).

Orbamia octomaculata (Wallengren, 1872)
BIN: BOLD: AAQ4039
Figures 1, 19, 37, 55, 73

Panagra octomaculata: Wallengren (1872): 60 (Holotype ♂ in NHRS, Stockholm; locus typicus: [South Africa]: “Caffraria orientalis interior“)

Examined material (ZSM). 25♂♀ from Tanzania, Zambia, Botswana, Mozambique, Malawi, Namibia, South Africa (ZSM G 20929/♀; ZSM G 20921/♂; ZSM G 20930/♂; ZSM G 20931/♂; ZSM G 20943/♂; ZSM G 13646/♂; ZSM G 13645/♀; ZSM G 20947/♀).

Differential features (COI sequences, photographs of adults and their genitalia see https://dx.doi.org/10.5883/DS-ORBAMIA): Adult: Forewing length: 11.5–13.5 mm. Upperside of wings: Ground colour pale brown with dark suffusion. Underside: Ground colour yellow or orange with much dark suffusion, terminal fascia on hind wing usually complete, on forewing restricted to apex. Male genitalia: Uncus long, triangular, valva strongly (rectangularly) bent, dorsal process with small spinule at tip, cornutus short and stout (1.4–1.7 mm). Female genitalia: Lamella antevaginalis U-shaped, long (0.75 mm), signum sclerotised, transversely flat, transverse ridge curved (0.4–0.5 mm).

Table 1. Barcode gap analysis of COI data of the genera *Orbamia*, *Rabomia*, and *Morabia* (https://dx.doi.org/10.5883/DS-ORBAMIA), showing intraspecific variation ("Mean Intra-Sp" and "Max. Intra-Sp.") and distances from Nearest Neighbour Species ("NN").

Species	Mean Intra-Sp	Max. Intra-Sp	Nearest species	Distance NN
Orbamia abiyi	0.51	0.93	*Orbamia clarior*	2.1
Orbamia balensis	0.61	0.61	*Orbamia ocellata*	7.65
Orbamia becki	0.97	2.68	*Orbamia marginata*	1.89
Orbamia clarior	0	0	*Orbamia abiyi*	2.1
Orbamia ocellata	0	0	*Orbamia clarior*	2.81
Orbamia emanai	1.43	2.17	*Orbamia clarior*	2.47
Orbamia marginata	0.53	0.62	*Orbamia becki*	1.89
Orbamia obliqua	1.35	1.87	*Orbamia abiyi*	3.63
Orbamia octomaculata	0.69	1.27	*Orbamia marginata*	2.34
Orbamia renimacula	0.42	1.08	*Orbamia becki*	2.18
Rabomia obscurata	N/A	0	*Rabomia subaurata*	5.19
Rabomia subaurata	0.41	0.62	*Rabomia obscurata*	5.19
Morabia brunnea	N/A	0	*Morabia politzari*	2.66
Morabia politzari	0.25	0.26	*Morabia brunnea*	2.66

Orbamia marginata Hausmann & Tujuba, sp. nov.

http://zoobank.org/6B79EAB5-4CE5-4B46-9176-5A47FF51E0AB
BIN: BOLD: AAZ5266
Figures 2, 20, 38, 56

Examined material. ***Holotype:*** ♂, Tanzania, Bukwa region, 14 km W Namanyere, 1290 m, 07°27.28'S, 030°54.49'E, 14.xi.2005, leg. Ph. Darge, coll. ZSM (ZSM G 20909).

Paratypes: 2♂, Tanzania, Rukwa region, 14 km W Namanyere, 1290 m, 07°27.28'S, 030°54.49'E, 14.xi.2005, leg. Ph. Darge, coll. ZSM (ZSM G 20941); 1♂, Tanzania, Rukwa region, Luafi Game Reserve (W. Namanyere), 1260 m, 07°26.98'S, 030°54.24'E, 31.i.2008, leg. Ph. Darge; 1♂, Tanzanie, Iringa region, Iyayi savanna, 1400 m, 08°51.47'S, 034°31.29'E, 14.iv.2007, Ph. Darge; 1♂, Tanzania, Morogoro region, Udzungwa N.P. camp site, 3315 m, 07°50.95'S, 036°50.95'E, 26.xi.2005, leg. Ph. Darge (all ZSM).

Etymology. The name refers to the uninterrupted black line at the hindwing margin (Lat. margo/marginis = edge, border).

Differential features (COI sequences, photographs of adults and their genitalia see https://dx.doi.org/10.5883/DS-ORBAMIA): Adult: Forewing length: 11.5–12.5 mm. Upper side of wings: Ground colour dirty grey with brown suffusion. Underside: Ground colour whitish beige with some dark suffusion, terminal fascia conspicuous, uninterrupted on all wings. Male genitalia: Uncus long, triangular, valva slightly bent, dorsal process with small spinule at tip, cornutus short and stout (1.6 mm). Female genitalia unknown.

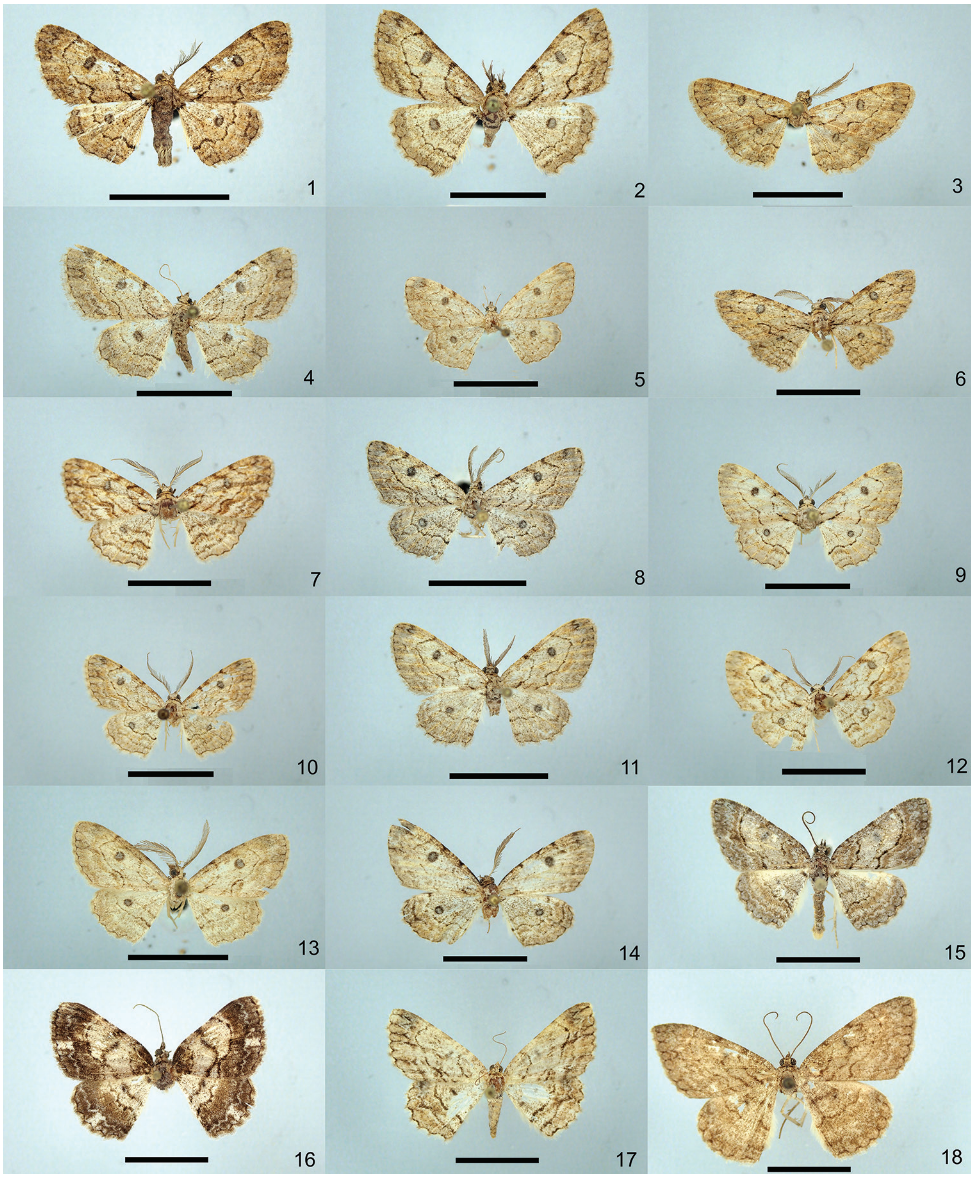

Figures 1–18. Specimens of the genera *Orbamia*, *Rabomia*, and *Morabia*, dorsal view. **1** *Orbamia octomaculata* **2** *O. marginata* (paratype) **3** *O. becki* (holotype) **4** *O. renimacula* **5** *O. clarissima* (holotype) **6** *O. clarior* (holotype) **7** *O. obliqua* (holotype) **8** *O. obliqua parva* (holotype) **9** *O. ocellata* **10** *O. abiyi* (holotype) **11** *O. emanai* (holotype) **12** *O. emanai lenzi* (holotype) **13** *O. pauperata* (holotype) **14** *O. balensis* (holotype) **15** *Rabomia subaurata* **16** *R. obscurior* (holotype) **17** *Morabia politzari* (holotype) **18** *M. brunnea* (holotype). Scale bars: 1 cm.

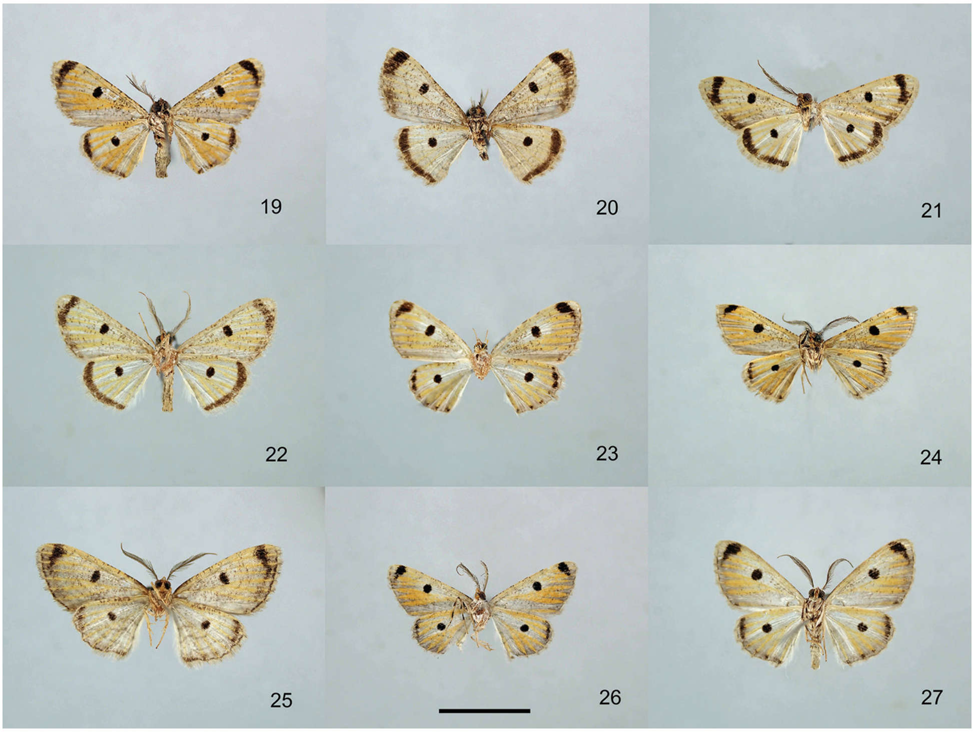

Figures 19–27. Specimens of the genus *Orbamia*, ventral view. **19** *Orbamia octomaculata* **20** *O. marginata* **21** *O. becki* **22** *O. renimacula* **23** *O. clarissima* **24** *O. clarior* **25** *O. obliqua* **26** *O. obliqua parva* **27** *O. ocellata*. Scale bars: 1 cm.

Orbamia becki **Hausmann, 2006**

BIN: BOLD: AAD8768
Figures 3, 21, 39, 57, 74

Orbamia becki: Hausmann (2006): 42 (Holotype ♂ in ZSM: G 13627; locus typicus: Yemen: Al Hudaydah, Jebel Burra).

Examined material (ZSM). 57♂♀ from Yemen, Ethiopia and Djibouti (ZSM G 13478/♂; ZSM G 13628/♀; ZSM G 13649/♀; ZSM G 13636/♂; ZSM G 13637/♀/ ZSM G 13650/♀; ZSM G 20927/♀).

Differential features (COI sequences, photographs of adults and their genitalia see https://dx.doi.org/10.5883/DS-ORBAMIA): Adult: Forewing length: 9.5–12 mm. Upperside of wings: Ground colour pale brown. Underside: Ground colour whitish with yellowish tinge, on forewing with some dark suffusion, terminal fascia on all wings complete. Male genitalia very similar to those of *O. octomaculata*: Uncus stout, triangular, valva strongly (rectangularly) bent, dorsal process with small spinule at tip, cornutus short and stout (1.5 mm). Female genitalia very similar to those of

O. octomaculata: Lamella antevaginalis U-shaped (0.6–0.7 mm), signum sclerotised, transversely oval, transverse ridge curved (0.3–0.5 mm).

Remarks. Allopatric vicariant of *O. octomaculata*. *Orbamia becki* is the only species of this genus that has also been recorded outside Africa in Yemen, southern Arabia.

Orbamia renimacula **(Prout, 1926)**

BIN: BOLD: AAE1536
Figures 4, 22, 40, 58, 75

Boarmia renimacula: Prout (1926): 184 (holotype ♀ in NHMUK; locus typicus: Senegal: Sédhiou).

Examined material (ZSM). 45♂♀ from Cameroon, Burkina Faso (Upper Volta), Guinea, Senegal, Togo, Mali, Gambia, Nigeria and Ivory Coast (ZSM G 13626/♂; ZSM G 61321/♀; ZSM G 13620/♂).

Differential features (COI sequences, photographs of adults and their genitalia see https://dx.doi.org/10.5883/DS-ORBAMIA): Adult: Forewing length: 8.5–12 mm, one of the smallest *Orbamia* species. Upperside of wings: Ground colour pale grey with brown suffusion. Underside: Ground colour white with very slight yellowish tinge, and slight dark suffusion, terminal fascia on all wings complete, conspicuous, at forewing apex dilated. Male genitalia: Uncus narrow digitiform, saccus round, valva almost straight, dorsal process with fine, curved hook at tip, cornutus of medium length (2.0 mm). Female genitalia: Lamella post-vaginalis weakly sclerotised, lamella ante-vaginalis U-shaped (0.6 mm), signum sclerotised, rhomboid, transverse ridge straight (0.25 mm).

Orbamia clarissima **Hausmann & Tujuba, sp. nov.**

http://zoobank.org/38E93700-3258-4497-B742-39B80BB75B0D
BIN: not yet assigned, DNA barcodes BC ZSM Lep 106553, 106554, 106555.
Figures 5, 23, 41, 59, 76

Examined material. ***Holotype:*** ♀, Kibwezi, B.E.A. [Kenya], 12 March 1917 (W. Feather), coll. ZSM (ZSM G 13618).

Paratypes: 1♂, Kibwezi, B.E.A. [Kenya], April 1922 (W. Feather); 1♂, Kenya, Mutha, 5.IV.69, Watulege; 1♀, Kenya, Musthomo, 13.III.69, Watulege (ZSM G 13617); 1♂, Somalia m., Caonole Fluß, 21.1.1988, leg. Dr. Politzar (all ZSM). ZSM G 13647/♂.

Etymology. The name refers to the very pale ground colour (Lat. clarissimus, -a, -um = palest, clearest).

Differential features (COI sequences, photographs of adults and their genitalia see https://dx.doi.org/10.5883/DS-ORBAMIA): Adult: Forewing length: 7.5–11 mm, one of the smallest *Orbamia* species. Upperside of wings: Ground colour whitish with slight grey brown suffusion. Underside: Ground colour white with slight orange tinge, mainly towards termen between veins, apical spots on all wings conspicuous, sharp. Male genitalia: Uncus long, digitiform, stout, valva straight, dorsal process with small spinule at tip, cornutus very short (1.0 mm) and tiny. Female genitalia: Apophyses stout, apophyses anteriores comparatively long (2/3 length of apophyses posteriores), lamella ante-vaginalis heart-shaped (length and width 0.45 mm), signum small, sclerotised, transverse ridge straight (0.15 mm).

Orbamia clarior **Hausmann & Tujuba, sp. nov.**

http://zoobank.org/79B39635-880A-411F-B9C8-563320CA5766
BIN: BOLD: ABW5825
Figures 6, 24, 42, 60

Examined material. Holotype: ♂, Kenya, South Ukanbasi, 6.V.1996, leg. Politzar (ZSM G 20944).

Etymology. The name refers to the comparatively pale ground colour.

Differential features (COI sequences, photographs of adults and their genitalia see https://dx.doi.org/10.5883/DS-ORBAMIA): Forewing length: 10 mm. Upperside of wings: Ground colour comparatively dark brownish, transverse lines of forewing oblique. Underside: Ground colour whitish beige, orange between veins, apical spot on forewing conspicuous, sharp, on hindwing narrow, elongate, remnants of dark colouration in the anal angle. Male genitalia: Uncus of medium length, digitiform, stout, dilated towards base, valva straight, dorsal process with conspicuous spinule at tip, cornutus very long (2.7 mm). Female genitalia unknown.

Orbamia obliqua **Hausmann & Tujuba, sp. nov.**

http://zoobank.org/BED6B29E-D967-419C-A998-6773D7BF078D
BIN: BOLD: AAM4892
Figures 7, 25, 43, 61

Examined material. ***Holotype:*** ♂, North-western Zambia, Hillwood farm, 11°16.01'S, 24°18.99'E, 17.ix.2009, 1420 m, UV, J. Lenz legit, coll. ZSM (G 20905).

Paratype: 1♂, Tanzania, Morogoro province, Nguru mounts, IV.2004 (ex coll. Philippe Darge, coll. ZSM, G 20906).

Etymology. The name refers to the oblique position of the transverse lines of the forewing (Lat. obliquus, -a, -um = oblique).

Differential features (COI sequences, photographs of adults and their genitalia see https://dx.doi.org/10.5883/DS-ORBAMIA): Adult: Forewing length: 11–12 mm. Upperside of wings: Ground colour pale grey with brown pattern, transverse lines oblique. Underside: Ground colour beige with slight yellowish tinge, and with strong dark suffusion, terminal area with pattern reduced to a dark apical spot and a dark shadow on the hindwing apex. Male genitalia: Uncus short, stout, hook-shaped, saccus projection shallow, valva straight, narrow at tip, dorsal process with a stout hook at tip, cornutus of medium length (1.9 mm). Female genitalia unknown.

Orbamia obliqua parva Hausmann & Tujuba, subsp. nov.

http://zoobank.org/3A0A5166-35FB-4D67-9BC2-B4C5C1024779
BIN: BOLD: AAM4892
Figures 8, 26, 44, 62

Examined material. ***Holotype:*** ♂, South Africa, Limpopo, Melkrivier Lapalala, Wilderness Kolobe camp, 1220 m -23.9094/28.2736, 13.xi.2017, leg. A. Hausmann, coll. Ditsong Museum, Pretoria, gen. prp. ZSM G 20933.

Paratypes: 6♂, South Africa, Limpopo, Melkrivier Lapalala, Wilderness, Kolobe camp, 1220 m -23.9094/28.2736, 13.xi.2017, leg. A. Hausmann; 2♂, RSA, Northwest prov. 7.5 km North Zeerust, 1180 m (lux), 25°27'S, 26°05'E, 17.II.2006, leg. Hacker (ZSM G 20949); 1♂, South Africa, Gauteng, Mogale's Gate Biodiversity Centre, near Bush Camp, -25.938, 27.639, 1420 m, 14.ii.2012, leg. P. Hebert, J. deWaard, coll. University of Guelph (Canada), Centre for Biodiversity Genomics.

Etymology. The name refers to the small size of this subspecies (Lat. parvus, -a, -um = small), being much smaller than the sympatric *O. octomaculata*.

Differential features (COI sequences, photographs of adults and their genitalia see https://dx.doi.org/10.5883/DS-ORBAMIA): Adult: Forewing length: 9–11 mm. Upperside of wings: Ground colour pale grey, darker in the terminal area, pattern dark grey. Underside: Ground colour whitish beige, orange between veins, on forewing apex a sharp black spot, dark colouration on the hindwing terminal area restricted to a small stripe or shadow in the apex. Male genitalia: Uncus comparatively short, stout, hook-shaped, saccus projection shallow, valva straight, narrow at tip, dorsal process with a stout hook at tip, cornutus of medium length (1.6–1.9 mm). Female genitalia unknown.

Orbamia ocellata (Warren, 1897), stat. nov.

BIN: BOLD: AAP8312
Figures 9, 27, 45, 63, 77

Lepiodes ocellata: Warren (1897): 94 (Syntypes 5♂1♀ in NHMUK; locus typicus: South Africa: Bathurst; [north-eastern Zambia]: Mpeta, Loangwa River [Luangwa], off the Zambesi [close to the border with northern Malawi]).

Note. Synonym of *O. octomaculata* according to Scoble (1999) but the type series of *ocellata* belongs to two different species. Herewith we designate the red-ring-labelled male specimen from Zambia, Mpeta, as lectotype to fix the identity of the name and to stabilise nomenclature. The taxon is herewith upgraded from synonymy to species rank (stat. nov.), based on the below mentioned differences in DNA barcodes and genitalia. Pattern of upper- and underside of wings of the lectotype exactly matches that of the examined material from Tanzania, partly collected in closely adjacent localities to the type locality (e.g., Ruvuma and Iringa provinces).

Examined material. 1♂, Tanzania, Pwani region, Manadera, 166m, 06°14.30'S, 038°23.19'E, 07.XII.2008, leg. Ph. Darge (ZSM G 20908); 1♀, Tanzanie, Tanga region, Savane prės, Usambara west. 475 m, 11.v.2005 leg. Ph. Darge; 2♀, Tanzanie, Tanga region, West Usambara mts, Magamba Forest, 1818 m, 04°42.76'S, 038°17.28'E, 01.XII.2008, leg. Ph. Darge; 1♀, Tanzanie, Morongoi region, Mikesse Hills, 375 m, 06°40.50'S, 037°58.12'E, 17.XI.2004, leg. Ph. Darge; 2♀, Tanzanie, Morogoro 1 km E Mikumi, 550 m, 5.III.2003, leg. M. Fibiger, H. Hacker, K.Larsen, H.P. Schreier; 1♀, Tanzania, Morogoro region, Uluguru mts, Bunduki Forest, 1275 m, 07°01.07'S, 037°37.94'E, 23.XI.2007, leg. Ph. Darge; 1♀, Tanzania, Morogoro region, face West des, Nguru mts, Makuyu, savane arborėe, 620 m, 25.IV.2005, leg. Ph. Darge (ZSM G 20942); 2♀, Tanzania, Morogoro region, West Nguru mts, Makuyu, alt. 620 m, 06°16.08'S, 037°20.54'E, 19.XI.2007, leg. Ph. Darge; 1♂, Tanzania, Rukwa prov, Kisengere/ Kasambo, 1193 m, 07°27.54'S, 030°52.81'E, 17.v.2004, leg. Ph. Darge; 1♂, Tanzania, Rukwa prov., Mbizi mts, entre Kisungu et Muze, 1415 m, 07°43.82'S, 031°32.4'E, 14.v.2004, leg. Ph. Darge; 1♀, Tanzanie, Iringa, Ulembwa, 2070 m, 09°18.70'S, 034°38.07'E, 22.XII.2008, leg. Ph. Darge (ZSM G 20911); 2♀, Tanzanie, Pwani region, Savane de Mandera, 170 m, 06°14.30'S, 038°23.19'E, 19.III.2006, leg. Ph. Darge; 1♂2♀, id., 15.I.2005; 1♀, Tanzanie, Ruvuma region, Kitai Savnna, 1020 m, 10°42.40'S, 035°12.33'E, 24.III.2006, leg. Ph. Darge (ZSM G 20946); 1♂, Tanzanie, Mbeya region, Igurusi savanna, 1150 m, 08°46.68'S, 033°46.17'E, 06.IV.2006, leg. Ph. Darge; 3♀, Tanzania, Ubenazomizi region, savannas and deciduous forest, 450 m, 06°40.57'S, 037°58.99'E, 13.XII.2002, leg. Ph. Darge and Th. Ebode; 1♀, Tanzanie, Ruvuma region, Kitai Savanna, 1020 m, 10°42.40'S, 035°12.33'E, 24.III.2006, leg. Ph. Darge.

Differential features (COI sequences, photographs of adults and their genitalia see https://dx.doi.org/10.5883/DS-ORBAMIA): Adult: Forewing length: 8.5–12 mm. Upperside of wings: Ground colour pale grey with slight brown suffusion, pattern brown with slight orange tinge. Underside: Ground colour whitish, orange between veins, apical spots on forewing conspicuous, sharply bordered, on hindwing terminal fascia usually diffuse, rarely restricted to apex. Male genitalia: Uncus narrow, digitiform, valva straight, broad, dorsal process with conspicuous, stout hook at tip, cornutus narrow and very long (2.8–3.0 mm). Female genitalia: Apophyses stout, apophyses anteriores comparatively long (2/3 length of apophyses posteriores), lamella ante- and post-vaginalis fused, oval, comparatively broad (length 0.7 mm, width 0.5 mm), signum weakly sclerotised, small, transverse ridge straight (0.2 mm).

Orbamia abiyi **Hausmann & Tujuba, sp. nov.**

http://zoobank.org/8AC03FE5-C57D-4BA1-9C63-44281F0AB521
BIN: BOLD: AAK5536
Figures 10, 28, 46, 64, 78

Examined material. ***Holotype:*** ♂, North Zambia, Mutinondo, 1390 m, wet Miombo, 29.XII. 2010, 12°23'30"S, 31°19'23"E, light trap, J. Lenz legit (ZSM G 20912).

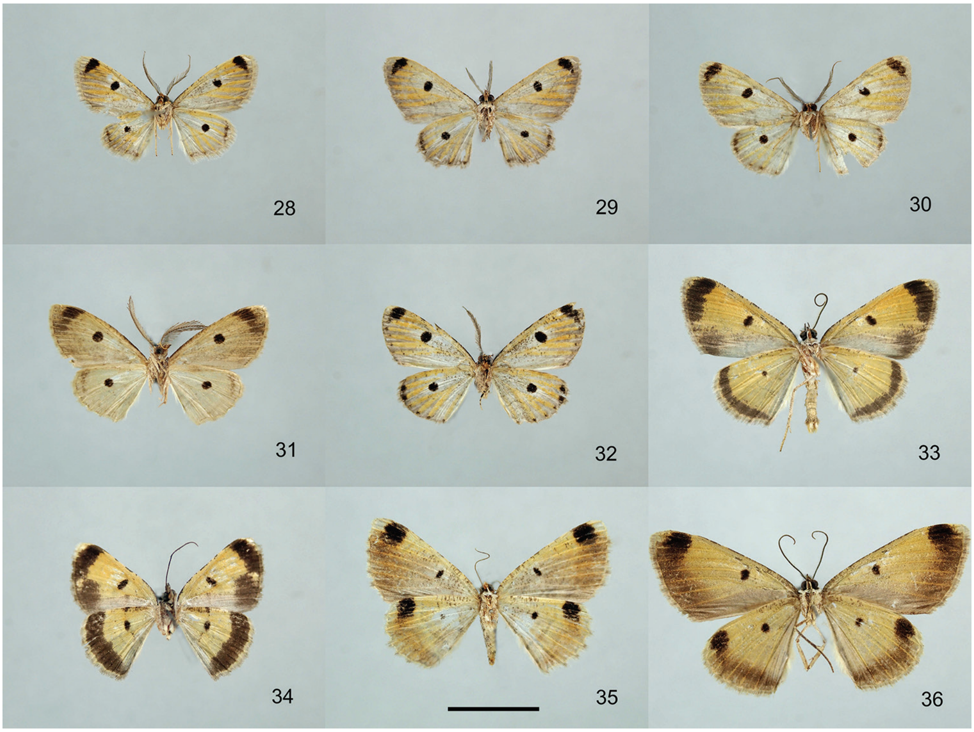

Figures 28–36. Specimens of the genera *Orbamia*, *Rabomia*, and *Morabia*, ventral view. **28** *Orbamia abiyi* **29** *O. emanai* **30** *O. emanai lenzi* **31** *O. pauperata* **32** *O. balensis* **33** *Rabomia subaurata* **34** *R. obscurior* **35** *Morabia politzari* **36** *M. brunnea*. Scale bars: 1 cm.

Paratypes: 1♂1♀, North Zambia, Mutinondo, 1390 m, wet Miombo, 29.XII.2010, 12°23'30"S, 31°19'23"E, light trap, J. Lenz legit (ZSM G 20913/♀); 1♂, S. Ethiopia SN, Arba Minch, below Hotel Bekele Molla, thornbush, 1310 m, 10°26'N, 39°53'E, 29.IV.2008, leg. Hacker & Schreier (ZSM G 20556); 1♂, Tanzania, Morogoro region, Mikesse Hills, 420 m, 06°40.15'S, 037°57.57'E, 21.XII.2005, Ph. Darge; 1♀, Tanzania, Rukwa prov., Mbizi mts, entre Kisungu et Muze, 1415 m, 07°43.82'S, 031°32.48'E, 14.v.2004, leg. Ph. Darge; 1♂, Namibia, Kavango distr., 17°52'N, 19°39'E, 16 km W Rundu, (Okavango) Kavango river area, 28.II.2006, leg. H. Hacker & H.P. Schreier (ZSM G 20932); 2♂, Rwanda, S.E. Rusumo, 1300 m, 29.XII.1975, leg. B. Turlin (ZSM G 13625; BC ZSM Lep); 1♂, id., 25.3.1975 (ZSM).

Etymology. The name honours his Excellency Dr Abiy Ahmed Ethiopia's Prime Minister, the 2019 Nobel Peace Prize Laureate, for his tremendous contributions to Ethiopia and the Horn of African geopolitics.

Differential features (COI sequences, photographs of adults and their genitalia see https://dx.doi.org/10.5883/DS-ORBAMIA): Adult: Forewing length: 10–12 mm. Upperside of wings: Ground colour pale grey with slight brown suffusion, pattern brown with very slight orange tinge. Underside: Ground colour whitish, orange between veins, apical spots on forewing conspicuous, sharply bordered, on hindwing terminal fascia usually diffuse, in Tanzania hindwing terminal fascia uninterrupted. Male genitalia: Uncus narrow, digitiform, valva straight, broad, dorsal process with conspicuous, stout hook at tip, cornutus narrow and long (2.2–2.3 mm). Female genitalia: Lamella ante- and post-vaginalis fused, oval (length 0.75–0.85 mm), signum weakly sclerotised, small, transverse ridge straight (0.17–0.2 mm).

Remarks. Populations from western Ethiopia with darker upperside of wings, on hindwing underside dark pattern reduced to apex. See also remarks to the following species.

Orbamia emanai Hausmann & Tujuba, sp. nov.

http://zoobank.org/5A4DFBCF-0D52-4378-AF90-84611329CBAE
BIN: BOLD: ABW6858
Figures 11, 29, 47, 65, 79

Examined material. ***Holotype:*** ♂, NW Ethiopia, 30 km SE Bahir Dar, Tis Isat, Blue Nile falls, 1640 m, 11°29'08"N, 37°35'28"E, 25.VI.2008, leg. Hacker & Schreier (ZSM G 20917).

Paratypes: 30♂8♀, NW Ethiopia, 30 km SE Bahir Dar, Tis Isat, Blue Nile falls, 1640 m, 11°29'08"N, 37°35'28"E, 25.VI.2008, leg. Hacker & Schreier; 1♂, S. Ethiopia S.N., 12 km W Jinka, border of Mago N.P., 930 M (lux), 05°18'47"N, 36°44'07"E, 6.V.2008, leg. Hacker & Schreier (ZSM G 20910/♀; ZSM G 20916/♀).

Additional material (exactly barcode-sharing): 8♂2♀, Botswana, Central distr. 15 km NW Francistown, river Tati, 1030 m, 21°02'S, 27°32'E, 19.II.2006, Hacker & Schreier (ZSM G 20919/♀; ZSM G 20920/♂); 1♀, Botswana, Kgatleng distr., 30 km NNE Gaborone, 980 m (lux), 19.II.2006, leg Hacker & Schreier; 2♂, Botswana, Central district 10 km SSE Nata, Sua pan, 930 m (lux) 20°09'S, 26°26'E, 20.II.2006, leg Hacker & Schreier.

Etymology. Named after Emana Getu, a senior professor of Entomology, at Addis Ababa University for his immense contributions to the field of entomology.

Differential features (COI sequences, photographs of adults and their genitalia see https://dx.doi.org/10.5883/DS-ORBAMIA): Adult: Forewing length: 9–12 mm. Upperside of wings: Ground colour comparatively dark. Underside: Ground colour pale grey, on hindwing with slight orange tinge, on forewing orange between veins, apical spots on forewing conspicuous, sharply bordered, on hindwing slightly darker at apex only. Male genitalia: Uncus narrow, digitiform, valva straight, broad, dorsal process with conspicuous, stout hook at tip, cornutus narrow and very long (2.5–3.0 mm). Female genitalia: Lamella ante- and post-vaginalis fused, oval (length 0.8–0.85 mm), signum weakly sclerotised, small, transverse ridge straight (0.17–0.2 mm).

Remarks. Morphological differences to the previous species small, but the genetic divergence correlates with darker wing colour, and a few characters in male genitalia (longer cornutus). Distribution areas of both species overlapping.

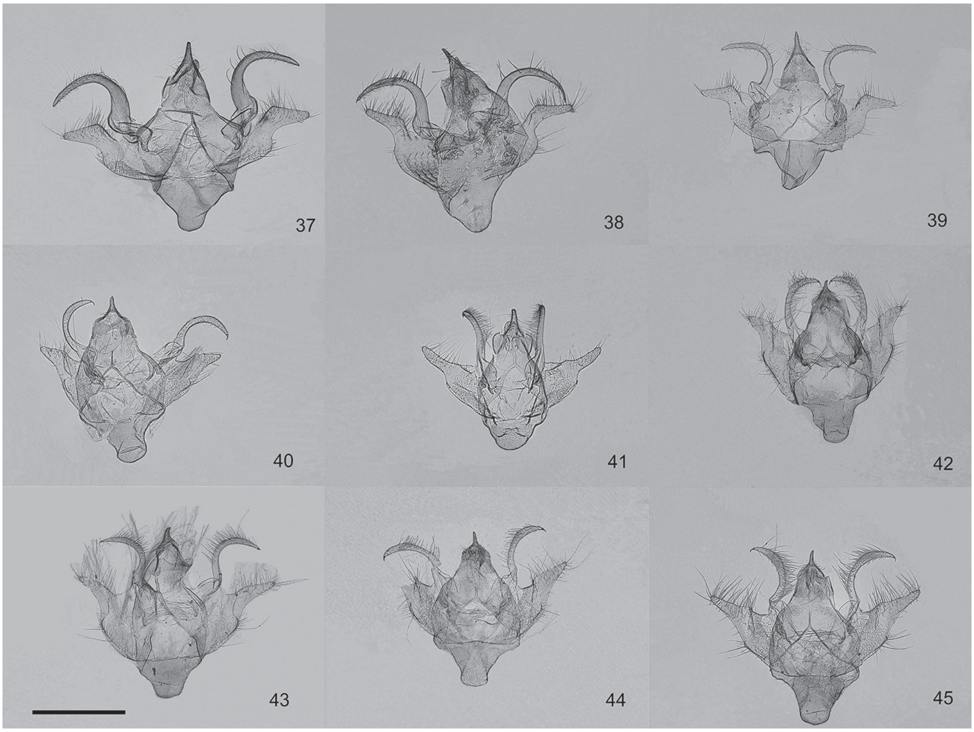

Figures 37–45. Male genitalia of the genus *Orbamia*. **37** *Orbamia octomaculata* **38** *O. marginata* **39** *O. becki* **40** *O. renimacula* **41** *O. clarissima* **42** *O. clarior* **43** *O. obliqua* **44** *O. obliqua parva* **45** *O. ocellata*. Scale bar: 1 mm.

Orbamia emanai lenzi Hausmann & Tujuba, subsp. nov.

http://zoobank.org/0FC250FF-B4AF-4461-8113-2D0CFEF85C5F
BIN: BOLD: ABW6858
Figures 12, 30, 48, 66, 80

Examined material. ***Holotype:*** ♂, Zambia, North Zambia, Mutinondo, 1390 m, wet Miombo, 01.I. 2011, 12°23'30"S, 31°19'23"E, light trap, J. Lenz legit, gen. prp. ZSM G 20917 (coll. ZSM G 20918).

Paratypes: 1♀, Zambia, North Zambia, Mutinondo, 1390 m, wet Miombo, 01.I.2011, 12°23'30"S, 31°19'23"E, light trap, J. Lenz legit (ZSM G 20922); 1♂, id., 29.XII.2010; 1♂, Zambia, Northwest prov., Chiwona riverine forest, 1330 m, -12.412S, 24.1910E, 12.IX.2015, leg Sàfiàn Szabolcs; 1♂, S. Africa [sic!], S. Malawi, Nsanje distr. 25 km S Blantyre, Mwabvi reserve, 16°39.20'S, 35°03.03'E, 10.XII.2010, 127 m, Ustjuzhanin & Kovtunovich (ZSM G 20907).

Etymology. Named after Jürgen Lenz, Harare - Leipzig, active and experienced researcher and collector of geometrids in Africa, mainly Zambia and Zimbabwe.

Differential features (COI sequences, photographs of adults and their genitalia see https://dx.doi.org/10.5883/DS-ORBAMIA): Adult: Forewing length: 10–11 mm.

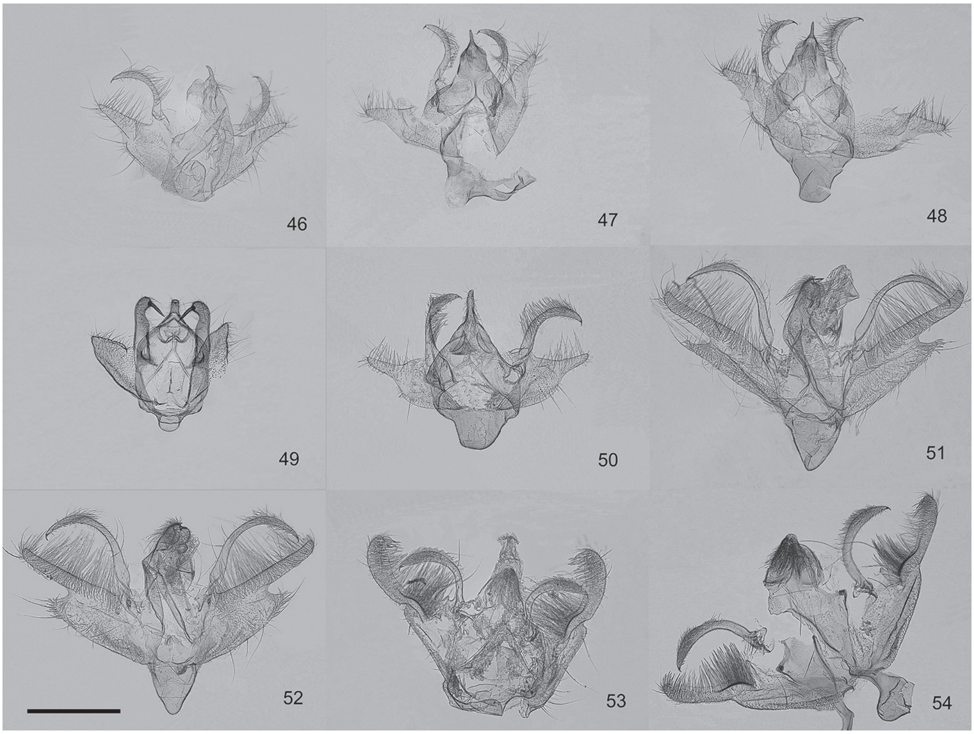

Figures 46–54. Male genitalia of the genera *Orbamia*, *Rabomia*, and *Morabia*. **46** *Orbamia abiyi* **47** *O. emanai* **48** *O. emanai lenzi* **49** *O. pauperata* **50** *O. balensis* **51** *Rabomia subaurata* **52** *R. obscurior* **53** *Morabia politzari* **54** *M. brunnea*. Scale bar: 1 mm.

Upperside of wings: Ground colour much paler than in the nominotypical subspecies, very pale grey, with slight brown suffusion, mainly in the terminal area, pattern grey brown. Underside: Ground colour whitish beige, orange on veins, apical spots on forewing conspicuous, sharply bordered, on hindwing terminal fascia usually diffuse over more or less the whole termen. Male genitalia: Uncus narrow, digitiform, valva straight, broad, dorsal process with conspicuous, stout hook at tip, cornutus narrow and long (2.7 mm). Female genitalia: Lamella ante- and post-vaginalis fused, oval (length 0.75–0.85 mm), signum weakly sclerotised, small, transverse ridge straight (0.17–0.2 mm).

Remarks. BIN-sharing but at 2.2 % distance, much paler than the nominotypical subspecies, but little difference in genitalia.

***Orbamia pauperata* Herbulot, 1966**

Figs 13, 31, 49, 67, 81

Orbamia pauperata: Herbulot (1966): 221 (Holotype § in ZSM: gen. prep. ZSM G 14466; locus typicus: Madagascar: Betioky, southern shore of Tsimanampetsotsa).

Note. So far, without BIN, holotype with short barcode fragment (BC ZSM Lep 81698).

Examined material. 2♂3♀ from Madagascar, including holotype (ZSM G 13619/♀).

Differential features (COI sequences, photographs of adults and their genitalia see https://dx.doi.org/10.5883/DS-ORBAMIA): Adult: Forewing length: 10–12 mm. Upperside of wings: Ground colour pale grey. Underside: Ground colour beige, without yellow tinge, apical spot present on forewing. Male genitalia: Uncus digitiform, saccus shortly projecting, round, valva short, broad, tapered at tip, dorsal process stoutly sclerotised, with a conspicuous, very long spine at tip, aedeagus short (1.2 mm), cornutus very short (0.7 mm) and S-shaped at tip. Female genitalia: Lamella ante- and post-vaginalis developed as two separate, narrow, transverse sclerites, posteriorly bilobed, signum rhomboid, transverse ridge straight (0.25 mm).

Remarks. Phylogenetically the most isolated species within this genus, based on large differences in morphology and genetics, the latter, however, just based on a short barcode fragment of the holotype.

Orbamia balensis Hausmann & Tujuba, sp. nov.

http://zoobank.org/:0948AD35-4B39-4FF5-A210-5AAD56A1BE4C
BIN: BOLD: AEA2800
Figures 14, 32, 50, 68

Examined material. ***Holotype:*** ♂, Ethiopia Oromia, Bale 8 km S. Dolo Mena, 1200 m, IV.2017, leg. R. Beck, coll. ZSM (ZSM G 20914).

Paratypes: 2♂2♀, Ethiopia Oromia, Bale 8 km S. Dolo Mena, 1200 m, IV.2017, leg. R. Beck (ZSM G 20948/♀); 1♀, Äthiopien, prov. Oromia, Dolo Mena, 30 km, S., 1080 m (savanna) 06°13.53'N, 39°46.82'E, 14.IV.2019, Robert Beck (ZSM).

Etymology. The name refers to the type locality in the Bale mountains.

Differential features (COI sequences, photographs of adults and their genitalia see https://dx.doi.org/10.5883/DS-ORBAMIA): Adult: Forewing length: 11–13 mm. Upperside of wings: Ground colour comparatively dark, with much dark brown suffusion, pattern not well contrasted. Underside: Ground colour beige, with pale orange tinge on veins, apical spots on forewing conspicuous, sharply bordered, on hindwing slightly darker at apex only, remnants of dotted terminal fascia on all wings. Male genitalia: Uncus stout, very long, saccus broad, valva straight, ´very broad at base, narrow at tip, dorsal process stoutly sclerotised, with conspicuous, stout hook at tip, cornutus narrow and short (1.1 mm). Female genitalia: Lamella ante- and post-vaginalis fused, heart-shaped, short (length 0.6 mm), signum small, transverse ridge straight (0.2 mm).

Rabomia Hausmann & Tujuba, gen. nov.

http://zoobank.org/C6E24B77-0F95-457D-9034-26348A26F071

Type species. *Ectropis*? *subaurata* Warren, 1899.

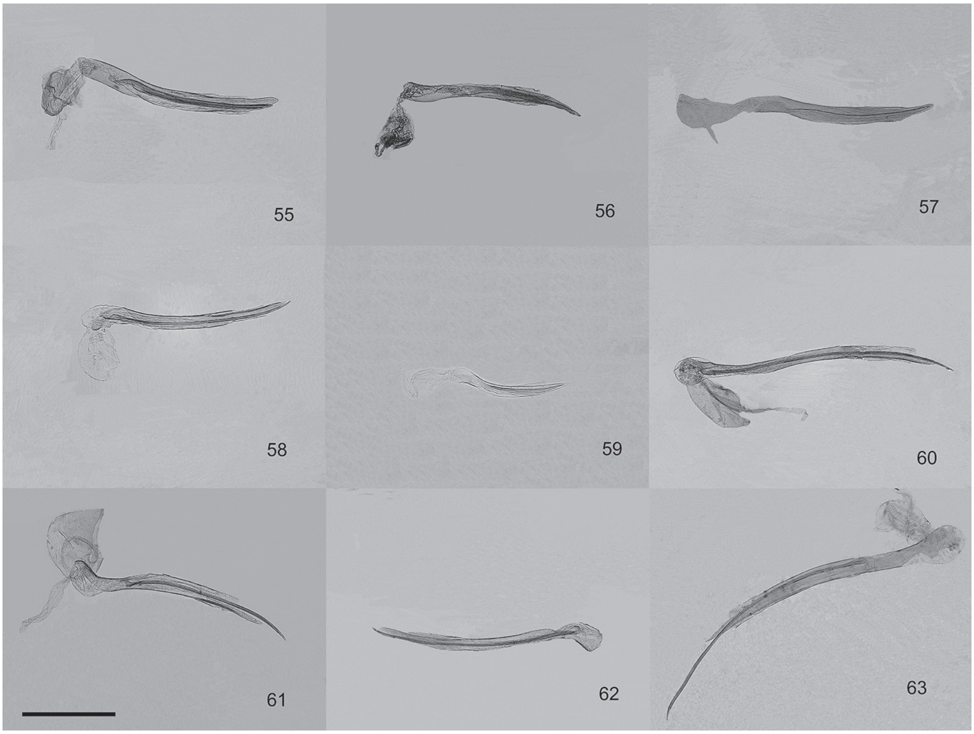

Figures 55–63. Aedeagus of male genitalia of the genus *Orbamia*. **55** *Orbamia octomaculata* **56** *O. marginata* **57** *O. becki* **58** *O. renimacula* **59** *O. clarissima* **60** *O. clarior* **61** *O. obliqua* **62** *O. obliqua parva* **63** *O. ocellata*. Scale bar: 1 mm.

Etymology. The name is an anagram of the sister genus *Orbamia*, similarly to the anagram used by Herbulot (1966) when transforming the name *Boarmia* to *Orbamia*.

Differential features (COI sequences, photographs of adults and their genitalia see https://dx.doi.org/10.5883/DS-ORBAMIA). Adult: Male antennae ciliate-fasciculate, female antennae filiform. Palpi of both sexes broad, bushy scaled, length in male 1.0, in female 1.5 times diameter of eye. Hind tibia of both sexes with two pairs of unequal spurs. Upperside of wings with inconspicuous, elongate discal spots, postmedial line of forewings sharp, strongly curved. Underside yellow, black terminal fascia conspicuous. Male genitalia: Uncus with three short sclerotised spines, lateral lobes below uncus swollen, saccus triangular, dorsal process of valva naked, with curved spinule at tip, aedeagus comparatively broad, with bundle of small cornuti at base, vesica condensed to a broad cornutus-like sclerite at tip. Female genitalia: Lamellae ante- and post-vaginalis sclerotised (elongate rhomboid), posteriorly rounded, ductus bursae sclerotised, long, helicoid, longitudinally furrowed, corpus bursae membranous, signum large, star-shaped.

Genetic data and phylogeny. The maximum likelihood analysis of COI barcode data supports the monophyly of the genus *Rabomia* gen. nov. and sister group relationship with (*Pycnostega*+*Dorsifulcrum*) (cf. Table 1, Fig. 85). However, phylogenies at genus level need to be considered with caution, when they are inferred from COI data. More research is needed to investigate the potential (re-) assignment of *Dorsifulcrum* to the Cassymini after having been excluded from that tribe in Brehm et al. (2019).

Remarks. In some morphological features (e.g., female signum and ductus bursae) the genus *Rabomia* gen. nov. is transitional to the genus *Dorsifulcrum* Herbulot, 1979, but is genetically clustering separately, underside of wings with black fascia only in the terminal area.

Rabomia subaurata (Warren, 1899), comb. nov.

BIN: BOLD: AAM3217
Figures 15, 33, 51, 69, 82

Ectropis? *subaurata*: Warren (1899): 306 (Holotype $ in NHMUK; locus typicus: [Zambia]: Mpeta, Loangwa River, off the Zambesi).

Examined material (ZSM). 10♂♀ from Zambia, Malawi, (southernmost) Democratic Republic of the Congo (Elisabethville [Lubumbashi]) (ZSM G 20923/♂; ZSM G20924 ♀).

Differential features (COI sequences, photographs of adults and their genitalia see https://dx.doi.org/10.5883/DS-ORBAMIA): Adult: Forewing length: 13–14 mm. Upperside of wings: Ground colour comparatively dark grey. Underside: Ground colour yellow, discal spots small, terminal fascia narrow at centre of forewing termen interrupted by a large yellow area. Male genitalia: Valva long and narrow, sacculus narrowly projecting at tip, at the base of aedeagus a bundle of eight comparatively long (0.3 mm) microcornuti. Female genitalia: Star-shaped signum large, diameter 0.7–0.9 mm.

Rabomia obscurior Hausmann & Tujuba, sp. nov.

http://zoobank.org/73A152CB-ADB8-4B67-AC34-A3F1BB1E16A2
BIN: BOLD: ABV9564
Figures 16, 34, 52, 70, 83

Examined material. ***Holotype:*** ♀, Burkina Faso (Upper Volta), Bobo Dioulesso, 6.10.81, leg. Dr Politzar, coll. ZSM (G 20915).

Paratypes: 1♀, Burkina Faso (Upper Volta), Bobo Dioulesso, 13.11.85, leg. Dr Politzar; 1♀: Burkina Faso (Upper Volta), Bobo Folonso, 28.7.79, leg. Dr Politzar; 1♂, id., 10.11.74; 1♂, Nigeria, Kaduna, 3.vii.1970, leg. Politzar, coll. ZSM (G 20926); 1♀, id., 28.vi.1970; 1♀, id., 26.vi.1970; 1♀, id., 8.vii.1970; 1♂, North Nigeria, Kogin Kano Game Reserve, 15.vi.1974, leg. Dr Politzar; 1♀, Cameroon, Yala Yarna, 40 km N of Ngaoundéré, 735 m, 22.vii.1974, leg. Gilles Clément (ZSM G 20925).

Etymology. The name refers to the darker colouration of wings (Lat. obscurior = darker).

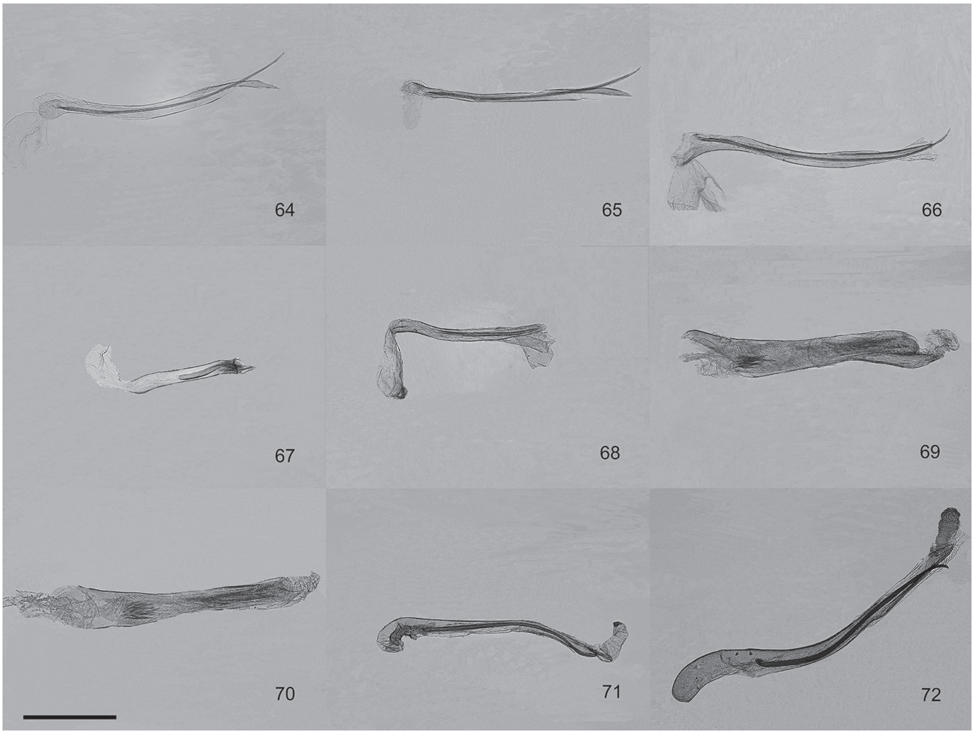

Figures 64–72. Aedeagus of male genitalia of the genera *Orbamia*, *Rabomia*, and *Morabia*. **64** *Orbamia abiyi* **65** *O. emanai* **66** *O. emanai lenzi* **67** *O. pauperata* **68** *O. balensis* **69** *Rabomia subaurata* **70** *R. obscurior* **71** *Morabia politzari* **72** *M. brunnea*. Scale bar: 1 mm.

Differential features (COI sequences, photographs of adults and their genitalia see https://dx.doi.org/10.5883/DS-ORBAMIA): Adult: Forewing length: 12–14 mm. Upperside of wings: Ground colour with darker suffusion than in *R. subaurata*, medial fascia dark and conspicuous on all wings, sometimes anastomosing with postmedial line on forewing. Underside: Ground colour yellow, discal spots larger than in *R. subaurata*, terminal fascia much broader, at centre of forewing termen interrupted by a small yellow spot or even uninterrupted. Male genitalia: Valva long and narrow, sacculus edged at tip, only shortly projecting, at the base of aedeagus a bundle of twelve comparatively short (0.15–0.2 mm) microcornuti. Female genitalia: Star-shaped signum large, diameter 0.8–1.0 mm.

Morabia Hausmann & Tujuba, gen. nov.

http://zoobank.org/D7BB6DF9-B1CD-4D00-8A15-A6906DFB2B56

Type species. *Morabia politzari* Hausmann & Tujuba, sp. nov.

Etymology. The name is an anagram of the sister genus *Orbamia*, similarly to the anagram used by Herbulot (1966) when transforming the name *Boarmia* to *Orbamia*.

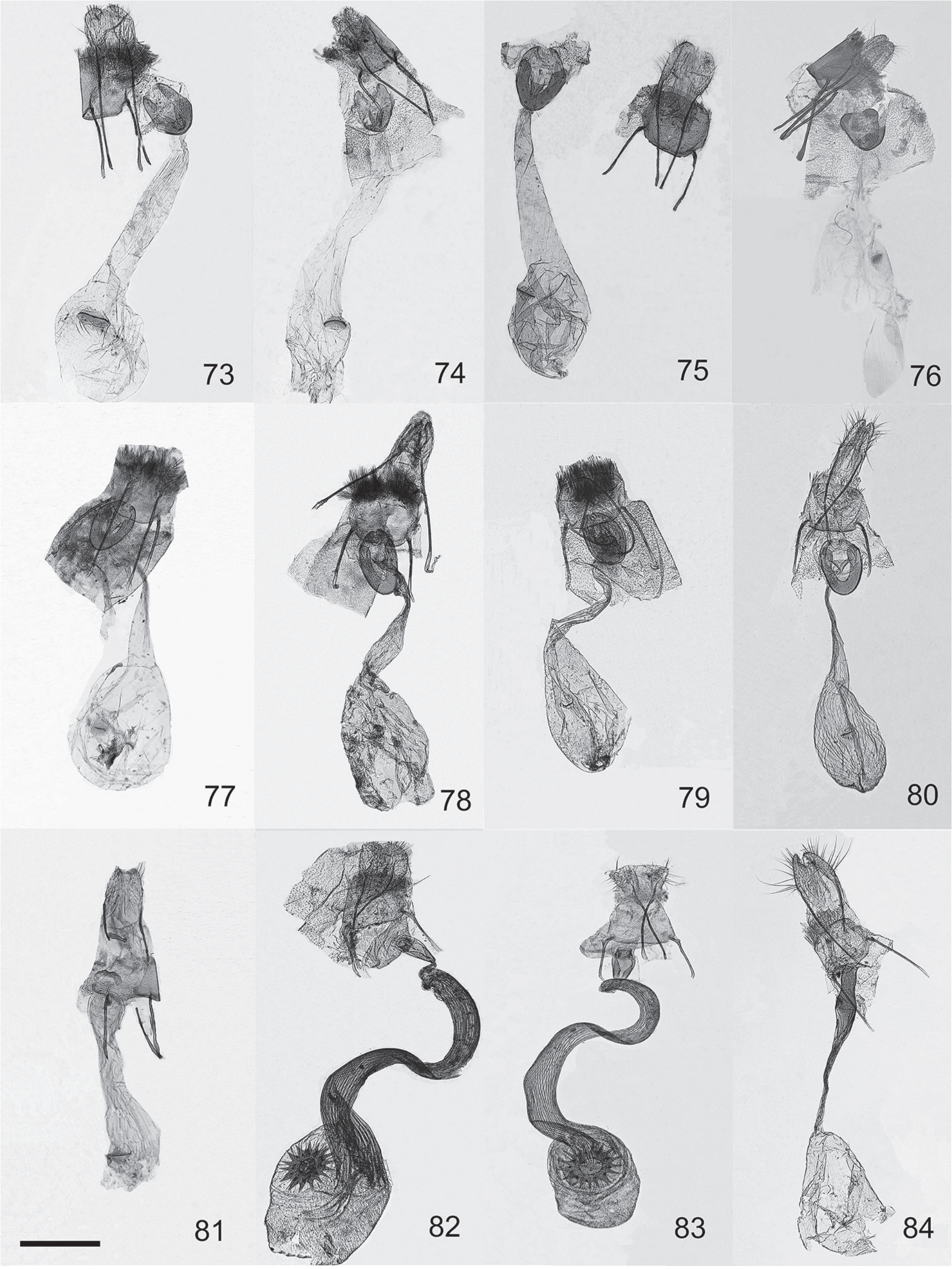

Figures 73–84. Female genitalia of the genera *Orbamia*, *Rabomia*, and *Morabia*. **73** *Orbamia octomaculata* **74** *O. becki* **75** *O. renimacula* **76** *O. clarissima* **77** *O. ocellata* **78** *O. abiyi* **79** *O. emanai* **80** *O. emanai lenzi* **81** *O. pauperata* **82** *Rabomia subaurata* **83** *R. obscurior* **84** *Morabia politzari*. Scale bar: 1 mm.

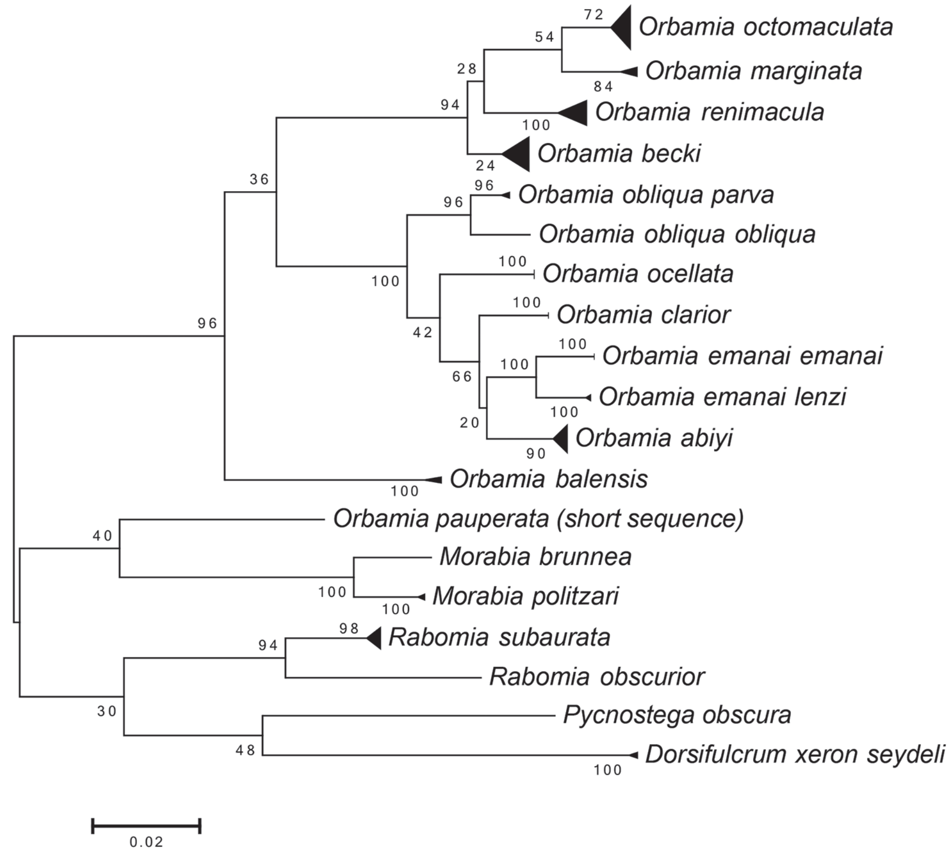

Figure 85. Maximum Likelihood Tree of COI data of the genera *Orbamia*, *Rabomia*, and *Morabia*, 50 Bootstrap Replications, Tamura-Nei model, uniform rates, built with Mega 6 software (Tamura et al. 2013; scale bar = 2 %), for original data see https://dx.doi.org/10.5883/DS-ORBAMIA.

Differential features (COI sequences, photographs of adults and their genitalia see https://dx.doi.org/10.5883/DS-ORBAMIA). Adult: Male antennae ciliate-fasciculate, female antennae filiform. Palpi of both sexes broad, bushy scaled, length 1.0–1.5 times diameter of eye. Hind tibia of both sexes with two pairs of unequal spurs. Upperside of wings with discal spots vestigial, medial line zigzagging, terminal line conspicuous, zigzagging on all wings. Underside beige, with a few yellowish scales and a sharp black spot in forewing apex. Male genitalia: Uncus very short, rounded saccus shallowly projecting, dorsal process of valva strongly setose, valva long and narrow, curved, strongly setose, mainly at centre, aedeagus with long and stout cornutus. Female genitalia: Apophyses long and fine. Lamellae ante- and post-vaginalis membranous, ductus bursae straight, anteriorly membranous, posteriorly dilated and towards antrum strongly sclerotised, corpus bursae membranous, pyriform, signum absent.

Genetic data and phylogeny. The maximum likelihood analysis of COI barcode data suggests the monophyly of the genus *Morabia* gen. nov. and an isolated position from (*Rabomia* gen. nov. (*Pycnostega+Dorsifulcrum*)) and from genus *Orbamia* (cf. Table 1, Fig. 85). However, phylogenies at genus level need to be considered with caution, when they are inferred from COI data.

Morabia politzari Hausmann & Tujuba, sp. nov.

http://zoobank.org/38C88B00-2394-4C29-81A9-9E58E06B058E
BIN: BOLD: ABX0432
Figures 17, 35, 53, 71, 84

Examined material. ***Holotype:*** ♀, Kenya, Sokoke Forest, 31.7.94, leg. Dr. Politzar, coll. ZSM.

Paratypes: 1♂, Kenya, Watama, 2.viii.1973, leg. Politzar, coll. ZSM (G 20934); 1♀, id., 30.vii.1973; 1♀, Kenya, Sokoke Forest, 31. Vii. 1994, leg. Politzar; 1♀, id, 2.vii.1994; 3♀, Tanzanie Bagamoyo dist. Vigwaza, 231 m, 06°42.89'S, 038°52.52'E, 30.III 2014, leg. Ph. Darge; 1♀, Tanzanie, Pwani region, Ruvu forest reserve, 220 m, 06°57.27'S, 038°49.36'E, 03.III.2014, leg. Ph. Darge (ZSM); 1♀, Coll. Mus. Tervuren, E.ville [DR Congo], 16.X.1955, Seydel (ZSM G 20935).

Etymology. The name refers to Dr. Heinz Politzar (1938–2007) for his great merits in collecting and studying African Lepidoptera (see Hacker and Hausmann 2010).

Differential features (COI sequences, photographs of adults and their genitalia see https://dx.doi.org/10.5883/DS-ORBAMIA): Adult: Forewing length: 12–14.5 mm. Upperside of wings: Ground colour whitish beige. Underside: Ground beige, with slight yellow or orange tinge, mainly on forewing, discal spots small, both wings with sharp, black apical spot. Male genitalia: Uncus very short, rounded, saccus shallowly projecting, dorsal process of valva strongly setose, valva long and narrow, curved, strongly setose, mainly at centre, aedeagus (length 2.5 mm) with long and stout cornutus (1.9 mm), sigmoid at tip. Female genitalia: Lamellae ante- and postvaginalis membranous, ductus bursae straight, anteriorly membranous, posteriorly dilated and towards antrum strongly sclerotised, corpus bursae membranous, pyriform, signum absent.

Morabia brunnea Hausmann & Tujuba, sp. nov.

http://zoobank.org/E25394ED-1400-454C-BDC5-882DAB89179C
BIN: BOLD: ABW6916
Figures 18, 36, 54, 72

Examined material. ***Holotype:*** 1♂, Zambia, North Zambia, Mutinondo, 1390 m, wet Miombo, 27.XII. 2010, 12°23'30"S, 31°19'23"E, light trap, J. Lenz legit, coll. ZSM (G 20945).

Etymology. The name refers to the unusual, brownish ground colour of the wings (Lat. brunneus, -a, um = brown).

Differential features (COI sequences, photographs of adults and their genitalia see https://dx.doi.org/10.5883/DS-ORBAMIA): Adult: Forewing length: 17.5 mm. Upperside of wings: Ground colour warm brown, pattern as in *M. politzari*. Underside: Ground pale brownish yellow, discal spots conspicuous, both wings with sharp, black apical spot and diffuse brown terminal fascia. Male genitalia: Uncus very short, rounded, strongly setose, saccus shallowly projecting, dorsal process of valva strongly setose, valva long and narrow, curved, strongly setose, mainly at centre, aedeagus longer (3.5 mm) than in the preceding species, S-shaped, with stout, S-shaped cornutus, longer than in the preceding species (2.3 mm). Female genitalia unknown.

Acknowledgements

The genetic analyses have received support from Paul DN Hebert and the Biodiversity Institute of Ontario (BIO) and the Canadian Centre for DNA Barcoding (CCDB University of Guelph). The data management and analysis system BOLD was provided by Sujeevan Ratnasingham.

References

Banki O, Hobern D, Döring M, Remsen D (2019) Catalogue of Life Plus: A collaborative project to complete the checklist of the world's species. Biodiversity Information Science and Standards 3: e37652. https://doi.org/10.3897/biss.3.37652

Brehm G (2015) Three new species of *Hagnagora* Druce, 1885 (Lepidoptera, Geometridae, Larentiinae) from Ecuador and Costa Rica and a concise revision of the genus. ZooKeys 537: 131–156. https://doi.org/10.3897/zookeys.537.6090

Brehm G (2018) Revision of the genus *Callipia* Guenée, 1858 (Lepidoptera, Geometridae), with the description of 15 new taxa. European Journal of Taxonomy 404: 1–54. https://doi.org/10.5852/ejt.2018.404

Brehm G, Murillo-Ramos L, Sihvonen P, Hausmann A, Schmidt BC, Õunap E, Moser A, Mörtter R, Bolt D, Bodner F, Lindt A, Parra LE, Wahlberg N (2019) New World geometrid moths (Lepidoptera: Geometridae): Molecular phylogeny, biogeography, taxonomic updates and description of 11 new tribes. Arthropod Systematics & Phylogeny 77(3): 457–486.

De Carvalho MR, Bockmann FA, Amorim DS, Brandao CRF, de Vivo M, de Figueiredo JL, Britski HA, de Pinna MCC, Menezes NA, Marques FPL, Papavero N, Cancello EM, Crisci JV, McEachran JD, Schelly RC, Lundberg JG, Gill AC, Britz R, Wheeler QD, Stiassny MLJ, Parenti LR, Page LM, Wheeler WC, Faivovich J, Vari RP, Grande L, Humphries CJ, DeSalle R, Ebach MC, Nelson GJ (2007) Taxonomic impediment or impediment to taxonomy? A commentary on systematics and the cybertaxonomic-automation paradigm. Evolutionary Biology 34(3–4): 140–143. https://doi.org/10.1007/s11692-007-9011-6

Forum Herbulot (2014) Forum Herbulot 2014 statement on accelerated biodiversity assessment statement (Community Consensus Position). In: Hausmann A (Ed.) Proceedings of the eighth Forum Herbulot 2014. How to accelerate the inventory of biodiversity (Schlettau, 30 June – 4 July 2014). Spixiana 37(2): 241–242.

Hacker H, Hausmann A (2010) Obituary to Dr. Karlheinz Politzar. Esperiana Memoir 5: 35–37.

Hardwick DF (1950) Preparation of slide mounts of lepidopterous genitalia. Canadian Entomologist 82: 231–235. https://doi.org/10.4039/Ent82231-11

Hausmann A (2003) Die afrotropischen Arten der Gattung *Hypochrosis* Guenée, [1858] mit Beschreibung einer neuen Gattung (*Cherbulois* gen. nov.) und 17 neuer Arten (Lepidoptera, Geometridae, Ennominae). Spixiana 26(2): 97–128.

Hausmann A (2006) The geometrid moths of Yemen – With 50 new records for the country and description of 20 new taxa (Lepidoptera: Geometridae). Esperiana 12: 9–62, 10 colour plates.

Hausmann A, Parisi F, Sciarretta A (2016) The Geometrinae of Ethiopia II: Tribus Hemistolini, genus *Prasinocyma* (Lepidoptera: Geometridae, Geometrinae). Zootaxa 4065(1): 1–63. https://doi.org/10.11646/zootaxa.4065.1.1

Herbulot C (1966) Nouveaux Geometridae du Sud-ouest de Madagascar. Bulletin Mensuel Société Linnéenne de Lyon 35: 216–221.

Ivanova NV, Dewaard JR, Hebert PDN (2006) An inexpensive, automation- friendly protocol for recovering high-quality DNA. Molecular Ecology Notes 6: 998–1002. https://doi.org/10.1111/j.1471-8286.2006.01428.x

Kimura M (1980) A simple method for estimating evolutionary rates of base substitutions through comparative studies of nucleotide sequences. Journal of Molecular and Evolution.16(2): 111–120. https://doi.org/10.1007/BF01731581

Löbel H, Hausmann A (2019) "Geometridae mundi", a new way of summarizing the diversity of global Geometrid species. In: Hausmann A (Ed.) Proceedings of the tenth Forum Herbulot 2018. Integrative taxonomy, a multidisciplinary approach to answer complicated taxonomic questions (Stuttgart, 11–16 June 2018). Spixiana 42(2): 291–320.

Meierotto S, Sharkey MJ, Janzen DH, Hallwachs W, Hebert PDN, Chapman EG, Smith MA (2019) A revolutionary protocol to describe understudied hyperdiverse taxa and overcome the taxonomic impediment. Deutsche Entomologische Zeitschrift 66(2): 119–145. https://doi.org/10.3897/dez.66.34683

Murillo-Ramos LdC, Brehm G, Sihvonen P, Hausmann A, Holm S, Ghanavi HR, Őunap E, Truuverk A, Staude H, Friedrich E, Tammaru T, Wahlberg N (2019) A comprehensive molecular phylogeny of Geometridae (Lepidoptera) with a focus on enigmatic small subfamilies. PeerJournal 7: e7386. https://doi.org/10.7717/peerj.7386

Prout LB (1926) New Geometridae in the Tring Museum. Novitates Zoologicae 33: 179–188. https://doi.org/10.5962/bhl.part.21141

Ratnasingham S, Hebert PDN (2007) BOLD: the barcode of life data systems. Molecular Ecology Notes 7: 355–364. https://doi.org/10.1111/j.1471-8286.2007.01678.x

Riedel A, Sagata K, Suhardjono YR, Tänzler R, Balke M (2013a) Integrative taxonomy on the fast track – towards more sustainability in biodiversity research. Frontiers in Zoology 10(15). https://doi.org/10.1186/1742-9994-10-15

Riedel A, Sagata K, Surbakti S, Tänzler R, Balke M (2013b) One hundred and one new species of *Trigonopterus* weevils from New Guinea. ZooKeys 280: 1–150. https://doi.org/10.3897/zookeys.280.3906

Scoble MJ (1999) Geometrid Moths of the World: A Catalogue. CSIRO Publishing, Collingwood, Stenstrup, 1016 pp. https://doi.org/10.1071/9780643101050

Scoble MJ, Hausmann A (2007) Online list of valid and available names of the Geometridae of the world. http://www.lepbarcoding.org/geometridae/species_checklists.php

Tamura K, Stecher G, Peterson D, Filipski A, Kumar S (2013) MEGA6: Molecular Evolutionary Genetics Analysis Version 6.0. Molecular Biology and Evolution 30: 2725–2729. https://doi.org/10.1093/molbev/mst197

Tujuba TF, Sciarretta A, Hausmann A, Abate GA (2019) Lepidopteran biodiversity of Ethiopia: current knowledge and future perspectives. ZooKeys 882: 87–125. https://doi.org/10.3897/zookeys.882.36634

Van Nieukerken EJ, Kaila L, Kitching IJ, Kristensen NP, Lees DC, Minet J, Mitter C, Mutanen M, Regier JC, Simonsen TJ, Wahlberg N, Yen S, Zahiri R, Adamski D, Baixeras J, Bartsch D, Bengtsson BÅ, Brown JW, Bucheli SR, Davis DR, Prins J de, De Prins W, Epstein ME, Gentili-Poole P, Gielis C, Hättenschwiler P, Hausmann A, Holloway JD, Kallies A, Karsholt O, Kawahara AY, Koster J, Kozlov M, Lafontaine JD, Lamas G, Landry J, Lee S, Nuss M, Park K, Penz C, Rota J, Schintlmeister A, Schmidt BC, Sohn J, Solis MA, Tarmann GM, Warren AD, Weller S, Yakovlev RV, Zolotuhin VV, Zwick A (2011) Order Lepidoptera Linnaeus, 1758. In: Zhang Z-Q (Ed.) Animal biodiversity: an outline of higher-level classification and survey of taxonomic richness. Zootaxa 3148: 212–221. https://doi.org/10.11646/zootaxa.3148.1.41

Wallengren HDJ (1872) Bidrag till Södra Afrikas Fjärilfauna. Öfversigt af Kongliga Vetenskaps-Akademiens Förhandlingar 29(3): 41–61.

Warren W (1899) New Drepanulidae, Thyrididae, and Geometridae from the Aethiopian region. Novitates Zoologicae 6(3): 287–312. https://doi.org/10.5962/bhl.part.22168

Wheeler QD (2008) Taxonomic shock and awe. In: Wheeler QD (Ed.) The New Taxonomy. 76. CRC Press, Boca Raton, 211–226. https://doi.org/10.1201/9781420008562.ch10

ZooKeys 929: 79–92 (2020)
doi: 10.3897/zookeys.929.35984
http://zookeys.pensoft.net

RESEARCH ARTICLE

A peer-reviewed open-access journal
ZooKeys
Launched to accelerate biodiversity research

Geographic boundaries and natural history notes of the microendemic endangered frog *Eupsophus migueli* Formas, 1977 (Alsodidae) in the Mahuidanche Range, southern Chile

César C. Cuevas[1], Rocío Sanhueza[2]

[1] *Departamento de Ciencias Biológicas y Químicas, Universidad Católica de Temuco, Rudecindo Ortega, Casilla 15-D, Temuco, Chile* [2] *Riparia LTDA, Valdivia, Chile*

Corresponding author: *César C. Cuevas* (cesar.cuevas@uct.cl; csr.cuevas@gmail.com)

Academic editor: *J. Penner* | Received 8 May 2019 | Accepted 23 September 2019 | Published 22 April 2020

http://zoobank.org/0A16E97F-FE44-488B-A3B1-2294E77BD84B

Citation: Cuevas CC, Sanhueza R (2020) Geographic boundaries and natural history notes of the microendemic endangered frog *Eupsophus migueli* Formas, 1977 (Alsodidae) in the Mahuidanche Range, southern Chile. ZooKeys 929: 79–92. https://doi.org/10.3897/zookeys.929.35984

Abstract

Eupsophus migueli is considered a microendemic endangered species inhabiting the temperate *Nothofagus* forests of the Mahuidanche Range of southern Chile. However, this categorization is based on scarce data about its distribution and natural history. In order to assess these parameters, this article reports new geographic records obtained through intensive fieldwork between 2011 and 2016. Considering this, an updated distribution map for *E. migueli* is proposed, and new data about natural history traits and habitat use are provided. The information obtained in this study is discussed considering the zoogeographical importance of *E. migueli*, and confirms the species IUCN conservation status.

Resumen

Eupsophus migueli está considerada como una especie microendémica en peligro de extinción que habita los bosques templados de *Nothofagus* de la Cordillera de Mahuidanche, sur de Chile. Sin embargo, esta categorización está basada en poca información acerca de su distribución e historia natural. Con el fin de evaluar ambos parámetros, en este artículo se reportan nuevos registros geográficos, obtenidos de manera intensiva entre los años 2011 y 2016. De esta forma, se propone un mapa de distribución actualizado para *E. migueli*, y se presentan nuevos datos sobre los rasgos de historia natural y sobre el uso del hábitat. Los nuevos antecedentes se discuten en referencia a la importancia zoogeográfica de *E. migueli*, y reafirman su categoría de conservación.

Keywords
conservation, frogs, microendemism, new geographic records, temperate forest

Introduction

Species of the genus *Eupsophus* (Feitzinger, 1843) are endemic to the temperate *Nothofagus* forests of central and southern Chile, and part of Argentina.

These species have a wide distribution range, being found from the remnant Maulino forest in the north (35°50'1.92"S, 72°30'36.31"W), to Isla Wellington in the south (46°25'S, 72°04'W) (Núñez et al. 2012). The extent of occurrence of the genus is about 191,978 km², however, microendemic conditions have been documented for *E. septentrionalis* (Ibarra-Vidal et al. 2004, Veloso et al. 2005), *E. insularis* (Formas and Vera 1982), *E. contulmoensis* (Ortiz et al. 1989), *E. nahuelbutensis* (Ortiz and Ibarra-Vidal 1992), *E. altor* (Núñez et al. 2012) and *E. migueli* (Formas 1979, Méndez et al. 2005). Here, we discuss the case of the microendemic frog *Eupsophus migueli* Formas, 1977.

Eupsophus migueli has been described in the Coastal Range of southern Chile. For a long time, its known distribution range was restricted only to a few sites neighbouring the type locality (Mehuín, 39°25'42.46"S, 73°12'42.35"W), covering an area of no more than 2.4 km². Later, its northern limit was located near Queule (39°22'S, 73°08'W; Méndez et al. 2005), seven kilometers north of the type locality (see Fig. 1). Although, Correa et al. (2017) synonymized *E. altor* with *E. migueli* extending the range of *E. migueli* south to the Lingue River, Suárez-Villouta et al. (2019) hypothesised that both are good species restoring the previous taxonomic situation. Bradford and Jaffré (2004) suggested that highly restricted endemism's, like the one exhibited by *E. migueli*, are typically attributed to a complex interplay of climatic, topographic, and geologic diversity, derived from environments with unique geography and severe levels of native habitat fragmentation. Although the microendemic status of *E. migueli* seems plausible in accordance with the description provided by Bradford and Jaffré (2004), intensive geographic studies have not been feasible since the species' description. Hence, we hypothesize that the highly restricted distribution of *E. migueli* is actually due to insufficient field sampling. Therefore, based on the compilation of sufficient data, its status as a microendemic species could be questioned. Consequently, the present study describes results of an exhaustive fieldwork conducted between 2011 and 2016, eastward and northward from the type locality of *E. migueli*. Finally, we comment on the taxonomic status of *E. migueli* and, on the base of all records available, we reassess and confirm its current conservation status according to the Chilean Regulation for Species Classification (RCE in spanish) and the International Union for Conservation of Nature (IUCN) Red List criteria.

Materials and methods

Study area

The study took place in a section of the Chilean Coastal Range known by the locals as Cordillera de Mahuidanche (about 55 km long and 20 km wide, with a maximum altitude 715 m a.s.l.). This mountain range is located in southern Chile between the mouths of Toltén (39°01'S, 73°06'W, Cautín Province) and Valdivia rivers (39°52'S, 73°23'W, Valdivia Province). The surveyed area comprises a polygon extending from south to north from the northern bank of the Lingue River (Mariquina, Los Ríos Region) to the southern bank of the Toltén River (Toltén, Araucanía Region); and from west to east, from the slopes of the Mahuidanche mountain (Lastarria, Araucanía Region), to the border between La Araucanía and Los Ríos Regions. The study area covered about 833.331 km^2 (Fig. 1).

The vegetation of the study area is characterized by the presence of the Laurifolia plant community, typically associated to the Valdivian rain forest (Gajardo 1993). Such community has been modified by human action, appearing today mostly forming remnants of mixed relict vegetation, belonging primarily to the associations of roble-laurel-lingue and temo-pitra in hillocks and low-lying areas, respectively (Hauenstein et al. 2002). Parts of these native forest remnants have been considered a priority for the conservation of biodiversity (CONAMA 2002).

Taxonomic criteria

Formas (1977), based on external morphometric, morphological qualitative characters, and chromosomic attributes, described *E. migueli*. Formas (1989) divided *Eupsophus* in two groups: "roseus" group (species presenting chromosome formula 2n = 30, snout–vent length < 6 cm; *E. altor*, *E. calcaratus*, *E. contulmoensis*, *E. insularis*, *E. migueli*, *E. nahuelbutensis*, *E. roseus* and *E. septentrionalis*), and the "vertebralis" group (species with 2n = 28, adult snout- vent length > 6 cm; *E. vertebralis* and *E. emiliopugini*). Correa et al. (2017) hypothesized that several species of the *Eupsophus* "roseus" group were synonyms, decreasing their number from eight to four. Among these, *E. altor* was synonymized with *E. migueli* increasing the range of the latter. Correa et al. (2017) downplay some diagnostic characters that identify *E. altor* (Núñez et al. 2012). They argue that the karyotype, the maximum frequency of the spectral elements of the mating call, the morphometric analyses, and the lack of knowledge about the reproductive cycle and the larva of *E. migueli*, do not allow the differentiation of two species (see Núñez et al. 2012). Subsequently, Suárez-Villouta et al. (2019) based on a new molecular analysis (including coalescence tests) concluded that the eight species recognized in the "roseus" group before the work of Correa et al. (2017) were valid, which was corroborated by Correa and Durán (2019). In summary, in this work we consider the "roseus" group to contain eight described species. Thus, in order to avoid confusion between the species of the "roseus" group potentially present in the study area, specific determination of frogs in the field followed the original diagnosis provided by Formas (1977) for *E. migueli*, Formas and Vera (1982) for *E. roseus* and *E. calcaratus* and by Núñez et al. (2012) for *E. altor*.

For genus nomenclature we followed Feitzinger (1843) and Pyron and Wiens (2011) for the family taxonomy.

Sampling

Systematic and standardized searches were conducted by applying Visual Encounter Surveys and time constrained search methods (Bury and Raphael 1983, Crump and Scott 1994) on transects of 100 m in length with a fixed width of 3 m. Searches were conducted in terrestrial environments within remnants of native secondary and mature forest, and exotic plantations. We focussed on adult frogs, performing a thorough visual examination of the area, and paying special attention to any possible shelters under rocks, logs, branches and leaves.

Calculations of two important IUCN criteria AOO (area of occupancy) and EOO (extent of occurrence) in km^2, were done with GeoCAT (Geospatial Conservation Assessment) software (Bachman et al. 2011). The AOO calculation was based on a default IUCN value of 2 km.

Specimens

Each collected specimen was placed into an individual plastic box, labelled with a characteristic colour and number. Collection sites were georeferenced and marked with the same colour of the respective specimen. Specimens were then transported to a near workstation, where they were measured with a calliper to the nearest 0.1 cm and photographed. Subsequently, each specimen was released at the exact place of capture. This study was conducted in strict accordance with published biosafety protocols in order to protect the health of amphibian populations, which involved the use of nitrile gloves and Virkon to disinfect any material used during the surveys (Soto-Azat et al. 2013). Sampling permits were granted by the Agricultural and Livestock Service (SAG) according to resolutions No. 4494/2012 and 5088/2016 to C. Cuevas.

As no specimens were taken away from their habitat, the taxonomic determination of specimens as *E. migueli* in all the new localities reported in this work was obtained through photography and analysis of live specimens (froglets and adults) during field trips conducted between 2011–2012 (August to November both years) and 2014–2016 (January to December both years). In one of the field trips, we were accompanied by the authority of the species *E. migueli* (Dr R. Formas), who confirmed the taxonomic determination of the specimens. Although some morphological variation was detected (see Fig. 2), all specimens were identified as *E. migueli* by the following combination of external characters: yellow iris and belly with whitish reticulations on a wine base (Formas 1977).

Results and discussion

New locality records reported here are located north of the town of Queule (Región de La Araucanía, Coastal Range), and south east of the village of Mehuín (Región de Los Ríos) (Table 1, Fig. 1). Some of the new localities, were detected during field trips conducted in 2007 by one of us (R. Sanhueza) and revisited for this study.

Early records considered herein include: Quebrada Casanova (Mehuín, type locality), Pichicuyín, and Queule located northern of Lingue River (Méndez et al. 2005). We also included others records reported by Contreras (2014) and Miranda (2015) (see map in Fig. 1). The taxonomic criteria used in this work to determine the specimens of *E. migueli* in the field, agrees with the results obtained by Suárez-Villouta et al. (2019), recognizing this taxon as a specific taxonomic unit different from *E. altor*. In this work we assume the conclusions of Suárez-Villouta et al. (2019), therefore, we consider the distribution of *E. migueli* from the Lingue River to the north. Consequently, all data available allows for the establishment of a broader distribution range for *E. migueli.* These new records reach ≈ 200 km^2 extending its range to the north, northeast and east of the previously known range of the species. Old and new localities (names, coordinates and additional data) are shown in Table 1.

External variation

Some froglets specimens detected from Boroa Norte in 2007 (Espinoza 2008, Sanhueza 2013) were misidentified as other *Eupsophus* spp., due to their iris colour and a very polymorphic dorsal pattern of pigmentation. In fact, the yellow colour of the iris of *E. migueli* is also shared with *E. altor* and *E. calcaratus*, however, their belly in a wine like pattern (Formas 1977) is quite different from both *E. calcaratus* and *E. altor*. In *E. altor* and *E. calcaratus* the belly is translucent (skin colour in *E. altor*), in addition, *E. calcaratus* exhibits a very characteristic black ribbon on the flanks of the head extending from the nares to the insertion of the forearms (Formas and Vera 1982). Moreover, *E. calcaratus* has never been reported north of the Valdivia River in Los Ríos Region (70 km south). Méndez et al. (2005) reported a population from the Mississippi locality south of the Lingue River (near Mehuín, type locality of *E. migueli*), however, the authors may have mistakenly identified specimens of *E. altor* as *E. calcaratus*. The current study confirms that identification as erroneous, since one of us (C. Cuevas) identified an *E. altor* specimen at the border of the Quilatrayen Stream (39°27'47.98"S, 73°9'18.68"W) (south of Lingue River) in December of 2015. This place is located 7 km north-east from the site reported by Méndez et al. (2005).

Specimens detected during our field work present intermediate patterns of pigmentation on the belly, as well as on the dorsum. Some specimens from El Socorro and Boroa Norte showed the back almost totally yellowish. Froglets and adults of *E. migueli* differed strongly in their dorsal colour patterns, especially those detected in El Socorro and Boroa Norte. Formas (1977) reported three different dorsal and ventral colour patterns in specimens from the type locality (Quebrada Casanova, Mehuín). The belly

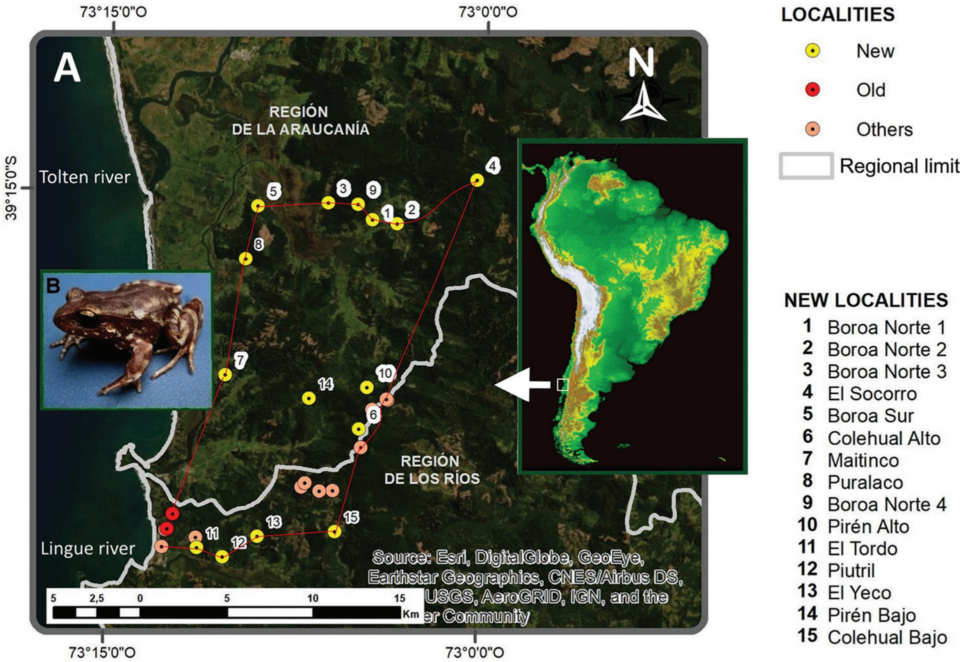

Figure 1. A Distribution map of *Eupsophus migueli*. The red polygon corresponds to an updated distribution area of *E. migueli*, and it is formed by georeferenced landmarks including new records (this paper), old records (including the type locality, Mehuín, and nearby localities Queule and Pichicuyín) and other documented points (Méndez et al. 2005, Contreras 2014, Miranda 2015) **B** specimen of *E. migueli* from Colehual Alto.

Table 1. New localities, coordinates and data (year, month, number (*N*) and mode of detection: calling (c) and/or visual (v)) of *E. migueli* specimens recorded during fieldwork reported in this paper.

ID	Locality	Coordinates	High	Year (month)	*N*	Detection
1	Boroa N 1	39°15'14.87"S, 73°06'16.91"W	4	2007–2015 (Jan)	20/1	v/c
2	Boroa N 2	39°15'44.72"S, 73°04'29.82"W	66	2007 (May)	10	v
3	Boroa N 3	39°14'57.44"S, 73°05'28.45"W	274	2007 (May)–2015 (Jan, Mar)	5/13	v
4	El Socorro	39°12'57.52"S, 73°00'45.32"W	450	2007 (Feb)–2015 (Mar)	10/7	v/c
5	Boroa Sur	39°15'04.15"S, 73°09'08.07"W	37	2011 (Sep)	5	c
6	Colehual Alto	39°22'28.83"S, 73°04'53.52"W	650	2011 (Sep)	13	c
7	Maitinco	39°20'45.23"S, 73°10'16.27"W	23	2011 (Nov)	3	v/c
8	Puralaco	39°17'04.83"S, 73°09'32.75"W	19	2012 (Aug)	5	c
9	Boroa N 4	39°15'17.23"S, 73°06'01.53"W	53	2015 (Apr)	4	v/c
10	Pirén Alto	39°21'38.91"S, 73°04'38.69"W	540	2015 (Apr)	7	v
11	El Tordo	39°26'07.55"S, 73°11'17.09"W	30	2015 (Dec)	2	c
12	Piutril	39°26'24.29"S, 73°10'14.37"W	40	2015 (Dec)	1	v
13	El Yeco	39°25'44.44"S, 73°08'52.00"W	86	2015 (Dec)	2	v
14	Pirén Bajo	39°21'24.12"S, 73°06'52.80"W	450	2016 (Dec)	3	v
15	Colehual Bajo	39°25'32.88"S, 73°05'44.97"W	282	2016 (Dec)	2	v

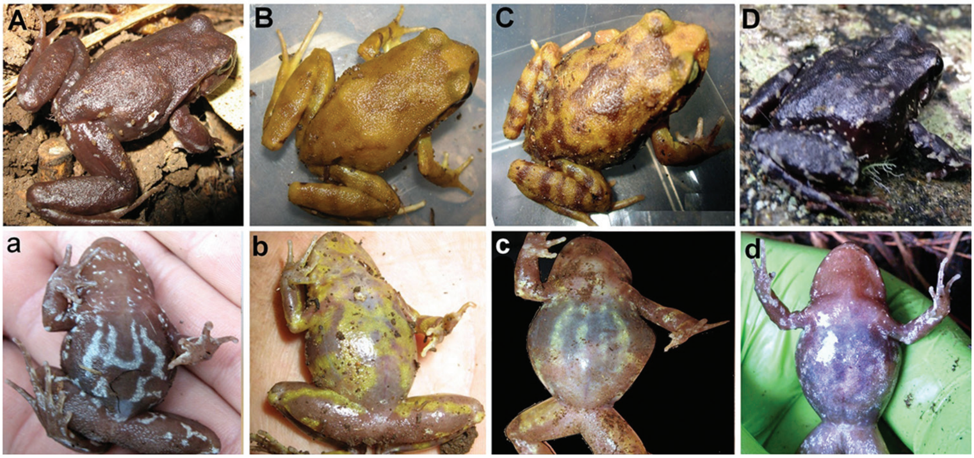

Figure 2. Dorsal (capitals) and ventral (lowercase) patterns of pigmentation in *Eupsophus migueli* from different localities along its distribution range. **A** Dorsal pattern of dark brown (Socorro) **a** ventral white with longitudinal spots (El Socorro, Boroa Norte) **B** dorsal yellow pattern and **b** belly with yellow crosslinks (El Socorro) **C** dorsal pattern yellow with brown spots and **c** belly with yellow longitudinal spots (El Socorro, Boroa Norte) **D** dorsal pattern dark brown and **d** belly with whitish faded spots. All specimens were adults ranging in size from 4 to 5 cm.

pattern showed a variation ranging from almost entirely dark with small white spots to completely white. Formas (opus cit.) suggested that the colour pattern for *E. roseus* and *E. migueli* were basically the same. However, when we compared both species, very different patterns were observed. Dorsal pigmentation in *Eupsophus roseus* ranges from the typical red (*roseus*) to dark with white bars on the dorsum and limbs (tabby like) with the belly having flesh-like tones. Conversely, most *E. migueli* specimens do not present spots or bars on the legs, and the belly has reticulations in different tones and patterns, but never flesh-coloured. Moreover, *E. roseus* and *E. calcaratus* present small whitish bars in the loreal region, which are not present in *E. migueli*. Figure 2 shows four new patterns of dorsal and ventral pigmentation for specimens of *E. migueli* from new localities considered in this study.

Reproductive strategy

A nidicolous reproductive strategy has been described for *E. altor*, *E. calcaratus*, *E. emiliopugini*, and *E. vertebralis* (Vera-Candioti et al. 2005, Núñez and Úbeda 2009, Núñez et al. 2012). The presence of calling males of *E. migueli* hidden in the moss or between roots of bushes on the banks of small streams, and the finding of newly metamorphosed frogs in the same environments in early austral spring, suggests that *E. migueli* exhibits this same strategy of larval development. At least 45 to 50 eggs can be found in each nest (ground cavity), which are cared by the male parent (Núñez et al. 2012). In mid-January 2017, a nest with 14 larvae in an advanced stage (42) of development was found on the banks of a stream in Pirén Bajo (Cuevas Personal observation). However, the male was no longer in the nest, therefore, the larvae could belong to *E. migueli* or *E. vertebralis*, considering both species have endotrophic tadpoles without a free-swimming phase (Formas 1979, Vera-Candioti et al. 2011, Núñez et al. 2012), and both species are sympatric in this area. Endotrophy has been considered an adaptive condition to the humid ground of the *Nothofagus* forest (Formas 1979, Cuevas and Cifuentes 2009) and is shared with other species that present parental care such as *Rhinoderma* spp. (Formas 2013) whose larvae are developed into the guttural sac (Formas et al. 1975).

Habitat preferences

In the last four decades, *Nothofagus* forests of the Coastal Range (33° to 38° South) have been disturbed and destroyed to a large extent by anthropogenic activities, including agriculture and forestation (Smith-Ramírez 2005). In addition, forest fires have also caused an important loss of native forest during summer months (Cuevas and Cifuentes 2009). Subsequently, the forest matrix has changed from native to mixed, being in many cases the dominant matrix (Lara et al. 2012). All these threats have important consequences in the quality and quantity of habitat available for the frogs, and represent one of the most important causes of their decline (IUCN 2019).

In these degraded forests, the detection of *E. migueli* occurred in four different habitats as follows (see Fig. 3): a) In **ecotonal zones**, adult males were detected by their advertisement call between August and the end of October (austral spring) on the banks of small streams (1 to 1.5 m wide; 20 cm deep) surrounded by swampy areas with a lot of moss and mud. In the same habitats, froglets (5–10 mm SVL) were found camouflaged among dried leaves, moss, and small wet branches near places where adults make their nests in the mud in early spring (September) until February (exceptionally); b) In **renewal forest**, adults (males and females), pre-adults and juveniles were collected among the leaf litter, under fallen logs and rocks, both on the shore and inland forest between December and May; c) In **pine monocultures,** adults were encountered under fallen branches or logs in April, d) In **remnant native forest**, adult frogs were found among the soil litter (dry leaves) and under fallen logs. In summary, from late winter to October adults were located through their vocalizations. Then, and until late summer, adults were found only through direct searches between the litter near water courses. During autumn, individuals were found hidden in refuges under fallen logs and rocks without emitting vocalizations, being detected exclusively by active searching. These findings suggest that *E. migueli* specimens move between streams and the inner forest after the breeding season.

In the aforementioned habitat, *E. migueli* was found to be sympatric with *E. vertebralis*, *Batrachyla taeniata*, *B. leptopus*, *Pleurodema thaul* and *Rhinoderma darwinii*

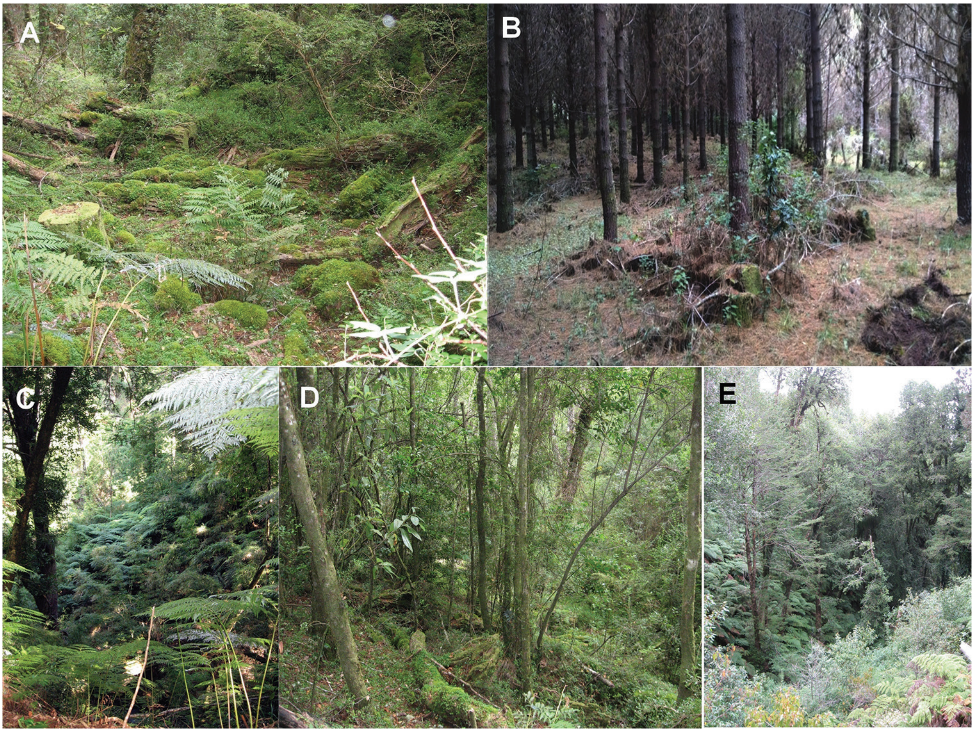

Figure 3. Habitat of *Eupsophus migueli* **A, D** native forest with anthropogenic disturbance in Boroa Norte 1 **B** pine monoculture with undergrowth habitat of *Aristotelia chilensis* in Boroa Norte 4 **C, E** native forest in El Socorro.

all along its distribution range (unpublished data). In fact, during the current study, mating calls from *B. leptopus*, *E. vertebralis* and *P. thaul* were detected; however, those differ notably from that of *E. migueli* (Penna and Veloso 1990). Lastly, *E. roseus* was also recorded in the area, although never at the same sites as *E. migueli*, suggesting that these are parapatric species (Cuevas pers. observation).

Conservation status

Currently, *E. migueli* is categorized as "Endangered" and "Rare" by the Species Classification Regulation of the Ministry of Environment of Chile (MINSEGPRES 2008), according to criteria **B1ab (iii)** (< 5000 km^2 presence extension) **+ B2ab (iii)** (< 500 km^2 occupancy area). The species has also been categorized as "Endangered" by the IUCN **B1ab (iii)** (IUCN 2017). In both categorizations, **B1** states that the EOO is estimated to be less than 5,000 km^2. **B1a** states that their habitat is severely fragmented or the species is known to exist at no more than five locations, and **(iii)** states that a continued decline is observed in the area, extent and quality of habitat.

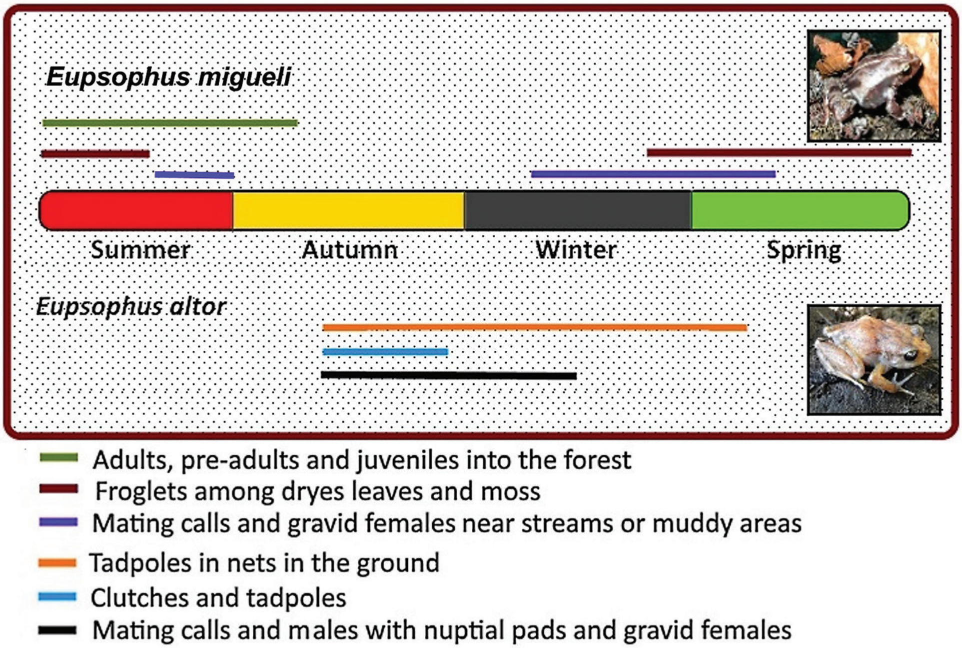

Figure 4. Scheme of the life history data of *E. migueli* (this paper) and *E. altor*. Data for *E. altor* were obtained from Núñez et al. (2012).

Criterion **B2**, indicates an estimated area of occupancy of less than 500 km^2, and **B2a** states that the habitat is severely fragmented, or the species is known to exist at no more than five locations, and **(iii)** establishes a continued decline observed in the area, extent and quality of habitat. Based on our surveys, both criteria are still valid regarding *E. migueli* status. The new data indicates its presence in more than five locations and new localities increase its range area from 3.223 km^2 (corresponding to type location) to over 200 km^2. Thus, the estimated values for AOO and EOO IUCN criteria was 80,000 km^2, and 223,811 km^2 respectively. Accordingly, *E. migueli* must remain categorized as an "Endangered" species.

On the other hand, the application of the criterion "rare species" must be revised in the case of *E. migueli*. This criterion explicitly refers to very infrequent species, and based on the surveys described here, it may have been misapplied in this case. This study verifies that *E. migueli* is a common species in the area.

Conclusions

The finding of additional *E. migueli* populations in small fragments within the Valdivian rainforest, and even into *Pinus* monoculture (with abundant native understory), has important implications for conservation. These findings raise questions regarding new practices for *Pinus* and *Eucalyptus* harvesting, and for vegetation management of streams, all of which are legislated in Chile. As it has been reported before, although these environments are not optimal for amphibians, they may indeed sustain some populations, as long as they have the minimal structural conditions of the undergrowth and microclimatic conditions (temperature, relative humidity, pH). However, the amphibian fauna detected in these altered environments remains in a "vulnerable" status which can be seriously affected if forest management (silviculture) interventions, such as, thinning and harvesting are not handled as "controlled disruptions" to mitigate their impacts. Disregarding these measures entails a serious risk for the amphibian diversity in the region.

Historically, the majority of the Mahuidanche Range has been covered by temperate *Nothofagus* forests (see Formas 1979, Veblen and Schlegel 1982). However, today the western slopes exhibit a high degree of human intervention (*Pinus* and *Eucalyptus* plantations, cattle raising and clearing of the native forest). Despite this, two recently described amphibians, *Alsodes norae* and *Eupsophus altor*, have been reported in the area (Cuevas 2008, Núñez et al. 2012). These species as well as *E. migueli*, *Insuetophrynus acarpicus*, *Telmatobufo australis* and in some cases *Rhinoderma darwinii* can all be found in native forest remnants. Such diversity makes the Cordillera de Mahuidanche a location of great zoogeographical and conservation interest.

Acknowledgements

The authors greatly appreciate to Don Atalibar Sanhueza, Sofía Pichilen, Milo Bustamante, Manuel Hernández Nieto, and the company Masisa S.A., for granting the corresponding permits to carry out amphibian surveys on their properties in the Coastal Range of southern Chile. To Dr Ramón Formas for his valuable help in field work and identification of *E. migueli* specimens. Also, we thank Gonzalo Rebolledo for his assistance during fieldwork and cartographical support, and Dr Claudio Soto-Azat and Dra Alexandra Peñafiel for comments and English editing through the manuscript. RS wish to thank to Dr Jaime Rau and the Program of Magister en Ciencias mención Producción, Conservación y Manejo de Recursos Naturales, Universidad de Los Lagos, Chile, for their support in the first stage of this work.

References

Bachman S, Moat J, Hill A, de la Torre J, Scott B (2011) Supporting Red List threat assessments with GeoCAT: geospatial conservation assessment tool. In: Smith V, Penev L (Eds) e-Infrastructures for data publishing in biodiversity science. Zookeys 150: 117–126. https://doi.org/10.3897/zookeys.150.2109

Bradford J, Jaffré T (2004) Plant species microendemism and conservation of montane maquis in New Caledonia: two new species of *Pancheria* (Cunoniaceae) from the Roche Ouaïème Biodiversity and Conservation 13: 2253. https://doi.org/10.1023/B:BIOC.0000047901.33761.3c

Bury R, Raphael M (1983) Inventory methods for amphibians and reptiles. In: Bell J, Atterbury T (Eds) Renewable Resource Inventories for Monitoring Changes and Trends. Oregon State University, Corvallis, 416–419.

CONAMA (2002) Estrategia Regional de Conservación y Uso Sustentable de la Biodiversidad – Región de La Araucanía. Comisión Nacional del Medio Ambiente. 170 pp.

Contreras C (2014) Diversidad de anfibios en un transecto longitudinal de la Cordillera de la Costa valdiviana, Chile. Trabajo de Titulación presentado como parte de los requisites para optar al título de Ingeniero en Conservación de Recursos Naturales. Facultad de Ciencias, Universidad Austral de Chile, 47 pp. [+ anexos]

Correa C, Durán F (2019) Taxonomy, systematics and geographic distribution of ground frogs (Alsodidae, *Eupsophus*): a comprehensive synthesis of the last six decades of research. Zookeys 863: 107–152. https://doi.org/10.3897/zookeys.863.35484

Correa C, Vasquez D, Castro-Carrasco C, Zuñiga-Reinoso A, Ortiz JC, Palma RE (2017) Species delimitation in frogs from South American temperate forests: The case of *Eupsophus*, a taxonomically complex genus with high phenotypic variation. PLoS ONE 12(8): e0181026. https://doi.org/10.1371/journal.pone.0181026

Crump M, Scott N (1994) Visual encounter surveys. In: Heyer WR, Donnelly MA, McDiarmid RW, Hayek LC, Foster MS (Eds) Measuring and Monitoring Biological Diversity: Standard Methods for Amphibians. Smithsonian Institution Press, Washington, 84–92.

Cuevas CC (2008) A new species of the genus *Alsodes* (Anura: Neobatrachia) from the *Nothofagus* forest, Coastal Range, Southern Chile, identified by its karyotype. Zootaxa 1771: 43–53. https://doi.org/10.11646/zootaxa.1771.1.4

Cuevas CC, Cifuentes SL (2009) Frogs and life strategies: an approach to evaluate forest ecosystems health in southern Chile. In: Oyarzún CE, Hoerst N (Eds) Ecological Advances in Temperate Rain Forest. Academic Press, Gent, 17–30.

Espinoza L (2008) Efectos de la fragmentación y tipo de hábitat sobre la distribución de anfibios en la cordillera de la costa de la Región de La Araucanía. Tesis para optar al grado de Licenciado en Recursos Naturales. Escuela de Ciencias Ambientales, Facultad de Recursos Naturales, Universidad Católica de Temuco, 110 pp.

Feitzinger LJ (1843) Systema Reptilium. Fasciculus Primus. Braumüller et Seidel, Wien, 31.

Formas JR (1977) A new species of leptodactylid frog (*Eupsophus*) from the coastal range in Southern Chile. Studies on Neotropical Fauna and Environment 13: 1–9. https://doi.org/10.1080/01650527809360528

Formas JR (1979) La herpetofauna de los bosques templados de Sudamérica. In: Duellman WE (Ed.) The South American Herpetofauna. Museum of Natural History, University of Kansas, Lawrence, Kansas, Monograph 7: 341–379.

Formas JR (1989) A new species of *Eupsophus* (Amphibia: Anura: Leptodactylidae) from southern Chile. Proceedings of the Biological Society of Washington 102: 568–576.

Formas R, Pugin E, Jorquera B (1975) La identidad del batracio chileno *Heminectes rufus* Philippi, 1902. Physis 34: 147–157.

Formas JR, Vera MA (1982) The status of two Chilean frogs of the genus *Eupsophus* (Anura: Leptodactylidae). Proceedings of the Biological Society of Washington 95: 594–601.

Gajardo R (1993) La vegetación natural de Chile. Clasificación y distribución geográfica. Editorial Universitaria, 165 pp.

Hauenstein E, González M, Peña-Cortés F, Muñoz-Pedreros AM (2002) Clasificación y caracterización de la flora y vegetación de los humedales de la costa de Toltén, IX Región, Chile. Gayana Botánica 59: 91–104. https://doi.org/10.4067/S0717-66432002000200006

IUCN Standards and Petitions Committee (2019) Guidelines for using the IUCN Red List Categories and Criteria. Version 14. Prepared by the Standards and Petitions Committee. http://www.iucnredlist.org/documents/RedListGuidelines.pdf

Ibarra-Vidal H, Ortiz JC, Torres-Pérez F (2004) *Eupsophus septentrionalis* n. sp., nueva especie de Leptodactylidae (Amphibia) de Chile central. Boletín de la Sociedad Biológica de Concepción 75: 91–102.

Lara A, Solari M, Prieto MDR, Peña MP (2012) Reconstrucción de la cobertura de la vegetación y uso del suelo hacia 1550 y sus cambios a 2007 en la ecorregión de los bosques valdivianos lluviosos de Chile (35°–43°, 30'S). Bosque 33: 13–23. https://doi.org/10.4067/S0717-92002012000100002

Méndez MA, Torres-Pérez F, Correa C, Soto ER, Veloso A, Armesto J (2005) Genetic divergence in the endangered frog *Insuetophrynus acarpicus* (Anura: Leptodactylidae). Herpetological Journal 16: 93–96.

MINSEGPRES, Ministerio Secretaría General del Presidencia (2008) Decreto Supremo N°50. Aprueba y oficializa nómina para el Segundo Proceso de Clasificación de Especies según su Estado de Conservación. Gobierno de Chile.

Miranda P (2015) Catastro de anfibios En Peligro y En Peligro Crítico de la Cordillera de Queule, Región de Los Ríos, Chile. Trabajo de Titulación presentado como parte de los requisitos para optar al título de Ingeniero en Conservación de Recursos Naturales. Facultad de Ciencias, Universidad Austral de Chile, 42 pp. [+ anexos]

Núñez JJ, Úbeda CA (2009) The tadpole of *Eupsophus nahuelbutensis* (Anura: Neobatrachia): external morphology, chondrocranium, and comments on its natural history. Zootaxa 2126: 58–68. https://doi.org/10.11646/zootaxa.2126.1.3

Núñez J, Rabanal F, Formas R (2012) Description of a new species of *Eupsophus* (Amphibia: Neobatrachia) from the Valdivian Coastal rage, Southern Chile: an integrative taxonomic approach. Zootaxa 3305: 53–68. https://doi.org/10.11646/zootaxa.3305.1.3

Ortiz JC, Ibarra-Vidal H (1992) Una nueva especie de Leptodactylidae (*Eupsophus*) de la Cordillera de Nahuelbuta (Chile). Acta Zoológica Lilloana (Argentina) 41: 75–79.

Ortiz JC, Ibarra-Vidal H, Formas R (1989) A new species of *Eupsophus* (Anura: Leptodactylidae) from Contulmo, Nahuelbuta range, southern Chile. Proceedings of the Biological Society of Washington 102: 1031–1035.

Penna M, Veloso AM (1990) Vocal diversity in frogs of the South American temperate forest. Journal of Herpetology 24: 23–33. https://doi.org/10.2307/1564285

Pyron RA, Wiens JJ (2011) A large-scale phylogeny of Amphibia including over 2800 species, and a revised classification of advanced frogs, salamanders, and caecilians. Molecular Phylogenetics and Evolution 61: 543–583. https://doi.org/10.1016/j.ympev.2011.06.012

Sanhueza R (2013) Efectos de la fragmentación del bosque nativo en mamíferos no voladores y anfibios en la Cordillera de la Costa de la Araucanía. Tesis Magíster en Ciencias, Mención Producción, Manejo y Conservación de Recursos Naturales. Universidad de Los Lagos. Vicerrectoría de Investigación y Postgrado, Escuela de Postgrado, Osorno, 103 pp.

Smith-Ramírez C (2005) The Chilean coastal range: a vanishing center of biodiversity and endemism in South American temperate forest. Biodiversity and Conservation 13: 373–393. https://doi.org/10.1023/B:BIOC.0000006505.67560.9f

Soto-Azat C, Valenzuela-Sánchez A, Collen B, Rowcliffe JM, Veloso A, Cunningham AA (2013) The Population Decline and Extinction of Darwin's Frogs. PLoS ONE 8(6): e66957. https://doi.org/10.1371/journal.pone.0066957

Suárez-Villouta EY, Quercia CA, Díaz LM, Vera-Sovier VA, Núñez JJ (2019) Speciation in a biodiversity hotspot: phylogenetic relationships, species delimitation, and divergence times of the Patagonian ground frogs of *Eupsophus roseus* group (Alsodidae). https://doi.org/10.1101/423202

Veblen TT, Schlegel FM (1982) Reseña ecológica de los bosques del sur de Chile. Bosque (4)2: 73–115. https://doi.org/10.4206/bosque.1982.v4n2-03

Veloso A, Celis Diez JL, Guerrero PC, Méndez MA, Iturra P, Simonetti JA (2005) Description of a new *Eupsophus* species (Amphibia, Leptodactylidae) from the remnants of Maulino forest, Central Chile. Herpetological Journal 15: 159–165.

Vera-Candioti MF, Úbeda C, Lavilla EO (2005) Morphology and metamorphosis of *Eupsophus calcaratus* tadpoles (Anura: Leptodactylidae). Journal of Morphology 264(2): 161–177. https://doi.org/10.1002/jmor.10320

Vera-Candioti MF, Núñez JJ, Úbeda C (2011) Development of the nidicolous tadpoles of *Eupsophus emiliopugini* (Anura: Cycloramphidae) until metamorphosis, with comments on systematic relationships of the species and its endotrophic developmental mode. Acta Zoologica 92: 27–45. https://doi.org/10.1111/j.1463-6395.2010.00448.x

ZooKeys 929: 93–115 (2020)
doi: 10.3897/zookeys.929.49748
http://zookeys.pensoft.net

RESEARCH ARTICLE

A peer-reviewed open-access journal
ZooKeys
Launched to accelerate biodiversity research

A new species of the toothed toad *Oreolalax* (Anura, Megophryidae) from Sichuan Province, China

Yinmeng Hou[1,2,3,*], Shengchao Shi[1,3,*], Daming Hu[2], Yue Deng[2], Jianping Jiang[1], Feng Xie[1,*], Bin Wang[1,*]

1 *CAS Key Laboratory of Mountain Ecological Restoration and Bioresource Utilization and Ecological Restoration Biodiversity Conservation Key Laboratory of Sichuan Province, Chengdu Institute of Biology, Chinese Academy of Sciences, Chengdu 610041, China* **2** *Management Center of Sichuan White River National Nature Reserve, Pengzhou 611900, China* **3** *University of Chinese Academy of Sciences, Beijing 100049, China*

Corresponding author: Bin Wang (wangbin@cib.ac.cn); Feng Xie (xiefeng@cib.ac.cn)

Academic editor: A. Ohler | Received 30 December 2019 | Accepted 24 March 2020 | Published 22 April 2020

http://zoobank.org/0C8EC8A1-CA52-4478-A7D2-47D3B167BB51

Citation: Hou Y, Shi S, Hu D, Deng Y, Jiang J, Xie F, Wang B (2020) A new species of the toothed toad *Oreolalax* (Anura, Megophryidae) from Sichuan Province, China. ZooKeys 929: 93–115. https://doi.org/10.3897/zookeys.929.49748

Abstract

The toad genus *Oreolalax* is widely distributed in southwest China and northern Vietnam. A new species of the genus is described from Sichuan Province, China. Phylogenetic analyses based on the mitochondrial 12S rRNA and 16S rRNA gene sequences supported the new species as an independent clade clustered into the clade also containing *O. nanjiangensis* and *O. chuanbeiensis*. The new species can be distinguished from its congeners by a combination of the following characters: body size moderate (SVL 51.2–64.2 mm in males); head broad; tympanum hidden; interorbital region with dark triangular pattern; belly with marbling; male lacking spines on lip margin; spiny patches on chest small with thick sparse spines in male; nuptial spines thick and sparse; tibio-tarsal articulation reaching beyond nostril when leg stretched forward; toe webbing at base.

Keywords

Molecular phylogenetic analyses, morphology, southwest China, taxonomy

---

[*] These authors have contributed equally to this work.

Introduction

The toothed toad genus *Oreolalax* Myers & Leviton, 1962 belongs to Leptobrachiinae Dubois, 1980 of Megophryidae Bonaparte, 1850 (Amphibia, Anura). The genus currently contains 18 species (see list of Frost 2019), of which 17 species are known from southwestern China throughout the provinces of Sichuan, Shaanxi, Guizhou, Yunnan, Chongqing, Hunan, and Hubei (Fei et al. 2012, 2016), and one from northernmost Vietnam (Nguyen et al. 2013). Roy et al. (2018) noted one specimen of *Oreolalax* from northeastern India, but the photo of the specimen (Roy et al. 2018: fig. 1f) seems to fit the generic characters of the genus *Scutiger* Theobald, 1868 (according to keys in Fei et al. 2016). Toads of *Oreolalax* inhabit mountain forests at elevations between ca. 500 and 3300 m a.s.l. (Fei et al. 2009, 2012, 2016; Nguyen et al. 2013).

Although taxonomic assignments of the genus *Oreolalax* have been controversial for decades (Liu 1950; Dubois 1980, 1983, 1986; Huang 1991; Zhao and Adler 1993; Dubois and Ohler 1998; Delorme 2001; Wei et al. 2007, 2009; Fei et al. 1989, 1990, 2005, 2009), most phylogenetic studies indicated the genus as a monophyletic group (Xu et al. 1992; Fu et al. 2007; Wei et al. 2009; Pyron and Wiens 2011; Nguyen et al. 2013), and most recent taxonomic arrangements also regarded it as a distinct genus (e.g., Fei et al. 2012, 2016; Frost et al. 2019). As noted, the phylogenetic relationships between many species of the genus have been not resolved (Fu et al. 2007; Nguyen et al. 2013) although species of the genus in China had been divided into several species groups based on morphology (Fei et al. 2005, 2009).

Hengduan Mountains with the adjacent eastern mountains were suggested as the centre of origin and differentiation of the *Oreolalax* toads (Fei et al. 1989) in view of twelve species (66.7% of total number 18) being distributed in the narrow but long zone in the central southern part of Hengduan Mountains (Fei et al. 2012, 2016). As well, this region forms an important part of a biodiversity hotspot (Myers et al. 2000), and is expected to support underestimated species diversity. However, for two decades, no new species of *Oreolalax* has been reported in China, being much poorer on species diversity in contrast to the high species richness of the co-family genera *Megophrys* Kuhl & Van Hasselt, 1822 and *Leptobrachella* Smith, 1925 (e.g., Li et al. 2018; Zhang et al. 2017), and still contain dozens of cryptic species (Liu et al. 2018; Chen et al. 2016). Obviously, lacking deep investigation is the most significant obstacle for detecting cryptic species of *Oreolalax* in view that there has been no detailed taxonomic evaluation on its populations for two decades based on molecular phylogenetic data.

During the field surveys in 2018 in the White River National Nature Reserve, Pengzhou City, Sichuan Province (Prov.), China, we collected nine *Oreolalax* specimens. Our detailed morphological comparisons and molecular phylogenetic analyses indicate that the specimens should represent an undescribed species. Herein we describe it as a new species.

Materials and methods

Specimens

Three adult males and six tadpoles of *Oreolalax longmenmontis* sp. nov. were collected in May 2018 in the White River National Nature Reserve, Pengzhou City, Sichuan Prov., China (Fig. 1; Table 1, Suppl. materials 1, 2). For comparisons, some specimens of congeneric species were also collected in Sichuan Prov., China: eight *O. major* (Liu & Hu, 1960) from E' mei Mountain (the type locality of the species) and Baoxing County (Co.), one *O. nanjiangensis* Fei & Ye, 1999 from Guangwu Mountain, Nanjiang Co., and four *O. omeimontis* (Liu & Hu, 1960) from E'mei Mountain (the type locality of the species; Fig. 1; Table 1, Suppl. materials 1, 2). After taking photographs, the toad and tadpole were euthanized using isoflurane, and the specimens were fixed and then preserved in 75% ethanol. Tissue samples were taken and preserved separately in 95% ethanol prior to fixation. Specimens were deposited in Chengdu Institute of Biology, Chinese Academy of Sciences (**CIB**, **CAS**).

Molecular data and phylogenetic analyses

Genomic DNA from each specimen collected in this work was extracted using a TIANamp Genomic DNA Kit by TIANGEN (BEIJING) BIOTECH, China. Fragments of the mitochondrial genes 12S rRNA and 16S rRNA were amplified. For 12S, the primers Fphe40L (5'-AAAGCACAGCACTGAAGAYGC) and 12S600H (5'-TTATCGATTATAGAACAGGCTCCTCT-3') were used following Zhang et al. (2013), and for 16S, the primers P7 (5'-CGCCTGTTTACCAAAAACAT-3') and P8 (5'-CCGGTCTGAACTCAGATCACGT-3') were used following Simon et al. (1994). PCR amplification was performed in a reaction volume of 25 ul. Fragments were amplified under the following conditions: an initial denaturing step at 95 °C for 4 min; 36 cycles of denaturing at 95 °C for 30 s, annealing at 55 °C (for 16S)/52 °C (for 12S) for 30 s and extending at 72 °C for 60 s. Sequencing was conducted using an ABI3730 automated DNA sequencer in Shanghai DNA BioTechnologies Co., Ltd. (Shanghai, China). New sequences were deposited in GenBank (for accession numbers see Table 1).

For phylogenetic analyses, the available sequence data for all related species of *Oreolalax*, one *Scutiger ningshanensis* Fang, 1985, and one *Leptobrachella oshanensis* (Liu, 1950) were downloaded from GenBank especially for the topotypes of *Oreolalax* species (for accession numbers see Table 1). *Leptobrachella oshanensis* was used as the outgroup following Fu et al. (2007).

Sequences were assembled and aligned using the Clustalw options in BioEdit v. 7.0.9.0 (Hall 1999) with default settings. Alignments were checked by eye and modified manually if necessary. To avoid bias in alignments, GBLOCKS v. 0.91.b (Cas-

Table 1. Sampling information and GenBank accession numbers for molecular samples used in this study.

ID	Species	Voucher number	Locality (County/City, Province, Country)	12S	16S
1	*Oreolalax longmenmontis* sp. nov.	CIB20180522001	Pengzhou, Sichuan, China	MN749799	MN688667
2	*Oreolalax longmenmontis* sp. nov.	CIB20180526001	Pengzhou, Sichuan, China	MN749802	MN688670
3	*Oreolalax longmenmontis* sp. nov.	CIB20180526002	Pengzhou, Sichuan, China	MN749803	MN688671
4	*Oreolalax longmenmontis* sp. nov.	CIB2018041501	Pengzhou, Sichuan, China	MN749798	MN688666
5	*Oreolalax longmenmontis* sp. nov.	CIB2018052201602	Pengzhou, Sichuan, China	MN749800	MN688668
6	*Oreolalax longmenmontis* sp. nov.	CIB2018052201603	Pengzhou, Sichuan, China	MN749801	MN688669
7	*Oreolalax longmenmontis* sp. nov.	CIB2018041301	Pengzhou, Sichuan, China	MN749795	MN688663
8	*Oreolalax longmenmontis* sp. nov.	CIB2018041302	Pengzhou, Sichuan, China	MN749796	MN688664
9	*Oreolalax longmenmontis* sp. nov.	CIB2018041303	Pengzhou, Sichuan, China	MN749797	MN688665
10	*Oreolalax chuanbeiensis*	CIB-ZYC074	Mao County, Sichuan, China	EF397266	EF397266
11	*Oreolalax chuanbeiensis*	DQR-Pingwu-001J	Ping Wu, Sichuan, China	/	EU180887
12	*Oreolalax nanjiangensis*	CIBSCNJNJ2006004	Nanjiang, Sichuan, China	MN749790	MN688658
13	*Oreolalax nanjiangensis*	CIB-XM804	NanJiang, Sichuan, China	EF397265	EF397265
14	*Oreolalax multipunctatus*	CIB2013wb091	Emei, Sichuan, China	NC_037382	NC_037382
15	*Oreolalax omeimontis*	CIBWWS180610018	Emei, Sichuan, China	MN749793	MN688661
16	*Oreolalax omeimontis*	CIBWWS180610022	Emei, Sichuan, China	MN749794	MN688662
17	*Oreolalax omeimontis*	CIBEMS18061203	Emei, Sichuan, China	MN749791	MN688659
18	*Oreolalax omeimontis*	CIBEMS18061205	Emei, Sichuan, China	MN749792	MN688660
19	*Oreolalax rhodostigmatus*	CIB-ZYCA 746	Da Fang, Guizhou, China	EF397248	EF397248
20	*Oreolalax xiangchengensis*	CIB-3LW008	Li Jiang, Yunnan, China	EF397250	EF397250
21	*Oreolalax jingdongensis*	IOZCAS2691	Jingdong, Yunnan, China	EF397255	EF397255
22	*Oreolalax liangbeiensis*	IOZCAS3796	Puxiong, Yuexi, Sichuan, China	EF397253	EF397253
23	*Oreolalax rugosus*	CIB-XM340	Shi Mian, Sichuan, China	EF397254	EF397254
24	*Oreolalax major*	CIB2019bx01	Baoxing, Sichuan, China	MN749782	MN688650
25	*Oreolalax major*	CIB2019bx02	Baoxing, Sichuan, China	MN749783	MN688651
26	*Oreolalax major*	CIB2019bx03	Baoxing, Sichuan, China	MN749784	MN688652
27	*Oreolalax major*	CIB2019bx04	Baoxing, Sichuan, China	MN749785	MN688653
28	*Oreolalax major*	CIB2019bx05	Baoxing, Sichuan, China	MN749786	MN688654
29	*Oreolalax major*	CIBEM1824	Emei, Sichuan, China	MN749787	MN688655
30	*Oreolalax major*	CIBEM1825	Emei, Sichuan, China	MN749788	MN688656
31	*Oreolalax major*	CIBEM1826	Emei, Sichuan, China	MN749789	MN688657
32	*Oreolalax schmidti*	ROM40457	Hongya, Sichuan, China	EF397257	EF397257
33	*Oreolalax pingii*	CIB-XM980	Xi Chang, Sichuan, China	EF397259	EF397259
34	*Oreolalax lichuanensis*	IZCASH30036	Lichuan, Hubei, China	EF544237	EF544237
35	*Oreolalax sterlingae*	IEBR A.2012.1	Sa Pa, Lao Cai, Vietnam	KC569979	KC569981
36	*Scutiger ningshanensis*	/	/	NC_031426	NC_031426
37	*Leptobrachella oshanensis*	CIB20050095	/	NC_020610	NC_020610

tresana 2000) was used to extract regions of defined sequence conservation from the length-variable 12S and 16S gene fragments with default settings. Non-sequenced fragments were regarded as missing loci. Two fragments were concatenated for the following phylogenetic analyses.

Phylogenetic analyses were conducted using maximum likelihood (ML) and Bayesian Inference (BI) methods, implemented in PhyML v. 3.0 (Guindon et al. 2010) and MrBayes v. 3.12 (Ronquist and Huelsenbeck 2003), respectively. Prior to phylogenetic analyses, 12S and 16S genes were defined as two partitions in the concatenated data, and jModelTest v. 2.1.2 (Darriba 2012) was used to select the best substitution model for each partition under the Bayesian Inference Criteria (BIC). The results suggested

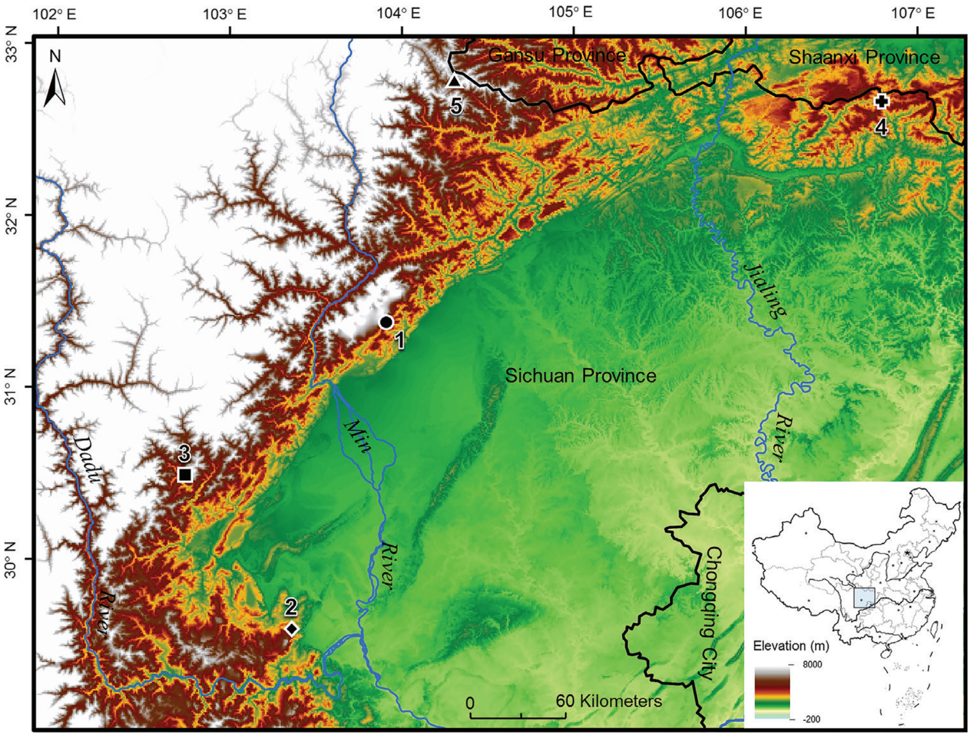

Figure 1. Localities for specimens used in this study. All localities are in Sichuan Province, China. Key: **1** Sichuan White River National Nature Reserve in Pengzhou City as the type locality of *Oreolalax longmenmontis* sp. nov.; **2** E mei Mountain as the common type locality of *O. major* and *O. omeimontis;* **3** Baoxing County as the type locality of *O. popei*, also as another sampling locality of *O. major;* **4** Guangwu Mountain in Nanjiang County as the type locality of *O. nanjiangensis;* **5** Pingwu County as the type locality of *O. chuanbeiensis*.

GTR + I + G model for all partitions. For the ML tree, branch supports were drawn from 10,000 nonparametric bootstrap replicates. In BI analyses, two runs each with four Markov chains were run for 40 million iterations with sampling every 1000 generations. The first 25% generations were removed as the "burn-in" stage followed by calculation of Bayesian posterior probabilities and the 50% majority-rule consensus of the post burn-in trees sampled at stationarity. Finally, genetic distance between *Oreolalax* species was calculated with the pairwise uncorrected *p*-distance model on 16S gene using MEGA v. 7 (Kumar et al. 2016).

Morphological comparisons

Three adult males of *Oreolalax longmenmontis* sp. nov., four *O. nanjiangensis*, 13 *O. chuanbeiensis* Tian, 1983, and ten *O. popei* (Liu, 1947) were measured (Suppl.

material 1). Sex of individuals was determined by presence of nuptial spines on finger and chest in males in breeding condition. The terminology and methods followed Fei et al. (2009) and Watters et al. (2016). Measurements were taken with a dial caliper to 0.1 mm. In total, 26 morphometric characters of adult specimen were measured:

ED	eye diameter (distance from the anterior corner to the posterior corner of the eye)
EN	eye to nostril distance (distance from anterior corner of the eye to the posterior margin of the nostril
FIIIL	third finger length (distance from base to tip of finger III)
FIIL	second finger length (distance from base to tip of finger II)
FIL	first finger length (distance from base to tip of finger I)
FIVL	fourth finger length (distance from base to tip of finger IV)
FL	foot length (distance from tarsus to the tip of fourth toe)
HDL	head length (distance from the tip of the snout to the articulation of jaw)
HDW	maximum head width (greatest width between the left and right articulations of jaw)
IND	internasal distance (minimum distance between the inner margins of the external nares)
IOD	interorbital distance (minimum distance between the inner edges of the upper eyelids)
LAL	length of lower arm and hand (distance from the elbow to the distal end of the finger III)
LW	lower arm width (maximum width of the lower arm)
NS	nostril–snout distance (distance from the tip of the snout to the naris)
SL	snout length (distance from the tip of the snout to the anterior corner of the eye)
SVL	snout-vent length (distance from the tip of the snout to the posterior edge of the vent)
TFL	length of foot and tarsus (distance from the tibiotarsal articulation to the distal end of the toe IV)
THL	thigh length (distance from vent to knee)
TL	tibia length (distance from knee to tarsus)
TOE1L	length of the first toe (distance from the metatarsal tubercle to the tip of toe I)
TOE2L	length of the second toe (distance from the metatarsal tubercle to the tip of toe II)
TOE3L	length of the third toe (distance from the metatarsal tubercle to the tip of toe III)
TOE4L	length of the fourth toe (distance from the metatarsal tubercle to the tip of toe IV)
TOE5L	length of the fourth toe (distance from the metatarsal tubercle to the tip of toe V)

TW	maximal tibia width
UEW	upper eyelid width (greatest width of the upper eyelid margins measured perpendicular to the anterior-posterior axis).

Six tadpoles (Suppl. material 2) were assigned to *O. longmenmontis* sp. nov. based on their phylogenetic positions very close to the adult specimens of the new species (see the results). Developmental stages were determined according to Gosner (1960). Twelve characters of tadpole specimen were measured:

BH	maximum body height
BW	maximum body width
ED	maximum eye diameter
IOD	interocular distance (minimum distance between eye)
MW	mouth width (distance between two corners of mouth)
SL	snout length (distance from the tip of the snout to the anterior corner of the eye)
SS	snout to spiraculum (distance from spiraculum to the tip of the snout)
SVL	snout-vent length
TAH	tail height (maximum height between upper and lower edges of tail)
TAL	tail length (distance from base of vent to the tip of tail)
TBW	maximum width of tail base
TOL	total length (distance from the tip of the snout to the tip of tail).

In order to reduce the impact of allometry, a corrected value from the ratio of each character to SVL was calculated and was log-transformed for subsequent morphometric analyses. Mann-Whitney *U* test was used to test the significance of differences on morphometric characters between species. The significance level was set at 0.05. Analyses were carried out in R.

We also compared morphological characters of *Oreolalax longmenmontis* sp. nov. with other *Oreolalax* species. Comparative morphological data were obtained from the literature for *O. chuanbeiensis* (Tian 1983; Fei et al. 2009, 2016), *O. granulosus* Fei, Ye & Chen, 1990 (Fei et al. 2009, 2016), *O. jingdongensis* Ma, Yang & Li, 1983 (Fei et al. 2009, 2016), *O. liangbeiensis* Liu & Fei, 1979 (Fei et al. 2009, 2016), *O. lichuanensis* Hu & Fei, 1979 (Fei et al. 2009, 2016), *O. major* (Fei et al. 2009, 2016), *O. multipunctatus* Wu, Zhao, Inger, and Shaffer, 1993 (Fei et al. 2009, 2016), *O. nanjiangensis* (Fei et al. 2009, 2016), *O. omeimontis* (Liu and Hu 1960; Fei et al. 2009, 2016), *O. pingii* (Liu, 1943) (Fei et al. 2009, 2016), *O. popei* (Liu 1947; Fei et al. 2009, 2016), *O. puxiongensis* Liu & Fei, 1979 (Fei et al. 2009, 2016), *O. rhodostigmatus* Hu & Fei, 1979 (Fei et al. 2009, 2016), *O. rugosus* (Liu, 1943) (Fei et al. 2009, 2016), *O. schmidti* (Liu, 1947) (Fei et al. 2009, 2016), *O. sterlingae* Nguyen, Phung, Le, Ziegler & Böhme, 2013 (Nguyen et al. 2013), *O. weigoldi* (Vogt, 1924) (Fei et al. 2009, 2016), and *O. xiangchengensis* Fei & Huang, 1983 (Fei et al. 2009, 2016). In addition, for comparison, we examined the holotype and/or topotype materials for

O. nanjiangensis, *O. puxiongensis*, *O. liangbeiensis*, *O. multipunctatus*, *O. granulosus*, *O. chuanbeiensis*, *O. pingii*, *O. rugosus*, *O. schmidti*, *O. omeimontis*, *O. jingdongensis*, *O. lichuanensis*, *O. popei*, and *O. major* (Suppl. materials 1, 3).

Results

Aligned sequence matrix of 12S+16S contained 896 bps. ML and BI trees presented almost consistent topology though relationships of some clades were unresolved (Fig. 2). The genus *Oreolalax* was strongly supported as a monophyletic group. All nine specimens of *O. longmenmontis* sp. nov. were clustered into one clade, which was independently clustered into a clade also containing *O. nanjiangensis* and *O. chuanbeiensis*. Genetic distance on 16S gene with uncorrected *p*-distance model between the nine specimens of *O. longmenmontis* was zero. Genetic distance between *O. longmenmontis* and its most closely related species *O. nanjiangensis* and *O. chuanbeiensis* were 1.4% and 1.6%, respectively, being higher than that between many pairs of species (Table 2), for example, *O. major* vs. *O. xiangchengensis* (0.6%), *O. rugosus* vs. *O. xiangchengensis* (1.3%), *O. rugosus* vs. *O. major* (1.0%), and *O. schmidti* vs. *O. pingii* (0.4%).

Mann-Whitney *U* tests indicated that *Oreolalax longmenmontis* was significantly different from *O. chuanbeiensis*, *O. nanjiangensis*, and *O. popei* on many morphometric characters (all P-values < 0.05; Table 3). *Oreolalax longmenmontis* could also be distinguished from its congeners based on morphological descriptions from the literature and from our examinations of specimens (Suppl. materials 1, 3). More detailed descriptions of results from morphological comparisons between the new taxon and its congeners are presented in the following sections.

Based on the molecular and morphological differences, the specimens from the Sichuan White River National Nature Reserve, Sichuan Prov., China represent an new species which is described as follows.

***Oreolalax longmenmontis* sp. nov.**

http://zoobank.org/9D057EEA-C908-41EF-B6EF-6A2FED872431
Figures 3, 4A, B, 5, 6; Tables 1, 2, Suppl. materials 1, 2

Holotype. CIB20180522001, adult male (Fig. 3), from Xia Jia Gou (31.293360N, 103.866190E, ca. 1335 m a. s. l.), White River National Nature Reserve, Pengzhou City, Sichuan Province, China, collected by SC Shi on 26 May 2018.

Paratype. Two adult males collected from the same place of the holotype. Specimen CIB20180526001 collected by SC Shi on 26 May 2018; CIB20180527002 collected by B Wang on 27 May 2018.

Diagnosis. *Oreolalax longmenmontis* sp. nov. is assigned to the genus *Oreolalax* by its molecular phylogenetic position and the following morphological characters: the maxillary teeth prominent; back rough scattered with large warts, covered with oval

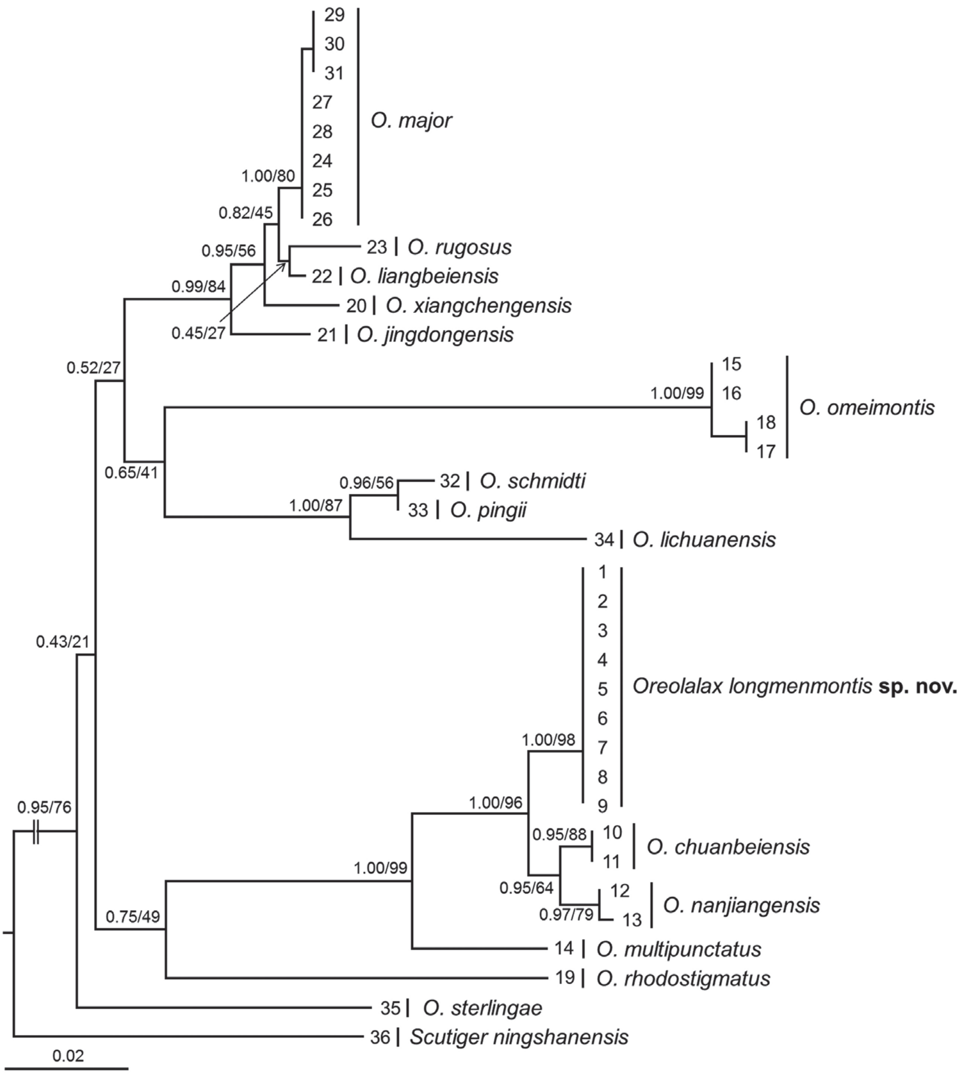

Figure 2. Maximum Likelihood tree based on the mitochondrial 12S and 16S gene sequences. Bayesian posterior probabilities from Bayesian Inference analyses/bootstrap supports from Maximum Likelihood analyses are labelled beside nodes. See information of samples 1–36 in Table 1.

black spots; pupil vertical; tongue oval, notched posteriorly; femoral glands prominent; pectoral and axillary gland present in males in breeding season; inner two fingers with black nuptial spines in males in breeding season.

Oreolalax longmenmontis could be distinguished from its congeners by a combination of the following characters: body size moderate (SVL 51.2–64.2 mm in males); head broad; tympanum hidden; interorbital region with dark triangular pattern; belly with marbling; male lacking spines on lip margin; spiny patches on chest small with

Table 2. Uncorrected *p*-distance between *Oreolalax* species of the 16S rRNA gene. Mean values of genetic distance are given in the lower half of the table.

	1	**2**	**3**	**4**	**5**	**6**	**7**	**8**	**9**	**10**	**11**	**12**	**13**	**14**
1. *Oreolalax longmenmontis* sp. nov.														
2. *Oreolalax nanjiangensis*	0.014													
3. *Oreolalax chuanbeiensis*	0.016	0.006												
4. *Oreolalax multipunctatus*	0.029	0.027	0.028											
5. *Oreolalax omeimontis*	0.085	0.093	0.091	0.087										
6. *Oreolalax rhodostigmatus*	0.065	0.065	0.066	0.059	0.096									
7. *Oreolalax xiangchengensis*	0.063	0.057	0.059	0.057	0.092	0.049								
8. *Oreolalax jingdongensis*	0.064	0.055	0.059	0.057	0.090	0.059	0.025							
9. *Oreolalax liangbeiensis*	0.063	0.056	0.058	0.056	0.088	0.049	0.007	0.018						
10. *Oreolalax rugosus*	0.057	0.056	0.058	0.055	0.087	0.047	0.013	0.025	0.011					
11. *Oreolalax major*	0.056	0.053	0.055	0.050	0.083	0.045	0.006	0.018	0.000	0.010				
12. *Oreolalax schmidti*	0.087	0.085	0.083	0.077	0.103	0.068	0.060	0.070	0.058	0.062	0.055			
13. *Oreolalax pingii*	0.080	0.079	0.076	0.069	0.097	0.061	0.055	0.066	0.054	0.055	0.049	0.004		
14. *Oreolalax lichuanensis*	0.095	0.089	0.086	0.084	0.113	0.080	0.066	0.082	0.069	0.069	0.067	0.032	0.032	
15. *Oreolalax sterlingae*	0.070	0.072	0.069	0.062	0.092	0.071	0.059	0.064	0.058	0.049	0.052	0.068	0.063	0.080

Table 3. Morphometric comparisons between *Oreolalax longmenmontis* sp. nov. and its relatives. P-value from Mann-Whitney U test between the new species and each relative. The significant level is 0.05. See abbreviations for characters in the Materials and methods section.

Characters	***Oreolalax longmenmontis* sp. nov.**		***Oreolalax popei***			***Oreolalax nanjiangensis***			***Oreolalax chuanbeiensis***		
	Male (*N* = 3)		**Male (*N* = 10)**		**P-value**	**Male (*N* = 4)**		**P-value**	**Male (*N* = 13)**		**P-value**
	Mean ± SD	**Range**	**Mean ± SD**	**Range**		**Mean ± SD**	**Range**		**Mean ± SD**	**Range**	
SVL	56.8 ± 6.7	51.2–64.2	64.3 ± 2.7	59.3–68.4	/	53.7 ± 1.6	51.4–55.0	/	50.9 ± 2.6	46.7–56.0	/
HDL	18.5 ± 1.9	17.2–20.6	24.0 ± 0.9	22.4–24.9	0.007	21.3 ± 0.4	21–21.8	0.057	17.9 ± 0.6	17.1–19.1	0.007
HDW	21.2 ± 2.1	19.1–23.3	23.9 ± 1.0	21.9–24.9	0.811	19.8 ± 0.9	19.1–21	0.857	17.7 ± 0.5	17.2–19.2	0.025
SL	8.2 ± 1.1	7.3–9.5	9.8 ± 0.4	9.0–10.5	0.014	8.1 ± 0.3	7.8–8.5	0.229	7.8 ± 0.4	7.1–8.4	0.014
NS	4.3 ± 0.4	3.8–4.6	4.6 ± 0.3	4.2–5.3	0.469	4.3 ± 0.2	4.1–4.5	0.114	4.3 ± 0.3	3.8–4.7	0.025
EN	4.0 ± 0.4	3.6–4.3	4.6 ± 0.3	4.1–5.3	0.692	3.7 ± 0.4	3.3–4.1	0.629	3.6 ± 0.2	3.2–4.0	0.800
IND	4.1 ± 0.4	3.7–4.5	4.7 ± 0.3	4.0–5.1	0.469	4.1 ± 0.1	3.9–4.2	0.114	4.7 ± 0.2	4.1–4.9	0.004
IOD	5.9 ± 0.4	5.5–6.2	6.4 ± 0.4	5.6–6.9	0.371	5.0 ± 0.5	4.3–5.4	0.229	5.8 ± 0.2	5.5–6.2	0.082
ED	6.1 ± 0.3	5.8–6.4	6.4 ± 0.4	5.5–6.8	0.112	5.0 ± 0.3	4.5–5.3	0.114	5.0 ± 0.2	4.6–5.5	0.189
UEW	5.3 ± 0.6	4.6–5.6	6.0 ± 0.2	5.6–6.3	0.573	5.0 ± 0.8	4.5–6.2	1.000	4.2 ± 0.2	3.9–4.5	0.014
LW	5.7 ± 0.7	5.0–6.3	6.5 ± 0.7	5.3–7.3	1.000	5.8 ± 0.5	5.1–6.3	0.229	5.7 ± 0.5	4.9–6.7	0.039
LAL	29.5 ± 1.6	28–31.2	30.2 ± 1.3	28.5–32.6	0.014	26.3 ± 1.2	24.5–27.2	0.229	26.5 ± 0.7	24.9–27.5	0.704
THL	29.8 ± 2.3	27.2–31.7	32.2 ± 1.4	30.1–34.3	0.161	27.4 ± 1.6	25.6–29.2	0.629	26.0 ± 1.0	23.6–27.3	0.364
TL	29.5 ± 3.5	25.7–32.8	31.4 ± 1.2	29.1–33.2	0.014	26.2 ± 0.9	25.1–27.4	0.114	25.1 ± 1.0	23–26.6	0.111
TW	6.5 ± 1.0	5.4–7.3	7.1 ± 0.5	6.5–7.8	1.000	6.0 ± 0.2	5.7–6.2	0.629	6.4 ± 0.9	4.4–7.4	0.439
TFL	44.1 ± 4.2	39.6–47.9	47.1 ± 1.7	44.6–49.7	0.770	39.0 ± 1.2	38.1–40.5	0.114	38.3 ± 1.3	36.0–40.5	0.189
FL	28.3 ± 3.3	25.4–31.9	31.4 ± 1.1	29.9–33.1	0.281	28.1 ± 1.7	26.5–30.0	0.114	25.8 ± 1.1	24.4–27.3	0.704

thick and sparse spines in male; nuptial spines thick and sparse; tibio-tarsal articulation reaching beyond nostril when leg stretched forward; toe webbing at base.

Description of holotype. Measurements in mm. Body size medium, SVL 64.2; body relatively slender and flat; head wider than long (HDW/HDL ratio 1.14); snout rounded in dorsal and lateral views, slightly projecting beyond lower jaw; maxillary teeth present; vomerine range absent; eye large (ED 6.3), shorter than snout length (SL 9.5); pupil vertical; interorbital region flat; tympanum hidden; vocal sac absent;

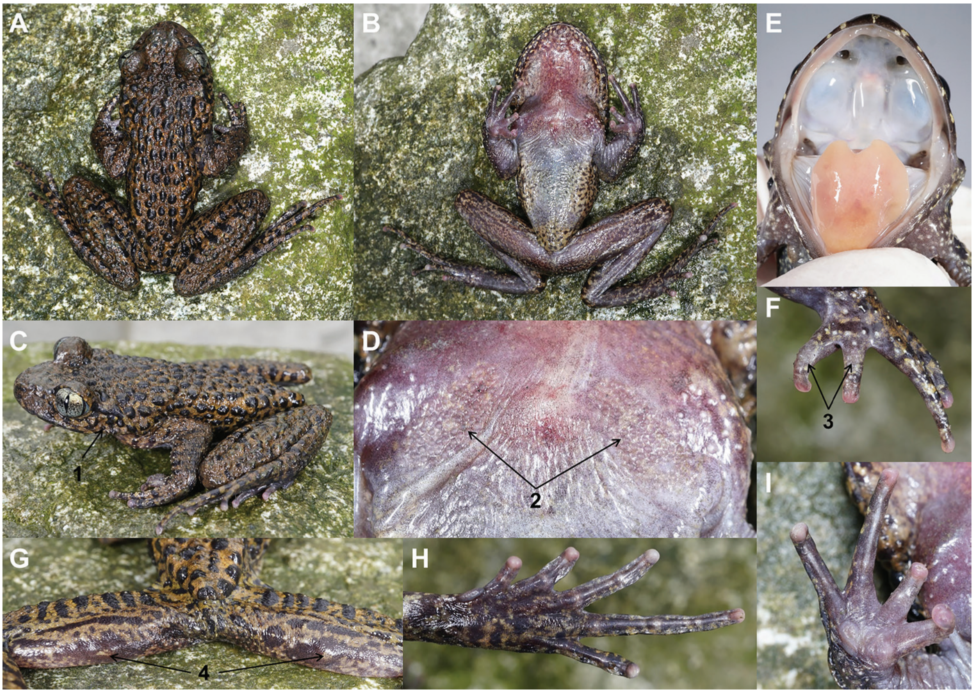

Figure 3. Photos of the holotype CIB20180522001 of *Oreolalax longmenmontis* sp. nov. in life **A** dorsal view **B** ventral view **C** lateral view **D** view of chest **E** view of oral cavity **E** dorsal view of fingers **G** view of femoris posterior **H** ventral view of foot **I** ventral view of hand. Key: 1 indicates tympanum hidden; 2 denotes a pair of spinal patches with large and sparse spines on chest; 3 denotes nuptial spines on the dorsal surface of fingers I and II; 4 denotes two small posterior femoral glands.

supratympanic fold significant; tongue longer than wide, free at the back, notched posteriorly; nostril oval, internarial distance (IND 4.5) shorter than upper eyelid (UEW 5.6), shorter than interorbital distance (IOD 6.2); nostril slightly closer to eye (EN 4.3) than to tip of the snout (NS 4.6).

Forelimbs moderately long and strong, length (LAL 31.2) approximately half of SVL; relative finger lengths: II < I < IV < III; fingers slender, distinct longitudinal ridges under fingers III and IV; finger tips rounded, two metacarpal tubercles oval, inner larger than outer; nuptial spines large and sparse on dorsal surface of fingers I and II.

Hindlimbs flat; toe webbing rudimentary, with narrow dermal fringes, distinct dermal ridges present under five toes; tibiotarsal articulation reaching beyond nostril when leg stretched forward; thigh length (THL 31.7) slightly shorter than tibia length (TL 32.8); foot length (FL 31.9) almost equal with thigh; relative toe lengths: I < II < V < III < IV; tips of toes rounded; subarticular tubercles distinct; inner metatarsal tubercle elliptical and narrow (IML 2.7), no outer metatarsal tubercle.

Rough skin on the back, lateral limb surfaces, large scattered tubercles with oval black spot; forehead and upper lip with scatted small tubercles; upper jaw protrudes slightly from lower jaw; supratympanic fold distinct, from posterior canthus above base of upper arm, mostly covered with dark spots. A pair of spinal patches small, present on chest, with relatively large and sparse spines; axillary glands small; posterior femoral gland small present. The backs of limbs with scatted differently sized tubercles; the forelimbs and hindlimbs have black longitudinal stripes, the hindlimbs are covered with medium-sized wart granules, the forelimbs are covered with many small white warty granules. Skin smooth on throat, belly, and ventral sides of the limbs.

Colouration of the holotype in life. In life, body dark brown dorsally, with large tubercles, tubercular region with scattered black, oval-shaped markings, tongue orange-yellow, limb surfaces dark brown, scattered with different sizes of white tubercles; five or six faint transverse black stripes on the dorsal surface of the forearm; most parts of supratympanic line covered with black spots; belly interlaced with two colours: flesh red and greyish-white with some black speckles, throat and anterior chest are darker than belly. Back of posterior limbs with nine or ten black stripes; finger and toe tips flesh-pink. Arms and fingers covered in many scattered small white tubercles. Dorsal surfaces of head and hind limbs scattered with black medium-sized tubercles; upper lip barred with yellowish brown and black spots; iris bicolored; slightly beige above, silver below, with black reticulations throughout. Posterior femoral glands yellow-brown. Nuptial spines light grey, chest spiny patches flesh-pink. Outer metacarpals grey-pink, inner metatarsals brown.

Preserved holotype colouration. In preservative (75% ethanol), the dorsal and lateral surfaces are dark brown; throat and anterior chest brown, belly grey, dark markings are evident on the abdomen and throat; the forelimbs and ventral surface of the thigh are brown, Inner and outer metacarpals brown; tongue creamy white; the colour of dorsal spots and stripes on limbs and posterior femoral glands become more conspicuous; the spiny patches become flat and indistinct (Fig. 4A, B).

Variations. The two paratypes CIB20180526001 (Fig. 5A, B) and CIB20180527002 (Fig. 5C, D) are smaller than holotype on body size (Table 2, Suppl. material 1). The colour of paratypes is brown, lighter than holotype. The arrangement and shape of the large tubercles on the dorsal surface are more irregular than of the holotype. The paratype CIB20180526001 has fewer abdominal streaks than the holotype. The paratype CIB20180527002 has fewer markings at the meeting of thighs to abdomen and more markings in the posterior abdomen than holotype. Iris colour also varies between individuals: the holotype is light blue-green, CIB20180526001 is yellowish orange, and CIB20180527002 is orange.

Secondary sexual characteristics. In breeding males, a pair of small spiny patches on chest, nuptial spines thick and sparse on dorsal surface of fingers I and II (Fig. 3D, H).

Tadpoles. Measurements in mm. Differences in measurements are shown in Suppl. material 2. Character description is based on the preserved tadpole specimen CIB2018041501 (Fig. 6). Stage 37. Labial tooth row formula: 1:5+5/5+5:1; body dark brown in the back and lateral view, creamy white in the ventral; tail light brown; snout rounded; eye positioned dorsolateral; the opening of the spiracle single in the lateral, without a free distal tube; tail end blunt; caudal fin light and broad.

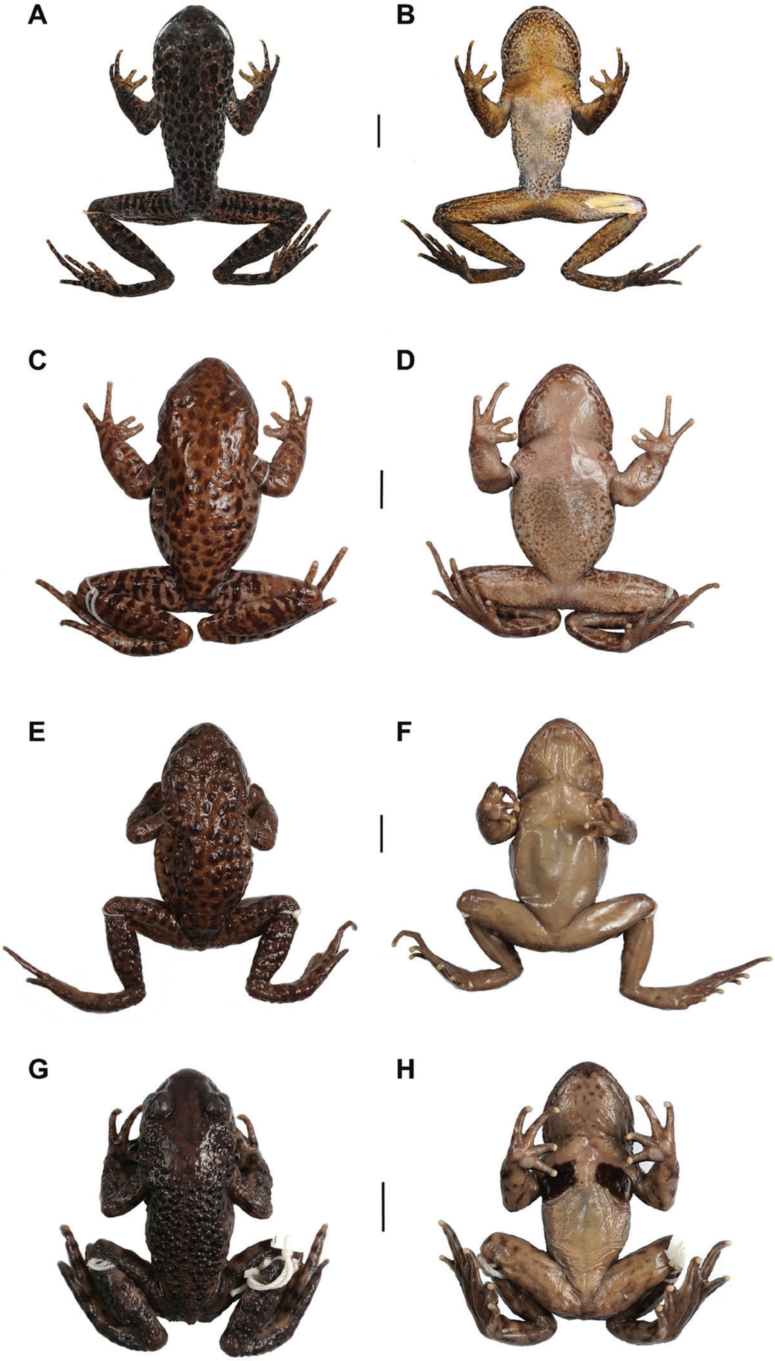

Figure 4. Specimen photos of *Oreolalax longmenmontis* sp. nov. and its relative species **A, B** dorsal and ventral view of the holotype CIB20180522001 of *Oreolalax longmenmontis* sp. nov. **C, D** dorsal and ventral view of the topotype CIB25142 of *O. popei* **E, F** dorsal and ventral view of the topotype CIB89700 of *O. nanjiangensis* **G, H** dorsal and ventral view of the topotype CIB89682 of *O. chuanbeiensis*. Scale bar: equal to 10 mm.

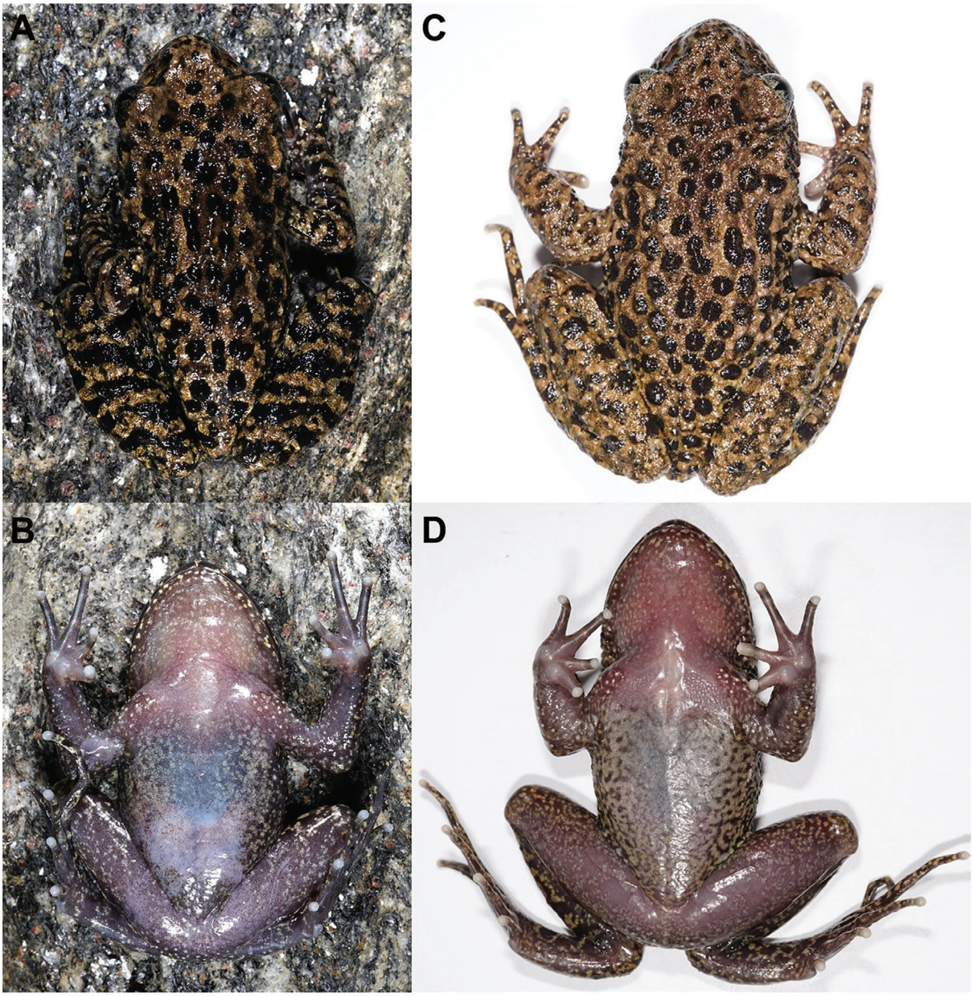

Figure 5. Colour variations in *Oreolalax longmenmontis* sp. nov. **A, B** dorsal and ventral view of the paratype CIB20180527002 **C, D** dorsal and ventral view of the paratype CIB20180526001.

Comparisons. By having a relatively larger body (SVL 51.2–64.2 mm in males; *N* = 3), *Oreolalax longmenmontis* sp. nov. differs from *O. pingii* (*N* = 20), *O. puxiongensis* (*N* = 20), *O. schmidti* (*N* = 30), *O. sterlingae* (*N* = 1), *O. multipunctatus* (*N* = 4), and *O. xiangchengensis* (*N* = 10) (vs. SVL < 51.0 mm in the latter).

By head wider than long, *O. longmenmontis* differs from *O. multipunctatus*, *O. rhodostigmatus*, and *O. schmidti* (vs. head longer than wide in the latter).

By the hidden tympanum, *Oreolalax longmenmontis* differs from *O. granulosus*, *O. jingdongensis*, *O. xiangchengensis*, and *O. rugosus* (tympanum absent in the latter) and differs from *O. rhodostigmatus* (tympanum rather visible).

By lacking spines on lip margin in male, *Oreolalax longmenmontis* sp. nov. differs from *O. sterlingae*, *O. granulosus*, *O. jingdongensis*, *O. liangbeiensis*, *O. lichuanensis*, *O. major*,

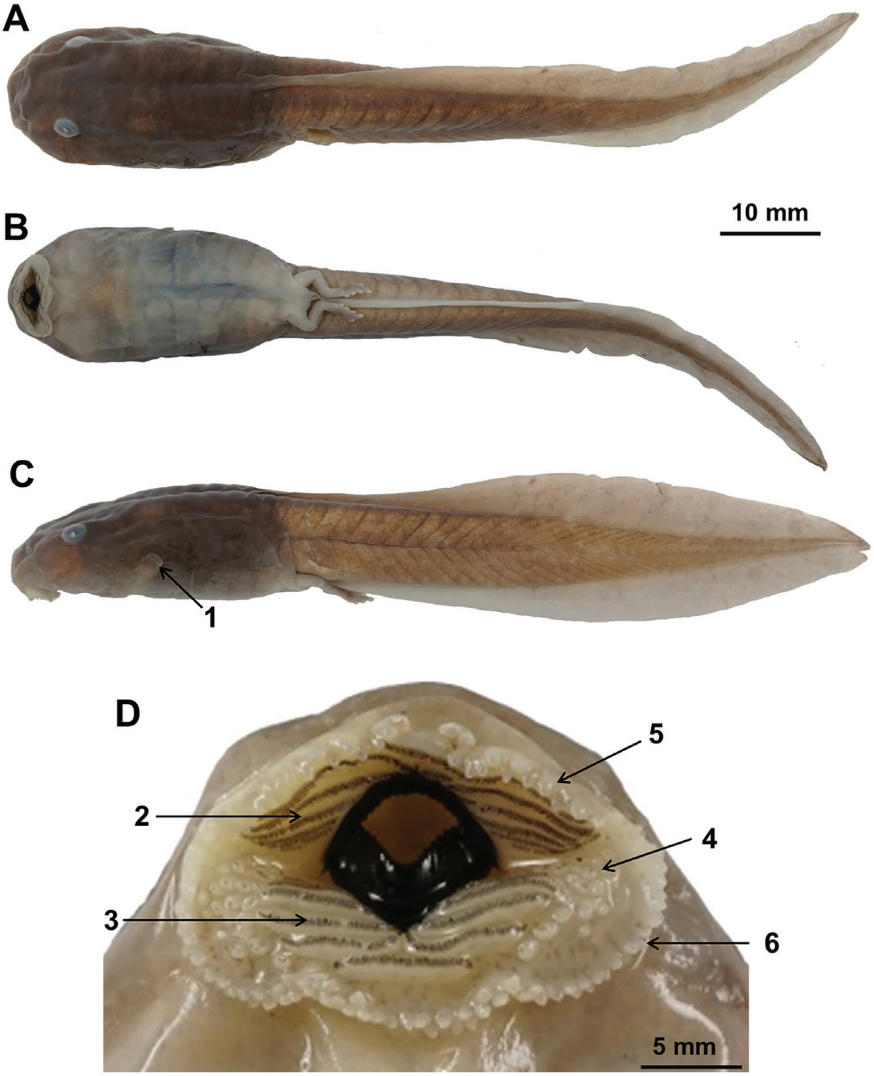

Figure 6. The tadpole specimen CIB2018041501 of *Oreolalax longmenmontis* sp. nov. **A** dorsal view **B** lateral view **C** ventral view **D** mouth structure. Key: 1 spiracle; 2 upper keratodonts; 3 lower keratodonts; 4 additional tubercles at the angles of mouth; 5 labial papillae on upper lips; 6 labial papillae on lower lips.

O. multipunctatus, *O. omeimontis*, *O. pingii*, *O. puxiongensis*, *O. rugosus*, *O. schmidti*, *O. weigoldi*, and *O. xiangchengensis* (vs. spines on lip margin visible in male in the latter).

By vocal sac absent, *Oreolalax longmenmontis* differs from *O. omeimontis* (vs. vocal sac present in male in the latter).

By interorbital region with dark triangular pattern, *Oreolalax longmenmontis* differs from *O. multipunctatus*, *O. granulosus*, *O. major*, *O. liangbeiensis*, *O. lichuanensis*, *O. pingii*, *O. rhodostigmatus*, *O. rugosus*, *O. weigoldi*, *O. sterlingae*, and *O. xiangchengensis* (vs. without in the latter).

By spiny patches on chest small in male, *Oreolalax longmenmontis* differs from *O. granulosus*, *O. liangbeiensis*, *O. major*, *O. omeimontis*, *O. pingii*, *O. rhodostigmatus*, *O. jingdongensis*, *O. weigoldi*, and *O. xiangchengensis* (vs. large in the latter).

By spines on spiny patches on chest thick and sparse in male, *Oreolalax longmenmontis* differs from *O. omeimontis*, *O. granulosus*, *O. major*, *O. liangbeiensis*, *O. pingii*, *O. puxiongensis*, *O. rugosus*, *O. schmidti*, *O. sterlingae*, and *O. xiangchengensis* (vs. spines thin and fine in the latter).

By nuptial spines on fingers thick and sparse, *Oreolalax longmenmontis* differs from *O. sterlingae*, *O. omeimontis*, *O. granulosus*, *O. liangbeiensis*, *O. major*, *O. rugosus*, *O. schmidti*, *O. pingii*, *O. puxiongensis*, and *O. xiangchengensis* (vs. thin and fine in the latter).

By tibio-tarsal articulation reaching beyond nostril when leg stretched forward, *Oreolalax longmenmontis* differs from *O. omeimontis*, *O. multipunctatus*, *O. granulosus*, *O. major*, *O. liangbeiensis*, *O. lichuanensis*, *O. pingii*, *O. puxiongensis*, *O. rhodostigmatus*, and *O. rugosus* (vs. reaching up to the posterior corner of eye in the latter).

By toe webbing at base, *Oreolalax longmenmontis* sp. nov. differs from *O. granulosus*, *O. jingdongensis*, *O. liangbeiensis*, *O. major*, *O. rugosus*, *O. weigoldi*, and *O. xiangchengensis* (vs. toe IV at least 1/4 webbed in the latter).

By belly with marble spots, *Oreolalax longmenmontis* differs from *O. omeimontis*, *O. liangbeiensis*, *O. pingii*, *O. rhodostigmatus*, *O. schmidti*, and *O. xiangchengensis* (vs. without spot in the latter).

Oreolalax longmenmontis sp. nov. most resembles *O. popei* in morphology and is also potentially sympatric with it. The new species could be distinguished from *O. popei* by a combination of following characters: comparatively small body size (mean male SVL 56.8 mm vs. 64.4 mm in *O. popei*), head wider than long (vs. head longer than wide in *O. popei*), tibio-tarsal articulation reaching beyond nostril when leg stretched forward (vs. just reaching the anterior angle of eye in *O. popei*), forelimb long (mean male LAL/SVL ratio 51.89% vs. 46.87% in *O. popei*), hindlimb long (mean male HLL/SVL ratio 182.05% vs. 172.02% in *O. popei*, and mean male TFL/SVL ratio 77.64% vs. 73.21% in *O. popei*), and short IML (4.46% of SVL vs. 5.03% *O. popei*).

Oreolalax longmenmontis is genetically closer to *O. nanjiangensis* and *O. chuanbeiensis*. The new species distinctly differs from *O. chuanbeiensis* by the following characters: broader head (vs. head wide almost equal to long in the latter), lacking spines on lip margin in male (vs. visible in male in the latter), spiny patches on chest small with thick sparse spines in male (vs. large with fine spines in the latter), nuptial spines thick sparse on fingers (vs. thin and fine in the latter), toe webbing at base (vs. toe IV 1/3 webbed in the latter), tibio-tarsal articulation reaching beyond nostril when leg stretched forward (vs. just reaching the level of eye in the latter), and having significant differences on HDL, HDW, SL,NS, IND, UEW, LW ($p < 0.05$ when comparing with the latter; Table 3). The new species differs from *O. nanjiangensis* by the following characters: broader head (vs. head wide almost equal to long in the latter), belly with marble spots (vs. without spot in the latter), tibio-tarsal articulation reaching beyond nostril when leg stretched forward (vs. just reaching the level of eye in the latter), interorbital region with dark triangular pattern (vs. without in the latter), comparatively long body size (mean

Figure 7. Habitats of *Oreolalax longmenmontis* sp. nov. in the type locality, Sichuan White River National Nature Reserve in Pengzhou City, Sichuan Province, China **A** landscape of montane forests **B** a montane stream with a small pond occupied by toad (*insert*: the holotype CIB20180522001 in life).

male SVL 56.8 vs. 53.7 in the latter), forelimb long (mean male LAL/SVL ratio 51.9% vs. 48.9% in the latter), and hindlimb long (mean male HLL/SVL ratio 182% vs. 172% in the latter, and mean male TFL/SVL ratio 77.6% vs. 72.7% in the latter; Table 3).

Distribution and ecology. *Oreolalax longmenmontis* sp. nov., is currently known only from the type locality, the White River National Nature Reserve, Pengzhou City, Sichuan Prov., China at elevations of 1300–1450 m. The new species inhabits subtropical evergreen broad-leaved forests and is frequently found near the ponds in the montane streams (Fig. 7). The breeding season is currently uncertain. Three sympatric amphibian species, i.e., *Amolops chunganensis* (Pope, 1929), *Odorrana margaratae* (Liu, 1950), and *Quasipaa boulengeri* (Günther, 1889), were found in the same habitat.

Etymology. The specific epithet *longmenmontis* refer to the type locality of the species, the central part of the Longmen Mountains, Pengzhou City of Sichuan Prov., China. We propose the common name "Longmen Mountains toothed toad" (English) and "long men shan chi chan" (Chinese).

Discussion

Superficial similarities in morphology between related species of the genus *Oreolalax* easily lead to misleading classifications in the field. Although *Oreolalax longmenmontis* sp. nov. resembles *O. popei*, our detailed comparisons can identify them by many morphological characters. A previous study regarded one sample from Pengzhou City, Sichuan Prov., China as *O. popei* (Fu et al. 2007), but which is phylogenetically nested with samples of *Oreolalax longmenmontis* sp. nov. This indicated that the populations from localities near Pengzhou City were probably the new species, such as populations from Maoxian Co. and Dujiangyan City which had been recognized as *O. popei* (Fei et al. 2009, 2012, 2016). These localities, all in the central part of Longmen

Mountains, are separated from the type locality of *O. popei*, the Jiajin Mountains in Baoxing Co., Sichuan Prov., by a straight-line distance of 150 km. Future investigation should focus on population composition and exact distributional ranges based on both detailed morphological comparisons and molecular phylogenetic data.

As noted above, basal relationships between major clades of the genus *Oreolalax* were not resolved in all phylogenetic studies (Fu et al. 2007; this study). This was possibly due to the relatively lower number of mutations in 12S and 16S gene sequences and/or historically tachytelic evolution for the basal relationships in the genus. We need more suitable genes or genomic information to resolve systematic profiles in these toads. However, the molecular phylogenetic framework of the genus (Fu et al. 2007; this study) could confirm that the four species groups in *Oreolalax* classified based on morphology by Fei et al. (2005) were all not monophyletic groups.

Unexpectedly, in many and detailed surveys in different seasons, we only found three adult individuals of *Oreolalax longmenmontis* sp. nov. in the White River National Nature Reserve. Obviously, the population, especially the adult population of the species, is extraordinarily small although its tadpole population seems to be rich. It is urgent for us to conduct investigation on its population status because the species suffers from disturbances from tourism, increasingly severe weather, and habitat loss due to intensifying human activities.

Acknowledgements

We are grateful to the editors and reviewers for their work on the manuscript. This work was supported by the Project for surveys on amphibians and reptiles in Sichuan White River National Nature Reserve, the National Natural Science Foundation of China (No. 31201702), National Key Research and Development Program of China (No. 2017YFC0505202), and Project supported by the Biodiversity investigation, Observation and Assessment Program (2019–2023) of Ministry of Ecology and Environment of China.

References

Bonaparte CLJL (1850) Conspectus Systematum. Herpetologiae et Amphibiologiae. Editio altera reformata [Lugdini Batavorum] Brill EJ, Leiden, 1 pp.

Castresana J (2000) Selection of conserved blocks from multiple alignments for their use in phylogenetic analysis. Molecular Biology and Evolution 17: 540–552. https://doi.org/10.1093/oxfordjournals.molbev.a026334

Chen JM, Zhou WW, Poyarkov NA, Stuart BL, Brown RM, Lathrop A, Wang YY, Hou M, Chen HM, Suwannapoom C, Nguyen SN, Duong TV, Papenfuss T, Murphy R, Zhang YP, Che J (2016) A novel multilocus phylogenetic estimation reveals unrecognized diversity in Asian horned toads, genus *Megophrys* sensu lato (Anura: Megophryidae). Molecular Phylogenetics and Evolution 106: 28–43. https://doi.org/10.1016/j.ympev.2016.09.004

Darriba D, Taboada GL, Doallo R, Posada D (2012) jModelTest 2: more models, new heuristics and parallel computing. Nature Methods 9(8): 772–772. https://doi.org/10.1038/nmeth.2109

Delorme M, Dubois A (2001) Une nouvelle espèce de *Scutiger* du Bhutan, et quelques remarques sur la classification subgénérique du genre *Scutiger* (Megophryidae, Leptobrachiinae). Alytes 19: 141–153.

Dubois A (1980) Notes sur la systématique et la répartition des amphibiens anoures de Chine et des régions avoisinantes IV. Classification générique et subgénérique des Pelobatidae Megophryinae. Bulletin Mensuel de la Société Linnéenne de Lyon 49: 469–482. https://doi.org/10.3406/linly.1980.10444

Dubois A (1983) Classification et nomenclature supragénérique des amphibiens anoures. Bulletin Mensuel de la Société Linnéenne de Lyon 52: 270–276. https://doi.org/10.3406/linly.1983.10607

Dubois A (1986) Miscellanea nomenclatoica batrachologica (XII). Alytes 5(4): 173–174.

Dubois A, Ohler A (1998) A new species of *Leptobrachium* (*Vibrissaphora*) from northern Vietnam, with a review of the taxonomy of the genus *Leptobrachium* (Pelobatidae, Megophyinae). Dumerilia 4(14): 1–32.

Fang RS (1985) A new species of *Scutiger* from Shaanxi, China. Acta Herpetologica Sinica, New Series, Chengdu 4(4): 305–307.

Fei L, Hu SQ, Ye CY, Huang YZ (2009) Fauna Sinica, Amphibia, Vol. 2, Anura. Science Press, Beijing, 957 pp.

Fei L, Ye CY (1990) Intergeneric relationships and diversification of the high-altitude pelobatid toads in Asia and their relation with the formation of Qinghai-Xizang Plateau (Amphibia: Pelobatidae). Acta Zoologica Sinica 36(4): 420–428.

Fei L, Ye CY (2016) Amphibians of China. Volume 1. China: Science Press, Beijing, 1040 pp.

Fei L, Ye CY, Li C (1999) Description of a new pelobatid toad of genus *Oreolalax* – *Oreolalax nanjiangensis* from Daba Mountain Region of China. Beijing, Acta Zootaxonomica Sinica 24: 107–113. https://doi.org/10.3969/j.issn.1000-0739.1999.01.021

Fei L, Ye CY, Li SS (1989) On the generic classification of Asian high altitude pelobatid toads (Amphibia: Pelobatidae). Acta Zoologica Sinica 35(4): 381–389.

Fei L, Ye CY, Jiang JP (2012) Colored atlas of Chinese amphibians and their distributions. Sichuan Publishing House of Science and Technology, Chengdu, 620 pp.

Fei L, Ye CY, Jiang JP, Xie F, Huang YZ (2005) An illustrated key to Chinese amphibians. Publishing House of Science and Technology, Chengdu, 340 pp.

Frost DR (2019) Amphibian species of the world: an online reference. Version 6.0 (accessed on 30 Dec 2019). Electronic Database accessible at http://research.amnh.org/herpetology/amphibia/index.html. American Museum of Natural History, New York, USA.

Fu JZ, Weadick CJ, Bi K (2007) A phylogeny of the high-elevation Tibetan megophryid frogs and evidence for the multiple origins of reversed sexual size dimorphism. Journal of Zoology 273: 315–325. https://doi.org/10.1111/j.1469-7998.2007.00330.x

Gosner KL (1960) A simplified table for staging anuran embryos and larvae with notes on identification. Herpetologica 16(3): 183–190.

Guindon S, Dufayard JF, Lefort V, Anisimova M, Hordijk W, Gascuel O (2010) New algorithms and methods to estimate maximum-likelihood phylogenies: assessing the performance of PhyML 3.0. Systematic Biology 59(3): 307–321. https://doi.org/10.2307/25677586

Günther DA (1889) XXIV. Third contribution to our knowledge of reptiles and fishes from the upper Yangtze-Kiang. Annals and Magazine of Natural History 4: 218–229.

Hall TA (1999) BioEdit: a user-friendly biological sequence alignment editor and analysis program for Windows 95/98/NT. Nucleic Acids Symposium Series 41: 95–98.

Huang YZ, Fei L, Ye CY (1991) Studies on internal oral structures of tadpoles of Chinese Pelobatidae. Journal of Plateau Biology 10: 71–99.

Kuhl H, Van Hasselt JC (1822) Uittreksels uit breieven van de Heeren Kuhl en van Hasselt, aan de Heeren C. J. Temminck, Th. van Swinderen en W. de Haan. Algemeene Konst-en Letter-Bode 7: 99–104.

Li SZ, Xu N, Liu J, Jiang JP, Wei G, Wang B (2018) A new species of the Asian toad genus *Megophrys sensu lato* (Amphibia: Anura: Megophryidae) from Guizhou Province, China. Asian Herpetological Research 9(4): 224–239. https://doi.org/10.16373/j.cnki.ahr.180072

Liu CC (1943) Two new *Scutigers* from Chao-Chiao-Hsien, Sikang. Journal of the West China Border Research Society, Series B 14: 35–38.

Liu CC (1947) Two new frogs of the genus *Scutiger* from West China. Copeia 1947(2): 123–126.

Liu CC (1950) Amphibians of Western China. Fieldiana Zoology Memoires 2: 1–397. [+ 10pl.]

Liu CC, Hu SQ (1960) New *Scutigers* from China with a discussion about the genus. Scientia Sinica 9: 760–779.

Myers GS, Leviton AE (1962) Generic classification of the high altitude pelobatid toads of Asia. (*Scutiger*, *Aelurophrye*, and *Oreolalax*). Copeia 1962(2): 287–291.

Liu CC, Hu SQ, Fei L (1979) Five new pelobatid toads from China. Beijing. Acta Zootaxonomica Sinica 4: 83–92.

Liu ZY, Chen GL, Zhu TQ, Zeng ZC, Lyu ZT, Wang J, Anthony KM, Greenberg J, Guo ZY, Yang ZH, Shi SH, Wang YY (2018) Prevalence of cryptic species in morphologically uniform taxa–Fast speciation and evolutionary radiation in Asian frogs. Molecular Phylogenetics and Evolution 127: 723. https://doi.org/10.1016/j.ympev.2018.06.020

Myers N, Mittermeier RA, Mittermeier CG, Fonseca GABD, Kent J (2000) Biodiversity hotspot for conservation priorities. Nature 403(6772): 853–858.

Nguyen TQ, Phung TM, Le MD, Ziegler T, Böhme W (2013) First record of the genus *Oreolalax* (Anura: Megophryidae) from Vietnam with description of a new species. Copeia 2013(2): 213–222. https://doi.org/10.1643/CH-12-021

Pope CH (1929) Four new frogs from Fukien Province, China. American Museum Novitates 352: 1–5.

Pyron RA, Wiens JJ (2011) A large-scale phylogeny of Amphibia including over 2800 species, and a revised classification of advanced frogs, salamanders, and caecilians. Molecular Phylogenetics and Evolution 61: 543–583. https://doi.org/10.1016/j.ympev.2011.06.012

Ronquist F, Huelsenbeck JP (2003) MrBayes 3: Bayesian phylogenetic inference under mixed models. Bioinformatics 19(12): 1572–1574. https://doi.org/10.1093/bioinformatics/btg180

Roy JK, Begum RH, Ahmed F (2018) Amphibians of the Dibang River Basin, Arunachal Pradesh: An annotated checklist with distribution records. Journal of Threatened Taxa 10: 12940–12952. https://doi.org/10.11609/jott.4249.10.15.12940-12952

Simon C, Frati F, Beckenbach A, Crespi B, Liu H, Flook P (1994) Evolution, weighting, and phylogenetic utility of mitochondrial gene sequences and a compilation of conserved polymerase chain reaction primers. Annals of the Entomological Society of America 87(6): 651–701. https://doi.org/10.1093/aesa/87.6.651

Smith MA (1925) Contributions to the herpetology of Borneo. Sarawak Museum Journal 3: 15–34.

Sudhir K, Glen S, Koichiro T (2016) MEGA7: Molecular evolutionary genetics analysis version 7.0 for bigger datasets. Molecular Biology and Evolution (7): 7. https://doi.org/10.1093/molbev/msw054

Theobald W (1868) Catalogue of reptiles in the Museum of the Asiatic Society of Bengal. Journal of the Asiatic Society of Bengal 37, suppl., i-vi + 7–88. [+ i-iii, 4 pl.]

Tian WS (1983) A new species of *Oreolalax* – *O. chuanbeiensis*. Acta Herpetologica Sinica 2(4): 59–62.

Vogt T (1924) Reptilien und Amphibien aus Szetschwan, Osttibet und Tschili. Zoologischer Anzeiger 60: 337–344.

Watters JL, Cummings ST, Flanagan RL, Siler CD (2016) Review of morphometric measurements used in anuran species descriptions and recommendations for a standardized approach. Zootaxa 4072(4): 477–495. https://doi.org/10.11646/zootaxa.4072.4.6

Wei G, Li ZZ, Xu N, Jiang JP (2007) Review on the systematics of the genus *Oreolalax*. Chinese Journal of Zoology 42: 169–173. http://www.en.cnki.com.cn/Article_en/CJFDTOTAL-BIRD200705032.htm

Wei G, Wang B, Xu N, Li ZZ, Jiang JP (2009) Morphological evolution from aquatic to terrestrial in the genus *Oreolalax* (Amphibia, Anura, Megophryidae). Progress in Natural Science 19: 1043–1048. https://doi.org/10.1016/j.pnsc.2009.02.010

Wu GF, Zhao EM, Inger RF, Shaffer HB (1993) A new frog of the genus *Oreolalax* (Pelobatidae) from Sichuan, China. Journal of Herpetology 27: 410–413. https://doi.org/10.2307/1564828

Xu N, Wei G, Li DJ, Ye CY, Fei L (1992) Studies on the interspecific phylogeny of the *Oreolalax* (Amphibia: Pelobatidae). Acta Herpetologica Sinica 1–2: 40–49.

Zhang P, Liang D, Mao LR, Hillis D, Wake D, Cannatella D (2013) Efficient sequencing of Anuran mtDNAs and a mitogenomic exploration of the phylogeny and evolution of frogs. Molecular Biology and Evolution 30: 1899–1915. https://doi.org/10.1093/molbev/mst091

Zhang YG, Li N, Xiao JL, Pan T, Wang H, Zhang B, Zhou J (2017) A new species of the genus *Xenophrys* (Amphibia: Anura: Megophryidae) from Libo County, Guizhou, China. Asian Herpetological Research 8: 75–85. https://doi.org/10.16373/j.cnki.ahr.160041

Zhao EM, Adler K (1993) Herpetology of China. Society for the Study of Amphibians & Reptiles, 522 pp.

Supplementary material 1

Table S1

Authors: Yinmeng Hou, Shengchao Shi, Daming Hu, Yue Deng, Jianping Jiang, Feng Xie, Bin Wang

Explanation note: Measurements of the *Oreolalax longmenmontis* sp. nov. and its three relatives. See abbreviations for characters in the Materials and methods section.

Link: https://doi.org/10.3897/zookeys.929.49748.suppl1

Supplementary material 2

Table S2

Authors: Yinmeng Hou, Shengchao Shi, Daming Hu, Yue Deng, Jianping Jiang, Feng Xie, Bin Wang

Explanation note: Measurements of the *Oreolalax longmenmontis* sp. nov. tadpoles. See abbreviations for characters in the Materials and methods section.

Link: https://doi.org/10.3897/zookeys.929.49748.suppl2

Supplementary material 3

Table S3

Authors: Yinmeng Hou, Shengchao Shi, Daming Hu, Yue Deng, Jianping Jiang, Feng Xie, Bin Wang

Explanation note: Examined specimens in this study.

Link: https://doi.org/10.3897/zookeys.929.49748.suppl3

ZooKeys 929: 117–161 (2020)
doi: 10.3897/zookeys.929.50240
https://zookeys.pensoft.net

RESEARCH ARTICLE

A peer-reviewed open-access journal
ZooKeys
Launched to accelerate biodiversity research

Evolutionary relationships and population genetics of the Afrotropical leaf-nosed bats (Chiroptera, Hipposideridae)

Bruce D. Patterson[1], Paul W. Webala[2], Tyrone H. Lavery[1,3], Bernard R. Agwanda[4], Steven M. Goodman[1,5], Julian C. Kerbis Peterhans[1,6], Terrence C. Demos[1]

1 Negaunee Integrative Research Center, Field Museum of Natural History, Chicago IL 60605, USA **2** *Department of Forestry and Wildlife Management, Maasai Mara University, Narok, Kenya* **3** *Threatened Species Recovery Hub, Fenner School of Environment and Society, The Australian National University, Canberra, ACT, Australia* **4** *Mammalogy Section, National Museums of Kenya, Nairobi, Kenya* **5** *Association Vahatra, BP 3972, Antananarivo 101, Madagascar* **6** *College of Arts and Sciences, Roosevelt University, Chicago, IL, 60605, USA*

Corresponding author: Bruce D. Patterson (bpatterson@fieldmuseum.org)

Academic editor: DeeAnn Reeder | Received 24 January 2020 | Accepted 16 March 2020 | Published 22 April 2020

http://zoobank.org/0DBE5B59-AF74-4D94-A1AD-4EBB3E114565

Citation: Patterson BD, Webala PW, Lavery TH, Agwanda BR, Goodman SM, Kerbis Peterhans JC, Demos TC (2020) Evolutionary relationships and population genetics of the Afrotropical leaf-nosed bats (Chiroptera, Hipposideridae). ZooKeys 929: 117–161. https://doi.org/10.3897/zookeys.929.50240

Abstract

The Old World leaf-nosed bats (Hipposideridae) are aerial and gleaning insectivores that occur throughout the Paleotropics. Both their taxonomic and phylogenetic histories are confused. Until recently, the family included genera now allocated to the Rhinonycteridae and was recognized as a subfamily of Rhinolophidae. Evidence that Hipposideridae diverged from both Rhinolophidae and Rhinonycteridae in the Eocene confirmed their family rank, but their intrafamilial relationships remain poorly resolved. We examined genetic variation in the Afrotropical hipposiderids *Doryrhina*, *Hipposideros*, and *Macronycteris* using relatively dense taxon-sampling throughout East Africa and neighboring regions. Variation in both mitochondrial (cyt-b) and four nuclear intron sequences (ACOX2, COPS, ROGDI, STAT5) were analyzed using both maximum likelihood and Bayesian inference methods. We used intron sequences and the lineage delimitation method BPP—a multilocus, multi-species coalescent approach—on supported mitochondrial clades to identify those acting as independent evolutionary lineages. The program StarBEAST was used on the intron sequences to produce a species tree of the sampled Afrotropical hipposiderids. All genetic analyses strongly support generic monophyly, with *Doryrhina* and *Macronycteris* as Afrotropical sister genera distinct from a Paleotropical *Hipposideros*; mitochondrial analyses interpose the genera *Asellia*, *Coelops*, and *Asellia* between these clades. Mitochondrial analyses also suggest at least two separate colonizations of Africa by Asian groups of *Hipposideros*, but the actual number and direction of faunal interchanges will hinge on placement of the unsampled African-Arabian species *H. megalotis.* Mitochondrial sequences further identify a large number of geographically structured clades within species of all three genera. However, in sharp contrast to this pattern, the four nuclear introns fail to distinguish many of these groups and their geographic structuring disappears. Various distinctive mitochondrial clades are consolidated in the intron-based gene trees and delimitation analyses, calling into question their evolutionary independence or else indicating their very recent divergence. At the same time, there is now compelling genetic evidence in both mitochondrial and nuclear sequences for several additional unnamed species among the Afrotropical *Hipposideros.* Conflicting appraisals of differentiation among the Afrotropical hipposiderids based on mitochondrial and nuclear loci must be adjudicated by large-scale integrative analyses of echolocation calls, quantitative morphology, and geometric morphometrics. Integrative analyses will also help to resolve the challenging taxonomic issues posed by the diversification of the many lineages associated with *H. caffer* and *H. ruber*.

Keywords
cryptic species, mtDNA, nuclear introns, Paleotropical, phylogeny, species delimitation, systematics

Introduction

The Old World leaf-nosed bats, family Hipposideridae, currently include seven genera and 90 species of insectivorous bats distributed over much of the Paleotropics (Monadjem 2019; Simmons and Cirranello 2019). Both the taxonomic and phylogenetic histories of this family are confused. Throughout much of its history (e.g., Koopman 1989), Hipposideridae was considered either a subfamily of the Rhinolophidae (the horseshoe bats) or as its sister family within the Rhinolophoidea. Recently, however, the “trident bats” (*Cloeotis*, *Paratriaenops*, *Rhinonicteris*, and *Triaenops*) were shown to comprise a family-ranked group, the Rhinonycteridae, which is separate from and sister to the Hipposideridae (Foley et al. 2015; Armstrong et al. 2016). Even the genus *Hipposideros* Gray, 1831, as it was traditionally understood, appears paraphyletic with respect to the allied genera *Asellia*, *Aselliscus*, *Coelops*, and *Anthops* (Foley et al. 2015; Amador et al. 2018). Re-validation of *Macronycteris* Gray, 1866 and *Doryrhina* Peters, 1871 for groups of Afrotropical endemic species more closely related to each other than to African and Asian members of *Hipposideros* sensu stricto resolved a number of those issues (Foley et al. 2017).

The species richness of *Doryrhina*, *Macronycteris*, and *Hipposideros* differs widely. Most authors recognize two species of *Doryrhina* (*D. cyclops* and *D. camerunensis*), five species of *Macronycteris* (*M. commersoni*, *M. cryptovalorona*, *M. gigas*, *M. thomensis*, and *M. vittata*), and 83 species of *Hipposideros*, 10 of which occur in Africa (Monadjem 2019; Simmons and Cirranello 2019). These are *H. beatus*, *H. caffer*, *H. curtus*, *H. fuliginosus*, *H. lamottei*, *H. ruber*, and *H. tephrus* in the *bicolor* group of *Hipposideros*; *H. jonesi* and *H. marisae* in the *speoris* group, and *H. megalotis* in the *megalotis* group (Hill 1963; Murray et al. 2012; Monadjem 2019). In addition, three extinct species of hipposiderid are known from the region: †*Macronycteris besaoka* (Madagascar), †*Hip-*

posideros amenhotepos (Egypt), and †*H. kaumbului* (Ethiopia). Type localities for valid species, subspecies, and synonyms for these three genera in Africa and Madagascar appear in Figure 1; after the removal of *Doryrhina* and *Macronycteris* taxa, group assignments for the species remaining in *Hipposideros* appear in Table 1.

As suggested by their checkered taxonomic history, phylogenetic understanding of the Hipposideridae has slowly come into focus. *Doryrhina* and *Macronycteris* are two of a dozen generic-group names that were synonymized with *Hipposideros* for all of the 20th century (Miller 1907; Allen 1939; Koopman 1994). Instead of subgenera, taxonomists used the species groups delineated by Andersen (1918) and refined by Tate (1941) and Hill (1963) in their generic revisions based on morphology. Assessment of rhinolophoid relationships using an intron supermatrix (Eick et al. 2005) confirmed the early divergence of hipposiderids and rhinolophids (estimated at 41 Ma), thereby substantiating their rank as a separate families. Despite earlier suppositions that the area of origin for Hipposideridae was in Asia (Koopman 1970; Bogdanowicz and Owen 1998) or Australia (Hand and Kirsch 1998), Eick et al. (2005) clearly demonstrated the ancestry of the family (and superfamily) was in Africa. A recent supermatrix analysis with the most comprehensive taxonomic sampling (42 species; Amador et al. 2018) confirmed the early divergence of hipposiderids and rhinolophids at 41.3 Ma, but this analysis questioned the validity of both *Doryrhina* and *Macronycteris*. Amador et al. attributed the paraphyly of *Hipposideros* sensu lato documented by Foley et al. (2015) to their limited taxonomic sampling. Amador et al. (2018) also challenged the integrity of the *commersoni*, *cyclops*, *speoris*, and *bicolor* species groups, arguing that all African species save for *H. jonesi* belonged in a single, exclusively African species group.

Although new species of hipposiderids are regularly discovered and described in Asia (Robinson et al. 2003; Guillen-Servent and Francis 2006; Bates et al. 2007; Douangboubpha et al. 2011; Thong et al. 2012; Murray et al. 2018), the pace of discovery has been much slower in Africa. Only one extant species has been described since the recognition of *Hipposideros lamottei* (Brosset 1985 [“1984”]), and that one was from Madagascar (Goodman et al. 2016). Surveys of mitochondrial sequences from African hipposiderids have strongly suggested that supposedly widespread species such as *Hipposideros caffer* and *H. ruber* actually represent complexes of cryptic species (Vallo et al. 2008, 2011; Monadjem et al. 2013). Phylogenetic analyses (e.g., Vallo et al. 2008) show that these named species complexes are not monophyletic, resolving clades comprised of bats identified as both *H. caffer* and *H. ruber*. These studies have characterized the clades in both morphological and genetic terms, even establishing them in sympatry (see also Vallo et al. 2011). However, the uncertain relationship of the identified clades to the many names already proposed for Afrotropical hipposiderids, many based on incomplete or formalin-preserved specimens, has precluded formally naming them. Incomplete geographic sampling and the lack of evidence from nuclear genes for these populations has also clouded interpretations of this mitochondrial diversity.

Our field surveys in Eastern Africa and adjoining regions offer a new basis for considering the taxonomy and phylogenetics of Afrotropical hipposiderids. We sought to answer these questions: (1) Is there compelling evidence to support the recognition of

Figure 1. Type localities for Afrotropical hipposiderids: *Doryrhina*, blue symbols; *Hipposideros*, white symbols; *Macronycteris*, black symbols. Stars denote valid species, whereas circles indicate taxa considered as subspecies or synonyms. Localities are projected onto the biome map of Olson et al. (2001). Taxa depicted are: *Hipposideros abae* J. A. Allen,1917; †*Hipposideros* (*Pseudorhinolophus*) *amenhotepos* Gunnell, Winkler, Miller, Head, El-Barkooky, Gawad, Sanders & Gingerich, 2015; *Phyllorhina angolensis* Seabra, 1898; *Hipposideros caffer* var. *aurantiaca* De Beaux, 1924; *Hipposideros beatus* K. Andersen, 1906; †*Hipposideros besaoka* Samonds, 2007; *Phyllorrhina bicornis* Heuglin, 1861; *Hipposideros braima* Monard, 1939; *Hipposideros caffer* Sundevall, 1846; *Phyllorhina caffra* Peters, 1852; *Hipposideros camerunensis* Eisentraut, 1956; *Hipposideros caffer centralis* K. Andersen, 1906; *Rhinolophus Commersonii* É. Geoffroy, 1813; *Hipposideros cryptovalorona* Goodman, Schoeman, Rakotoarivelo & Willows-Munro, 2016; *Hipposideros curtus* G. M. Allen, 1921; *Phyllorrhina cyclops* Temminck, 1853; *Phyllorrhina fuliginosa* Temminck, 1853; *Hipposideros gigas gambiensis* K. Andersen, 1906; *Rhinolophus gigas* Wagner, 1845; *Phyllorrhina gracilis* Peters, 1852; *Hipposideros caffer guineensis* K. Andersen, 1906; *Hipposideros jonesi* Hayman, 1947; †*Hipposideros kaumbului* Wesselman, 1984; *Hipposideros lamottei* Brosset, 1985; *Hipposideros langi* J. A. Allen, 1917; *Hipposideros marisae* Aellen, 1954; *Phyllorhina Commersoni*, var. *marungensis* Noack, 1887; *Hipposideros beatus maximus* Verschuren, 1957; *Phyllorrhina megalotis* Heuglin, 1861; *Rhinolophus micaceus* de Winton, 1897; *Hipposideros Commersoni mostellum* Thomas, 1904; *Hipposideros nanus* J. A. Allen, 1917; *Hipposideros gigas niangarae* J. A. Allen, 1917; *Hipposideros caffer niapu* J. A. Allen, 1917; *Phyllorrhina rubra* Noack, 1893; *Hipposideros sandersoni* Sanderson, 1937; *Hipposideros tephrus* Cabrera, 1906; *Phyllorhina Commersoni*, var. *thomensis* Bocage, 1891; *Hipposideros gigas viegasi* Monard, 1939; *Phyllorhina vittata* Peters, 1852.

Table 1. Species groups of *Hipposideros* (modified from Murray et al. 2012 to include newly recognized forms and to remove species now recognized in *Doryrhina* and *Macronycteris*).

Armiger group
H. alongensis
H. armiger
H. griffini[a]
H. pendelburyi[a]
H. turpis
Bicolor group
ater subgroup
H. ater[b]
H. atrox[a]
H. bicolor[b]
H. breviceps[b]
H. cineraceus[b]
H. coronatus[b]
H. dyacorum[b]
H. einnaythu[a,b]
H. halophyllus[b]
H. khaokhouayensis[b]
H. nicobarulae[a,b]
H. pomona[b]
H. ridleyi[b]
H. rotalis[b]
calcaratus subgroup
H. calcaratus[c]
H. cervinus[c]
H. coxi[c]
H. galeritus[c]
ruber subgroup
H. abae[d]
H. beatus[e]
H. caffer[e]
H. fuliginosus[e]
H. lamottei[e]
H. ruber[e]
H. tephrus[a,e]
subgroup uncertain
H. cruminiferus
H. curtus
H. doriae
H. durgadasi
H. fulvus
H. gentilis[a]
H. hypophyllus
H. kunzi[a]
H. macrobullatus
H. maggietaylorae
H. nequam
H. obscurus
H. orbiculus
H. papua
H. pygmaeus
Boeadii group
H. boeadii
Cyclops group[f]
H. corynophyllus
H. edwardshilli
H. muscinus
H. semoni
H. stenotis
H. wollastoni
Diadema group
H. demissus
H. diadema
H. dinops
H. inexpectatus
H. inornatus
H. lankadiva
H. lekaguli
H. pelingensis
Larvatus group
H. grandis
"H. khasiana"[a,g]
H. larvatus
H. madurae
H. sorenseni
H. sumbae
Megalotis group
H. megalotis
Pratti group
H. lylei
H. pratti
H. scutinares
Speoris group
H. jonesi[h]
H. marisae[g]
H. speoris

(Endnotes)

a Added to species list subsequent to Murray et al. (2012)

b Recognized in the Ater species group by Monadjem (2019)

c Recognized in the Calcaratus species group by Monadjem (2019)

d Formerly listed in the Speoris group but transferred to the Ruber group by Monadjem (2019)

e Recognized in the Ruber species group by Monadjem (2019)

f *H. cyclops* and *H. camerunensis* are now recognized as members of *Doryrhina*; listed species were treated as *Doryrhina* in Monadjem (2019) on the basis of similar morphology but were recognized as the Muscinus group by Tate (1941); they might represent an unnamed genus or subgenus.

g Invalid name accorded to what is likely a real biological entity (cf. Monadjem 2019)

h Formerly in the Bicolor species group but transferred to the Speoris group by Monadjem (2019).

Doryrhina and *Macronycteris* as distinct Afrotropical genera alongside the Paleotropical *Hipposideros*? (2) Which species belong to these groups? (3) Are the traditional species groups of African hipposiderids monophyletic? Using both mitochondrial and nuclear intron sequences, we also evaluate the question of cryptic species among African hipposiderids and the possibility of mitochondrial-nuclear discordance.

Material and methods

Selection of taxa and sampling

Our genetic dataset is based on 453 hipposiderid individuals, the vast majority being represented by museum vouchers. We generated original genetic data from 319 individuals collected at 102 georeferenced localities, and complemented them with 134 mitochondrial sequences from 90 localities downloaded from GenBank (we obtained new sequence data for five individuals with prior GenBank records; see Suppl. material 1: Figure S1 and Appendix I). All individuals were sequenced for Cytochrome-b (cyt-b) in order to maximize assessment of genetic diversity; however, redundant haplotypes were removed for subsequent phylogenetic analyses (see Appendix I for complete list of individuals sequenced). The bats newly sequenced for this study were obtained over several decades in the course of small mammal surveys across sub-Saharan Africa and Madagascar, with relatively dense sampling in East Africa. Initial assignment of East African individuals to species was determined using meristic, mensural, and qualitative characters published in the bat keys of Thorn et al. (2009) and Patterson and Webala (2012). Collection methods followed mammal guidelines for the use of wild mammals in research and education (Sikes and the Animal Care and Use Committee of the American Society of Mammalogists 2016) and the most recent collections were approved under Field Museum of Natural History's IACUC #2012-003. Only GenBank records for cyt-b were available for records of the Arabian-North African hipposiderid *Asellia*, which was included for context in the phylogenetic analyses. Lacking information from nuclear introns, we draw no firm conclusions from their placement and do not discuss *Asellia* in this paper (see Benda et al. 2011; Bray and Benda 2016).

Appendix I contains the institutions and voucher numbers, GenBank accession numbers, and locality information for our samples. The fact that museum voucher specimens were used wherever possible for the genetic analyses permits the genetic analysis to serve as a foundation for integrative taxonomic analyses of dental, cranial, and skeletal variation, using the same specimens. To avoid adding to current taxonomic confusion, we take a conservative approach in assigning names to clades in our analyses. Where a clade's taxonomic identity was ambiguous or unknown, we referred to it simply as a numbered clade. Integrative taxonomic diagnoses of the various clades supported by our analyses will be necessary to determine which, if any, existing names may apply to them. However, to relate our results to those of earlier studies of African *Hipposideros* (Vallo et al. 2008, 2011; Monadjem et al. 2013), we cross-referenced specimens used in two or more analyses to equate the various non-binomial names that have been applied to these cryptic lineages.

DNA extraction, amplification, and sequencing

Genomic DNA from preserved tissue samples was extracted using the Wizard SV 96 Genomic DNA Purification System (Promega Corporation, WI, USA). Fresh specimens were sequenced for mitochondrial cytochrome-b (cyt-b), using the primer pair LGL 765F and LGL 766R (Bickham et al. 1995; Bickham et al. 2004), and four unlinked autosomal nuclear introns: ACOX2 intron 3, COPS7A intron 4, ROGDI intron 7 (Salicini et al. 2011), and STAT5B (Matthee et al. 2001) for hipposiderid specimens and the sister group *Triaenops afer* (Rhinonycteridae; see Table 1 for primer information). PCR amplification, thermocycler conditions, and sequencing were identical to Patterson et al. (2018) and Demos et al. (2018). Sequences were assembled and edited using GENEIOUS PRO v.11.1.5 (Biomatters Ltd). Sequence alignments were made using MUSCLE (Edgar 2004) with default settings in GENEIOUS. Protein coding data from cyt-b were translated to amino acids to determine codon positions and confirm the absence of premature stop codons, deletions, and insertions. Several gaps were incorporated in the nuclear intron alignments, but their positions were unambiguous.

Sequence alignments used in this study have been deposited on the FIGSHARE data repository (https://doi.org/10.6084/m9.figshare.11936250). All newly generated sequences were deposited in GenBank with accession numbers MT149315–MT149893 (see also Appendix I).

Phylogenetic analyses

jMODELTEST2 (Darriba et al. 2012) on CIPRES Science Gateway v. 3.3 (Miller et al. 2010) was used to determine the sequence substitution models that best fit the data using the Bayesian Information Criterion (BIC) for cyt-b and the four nuclear introns. PARTITIONFINDER2 (Lanfear et al. 2016) on CIPRES was used to determine the sequence substitution models for the concatenated alignment of four nuclear introns using the Bayesian Information Criterion (BIC) with the 'greedy' search algorithm. Uncorrected sequence divergences (*p*-distances) between and within species/clades were calculated for cyt-b using MEGA X v. 10.0.5 (Kumar et al. 2018). Maximum-likelihood (ML) analyses were performed using the program IQ-TREE v. 1.6.10 (Chernomor et al. 2016; Nguyen et al. 2015) on the CIPRES portal for separate gene trees (cyt-b, ACOX2, COPS7A, ROGDI, and STAT5B) and a concatenated alignment, partitioned by gene, using the four nuclear introns. As in Hillis and Bull (1993), nodes supported by bootstrap values (BP) ≥ 70% were considered strongly supported. Gene tree analyses under a Bayesian Inference (BI) framework were inferred in MRBAYES v. 3.2.7 (Ronquist et al. 2012) on the CIPRES portal for the same set of genes as the ML analyses. Two independent runs were conducted in MrBayes, and nucleotide substitution models were unlinked across partitions for each nuclear locus in the concatenated alignment. Four Markov chains were run for 1×10^8 generations for individual gene trees, and 2×10^7 generations for the concatenated analysis, using default heating values and sampled every 1000th generation. A conservative 25% burn-in was applied and stationarity of the MRBAYES results was assessed in Tracer v. 1.7 (Rambaut et al. 2018). Majority-rule consensus trees were constructed for each Bayesian analysis. Following Erixon et al. (2003), nodes supported by posterior probabilities (PP) ≥0.95 were considered strongly supported.

Haplotype networks for cyt-b were inferred using the median-joining network algorithm in PopArt v. 1.7 (Leigh and Bryant 2015). Separate analyses were carried out for the following clades, each consisting of four subclades: (1) *Doryhina* (*D. camerunensis*, *D.* cf. *camerunensis*, *D. cyclops*1, and *D. cyclops*2); (2) *Macronycteris* (*M. commersoni*, *M. cryptovalorona*, *M. gigas*, and *M. vittata*); (3) *Hipposideros caffer*1–4; (4) *Hipposideros caffer*5–8; and (5) *Hipposideros ruber*1–4.

Hipposiderid taxa included in the species tree analyses were assigned to either species or numbered clades based on clade support in the ML and BI gene-tree analyses of the cyt-b dataset. This in turn identified populations to be used as 'candidate species' in a coalescent-based species-tree approach implemented in StarBEAST2 (Ogilvie et al. 2017), an extension of BEAST v. 2.5.1 (Drummond et al. 2012; Bouckaert et al. 2014). Species tree analysis was conducted using the four nuclear intron alignments. Substitution, clock, and tree models were unlinked across all loci. A lognormal relaxed-clock model was applied to each locus under a Yule tree prior and a linear with constant root population size model. Four independent replicates were run with random starting seeds, and chain lengths of 1×10^8 generations and parameters were sampled every 5,000 steps. For the StarBEAST2 analyses, evidence of convergence and stationarity of posterior distributions of model parameters was assessed based on ESS values >200 and examination of trace files in Tracer v. 1.7. The burn-in was set at 10% and separate runs were assembled using LOGCOMBINER v. 2.5.1 and TREEANNOTATOR v. 2.5.1 (Rambaut et al. 2018).

Coalescent lineage delimitation

Based on the well supported clades obtained in the cyt-b gene tree analyses and available intron samples, a lineage delimitation scenario with 18 candidate species was tested. We inferred the evolutionary isolation of their gene pools using the phased nuclear DNA dataset (ACOX2, COPS7A, ROGDI, and STAT5A; 104 individuals) for joint independent lineage delimitation and species-tree estimation evaluated under the multi-species coalescent model using the program BPP v. 3.3 (Yang and Rannala 2014; Rannala and Yang 2017). This analysis was carried out to guide future investigations of the species status of evolutionarily isolated lineages inferred here. Supported lineages will be examined using an integrative species taxonomic approach, including morphological, morphometric, and acoustic characters, as well as ectoparasite associations and distributional data. Species/clade memberships for BPP were identical to individuals assigned to lineages in the species tree analyses. The validity of our assignment of individuals to populations was tested using the guide-tree-free algorithm (A11) in BPP. Because the probability of delimitation by BPP is sensitive to selected parameters (Leaché and Fujita 2010; Yang 2015), we evaluated two independent runs for each of four different combinations of divergence depth and effective population sizes priors (τ and θ, respectively; Table 2). Two independent MCMC chains were run for 5×10^4 generations. The burn-in was 20% and samples drawn every 50th generation. In total, eight BPP runs were carried out using four phased nuclear intron alignments. Lineages were considered to be statistically well supported when the delimitation posterior probabilities generated were ≥0.95 under all four combinations of priors.

Results

In terms of cyt-b sequence divergence, clades within *Doryrhina* are separated by 3.0–5.7% genetic distances, whereas less than 3% separates the four recognized species of

Table 2. Primer information and chosen substitution models for regions amplified in this study. Substitution models before “/” are the best-supported models inferred by jMODELTEST2 and models after “/” indicate those inferred by PARTITIONFINDER2 for the concatenated intron alignment.

Primer name	Sequence	Primer publication	Substitution model
ACOX2-3-F	5’-CCTSGGCTCDGAGGAGCAGAT-3’	Salicini et al. 2011	K80+G / K81+G
ACOX2-3-R	5’-GGGCTGTGHAYCACAAACTCCT-3’		
COPS7A-4-F	5’-TACAGCATYGGRCGRGACATCCA-3’	Salicini et al. 2011	HKY / K80
COPS7A-4-R	5’-TCACYTGCTCCTCRATGCCKGACA-3’		
ROGDI-7-F	5’-CTGATGGAYGCYGTGATGCTGCA-3’	Salicini et al. 2011	K80+G / K81+G
ROGDI-7-R	5’-CACGGTGAGGCASAGCTTGTTGA-3’		
STAT5B-16-F	5’--CTGCTCATCAACAAGCCCGA-3’	Matthee et al. 2001	GTR+G / K81+G
STAT5B-16-R	5’-GGCTTCAGGTTCCACAGGTTGC-3’		
cyt-b-LGL-765-F	5’-GGCTTCAGGTTCCACAGGTTGC-3’	Trujillo et al. 2009	GTR+I+G
cyt-b -LGL-766-R	5’-GTTTAATTAGAATYTYAGCTTTGGG-3’		

Table 3. Prior Schemes (PS) used in BPP analyses. Prior distributions on τ represent two relative divergence depths (deep and shallow) and on θ represent two relative effective population sizes (large and small) scaling mutation rates.

PS	Effective pop. size	Divergence depth	Gamma distribution for prior
1	Large	Deep	$\theta = \Gamma$ [1, 10] and $\tau = \Gamma$ [1, 10]
2	Large	Shallow	$\theta = \Gamma$ [1, 10] and $\tau = \Gamma$ [2, 2000]
3	Small	Shallow	$\theta = \Gamma$ [2, 2000] and $\tau = \Gamma$ [2, 2000]
4	Small	Deep	$\theta = \Gamma$ [2, 2000] and $\tau = \Gamma$ [1, 10]

Macronycteris. Between Afrotropical *Hipposideros*, the greatest distances separate *H. jonesi* from other lineages (13.4–16.1%). The various numbered clades allied to *Hipposideros caffer* differ from one another in cyt-b sequences by 2.5–10.3% and clades allied to *H. ruber* differ by 3.0–8.2% (Table 4).

Maximum likelihood and Bayesian phylogenies from a 452-individual alignment of cyt-b are shown in Suppl. material 2: Figures S2, Suppl. material 3: Figures S3. Identical haplotypes were pruned from this tree to produce the 303 unique-haplotype alignment shown in Figure 2. The 303 haplotype alignment used in the ML and BI gene tree analyses ranged from 413 to 1140 base pairs (bp) in length (89.9% complete matrix). Only the Bayesian topology is shown, but both posterior probabilities and bootstrap values are depicted at common, well supported nodes. Multiple, geographically cohesive clades are evident for the three widely distributed Afrotropical *Hippposideros*, *H. beatus*, *H. caffer*, and *H. ruber*.

Substitution networks for cyt-b haplotypes for *Doryrhina*, *Macronycteris*, and *Hipposideros* are shown in Figures 3, 4, showing the genetic and geographic relationships of the clades identified in Figure 2.

Maximum likelihood and Bayesian phylogenies from a 103-individual alignment of four concatenated introns for *Doryrhina*, *Macronycteris*, and *Hipposideros* are shown in Figure 5. Many of the numbered clades in Figures 2–4 are jumbled in Figure 5; they are not recovered as monophyletic units and the geographic structure evident in mtDNA analyses disappears.

Table 4. Uncorrected cyt-b p-distances between (off diagonal) and within (on diagonal) Afrotropical hipposiderid clades, showing the number of base differences per site averaged over all sequence pairs between groups. The analysis involved 386 nucleotide sequences and all ambiguous positions were removed; na (not available) reflects a sample size of one individual.

		[1]	[2]	[3]	[4]	[5]	[6]	[7]	[8]	[9]	[10]	[11]	[12]	[13]	[14]	[15]
[1]	*Doryrhina camerunensis*	**0.003**														
[2]	*Doryrhina* cf. *camerunensis*	0.055	**na**													
[3]	*Doryrhina cyclops* 1	0.057	0.048	**0.008**												
[4]	*Doryrhina cyclops* 2	0.055	0.041	0.030	**0.006**											
[5]	*Hipposideros abae*	0.176	0.173	0.168	0.166	**0.033**										
[6]	*Hipposideros beatus* 1	0.152	0.156	0.160	0.152	0.116	**0.007**									
[7]	*Hipposideros beatus* 2	0.146	0.149	0.151	0.147	0.117	0.044	**0.006**								
[8]	*Hipposideros caffer* 1	0.157	0.154	0.150	0.148	0.108	0.103	0.106	**0.006**							
[9]	*Hipposideros caffer* 2	0.153	0.150	0.150	0.147	0.106	0.096	0.108	0.045	**0.01**						
[10]	*Hipposideros caffer* 3	0.152	0.148	0.150	0.149	0.108	0.110	0.111	0.046	0.052	**0.011**					
[11]	*Hipposideros caffer* 4	0.162	0.159	0.160	0.154	0.106	0.105	0.114	0.077	0.078	0.079	**0.018**				
[12]	*Hipposideros caffer* 5	0.150	0.155	0.159	0.148	0.113	0.091	0.096	0.095	0.101	0.103	0.098	**0.005**			
[13]	*Hipposideros caffer* 6	0.155	0.156	0.164	0.153	0.112	0.093	0.102	0.090	0.097	0.099	0.094	0.028	**0.011**		
[14]	*Hipposideros caffer* 7	0.151	0.154	0.161	0.148	0.108	0.084	0.094	0.094	0.094	0.098	0.096	0.025	0.032	**0.011**	
[15]	*Hipposideros caffer* 8	0.154	0.155	0.160	0.152	0.111	0.090	0.092	0.092	0.095	0.102	0.093	0.033	0.039	0.029	**0.021**
[16]	*Hipposideros fuliginosus*	0.155	0.149	0.154	0.142	0.101	0.095	0.096	0.078	0.084	0.087	0.094	0.088	0.086	0.080	0.085
[17]	*Hipposideros jonesi*	0.153	0.143	0.154	0.147	0.160	0.145	0.138	0.135	0.140	0.140	0.139	0.134	0.134	0.137	0.139
[18]	*Hipposideros lamottei*	0.171	0.173	0.174	0.163	0.106	0.097	0.118	0.094	0.086	0.095	0.097	0.057	0.059	0.052	0.060
[19]	*Hipposideros* cf. *lamottei*	0.158	0.158	0.156	0.149	0.107	0.103	0.107	0.091	0.099	0.095	0.097	0.053	0.058	0.052	0.054
[20]	*Hipposideros marisae*	0.177	0.180	0.178	0.172	0.159	0.153	0.153	0.144	0.148	0.140	0.152	0.148	0.144	0.154	0.159
[21]	*Hipposideros ruber* 1	0.155	0.151	0.152	0.142	0.104	0.099	0.101	0.081	0.084	0.085	0.086	0.090	0.081	0.082	0.082
[22]	*Hipposideros ruber* 2	0.155	0.155	0.156	0.142	0.103	0.097	0.102	0.081	0.082	0.089	0.089	0.086	0.078	0.083	0.081
[23]	*Hipposideros ruber* 3	0.159	0.149	0.155	0.147	0.105	0.094	0.101	0.084	0.082	0.096	0.088	0.090	0.083	0.082	0.082
[24]	*Hipposideros ruber* 4	0.153	0.147	0.151	0.141	0.100	0.094	0.097	0.073	0.073	0.085	0.082	0.083	0.077	0.078	0.078
[25]	*Hipposideros* cf. *ruber*	0.164	0.161	0.161	0.153	0.099	0.094	0.100	0.086	0.084	0.095	0.093	0.081	0.080	0.080	0.083
[26]	*Macronycteris commersoni*	0.157	0.156	0.155	0.145	0.164	0.159	0.154	0.164	0.169	0.168	0.171	0.166	0.170	0.167	0.162
[27]	*Macronycteris cryptovalorona*	0.147	0.143	0.147	0.142	0.157	0.152	0.146	0.156	0.162	0.161	0.165	0.159	0.164	0.158	0.157
[28]	*Macronycteris gigas*	0.151	0.149	0.154	0.144	0.164	0.163	0.158	0.162	0.168	0.165	0.170	0.165	0.171	0.164	0.165
[29]	*Macronycteris vittata*	0.147	0.148	0.149	0.140	0.162	0.158	0.147	0.160	0.161	0.166	0.165	0.164	0.169	0.164	0.163

Table 4. Continued.

		[16]	[17]	[18]	[19]	[20]	[21]	[22]	[23]	[24]	[25]	[26]	[27]	[28]	[29]
[16]	*Hipposideros fuliginosus*	**0.003**													
[17]	*Hipposideros jonesi*	0.137	**0.008**												
[18]	*Hipposideros lamottei*	0.100	0.161	**0.038**											
[19]	*Hipposideros* cf. *lamottei*	0.091	0.142	0.054	**0.006**										
[20]	*Hipposideros marisae*	0.145	0.092	0.156	0.158	**na**									
[21]	*Hipposideros ruber* 1	0.082	0.144	0.093	0.087	0.152	**0.013**								
[22]	*Hipposideros ruber* 2	0.084	0.147	0.093	0.091	0.157	0.030	**0.007**							
[23]	*Hipposideros ruber* 3	0.082	0.142	0.085	0.088	0.158	0.052	0.057	**0.022**						
[24]	*Hipposideros ruber* 4	0.078	0.140	0.087	0.088	0.154	0.053	0.051	0.057	**na**					
[25]	*Hipposideros* cf. *ruber*	0.084	0.142	0.094	0.089	0.157	0.081	0.081	0.082	0.072	**0.033**				
[26]	*Macronycteris commersoni*	0.155	0.186	0.183	0.167	0.193	0.163	0.162	0.161	0.168	0.174	**0.012**			
[27]	*Macronycteris cryptovalorona*	0.149	0.176	0.170	0.163	0.185	0.161	0.161	0.158	0.160	0.162	0.028	**0.003**		
[28]	*Macronycteris gigas*	0.153	0.179	0.178	0.169	0.190	0.165	0.165	0.161	0.165	0.169	0.026	0.029	**0.012**	
[29]	*Macronycteris vittata*	0.150	0.181	0.180	0.168	0.192	0.158	0.159	0.158	0.159	0.164	0.026	0.029	0.027	**0.006**

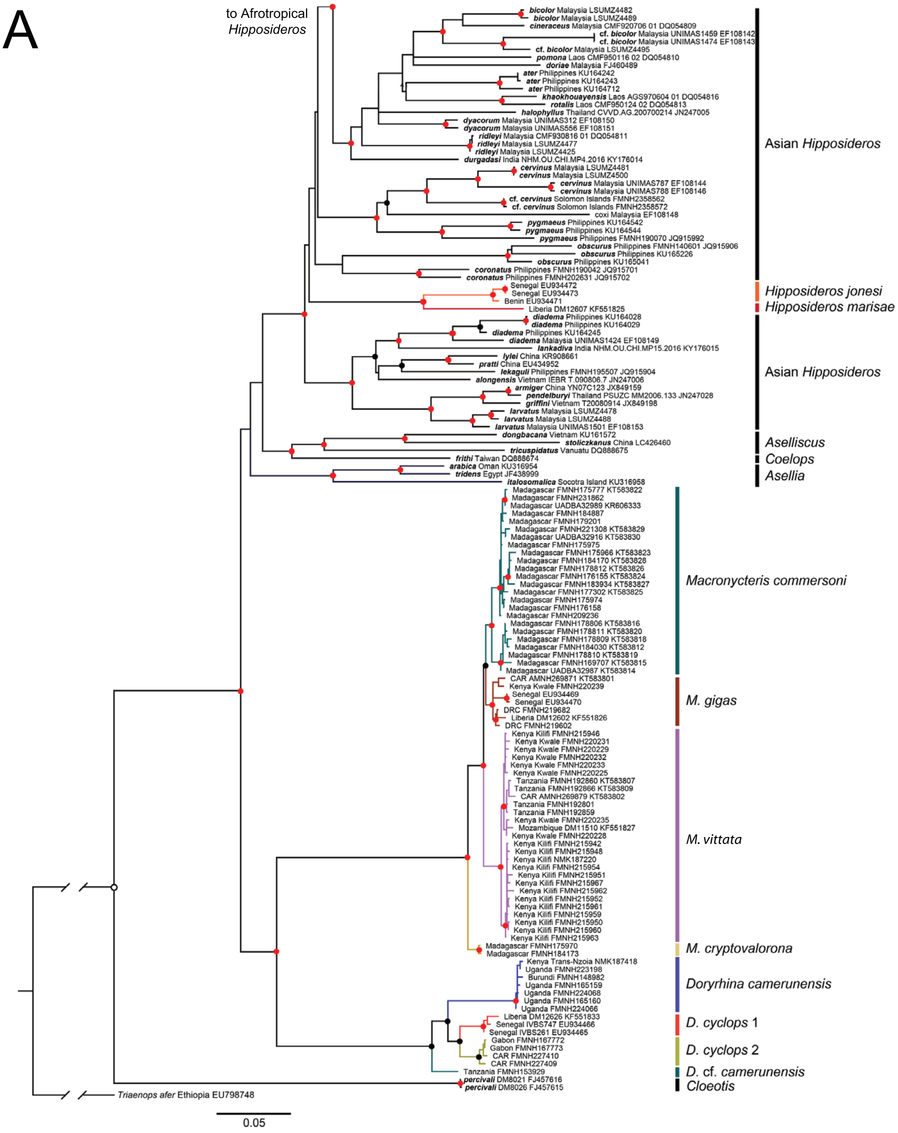

Figure 2. Parts **A** and **B**. Phylogeny of Hipposideridae based on Bayesian analysis of 303 cyt-b sequences. Colored lines denote well supported clades and symbols denote nodal support: red circles, BS ≥ 70%, PP ≥ 0.95; black circles BS ≥ 70%, PP ≤ 0.95; open circles BS ≤ 70%, PP ≥ 0.95.

A species tree generated using StarBEAST from the four introns appears in Figure 6. It depicts well-supported relationships among the various clades allied with *H. caffer*, *H. ruber*, and *H. beatus*. Remarkably, and in contrast with the concatenated analyses,

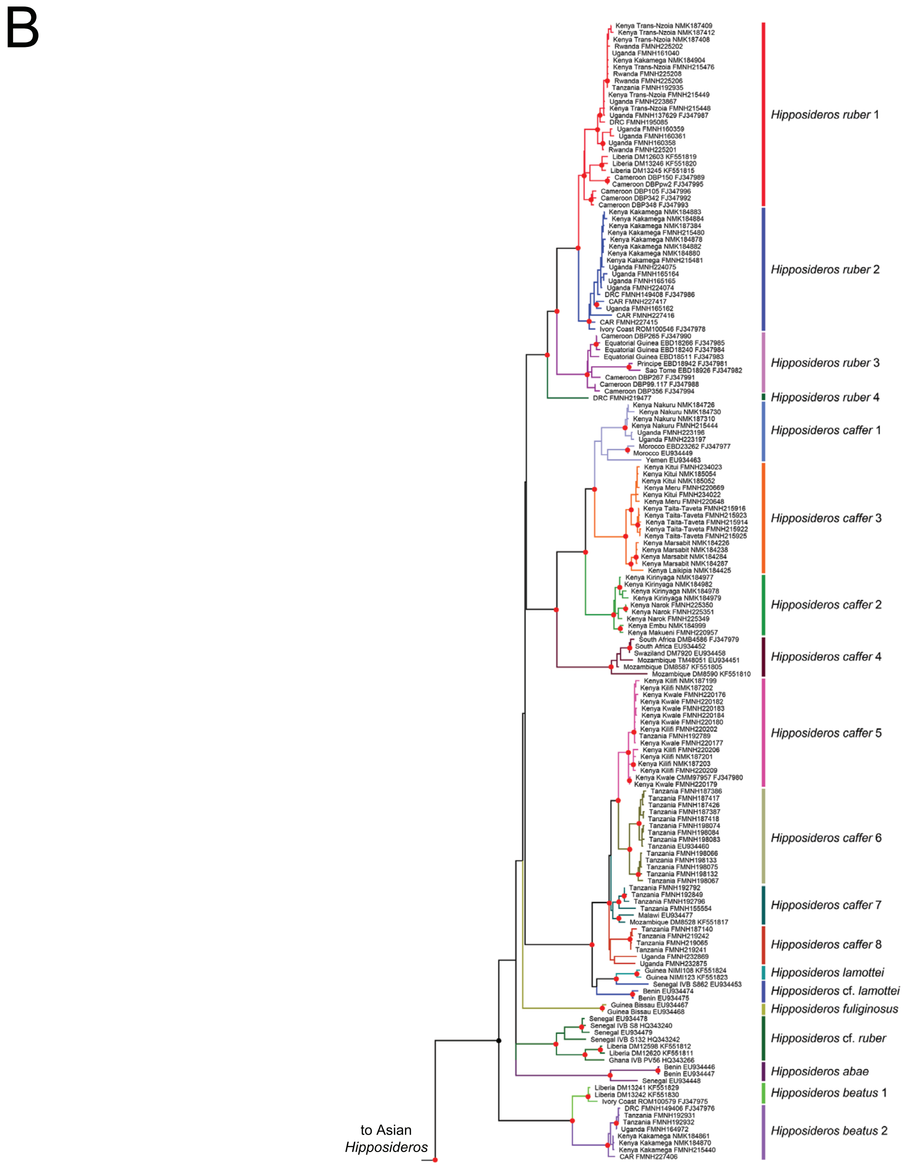

Figure 7. Continued.

it shows support for the Asian dyad *H. diadema* and *H. larvatus* as sister to these *ruber* subgroup members, with the Asian *ater* subgroup outside this pairing. There is little support for the deeper phylogenetic nodes.

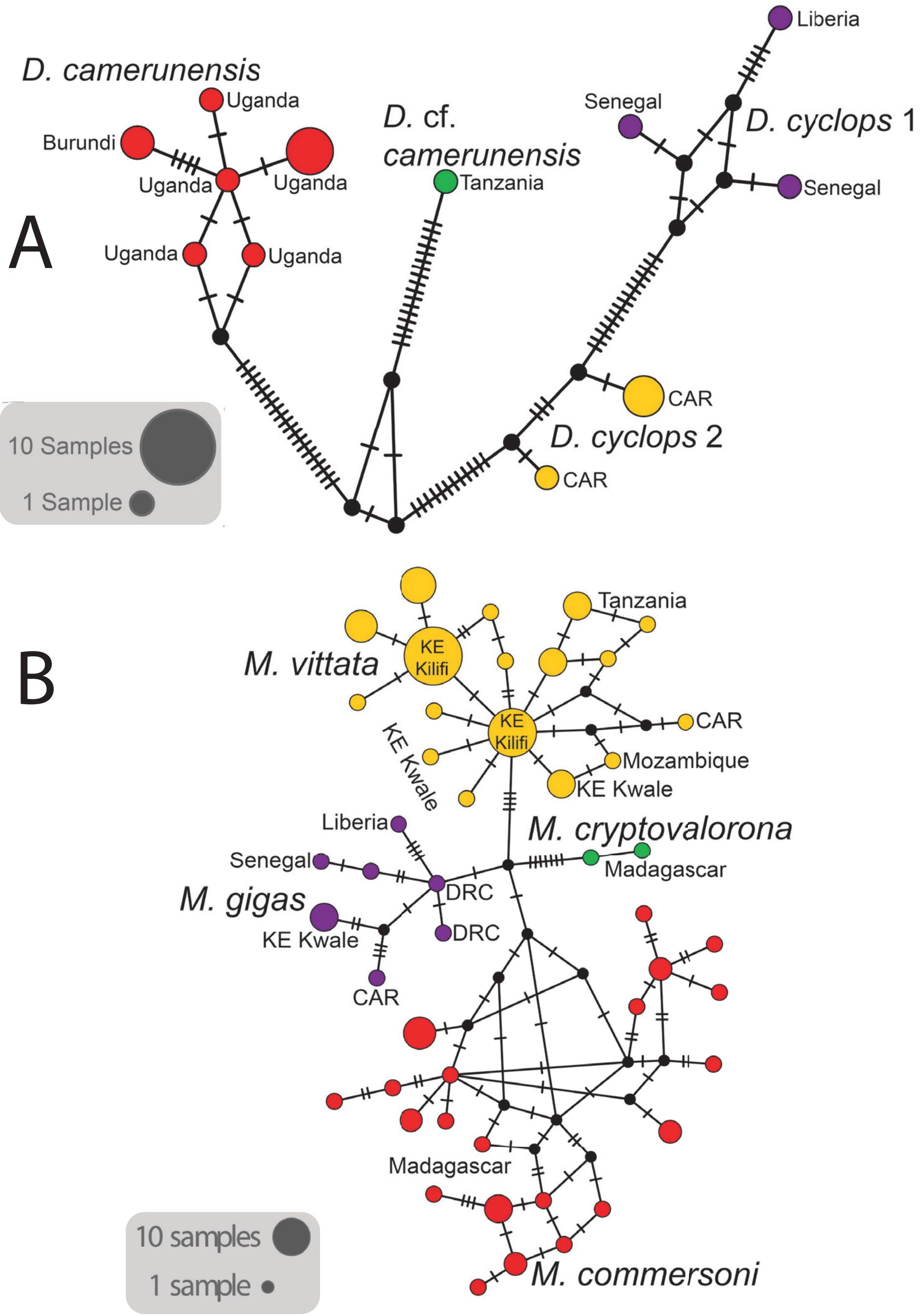

Figure 3. Substitution network plots for Afrotropical hipposiderids **A** *Doryrhina* **B** *Macronycteris*.

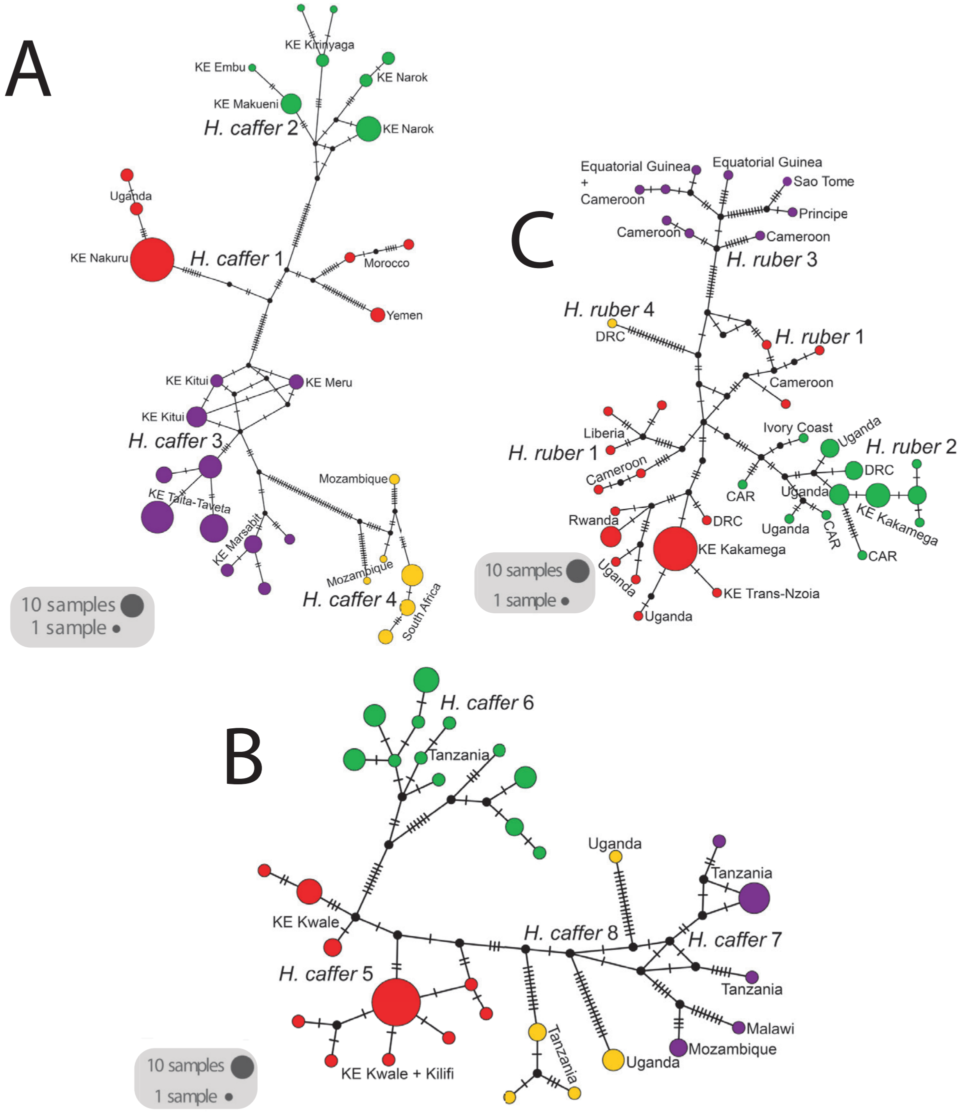

Figure 4. Substitution network plots for Afrotropical hipposiderids **A** *Hipposideros caffer* clades 1–4 **B** *Hipposideros caffer* clades 5–8 **C** *H. ruber* clades.

Discussion

Overall genetic variability

The three Afrotropical hipposiderid genera differ substantially in terms of their internal genetic differentiation. Clades of *Hipposideros* are separated by cyt-b *p*-distances averaging 9.7% (2.5–16.1%), whereas *Doryrhina* clades average p-distances of 4.8% (3.0–5.7%) and *Macronycteris* clades 2.7% (2.6–2.9%). Distance values for these genera tend to fall at the lower end of values obtained with similar sampling intensity for species-ranked clades in other Afrotropical bat genera: 2.5% for *Otomops* (Patterson et al. 2018), 9.3% for *Miniopterus* (Demos et al. 2020), 10% for *Scotophilus* and *Rhinolophus* (Demos et al. 2018, 2019a), 13.5% for *Myotis* (Patterson et al. 2019), and 17% for *Nycteris* (Demos et al. 2019b). Fewer cyt-b substitutions on average for these hipposiderids does not limit support for individual clades, and because distances do not approach those characteristic of substitutional saturation, the cyt-b tree recovers much of the deeper phylogenetic structure evident with nuclear intron sequences (compare Figs 2, 5).

Phylogenetics

Both cyt-b and intron analyses securely recovered *Doryrhina*, *Macronycteris*, and *Hipposideros* as monophyletic. *Doryrhina* + *Macronycteris* are sister to the remaining hipposiderids. However, only the cyt-b analysis included the hipposiderid genera *Aselliscus*, *Coelops*, and *Asellia* alongside *Hipposideros*. That analysis recovered all four genera as monophyletic with strong support. *Aselliscus* and *Coelops* were recovered as sister to *Hipposideros*, with *Asellia* joining later, but these relationships lacked confident support.

Using a supermatrix approach on exemplars of 46 species of hipposiderids, Amador et al. (2018) found *Hipposideros* sensu stricto to be paraphyletic. They recovered a mostly Asian group of *Hipposideros* as sister to two subclades, *Coelops* + *Aselliscus* and *Asellia* + African hipposiderids excluding *H. jonesi*, which was recovered with the Asian taxa. Paraphyly in this molecular analysis echoed earlier indications of *Hipposideros* paraphyly from morphology (Bogdanowicz and Owen 1998; Hand and Kirsch 1998, 2003). In another supermatrix analysis of exemplars belonging to 49 hipposiderid species, Shi and Rabosky (2015) failed to recover *Macronycteris* as monophyletic; *M. commersoni* was sister to all remaining hipposiderids, but strangely it did not group with *M. gigas*. When the anomalous position of *M. commersoni* in their tree is ignored, their topology is highly similar to that of Figure 2, except that *Asellia* (*Aselliscus*, *Coelops*) become the sister of *Hipposideros* (*Macronycteris*, *Doryrhina*), rather than sister of just *Hipposideros*. Using both mitochondrial and nuclear loci, Lavery et al. (2014) found that 17 species of Asian, Oceanian and Australasian *Hipposideros* were monophyletic with respect to the genera *Aselliscus*, *Coelops*, and *Anthops*. Clearly, missing data and missing taxa compromise all of these phylogenetic appraisals, so that the question of hipposiderid and *Hipposideros* monophyly remains open. However, subject to its sampling limitations, there is clear support in our analyses of monophyly for *Doryrhina*, *Macronycteris*, and *Hipposideros* as we apply these names.

Despite employing different mitochondrial and nuclear loci and using different sets of taxa, the phylogeny recovered by Lavery et al. (2014) is largely congruent with that in Figure 5. Their earliest diverging species group of *Hipposideros* is the *calcaratus* group, not represented in our tree unless *H. obscurus* is a member (Table 1). Their next diverging unit is the *diadema* group, which is also positioned near the base of our tree. Their other two groups are paired: the *galeritus* group (which includes *H. cervinus*, indicating that this species is misclassified as a *calcaratus* member) joined with the

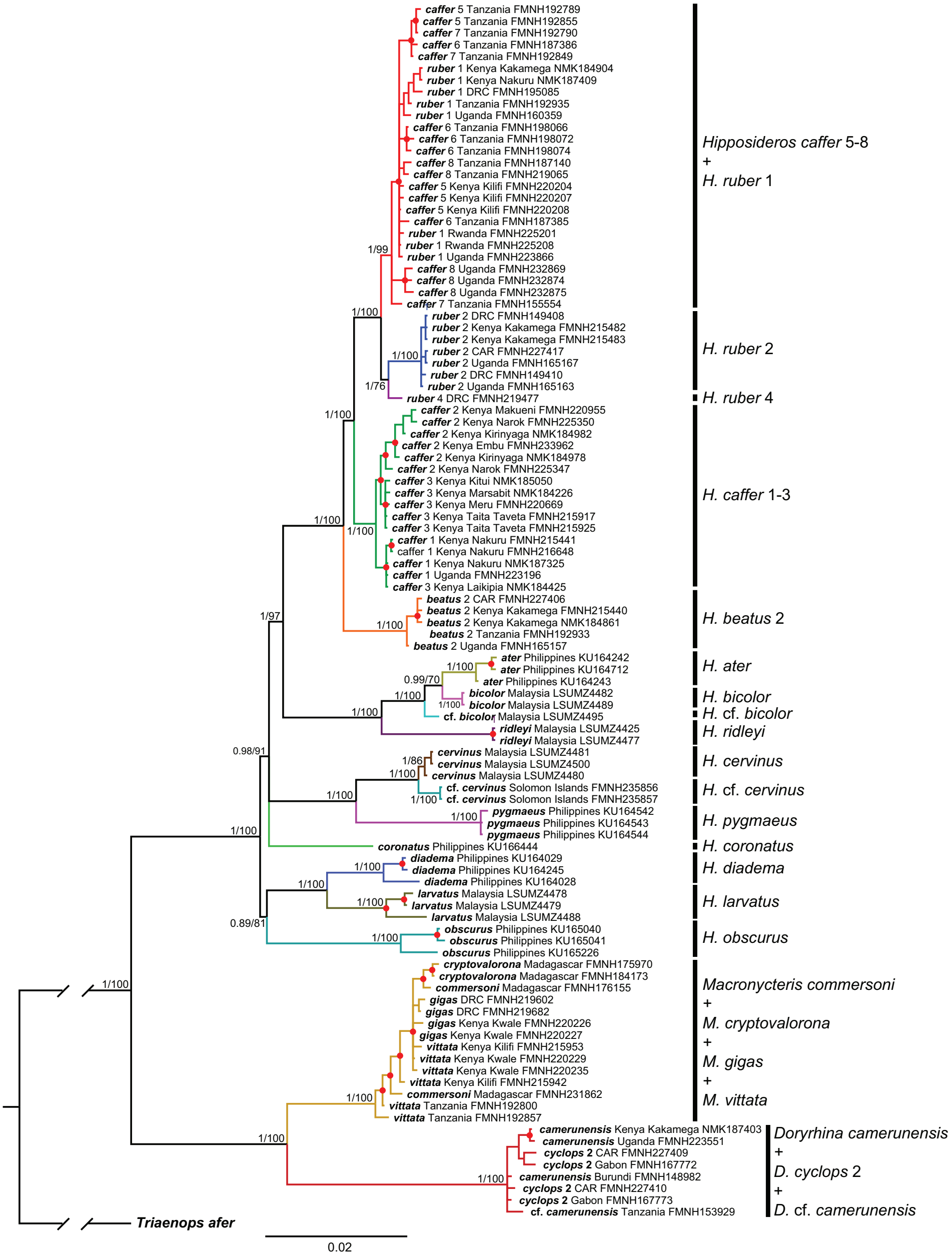

Figure 5. Phylogeny of Hipposideridae based on Bayesian analysis of 103 concatenated nuclear intron sequences. Numbers denote posterior probabilities (BI) and bootstrap percentages (ML); red circles at more terminal nodes indicate BS ≥ 70%, PP ≥ 0.95.

bicolor/*ater* group. In our intron analysis (Fig. 5), members of the *larvatus* and *diadema* groups join *H. obscurus* as sister to all remaining *Hipposideros* groups. The remainder form a trichotomy: *H. coronatus*, typically considered in the *bicolor* group; *H. pygmaeus* and *H. cervinus*, which are listed in different groups but were both considered members of the *galeritus* unit by Tate (1941); and the erstwhile *bicolor* group (sensu Hill 1963), which was subdivided into the *ater* subgroup (for Asian, Oceanian, and Australasian species) and the *ruber* subgroup (for Atrotropical ones) by Monadjem (2019).

The *ater* subgroup members included in our mitochondrial analysis (Fig. 2) form a well-supported clade consisting of *H. bicolor*, *H. cineraceus*, *H. pomona*, *H. doriae*, *H. ater*, *H. khaokhouayensis*, *H. rotalis*, *H. halophyllus H. dyacorum*, *H. ridley*, and *H. durgadasi*. This group is sister to all analyzed members of the *ruber* subgroup: the various clades allied with *Hipposideros beatus*, *H. caffer*, and *H. ruber*, as well as individuals of the Afrotropical species *H. lamottei* and *H. fuliginosus*. *H. abae*, which was previously considered in the *speoris* group (Simmons 2005; Murray et al. 2012), is clearly a member of the *ruber* group. Outside this pairing are the Asian species *H. cervinus*, *H. coronatus*, *H. coxi*, *H. obscurus*, and *H. pygmaeus*. Two Afrotropical species also lie outside the *ruber* + *ater* clade: *H. jonesi* and *H. marisae*, both thought to belong to the *speoris* group, appear as sisters in Figure 2A.

Parsimony, topological position, and the strong support of branching relationships in the mitochondrial and intron trees (Fig. 5; also Lavery et al. 2014) make it clear that the Afrotropical *ruber* group represents a comparatively recent colonization event from Asian ancestors–the *ruber* group is sister to the *ater* group and this pair has Asian sisters. However, although the basal dichotomy within *Hipposideros* includes an all Asian clade, lack of support for its sister(s) clouds the phylogenetic position of the *H. jonesi-H. marisae* clade–possibly sister to all sampled *Hipposideros* but more likely sandwiched between Asian clades. In any case, Figure 2 suggests that the *H. jonesi-H. marisae* clade resulted from an earlier African-Asian colonization event.

The lack of agreement in the phylogenetic position of *H. diadema* and *H. larvatus* between the concatenated intron tree (Fig. 5) and the species tree (Fig. 6) deserves comment, as both analyses were based on the same genetic dataset. The position of *H. diadema-H. larvatus* as sister to the *ruber* group (Fig. 6) runs counter to both our other genetic analyses (Figs 2, 5) and morphological assessments (Hill 1963; Murray et al. 2012; Table 1). This discrepancy is likely due to the generally weaker support for deep nodes within the tree; in the absence of saturation, this is often taken as evidence of rapid evolutionary radiations (e.g., Almeida et al. 2011). Lanier and Knowles (2014) used simulated data on deep phylogenies to show that species-tree methods do account for coalescent variance at deep nodes but that mutational variance among lineages poses the primary challenge for accurate reconstruction. In either case, vastly expanded genetic sampling via NGS techniques offers the most plausible avenues to clearer resolution.

However, the highly distinctive species *H. megalotis* belongs to its own species group (Table 1) and has not been included in any genetic analysis. Distributed in the Horn of Africa and the Arabian Peninsula, *H. megalotis* is the only hipposiderid with a fold of skin joining the base of the ear pinnae. Its uniquely specialized auditory system and derived dentition (e.g., loss of anterior premolars and enlargement of outer lower incisors), led Hill (1963) to regard it as a species that diverged early from the other

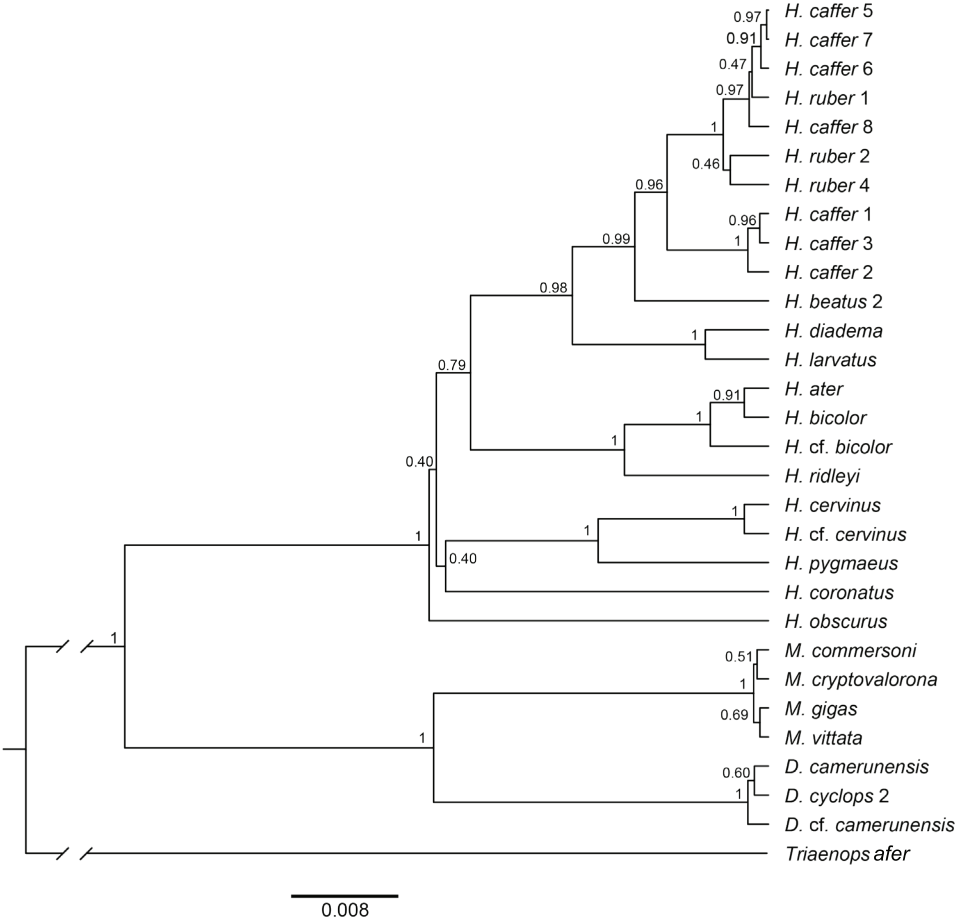

Figure 6. Species tree Hipposideridae based on StarBEAST analysis of four introns. Posterior probabilities appear at all nodes.

groups of African *Hipposideros*. Including this species in future analyses would shed light on the group's biogeography. Were there three colonizations of Africa by Asian groups of *Hipposideros* or could *H. megalotis* be sister to all Asian lineages of this genus? This information would greatly clarify ancestral geographic range inference.

Species limits

The lineage delimitation analyses indicate that a number of hipposiderid lineages are either unnamed or unidentified, and also that a number of recognized species may not be genetically and evolutionarily independent.

Previous studies had indicated that both *Hipposideros caffer* (Vallo et al. 2008) and *H. ruber* (Vallo et al. 2011) appear to be complexes of cryptic species. The two are traditionally distinguished on the basis of size and pelage color, *H. ruber* being the larger and more brightly colored form, but this distinction is clouded by geographic variation in size and the presence of both reddish and gray-brown phases in both species. Our mitochondrial analyses identified four *H. ruber* lineages and eight *H. caffer* lineages in two distinct groupings among the sampled populations (Fig. 2). Four of the *caffer* lineages and three of the *ruber* clades were identified as putative species by the BPP analyses (Table 5). The large number of clades in East Africa is remarkable: Kenya and Tanzania each support four of the eight clades allied with *H. caffer*, and all but one of the eight clades known from throughout the continent occur in one or the other East African country. This undoubtedly reflects the region's great landscape diversity, where West and Central African rainforests reach their eastern limit, southern savannas reach their northern limits, the Sahel reaches its southern limits, and all are riven by the African Rift Valley. It also is a product of our sampling intensity (see Suppl. material 1: Fig. S1).

Because some cyt-b sequences were used in multiple studies of this group, it is possible to relate our clade labels to those used by earlier studies (Table 6). Based on attributions made on morphological grounds by Vallo et al. (2008) and Monadjem et al. (2013), some well-supported but unnamed clades in our analysis can be identified. For instance, *caffer*1 has a distributional range and includes specimens previously identified as *Hipposideros tephrus* (Appendix I), while specimens of *caffer*4 come from near the type locality of *H. caffer* Sundevall, 1846, and may well represent that species. However, no samples confidently identified as *H. ruber* from the vicinity of its type locality have been sequenced, leaving the application of that name to clades in any of these trees purely conjectural. Applying formal names only after integrative taxonomic assessment is a responsible course as multispecies coalescent models like BPP can lead to over-splitting of species, especially when applied to geographically variable species complexes with parapatric distributions (Chambers and Hillis 2020).

Doryrhina is a poorly known genus characterized morphologically by the peculiar club-shaped processes on the central and posterior nose leaves. This trait is shared by the two recognized African species, *D. cyclops* and *D. camerunensis*, which differ chiefly in size (the latter is larger, with forearm lengths >75 mm). Although *D. cyclops* is considered to be monotypic, mitochondrial sequences clearly separate West African populations in Liberia and Senegal (*cyclops*1) from Central African populations in Gabon and Central African Republic (*cyclops*2), and these are substantially separated from *D. camerunensis* and a specimen referred to that species from Tanzania (Figs 2, 3). However, both the intron analysis (Fig. 5) and the species tree (Fig. 6) show little or no geographic structure. The BPP analyses confirm that none of the mitochondrial clades is behaving as an independent evolutionary lineage (Table 5). Geographic structure in mtDNA but continent-wide admixture in the nuclear genome could result from either male-biased dispersal with female philopatry or highly structured seasonal migrations, which are known in other hipposiderids. In any case, the genetic patterns of *Doryrhina* are hard to reconcile with its space-use behavior; individuals appear to have very small home ranges, on the order of a few hectares (Monadjem 2019). An integrative taxo-

Table 5. Lineage delimitation results from BPP based on the four intron dataset for mtDNA-supported clades of Afrotropical Hipposideridae. PS1-PS4 refer to four different prior schemes based on population size and age of divergence priors (see Table 3 for parameter details). Bold font indicates that the putative species was delimited under all parameter settings.

Putative Species	PS1	PS2	PS3	PS4
Doryrhina camerunensis	0.30	0.76	0.95	0.51
D. cf. *camerunensis*	0.32	0.73	0.97	0.79
D. cyclops 2	0.23	0.68	0.95	0.51
***Hipposideros beatus* 2**	**1**	**1**	**1**	**1**
***H. caffer* 1**	**0.99**	**0.99**	**0.99**	**0.99**
***H. caffer* 2**	**0.99**	**1**	**1**	**1**
***H. caffer* 3**	**0.99**	**0.99**	**0.99**	**0.99**
H. caffer 5	0.14	0.18	0.11	0.08
H. caffer 6	0.56	0.61	0.85	0.82
H. caffer 7	0.14	0.18	0.11	0.08
***H. caffer* 8**	**0.99**	**0.99**	**0.99**	**0.99**
***H. ruber* 1**	**0.99**	**0.99**	**0.99**	**0.99**
***H. ruber* 2**	**1**	**0.99**	**1**	**0.99**
***H. ruber* 4**	**0.99**	**0.99**	**0.99**	**0.99**
Macronycteris commersoni	0.24	0.72	0.94	0.52
M. cryptovalorona	0.35	0.81	0.97	0.76
M. gigas	0.09	0.43	0.91	0.38
M. vittata	0.11	0.44	0.90	0.34

nomic review of the genus *Doryrhina* is needed to determine the validity of *D. cyclops* and *D. camerunensis*. It would also shed light on whether six Australo-Papuan species tentatively allocated to that genus (cf. Monadjem 2019) belong there or elsewhere. Tate (1941) had earlier allocated those species to the Australasian *muscinus* group, convergent on but separate from his Afrotropical *cyclops* group, but Hill (1963) later united these groups.

Our analysis included four of the five recognized species of *Macronycteris*, lacking only *M. thomensis*, which is endemic to São Tomé Island in the Gulf of Guinea. Two species, *M. gigas* and *M. vittata*, occur on the African mainland and two others, *M. commersoni* and *M. cryptovalorona*, occur on Madagascar. *Macronycteris cryptovalorona* was named only in 2016, on the basis of its strong genetic divergence from *M. commersoni*; it appears in Figure 2 as sister to all three remaining species of *Macronycteris*. Despite a search for diagnostic characters, Goodman et al. (2016) could not distinguish it morphologically from *M. commersoni*. Both species are known to occur in the same caves in south central and southwestern Madagascar (Goodman et al. 2016; Rakotoarivelo et al. 2019). On the other hand, *M. vittata* and *M. gigas* are distinguished typically on the basis of size and pelage color (cf. Monadjem 2019). They are also known to occur together in the same cave (Shimoni Cave in Kwale, Kenya; Webala et al. 2019), where they utilize echolocation calls with different peak frequencies: *vittata* at 64–70 kHz and *gigas* at 53.4–54.8 kHz. Both in Africa and on Madagascar, these pairs of taxa appear to act as distinct species, but the monophyly evident in the cyt-b sequences (Figs 2, 4) disappears in the nuclear intron analyses. BPP analyses fail to

Table 6. Clade names and associated binomials (if used) for three analyses of cryptic lineages within the *ruber* species group of *Hipposideros*. No genetic analysis of this group has included type material; consequently, the application of binomials hinges on the robustness of ancillary morphological analyses, which were not conducted in our study. Boldfaced names denote clades supported by all four prior schemes in our BPP delimitation analyses.

Vallo et al. (2008)		**Monadjem et al. (2013)**		**This paper**
A1	*H. caffer*			caffer 4
		A1a	*H. caffer*	caffer 4
		A1b	*H. caffer*	caffer 4
A2	*H. caffer*		*H. caffer tephrus*	**caffer 1**
B	*H. ruber*			caffer 5
		B1	*H. ruber*	cf. lamottei
		B2	*H. ruber*	caffer 7
C1	*H. ruber*			**ruber 1**, **ruber 2**
		C1a	*H. cf. ruber*	**ruber 1**
		C1b	*H. cf. ruber*	**ruber 1**
C2	*H. ruber*	C2	*H. cf. ruber*	ruber 3
				ruber 4
D	*H. ruber*		*H. cf. ruber*	cf. ruber
		D1	*H. cf. ruber*	cf. ruber
		D2	*H. cf. ruber*	cf. ruber
–		E1	*H. cf. ruber*	cf. ruber
–		E2	*H. cf. ruber*	cf. ruber
–		–		**caffer 2**
–		–		**caffer 3**
–		–		caffer 6
–		–		**caffer 8**
abae	*H. abae*	abae	*H. abae*	abae
beatus	*H. beatus*	beatus	*H. beatus*	beatus1, **beatus 2**
fuliginosus	*H. fuliginosus*	fuliginosus	*H. fuliginosus*	fuliginosus
lamottei	*H. lamottei*	lamottei	*H. lamottei*	lamottei

resolve any of the *Macronycteris* species, and none appear as monophyletic in the concatenated intron analyses.

Our results clearly underscore the importance of using multilocus datasets to evaluate phylogenetic and phylogeographic relationships at the genus and species level in mammals. Use of a single genetic system may lead to widely divergent conclusions regarding species identity and distribution. Toews and Brelsford (2012) reviewed cases of mito-nuclear discordance in animals generally. Fully 18% of the cases they reviewed had discordant patterns of mitochondrial and nuclear DNA. In most cases, such patterns are attributable to adaptive introgression of mtDNA, demographic disparities, and sex-biased asymmetries; in some cases they found evidence for hybrid zone movement or human agency. Discordant patterns of variation between mitochondrial and nuclear DNA have been reported in at least six other families of bats (Nesi et al. 2011; Furman et al. 2014; Naidoo et al. 2016; Hassanin et al. 2018; Demos et al. 2019a; Gürün et al. 2019). Gürün et al. (2019) implicated the role of sex-biased dispersal in causing such discordance, male dispersal spreading nuclear variation farther and faster than the movement of mitochondria. This may be a more general pattern in bats (see also Demos et al. 2019b). To understand the processes responsible for these discordant patterns of genome evolution, extensive genomic sampling and far fuller knowledge of natural history will be required.

Acknowledgments

We thank Michael Bartonjo, Carl Dick, Ruth Makena, Beryl Makori, David Wechuli, Richard Yego, and Aziza Zuhura for help in obtaining specimens in the field. We acknowledge with special thanks the assistance of Simon Musila (National Museums of Kenya), Donna Dittman and Jacob Esselstyn (Louisiana State University) and Maria Eifler (University of Kansas) for loans of material. We also appreciate the efforts of curators and collection managers in all the institutions cited in Appendix I for maintaining the museum voucher specimens that enable integrative taxonomic studies to confidently name our numbered lineages. Fieldwork in eastern and southern Africa was funded by various agencies in cooperation with the Field Museum, especially the JRS Biodiversity Foundation. Field Museum's Council on Africa, Marshall Field III Fund, and Barbara E. Brown Fund for Mammal Research were critical to fieldwork and analyses, as were supporters Bud and Onnolee Trapp and Walt and Ellen Newsom. The John D. and Catherine T. MacArthur Foundation, Fulbright Program of US Department of State, Wildlife Conservation Society, and the Centers for Disease Control and Prevention sponsored and/or assisted in providing samples from DRC, Malawi, Mozambique, and Uganda. WWF Gabon supported fieldwork in Gabon, as did the Partenariat Mozambique-Réunion dans la Recherche en Santé: pour une approche intégrée d'étude des maladies infectieuses à risque épidémique (MoZaR; Fond Européen de Développement Régional, Programme Opérationnel de Coopération Territoriale) in Mozambique. We thank Ara Monadjem and Daniela Rossoni for reviews of an earlier draft of this manuscript.

References

Aellen V (1954) Description d'un nouvel *Hipposideros* (Chiroptera) de la Côte d'Ivoire. Revue Suisse de Zoologie 61: 473–483. https://doi.org/10.5962/bhl.part.75404

Allen GM (1921) A new horseshoe bat from West Africa. Revue de Zoologie Africaine 9: 193–196. https://doi.org/10.5962/bhl.part.24480

Allen GM (1939) A checklist of African mammals. Bulletin of the Museum of Comparative Zoology at Harvard College 83: 1–763.

Allen JA, Lang H, Chapin JP (1917) The American Museum Congo Expedition collection of bats. Bulletin of the American Museum of Natural History 37: 405–563. https://doi.org/10.5962/bhl.title.82385

Almeida F, Giannini N, DeSalle R, Simmons N (2011) Evolutionary relationships of the Old World fruit bats (Chiroptera, Pteropodidae): another star phylogeny? BMC Evolutionary Biology 11: 1–281. https://doi.org/10.1186/1471-2148-11-281

Amador LI, Moyers Arévalo RL, Almeida FC, Catalano SA, Giannini NP (2018) Bat systematics in the light of unconstrained analyses of a comprehensive molecular supermatrix. Journal of Mammalian Evolution 25: 37–70. https://doi.org/10.1007/s10914-016-9363-8

Andersen K (1906a) On *Hipposideros caffer*, Sund. and its closest allies; with some notes on *H. fuliginosus*, Temm. Annals and Magazine of Natural History (Series 7) 17: 269–282. https://doi.org/10.1080/00222930608562523

Andersen K (1906b) On the bats of the *Hipposideros armiger* and *commersoni* types. Annals and Magazine of Natural History (Series 7) 17: 35–48. https://doi.org/10.1080/00222930608562488

Andersen K (1918) Diagnoses of new bats of the families Rhinolophidæ and Megadermatidæ. Annals and Magazine of Natural History (Series 9) 2: 374–384. https://doi.org/10.1080/00222931808562380

Armstrong KN, Goodman SM, Benda P, Hand SJ (2016) A common name for the bat family Rhinonycteridae–the Trident Bats. Zootaxa 4179: 115–117. https://doi.org/10.11646/zootaxa.4179.1.7

Bates PJJ, Rossiter SJ, Suyanto A, Kingston T (2007) A new species of *Hipposideros* (Chiroptera: Hipposideridae) from Sulawesi. Acta Chiropterologica 9: 13–26. https://doi.org/10.3161/1733-5329(2007)9[13:ANSOHC]2.0.CO;2

Benda P, Vallo P, Reiter A (2011) Taxonomic revision of the genus *Asellia* (Chiroptera: Hipposideridae) with a description of a new species from southern Arabia. Acta Chiropterologica 13: 245–270. https://doi.org/10.3161/150811011X624749

Bickham JW, Patton JC, Schlitter DA, Rautenbach IL, Honeycutt RL (2004) Molecular phylogenetics, karyotypic diversity, and partition of the genus *Myotis* (Chiroptera: Vespertilionidae). Molecular Phylogenetics and Evolution 33: 333–338. https://doi.org/10.1016/j.ympev.2004.06.012

Bickham JW, Wood CC, Patton JC (1995) Biogeographic implications of cytochrome b sequences and allozymes in sockeye (*Oncorhynchus nerka*). Journal of Heredity 86: 140–144. https://doi.org/10.1093/oxfordjournals.jhered.a111544

Bocage JVBd (1891) Sur une variété de "*Phyllorhina commersoni*" de l'île St. Thomé. Jornal de Sciencias Mathematicas, Physicas e Naturaes, Academia Real das Sciencias de Lisboa (serie 2) 2: 1–88.

Bogdanowicz W, Owen RD (1998) In the Minotaur's labrinth: phylogeny of the bat family Hipposideridae. In: Kunz TH, Racey PA (Eds) Bat Biology and Conservation. Smithsonian Institution Press, Washington, 27–42.

Bouckaert R, Heled J, Kühnert D, Vaughan T, Wu C-H, Xie D, Suchard MA, Rambaut A, Drummond AJ (2014) BEAST 2: a software platform for Bayesian evolutionary analysis. PLoS Computational Biology 10: e1003537. https://doi.org/10.1371/journal.pcbi.1003537

Bray TC, Benda P (2016) Distribution of *Asellia tridens* (Chiroptera: Hipposideridae) lineages including representatives from Saudi Arabia. Zoology in the Middle East 62: 283–287. https://doi.org/10.1080/09397140.2016.1250708

Brosset A (1985 ["1984"]) Chiroptères d'altitude du Mont Nimba (Guinée). Description d'une espèce nouvelle, *Hipposideros lamottei*. Mammalia 48: 545–556. https://doi.org/10.1515/mamm.1984.48.4.545

Cabrera A (1906) Mamiferos de Mogador. Boletín de la Real Sociedad Española de Historia Natural 6: 357–368.

Chambers EA, Hillis DM (2020) The multispecies coalescent over-splits species in the case of geographically widespread taxa. Systematic Biology 69: 184–193. https://doi.org/10.1093/sysbio/syz042

Chernomor O, von Haeseler A, Minh BQ (2016) Terrace aware data structure for phylogenomic inference from supermatrices. Systematic Biology 65: 997–1008. https://doi.org/10.1093/sysbio/syw037

Darriba D, Taboada GL, Doallo R, Posada D (2012) jModelTest 2: more models, new heuristics and parallel computing. Nature Methods 9: 772–772. https://doi.org/10.1038/nmeth.2109

De Beaux O (1924) Mammiferi della Somalia Italiana. Atti della Società Italiana di Scienze Naturali Milano 62: 1–254.

De Winton WE (1897) Descriptions of two new mammals from West Africa. Annals and Magazine of Natural History (Series 6) 20: 1–524. https://doi.org/10.1080/00222939709487396

Demos TC, Webala PW, Bartonjo M, Patterson BD (2018) Hidden diversity of African yellow house bats (Vespertilionidae, *Scotophilus*): insights from multilocus phylogenetics and lineage delimitation. Frontiers in Ecology and Evolution 6: 1–86. https://doi.org/10.3389/fevo.2018.00086

Demos TC, Webala PW, Goodman SM, Kerbis Peterhans JC, Bartonjo M, Patterson BD (2019a) Molecular phylogenetics of the African horseshoe bats (Chiroptera: Rhinolophidae): expanded geographic and taxonomic sampling of the Afrotropics BMC Evolutionary Biology 19: 1–166. https://doi.org/10.1186/s12862-019-1485-1

Demos TC, Webala PW, Kerbis Peterhans JC, Goodman SM, Bartonjo M, Patterson BD (2019b) Molecular phylogenetics of slit-faced bats (Chiroptera: Nycteridae) reveals deeply divergent African lineages. Journal of Zoological Systematics and Evolutionary Research 57: 1019–1038. https://doi.org/10.1111/jzs.12313

Demos TC, Webala PW, Lutz HL, Peterhans JCK, Goodman SM, Cortés-Delgado N, Bartonjo M, Patterson BD (2020) Multilocus phylogeny of a cryptic radiation of Afrotropical long-fingered bats (Chiroptera, Miniopteridae). Zoologica Scripta 49: 1–3. https://doi.org/10.1111/zsc.12388

Douangboubpha B, Bumrungsri S, Satasook C, Soisook P, Bu SSH, Aul B, Harrison DL, Pearch MJ, Thomas NM, Bates PJJ (2011) A new species of small *Hipposideros* (Chiroptera: Hipposideridae) from Myanmar and a revaluation of the taxon *H. nicobarulae* Miller, 1902 from the Nicobar Islands. Acta Chiropterologica 13: 61–78. https://doi.org/10.3161/150811011X578624

Drummond AJ, Suchard MA, Xie D, Rambaut A (2012) Bayesian phylogenetics with BEAUti and the BEAST 1.7. Molecular Biology and Evolution 29: 1969–1973. https://doi.org/10.1093/molbev/mss075

Edgar RC (2004) MUSCLE: multiple sequence alignment with high accuracy and high throughput. Nucleic Acids Research 32: 1792–1797. https://doi.org/10.1093/nar/gkh340

Eick GN, Jacobs DS, Matthee CA (2005) A nuclear DNA phylogenetic perspective on the evolution of echolocation and historical biogeography of extant bats (Chiroptera). Molecular Biology and Evolution 22: 1869–1886. https://doi.org/10.1093/molbev/msi180

Eisentraut M (1956) Beitrage zur Chiropteran-Fauna von Kamerun (Westafrika). Zeitschrift für Morphologie und Ökologie der Tiere 84: 525–540.

Erixon P, Svennblad B, Britton T, Oxelman B (2003) Reliability of Bayesian posterior probabilities and bootstrap frequencies in phylogenetics. Systematic Biology 52: 665–673. https://doi.org/10.1080/10635150390235485

Foley NM, Goodman SM, Whelan CV, Puechmaille SJ, Teeling E (2017) Towards navigating the Minotaur's labyrinth: cryptic diversity and taxonomic revision within the speciose genus *Hipposideros* (Hipposideridae). Acta Chiropterologica 19: 1–18. https://doi.org/10.3161/15081109ACC2017.19.1.001

Foley NM, Thong VD, Soisook P, Goodman SM, Armstrong KN, Jacobs DS, Puechmaille SJ, Teeling EC (2015) How and why overcome the impediments to resolution: lessons from rhinolophid and hipposiderid bats. Molecular Biology and Evolution 32: 313–333. https://doi.org/10.1093/molbev/msu329

Furman A, Çoraman E, Çelik YE, Postawa T, Bachanek J, Ruedi M (2014) Cytonuclear discordance and the species status of *Myotis myotis* and *Myotis blythii* (Chiroptera). Zoologica Scripta 43: 549–561. https://doi.org/10.1111/zsc.12076

Geoffroy Saint-Hilaire É (1813) Sur un genre de chauve-souris, sous le nom de Rhinolophes. Annales du Muséum National d'Histoire Naturelle, Paris 20: 254–266.

Goodman SM, Schoeman MC, Rakotoarivelo A, Willows-Munro S (2016) How many species of *Hipposideros* have occurred on Madagascar since the Late Pleistocene? Zoological Journal of the Linnean Society 177: 428–449. https://doi.org/10.1111/zoj.12368

Guillen-Servent A, Francis CM (2006) A new species of bat of the *Hipposideros bicolor* group (Chiroptera: Hipposideridae) from Central Laos, with evidence of convergent evolution with Sundaic taxa. Acta Chiropterologica 8: 39–61. https://doi.org/10.3161/1733-5329(2006)8[39:ANSOBO]2.0.CO;2

Gunnell GF, Butler PM, Greenwood M, Simmons NB (2015) Bats (Chiroptera) from Olduvai Gorge, early Pleistocene, bed I (Tanzania). American Museum Novitates 3846: 1–36. https://doi.org/10.1206/3846.1

Gürün K, Furman A, Juste J, Ramos Pereira MJ, Palmeirim JM, Puechmaille SJ, Hulva P, Presetnik P, Hamidovic D, Ibáñez C (2019) A continent-scale study of the social structure and phylogeography of the bent-wing bat, *Miniopterus schreibersii* (Mammalia: Chiroptera), using new microsatellite data. Journal of Mammalogy 100: 1865–1878. https://doi.org/10.1093/jmammal/gyz153

Hand SJ, Kirsch JAW (1998) A southern origin for the Hipposideridae (Microchiroptera)? Evidence from the Australian fossil record. In: Kunz TH, Racey PA (Eds) Bat Biology and Conservation. Smithsonian Institution Press, Washington, 72–90.

Hand SJ, Kirsch JAW (2003) *Archerops*, a new annectent hipposiderid genus (Mammalia: Microchiroptera) from the Australian Miocene. Journal of Paleontology 77: 1139–1151. https://doi.org/10.1666/0022-3360(2003)077<1139:AANAHG>2.0.CO;2

Hassanin A, Colombo R, Gembu GC, Merle M, Tu VT, Görföl T, Akawa PM, Csorba G, Kearney T, Monadjem A, Ing RK (2018) Multilocus phylogeny and species delimitation within the genus *Glauconycteris* (Chiroptera, Vespertilionidae), with the description of a new bat species from the Tshopo Province of the Democratic Republic of the Congo. Journal of Zoological Systematics and Evolutionary Research 56: 1–22. https://doi.org/10.1111/jzs.12176

Hayman RW (1947) A new *Hipposideros* from Sierra Leone. Annals and Magazine of Natural History (Series 14) 109: 71–73. https://doi.org/10.1080/00222934708654611

Heuglin T (1861) Beiträge zur fauna der Säugetheire N.O.-Afrika's. I. Chiroptera. Nova acta Academiae Caesareae Leopoldino-Carolinae Germanicae Naturae Curiosorum 29: 1–18.

Hill JE (1963) A revision of the genus *Hipposideros*. Bulletin of the British Museum (Natural History): Zoology 11: 1–129. https://doi.org/10.5962/bhl.part.4716

Hillis DM, Bull JJ (1993) An empirical test of bootstrapping as a method for assessing confidence in phylogenetic analysis. Systematic Biology 42: 182–192. https://doi.org/10.1093/sysbio/42.2.182

Koopman KF (1970) Zoogeography of bats. In: Slaughter BH, Walton DW (Eds) About Bats: A Chiropteran Symposium. Southern Methodist University Press, Dallas, 29–50.

Koopman KF (1989) Systematic notes on Liberian bats. American Museum Novitates 2946: 1–11. http://hdl.handle.net/2246/5100

Koopman KF (1994) Chiroptera: Systematics. Handbuch der Zoologie (Vol. 8). Mammalia, part 60. Walter de Gruyter, Berlin, 217 pp.

Kruskop SV, Benda P, Vasenkov DA, Lavrenchenko LA (2016) First records of bats from the Alatish National Park, north-western Ethiopia (Chiroptera). Lynx (Series Nova) 47: 51–69. https://doi.org/10.2478/lynx-2016-0004

Kumar S, Stecher G, Li M, Knyaz C, Tamura K (2018) MEGA X: Molecular Evolutionary Genetics Analysis across computing platforms. Molecular Biology and Evolution 35: 1547–1549. https://doi.org/10.1093/molbev/msy096

Lanfear R, Frandsen PB, Wright AM, Senfeld T, Calcott B (2016) PartitionFinder 2: new methods for selecting partitioned models of evolution for molecular and morphological phylogenetic analyses. Molecular Biology and Evolution 34: 772–773. https://doi.org/10.1093/molbev/msw260

Lanier HC, Knowles LL (2014) Applying species-tree analyses to deep phylogenetic histories: challenges and potential suggested from a survey of empirical phylogenetic studies. Molecular Phylogenetics and Evolution 83: 191–199. https://doi.org/10.1016/j.ympev.2014.10.022

Lavery TH, Leung LKP, Seddon JM (2014) Molecular phylogeny of hipposiderid bats (Chiroptera: Hipposideridae) from Solomon Islands and Cape York Peninsula, Australia. Zoologica Scripta 43: 429–442. https://doi.org/10.1111/zsc.12068

Leaché AD, Fujita MK (2010) Bayesian species delimitation in West African forest geckos (*Hemidactylus fasciatus*). Proceedings of the Royal Society B 277: 3071–3077. https://doi.org/10.1098/rspb.2010.0662

Leigh JW, Bryant D (2015) POPART: Full-feature software for haplotype network construction. Methods in Ecology and Evolution 6: 1110–1116. https://doi.org/10.1111/2041-210X.12410

Matthee CA, Burzlaff JD, Taylor JF, Davis SK (2001) Mining the mammalian genome for artiodactyl systematics. Systematic Biology 50: 367–390. https://doi.org/10.1080/10635150119683

Miller Jr GS (1907) The Families and Genera of Bats. Government Printing Office, Washington, 282 pp. [+214 pls.] https://doi.org/10.5962/bhl.title.55695

Miller MA, Pfeiffer W, Schwartz T (2010) Creating the CIPRES Science Gateway for inference of large phylogenetic trees. Gateway Computing Environments Workshop (GCE). IEEE, New Orleans. https://doi.org/10.1109/GCE.2010.5676129

Monadjem A (2019) Family Hipposideridae (Old World leaf-nosed bats). In: Wilson DE, Mittermeier RA (Eds) Handbook of the Mammals of the World (Vol. 9). Bats. Lynx Ediciones, Barcelona, 210–227.

Monadjem A, Richards L, Taylor PJ, Denys C, Dower A, Stoffberg S (2013) Diversity of Hipposideridae in the Mount Nimba massif, West Africa, and the taxonomic status of *Hipposideros lamottei*. Acta Chiropterologica 15: 341–352. https://doi.org/10.3161/150811013X678964

Monard A (1939) Résultats de la Mission Scientifique du Dr. Monard en Guinée Portugaise 1937–1938. III. Chiroptères. Arquivos do Museu Bocage 10: 49–80.

Murray SW, Campbell P, Kingston T, Zubaid A, Francis CM, Kunz TH (2012) Molecular phylogeny of hipposiderid bats from Southeast Asia and evidence of cryptic diversity. Molecular Phylogenetics and Evolution 62: 597–611. https://doi.org/10.1016/j.ympev.2011.10.021

Murray SW, Khan FA, Kingston T, Zubaid A, Campbell P (2018) A new species in the *Hipposideros bicolor* group (Chiroptera: Hipposideridae) from Peninsular Malaysia. Acta Chiropterologica 20: 1–29. https://doi.org/10.3161/15081109ACC2018.20.1.001

Naidoo T, Schoeman MC, Goodman SM, Taylor PJ, Lamb JM (2016) Discordance between mitochondrial and nuclear genetic structure in the bat *Chaerephon pumilus* (Chiroptera: Molossidae) from southern Africa. Mammalian Biology-Zeitschrift für Säugetierkunde 81: 115–122. https://doi.org/10.1016/j.mambio.2015.11.002

Nesi N, Nakoune E, Cruaud C, Hassanin A (2011) DNA barcoding of African fruit bats (Mammalia, Pteropodidae). The mitochondrial genome does not provide a reliable discrimination between *Epomophorus gambianus* and *Micropteropus pusillus*. Comptes Rendus Biologies 334: 544–554. https://doi.org/10.1016/j.crvi.2011.05.003

Nguyen L-T, Schmidt HA, von Haeseler A, Minh BQ (2015) IQ-TREE: a fast and effective stochastic algorithm for estimating maximum-likelihood phylogenies. Molecular Biology and Evolution 32: 268–274. https://doi.org/10.1093/molbev/msu300

Noack T (1893) Neue Beiträge zur Kenntniss der Säugethier-Fauna von Ostafrika. Zoologische Jahrbücher Abteilung für Systematik Oekologie und Geographie der Tiere 7: 523–594. https://doi.org/10.5962/bhl.part.24067

Ogilvie HA, Bouckaert RR, Drummond AJ (2017) StarBEAST2 brings faster species tree inference and accurate estimates of substitution rates. Molecular Biology and Evolution 34: 2101–2114. https://doi.org/10.1093/molbev/msx126

Olson DM, Dinerstein E, Wikramanayake ED, Burgess ND, Powell GVN, Underwood EC, D'Amico JA, Itoua I, Strand HE, Morrison JC, Loucks CJ, Allnutt TF, Ricketts TH, Kura Y, Lamoreux JF, Wettengel WW, Hedao P, Kassem KR (2001) Terrestrial ecoregions of the world: a new map of life on Earth BioScience 51: 933–938. https://doi.org/10.1641/0006-3568(2001)051[0933:TEOTWA]2.0.CO;2

Patterson BD, Webala PW (2012) Keys to the bats (Mammalia: Chiroptera) of East Africa. Fieldiana: Life and Earth Sciences 6: 1–60. https://doi.org/10.3158/2158-5520-12.6.1

Patterson BD, Webala PW, Bartonjo M, Nziza J, Dick CW, Demos TC (2018) On the taxonomic status and distribution of African species of *Otomops* (Chiroptera: Molossidae). PeerJ 6: e4864. https://doi.org/10.7717/peerj.4864

Patterson BD, Webala PW, Kerbis Peterhans JC, Goodman SM, Bartonjo M, Demos TC (2019) Genetic variation and relationships among Afrotropical species of *Myotis* (Chiroptera: Vespertilionidae). Journal of Mammalogy 100: 1130–1143. https://doi.org/10.1093/jmammal/gyz087

Peters WCH (1852) Naturwissenschaftliche Reise nach Mossambique: auf Befehl Seiner Majestät des Königs Friedrich Wilhelm IV, in den Jahren 1842 bis 1848 ausgeführt. Zoologie. G. Reimer, Berlin, 202 pp. https://doi.org/10.5962/bhl.title.48863

Rakotoarivelo AR, Goodman SM, Schoeman MC, Willows-Munro S (2019) Phylogeography and population genetics of *Macronycteris commersonii* s.s. (Chiroptera: Hipposideridae), an endemic Malagasy bat. PeerJ 7: e5866. https://doi.org/10.7717/peerj.5866

Rambaut A, Drummond AJ, Xie D, Baele G, Suchard MA (2018) Posterior summarization in Bayesian phylogenetics using Tracer 1.7. Systematic Biology 67: 901–904. https://doi.org/10.1093/sysbio/syy032

Rannala B, Yang Z (2017) Efficient Bayesian species tree inference under the multispecies coalescent. Systematic Biology 66: 823–842. https://doi.org/10.1093/sysbio/syw119

Robinson MF, Jenkins PD, Francis CM, Fulford AJC (2003) A new species of the *Hipposideros pratti* group (Chiroptera, Hipposideridae) from Lao PDR and Vietnam. Acta Chiropterologica 5: 31–48. https://doi.org/10.3161/001.005.0103

Ronquist F, Teslenko M, van der Mark P, Ayres DL, Darling A, Höhna S, Larget B, Liu L, Suchard MA, Huelsenbeck JP (2012) MrBayes 3.2: efficient Bayesian phylogenetic inference and model choice across a large model space. Systematic Biology 61: 539–542. https://doi.org/10.1093/sysbio/sys029

Salicini I, Ibáñez C, Juste J (2011) Multilocus phylogeny and species delimitation within the Natterer's bat species complex in the Western Palearctic. Molecular Phylogenetics and Evolution 61: 888–898. https://doi.org/10.1016/j.ympev.2011.08.010

Samonds KE (2007) Late Pleistocene bat fossils from Anjohibe Cave, northwestern Madagascar. Acta Chiropterologica 9: 39–65. https://doi.org/10.3161/1733-5329(2007)9[39:LPBFFA]2.0.CO;2

Sanderson I (1937) Animal Treasure. Viking Press, New York, 325 pp. https://doi.org/10.2307/1436145

Seabra AF (1898) Sobre um caracter importante para a determinação dos generos e especies dos "Microchiroptera" e lista da especies d'este grupo existantes nas colleçoes de Museo Nacional. Jornal de Sciencias, Mathematicas, Physicas e Naturaes Lisboa (Serie 2) 5: 247–258.

Shi JJ, Rabosky DL (2015) Speciation dynamics during the global radiation of extant bats. Evolution 69: 1528–1545. https://doi.org/10.1111/evo.12681

Sikes RS, Animal Care and Use Committee of the American Society of Mammalogists (2016) 2016 Guidelines of the American Society of Mammalogists for the use of wild mammals in research and education. Journal of Mammalogy 97: 663–688. https://doi.org/10.1093/jmammal/gyw078

Simmons NB (2005) Chiroptera. In: Wilson DE, Reeder DAM (Eds) Mammal Species of the World: A Taxonomic and Geographic Reference (3rd edn.). Johns Hopkins University Press, Baltimore, 312–529.

Simmons NB, Cirranello AL (2019) Bat Species of the World: A Taxonomic and Geographic Database. http://www.batnames.org [Accessed on: 2019-8-21]

Sundevall CJ (1846) Nya Mammalia från Sydafrika. Öfversigt. Kungliga Svenska Vetenskapsakademiens Handlinger 3(5): 118–121.

Tate GHH (1941) Results of the Archbold Expeditions. No. 35. A review of the genus *Hipposideros* with special reference to Indo-Australian species. Bulletin of the American Museum of Natural History 78: 353–393. http://hdl.handle.net/2246/1780

Temminck CJ (1853) Esquisses zoologiques sur la côte de Guiné. I. Mammifères. C. C. Vander Hoek, Leiden, 256 pp. https://doi.org/10.5962/bhl.title.14828

Thomas O (1904) Three new bats, African and Asiatic. Annals and Magazine of Natural History (Series 7) 13: 384–388. https://doi.org/10.1080/00222930408562462

Thong VD, Puechmaille SJ, Denzinger A, Dietz C, Csorba G, Bates PJJ, Teeling EC, Schnitzler HU (2012) A new species of *Hipposideros* (Chiroptera: Hipposideridae) from Vietnam. Journal of Mammalogy 93: 1–11. https://doi.org/10.1111/j.1365-2907.2011.00202.x

Thorn E, Kerbis Peterhans JC, Baranga J (2009) Chiroptera. In: Thorn E, Kerbis Peterhans JC (Eds) Small mammals of Uganda. Bonner Zoologische Monographien 55: 12–75.

Toews DP, Brelsford A (2012) The biogeography of mitochondrial and nuclear discordance in animals. Molecular Ecology 21: 3907–3930. https://doi.org/10.1111/j.1365-294X.2012.05664.x

Vallo P, Benda P, Martínková N, Kanuch P, Kalko EKV, Cervený J, Koubek P (2011) Morphologically uniform bats *Hipposideros* aff. *ruber* (Hipposideridae) exhibit high mitochondrial genetic diversity in southeastern Senegal. Acta Chiropterologica 13: 79–88. https://doi.org/10.3161/150811011X578633

Vallo P, Guillén-Servent A, Benda P, Pires DB, Koubek P (2008) Variation of mitochondrial DNA in the *Hipposideros caffer* complex (Chiroptera: Hipposideridae) reveals high cryptic diversity Acta Chiropterologica 10: 193–206. https://doi.org/10.3161/150811008X414782

Verschuren J (1957) Introduction á l'ecologie, biologie et systématique de cheiroptères. In: de Saeger ZH (Ed.) Exploration du Parc National de la Garamba. Fascicule 7. Institut Parcs Nationaux du Congo Belge, Bruxelles, 25–65.

Wagner A (1845) Diagnosen einiger neuen Arten von Nagern und Handflügern. Archiv für Naturgeschichte 11: 145–149.

Webala PW, Rydell J, Dick CW, Musila S, Patterson BD (2019) Echolocation calls of high duty-cycle bats (Hipposideridae and Rhinonycteridae) from Kenya. Journal of Bat Research and Conservation 12: 10–20. https://doi.org/10.14709/BarbJ.12.1.2019.02

Wesselman HB (1984) The Omo micromammals: systematics and paleoecology of Early Man sites from Ethiopia. S. Karger, Basel, 222 pp.

Yang Z (2015) The BPP program for species tree estimation and species delimitation. Current Zoology 61: 854–865. https://doi.org/10.1093/czoolo/61.5.854

Yang Z, Rannala B (2014) Unguided species delimitation using DNA sequence data from multiple loci. Molecular Biology and Evolution 31: 3125–3135. https://doi.org/10.1093/molbev/msu279

Appendix I

Genetic sampling of Hipposideridae. Wherever possible, the voucher numbers associated with the genetic samples are specified. Accession numbers identify sequences downloaded from GenBank or accessioned to Genbank for this study. The designation 'redundant' indicates a cyt-b sequence that was omitted from the 303 individual alignment because of its identity to another. Institutional acronyms are as follows: AMNH – American Museum of Natural History, New York; CM – Carnegie Museum, Pittsburgh; CVVD – ?; DM – Durban Natural Science Museum, Durban; EBD – Estación Biológica de Doñana, Sevilla; FMNH – Field Museum of Natural History, Chicago; IEBR-T – Thong collection at Institute of Ecology and Biological Resources, Hanoi; IVB – Institute of Vertebrate Biology, Brno; KU – Biodiversity Institute and Natural History Museum, University of Kansas, Lawrence; Czech Academy of Sciences, Prague; LSUMZ – Lousiana State University Museum of Natural Science-Mammal Tissues, Baton Rouge; NHMOU – Natural History Museum of Osmania University, Hyderabad; NMK – National Museums of Kenya, Nairobi; NMP – National Museum, Prague; PSUZC – Princess Maha Chakri Sirindhorn Natural History Museum, Songkhla; ROM – Royal Ontario Museum, Toronto; SMF – Senckenberg Museum, Frankfurt; TM – Transvaal Museum, Pretoria; TTU – Texas Tech University Museum, Lubbock; UADBA – Université d'Antananarivo, Département de Biologie Animale, Antananarivo; UNIMAS – University of Malaysia Sarawak Natural History Museum, Kuching.

Table 7. RGHAEPRGJH

Voucher	cyt-b	ACOX2	COPS	ROGDI	STAT5	ScientificName	Country	Latitude	Longitude
	KU316954					*Asellia arabica*	Oman	17.100	54.080
	KU316958					*Asellia italosomalica*	Yemen	12.670	54.120
	JF438999					*Asellia tridens*	Libya	24.933	10.167
IEBR-T	KU161572					*Aselliscus dongbacana*	Vietnam	22.360	105.395
	LC426460					*Aselliscus stoliczkanus*	China		
	DQ888675					*Aselliscus tricuspidatus*	Vanuatu	-15.307	166.926
DM 8021	FJ457616					*Cloeotis percivali*	Swaziland	-25.817	31.283
DM 8026	FJ457615					*Cloeotis percivali*	Swaziland	-25.817	31.283
	DQ888674					*Coelops frithi*	Taiwan	21.948	120.780
FMNH 148981	redundant					*Doryrhina camerunensis*	Burundi	-2.100	29.383
FMNH 148982	MT149719	MT149615	MT149513	MT149418	MT149317	*Doryrhina camerunensis*	Burundi	-2.850	29.400
NMK 187403	redundant	MT149616	MT149514	MT149419	MT149318	*Doryrhina camerunensis*	Kenya	0.344	34.857
NMK 187418	MT149720					*Doryrhina camerunensis*	Kenya	0.344	34.857

Voucher	cyt-b	ACOX2	COPS	ROGDI	STAT5	ScientificName	Country	Latitude	Longitude
FMNH 165159	MT149721					*Doryrhina camerunensis*	Uganda	1.683	31.533
FMNH 165160	MT149722					*Doryrhina camerunensis*	Uganda	1.683	31.533
FMNH 223198	MT149723					*Doryrhina camerunensis*	Uganda	0.445	32.889
FMNH 223551	redundant	MT149617	MT149515	MT149420	MT149319	*Doryrhina camerunensis*	Uganda	0.445	32.889
FMNH 224066	MT149724					*Doryrhina camerunensis*	Uganda	0.501	30.426
FMNH 224068	MT149725					*Doryrhina camerunensis*	Uganda	0.501	30.426
FMNH 153929	MT149726	MT149618	MT149516	MT149421	MT149320	*Doryrhina* cf. *camerunensis*	Tanzania	-4.942	38.733
DM 12626	KF551833					*Doryrhina cyclops1*	Liberia	7.553	-8.492
IVB S261	EU934465					*Doryrhina cyclops1*	Senegal	12.883	-12.717
IVB S747	EU934466					*Doryrhina cyclops1*	Senegal	13.333	-13.217
FMNH 227409	MT149727	MT149619	MT149517	MT149422	MT149321	*Doryrhina cyclops2*	Central African Republic	3.033	16.410
FMNH 227410	MT149728	MT149620	MT149518	MT149423	MT149322	*Doryrhina cyclops2*	Central African Republic	3.033	16.410
FMNH 167772	MT149729	MT149621	MT149519	MT149424	MT149323	*Doryrhina cyclops2*	Gabon	-2.283	10.497
FMNH 167773	MT149730	MT149622	MT149520	MT149425	MT149324	*Doryrhina cyclops2*	Gabon	-2.283	10.497
NMP 91850	EU934446					*Hipposideros abae*	Benin	7.783	2.267
NMP 91851	EU934447					*Hipposideros abae*	Benin	7.783	2.267
IVB S822	EU934448					*Hipposideros abae*	Senegal	12.350	-12.317
IEBR-T 90806.7	JN247006					*Hipposideros alongensis*	Vietnam		
YN07C123	JX849159					*Hipposideros armiger*	China	23.600	102.002
UNIMAS 729	EF108140 redundant					*Hipposideros ater*	Malaysia	1.407	110.169
UNIMAS 1577	EF108139 redundant					*Hipposideros ater*	Malaysia	3.801	113.785
KU 164242	MT149731	MT149623	MT149521	MT149426	MT149325	*Hipposideros ater*	Philippines	13.796	120.159
KU 164243	MT149732	MT149624	MT149522	MT149427	MT149326	*Hipposideros ater*	Philippines	13.796	120.159
KU 164712	MT149733	MT149625	MT149523	MT149428	MT149327	*Hipposideros ater*	Philippines	19.085	121.241
ROM 100579	FJ347975					*Hipposideros beatus1*	Ivory Coast	6.930	-7.217
DM 13241	KF551829					*Hipposideros beatus1*	Liberia	7.553	-8.492
DM 13242	KF551830					*Hipposideros beatus1*	Liberia	7.553	-8.492
FMNH 227406	MT149734	MT149613	MT149524	MT149429	MT149328	*Hipposideros beatus2*	Central African Republic	3.033	16.410
FMNH 149406	FJ347976					*Hipposideros beatus2*	Democratic Republic of Congo	-1.417	28.583
FMNH 215440	MT149735	MT149626	MT149525	MT149430	MT149329	*Hipposideros beatus2*	Kenya	0.352	34.865
NMK 184861	MT149736	MT149627	MT149526	MT149431	MT149330	*Hipposideros beatus2*	Kenya	0.356	34.861
NMK 184864	redundant					*Hipposideros beatus2*	Kenya	0.360	34.861
NMK 184870	MT149737					*Hipposideros beatus2*	Kenya	0.352	34.865
FMNH 192931	MT149738					*Hipposideros beatus2*	Tanzania	-1.094	31.515

Voucher	cyt-b	ACOX2	COPS	ROGDI	STAT5	ScientificName	Country	Latitude	Longitude
FMNH 192932	MT149739					*Hipposideros beatus2*	Tanzania	-1.094	31.515
FMNH 192933	redundant	MT149628	MT149527	MT149432	MT149331	*Hipposideros beatus2*	Tanzania	-1.094	31.515
FMNH 164972	MT149740					*Hipposideros beatus2*	Uganda	1.733	31.467
FMNH 165157	redundant	MT149629	MT149528	MT149433	MT149332	*Hipposideros beatus2*	Uganda	1.683	31.533
LSUMZ MT-4482	MT149741	MT149630	MT149529	MT149434	MT149333	*Hipposideros bicolor*	Malaysia	1.970	103.500
LSUMZ MT-4489	MT149742	MT149631	MT149530		MT149334	*Hipposideros bicolor*	Malaysia	1.970	103.500
FMNH 215441	redundant	MT149632	MT149531	MT149435	MT149335	*Hipposideros caffer1*	Kenya	-0.346	36.119
FMNH 215442	redundant					*Hipposideros caffer1*	Kenya	-0.346	36.119
FMNH 215443	redundant					*Hipposideros caffer1*	Kenya	-0.346	36.119
FMNH 215444	MT149743					*Hipposideros caffer1*	Kenya	-0.346	36.119
FMNH 215445	redundant					*Hipposideros caffer1*	Kenya	-0.346	36.119
FMNH 215446	redundant					*Hipposideros caffer1*	Kenya	-0.346	36.119
FMNH 215447	redundant					*Hipposideros caffer1*	Kenya	-0.346	36.119
FMNH 216628	redundant					*Hipposideros caffer1*	Kenya	-0.346	36.119
FMNH 216629	redundant					*Hipposideros caffer1*	Kenya	-0.346	36.119
FMNH 216630	redundant					*Hipposideros caffer1*	Kenya	-0.346	36.119
FMNH 216631	redundant					*Hipposideros caffer1*	Kenya	-0.346	36.119
FMNH 216632	redundant					*Hipposideros caffer1*	Kenya	-0.346	36.119
FMNH 216645	redundant					*Hipposideros caffer1*	Kenya	-0.346	36.119
FMNH 216646	redundant					*Hipposideros caffer1*	Kenya	-0.346	36.119
FMNH 216647	redundant					*Hipposideros caffer1*	Kenya	-0.346	36.119
FMNH 216648	redundant	MT149633	MT149532	MT149436	MT149336	*Hipposideros caffer1*	Kenya	-0.346	36.119
FMNH 225346	redundant					*Hipposideros caffer1*	Kenya	-0.346	36.119
FMNH 225747	redundant					*Hipposideros caffer1*	Kenya	-0.564	36.254
FMNH 225748	redundant					*Hipposideros caffer1*	Kenya	-0.564	36.254
FMNH 225749	redundant					*Hipposideros caffer1*	Kenya	-0.564	36.254
FMNH 225750	redundant					*Hipposideros caffer1*	Kenya	-0.564	36.254
FMNH 225751	redundant					*Hipposideros caffer1*	Kenya	-0.564	36.254
NMK 184726	MT149744					*Hipposideros caffer1*	Kenya	-0.564	36.254
NMK 184727	redundant					*Hipposideros caffer1*	Kenya	-0.564	36.254
NMK 184728	redundant					*Hipposideros caffer1*	Kenya	-0.564	36.254
NMK 184729	redundant					*Hipposideros caffer1*	Kenya	-0.564	36.254
NMK 184730	MT149745					*Hipposideros caffer1*	Kenya	-0.564	36.254
NMK 184760	redundant					*Hipposideros caffer1*	Kenya	-0.430	36.174
NMK 184842	redundant					*Hipposideros caffer1*	Kenya	-0.539	36.294

Voucher	cyt-b	ACOX2	COPS	ROGDI	STAT5	ScientificName	Country	Latitude	Longitude
NMK 184843	redundant					*Hipposideros caffer1*	Kenya	-0.539	36.294
NMK 187310	MT149718					*Hipposideros caffer1*	Kenya	-0.539	36.294
NMK 187311	redundant					*Hipposideros caffer1*	Kenya	-0.539	36.294
NMK 187312	redundant					*Hipposideros caffer1*	Kenya	-0.539	36.294
NMK 187323	redundant					*Hipposideros caffer1*	Kenya	-0.346	36.119
NMK 187324	redundant					*Hipposideros caffer1*	Kenya	-0.346	36.119
NMK 187325	redundant	MT149634	MT149533	MT149437	MT149337	*Hipposideros caffer1*	Kenya	-0.346	36.119
NMK 187326	redundant					*Hipposideros caffer1*	Kenya	-0.346	36.119
EBD 23262	FJ347977					*Hipposideros caffer1*	Morocco	30.630	9.830
NMP	EU934449					*Hipposideros caffer1*	Morocco	30.067	-9.667
FMNH 223196	MT149746	MT149635	MT149534	MT149438	MT149338	*Hipposideros caffer1*	Uganda	0.445	32.889
FMNH 223197	MT149747					*Hipposideros caffer1*	Uganda	0.445	32.889
NMP	EU934463					*Hipposideros caffer1*	Yemen	15.283	44.167
FMNH 220955	redundant	MT149639	MT149538	MT149441	MT149342	*Hipposideros caffer2*	Kenya	-2.203	37.714
FMNH 220956	redundant					*Hipposideros caffer2*	Kenya	-2.203	37.714
FMNH 220957	MT149753					*Hipposideros caffer2*	Kenya	-2.203	37.714
FMNH 220958	redundant					*Hipposideros caffer2*	Kenya	-2.203	37.714
FMNH 225347	redundant	MT149640	MT149539	MT149442	MT149343	*Hipposideros caffer2*	Kenya	-1.547	35.306
FMNH 225348	redundant					*Hipposideros caffer2*	Kenya	-1.531	35.320
FMNH 225349	MT149754					*Hipposideros caffer2*	Kenya	-1.531	35.320
FMNH 225350	MT149755	MT149641	MT149540	MT149443		*Hipposideros caffer2*	Kenya	-1.531	35.320
FMNH 225351	MT149756					*Hipposideros caffer2*	Kenya	-1.531	35.320
FMNH 225352	redundant					*Hipposideros caffer2*	Kenya	-1.531	35.320
NMK 184977	MT149749					*Hipposideros caffer2*	Kenya	-0.117	34.541
NMK 184978	MT149750	MT149637	MT149536	MT149440	MT149340	*Hipposideros caffer2*	Kenya	-0.117	34.541
NMK 184979	MT149751					*Hipposideros caffer2*	Kenya	-0.117	34.541
NMK 184981	redundant					*Hipposideros caffer2*	Kenya	-0.117	34.541
NMK 184982	MT149752	MT149638	MT149537		MT149341	*Hipposideros caffer2*	Kenya	-0.117	34.541
NMK 184999	MT149748	MT149636	MT149535	MT149439	MT149339	*Hipposideros caffer2*	Kenya	-0.555	37.388
FMNH 215914	MT149768					*Hipposideros caffer3*	Kenya	-3.706	38.776
FMNH 215915	redundant					*Hipposideros caffer3*	Kenya	-3.706	38.776
FMNH 215916	MT149769					*Hipposideros caffer3*	Kenya	-3.706	38.776
FMNH 215917	redundant	MT149646	MT149545	MT149448	MT149348	*Hipposideros caffer3*	Kenya	-3.706	38.776
FMNH 215918	redundant					*Hipposideros caffer3*	Kenya	-3.706	38.776
FMNH 215921	redundant					*Hipposideros caffer3*	Kenya	-3.076	39.217

Voucher	cyt-b	ACOX2	COPS	ROGDI	STAT5	ScientificName	Country	Latitude	Longitude
FMNH 215922	MT149770					*Hipposideros caffer3*	Kenya	-3.076	39.217
FMNH 215923	MT149771					*Hipposideros caffer3*	Kenya	-3.076	39.217
FMNH 215924	redundant					*Hipposideros caffer3*	Kenya	-3.076	39.217
FMNH 215925	MT149772	MT149647	MT149546	MT149449	MT149349	*Hipposideros caffer3*	Kenya	-3.076	39.217
FMNH 220648	MT149766					*Hipposideros caffer3*	Kenya	0.170	38.194
FMNH 220669	MT149767	MT149645	MT149544	MT149447	MT149347	*Hipposideros caffer3*	Kenya	0.024	38.066
FMNH 234022	MT149757					*Hipposideros caffer3*	Kenya	-1.019	38.326
FMNH 234023	MT149758					*Hipposideros caffer3*	Kenya	-0.992	38.330
NMK 184226	MT149762	MT149644	MT149543	MT149446	MT149346	*Hipposideros caffer3*	Kenya	2.320	37.994
NMK 184238	MT149763					*Hipposideros caffer3*	Kenya	2.320	37.994
NMK 184284	MT149764					*Hipposideros caffer3*	Kenya	2.320	37.994
NMK 184287	MT149765					*Hipposideros caffer3*	Kenya	2.283	37.954
NMK 184425	MT149761	MT149643	MT149542	MT149445	MT149345	*Hipposideros caffer3*	Kenya	0.228	37.113
NMK 185050	redundant	MT149642	MT149541	MT149444	MT149344	*Hipposideros caffer3*	Kenya	-0.992	38.330
NMK 185051	redundant					*Hipposideros caffer3*	Kenya	-0.992	38.330
NMK 185052	MT149759					*Hipposideros caffer3*	Kenya	-0.992	38.330
NMK 185053	redundant					*Hipposideros caffer3*	Kenya	-0.992	38.330
NMK 185054	MT149760					*Hipposideros caffer3*	Kenya	-0.992	38.330
DM 8587	KF551805					*Hipposideros caffer4*	Mozambique	-23.205	32.499
DM 8590	KF551810					*Hipposideros caffer4*	Mozambique	-12.182	37.550
TM 48051	EU934451					*Hipposideros caffer4*	Mozambique	-21.517	35.100
DM 11007	KF551806 redundant					*Hipposideros caffer4*	South Africa	-27.596	32.220
	FJ347979					*Hipposideros caffer4*	South Africa	-27.660	32.251
	EU934452					*Hipposideros caffer4*	South Africa	-23.999	31.645
DM 7920	EU934458					*Hipposideros caffer4*	Swaziland	-26.870	31.463
FMNH 215941	redundant					*Hipposideros caffer5*	Kenya	-3.300	39.995
FMNH 220176	MT149780					*Hipposideros caffer5*	Kenya	-4.590	39.331
FMNH 220177	MT149781					*Hipposideros caffer5*	Kenya	-4.590	39.331
FMNH 220178	redundant					*Hipposideros caffer5*	Kenya	-4.590	39.331
FMNH 220179	MT149782					*Hipposideros caffer5*	Kenya	-4.590	39.331
FMNH 220180	MT149783					*Hipposideros caffer5*	Kenya	-4.590	39.331
FMNH 220182	MT149784					*Hipposideros caffer5*	Kenya	-4.082	39.483
FMNH 220183	MT149785					*Hipposideros caffer5*	Kenya	-4.082	39.483
FMNH 220184	MT149786					*Hipposideros caffer5*	Kenya	-4.082	39.483
FMNH 220185	redundant					*Hipposideros caffer5*	Kenya	-4.082	39.483

Voucher	cyt-b	ACOX2	COPS	ROGDI	STAT5	ScientificName	Country	Latitude	Longitude
FMNH 220186	redundant					*Hipposideros caffer5*	Kenya	-4.082	39.483
FMNH 220202	MT149773					*Hipposideros caffer5*	Kenya	-3.300	39.995
FMNH 220203	redundant					*Hipposideros caffer5*	Kenya	-3.300	39.995
FMNH 220204	redundant	MT149648	MT149547	MT149450	MT149350	*Hipposideros caffer5*	Kenya	-3.300	39.995
FMNH 220205	redundant					*Hipposideros caffer5*	Kenya	-3.323	40.042
FMNH 220206	MT149774					*Hipposideros caffer5*	Kenya	-3.323	40.042
FMNH 220207	redundant	MT149649	MT149548	MT149451	MT149351	*Hipposideros caffer5*	Kenya	-3.323	40.042
FMNH 220208	redundant	MT149650	MT149549	MT149452	MT149352	*Hipposideros caffer5*	Kenya	-3.323	40.042
FMNH 220209	MT149775					*Hipposideros caffer5*	Kenya	-3.323	40.042
FMNH 233985	redundant					*Hipposideros caffer5*	Kenya	-3.335	40.031
NMK 187199	MT149776					*Hipposideros caffer5*	Kenya	-3.323	40.042
NMK 187200	redundant					*Hipposideros caffer5*	Kenya	-3.323	40.042
NMK 187201	MT149777					*Hipposideros caffer5*	Kenya	-3.323	40.042
NMK 187202	MT149778					*Hipposideros caffer5*	Kenya	-3.323	40.042
NMK 187203	MT149779					*Hipposideros caffer5*	Kenya	-3.323	40.042
CM 97957	FJ347980					*Hipposideros caffer5*	Kenya	-4.250	39.383
FMNH 192789	MT149787	MT149651	MT149550	MT149453	MT149353	*Hipposideros caffer5*	Tanzania	-4.902	39.688
FMNH 192855	redundant	MT149652	MT149551	MT149454	MT149354	*Hipposideros caffer5*	Tanzania	-4.902	39.688
FMNH 187385	redundant	MT149653	MT149552	MT149455	MT149355	*Hipposideros caffer6*	Tanzania	-8.003	39.762
FMNH 187386	MT149788	MT149654	MT149553	MT149456		*Hipposideros caffer6*	Tanzania	-8.003	39.762
FMNH 187387	MT149789					*Hipposideros caffer6*	Tanzania	-7.993	39.792
FMNH 187388	redundant					*Hipposideros caffer6*	Tanzania	-7.993	39.792
FMNH 187417	MT149790					*Hipposideros caffer6*	Tanzania	-7.891	39.843
FMNH 187418	MT149791					*Hipposideros caffer6*	Tanzania	-7.891	39.843
FMNH 187426	MT149792					*Hipposideros caffer6*	Tanzania	-7.891	39.843
FMNH 187428	redundant					*Hipposideros caffer6*	Tanzania	-7.993	39.792
FMNH 198066	MT149793	MT149655	MT149554	MT149457	MT149356	*Hipposideros caffer6*	Tanzania	-5.878	39.311
FMNH 198067	MT149794					*Hipposideros caffer6*	Tanzania	-5.878	39.311
FMNH 198072	redundant	MT149656	MT149555	MT149458	MT149357	*Hipposideros caffer6*	Tanzania	-6.244	39.320
FMNH 198073	redundant					*Hipposideros caffer6*	Tanzania	-6.244	39.320
FMNH 198074	MT149795	MT149657	MT149556	MT149459	MT149358	*Hipposideros caffer6*	Tanzania	-6.244	39.320
FMNH 198075	MT149796					*Hipposideros caffer6*	Tanzania	-6.244	39.320
FMNH 198076	redundant					*Hipposideros caffer6*	Tanzania	-6.244	39.320
FMNH 198082	redundant					*Hipposideros caffer6*	Tanzania	-6.280	39.451
FMNH 198083	MT149797					*Hipposideros caffer6*	Tanzania	-6.280	39.451

Voucher	cyt-b	ACOX2	COPS	ROGDI	STAT5	ScientificName	Country	Latitude	Longitude
FMNH 198084	MT149798					*Hipposideros caffer6*	Tanzania	-6.280	39.451
FMNH 198131	redundant					*Hipposideros caffer6*	Tanzania	-5.878	39.311
FMNH 198132	MT149799					*Hipposideros caffer6*	Tanzania	-5.878	39.311
FMNH 198133	MT149800					*Hipposideros caffer6*	Tanzania	-5.878	39.311
NMP	EU934460					*Hipposideros caffer6*	Tanzania	-5.998	39.187
NMP	EU934477					*Hipposideros caffer7*	Malawi	-16.033	35.500
DM 8528	KF551817					*Hipposideros caffer7*	Mozambique	-13.401	34.870
DM 8550	KF551816 redundant					*Hipposideros caffer7*	Mozambique	-13.401	34.870
FMNH 155554	MT149801	MT149658	MT149557	MT149460	MT149359	*Hipposideros caffer7*	Tanzania	-8.519	35.904
FMNH 192790	redundant	MT149659	MT149558	MT149461	MT149360	*Hipposideros caffer7*	Tanzania	-4.902	39.688
FMNH 192792	MT149802					*Hipposideros caffer7*	Tanzania	-5.367	39.645
FMNH 192793	redundant					*Hipposideros caffer7*	Tanzania	-5.367	39.645
FMNH 192794	redundant					*Hipposideros caffer7*	Tanzania	-5.367	39.645
FMNH 192795	redundant					*Hipposideros caffer7*	Tanzania	-5.367	39.645
FMNH 192796	MT149803					*Hipposideros caffer7*	Tanzania	-5.367	39.645
FMNH 192849	MT149804	MT149660	MT149559	MT149462	MT149361	*Hipposideros caffer7*	Tanzania	-4.902	39.688
FMNH 187140	MT149805	MT149661	MT149560	MT149463	MT149362	*Hipposideros caffer8*	Tanzania	-3.798	36.069
FMNH 219065	MT149806	MT149662	MT149561	MT149464	MT149363	*Hipposideros caffer8*	Tanzania	-8.037	34.502
FMNH 219241	MT149807					*Hipposideros caffer8*	Tanzania	-8.037	34.502
FMNH 219242	MT149808					*Hipposideros caffer8*	Tanzania	-7.707	34.031
FMNH 232868	redundant					*Hipposideros caffer8*	Uganda	2.240	31.688
FMNH 232869	MT149809	MT149663	MT149562	MT149465	MT149364	*Hipposideros caffer8*	Uganda	2.240	31.688
FMNH 232874	redundant	MT149664	MT149563	MT149416	MT149365	*Hipposideros caffer8*	Uganda	2.240	31.688
FMNH 232875	MT149810	MT149665	MT149564		MT149366	*Hipposideros caffer8*	Uganda	2.240	31.688
LSUMZ MT-4480	redundant	MT149666		MT149466	MT149367	*Hipposideros cervinus*	Malaysia	1.970	103.500
LSUMZ MT-4481	MT149811	MT149667	MT149565	MT149467	MT149368	*Hipposideros cervinus*	Malaysia	1.970	103.500
LSUMZ MT-4500	MT149812	MT149668	MT149566	MT149468	MT149369	*Hipposideros cervinus*	Malaysia	1.970	103.500
UNIMAS 787	EF108144					*Hipposideros cervinus*	Malaysia	3.316	113.125
UNIMAS 788	EF108146					*Hipposideros cervinus*	Malaysia	3.316	113.125
LSUMZ MT-4495	MT149813	MT149669		MT149469	MT149370	*Hipposideros* cf. *bicolor*	Malaysia	1.970	103.500
UNIMAS 1459	EF108142					*Hipposideros* cf. *bicolor*	Malaysia	1.716	110.467
UNIMAS 1474	EF108143					*Hipposideros* cf. *bicolor*	Malaysia	1.716	110.467
FMNH 235856	MT149814	MT149670	MT149567	MT149470	MT149371	*Hipposideros* cf. *cervinus*	Solomon Islands	-10.569	161.913
FMNH 235857	MT149815	MT149671	MT149568	MT149471	MT149372	*Hipposideros* cf. *cervinus*	Solomon Islands	-10.569	161.913
NMP 91848	EU934474					*Hipposideros* cf. *lamottei*	Benin	7.783	2.267

Voucher	cyt-b	ACOX2	COPS	ROGDI	STAT5	ScientificName	Country	Latitude	Longitude
NMP 91849	EU934475					*Hipposideros* cf. *lamottei*	Benin	7.783	2.267
IVB S862	EU934453					*Hipposideros* cf. *lamottei*	Senegal	12.350	-12.317
IVB PV56	HQ343266					*Hipposideros* cf. *ruber*	Ghana	7.668	-1.962
DM 12598	KF551812					*Hipposideros* cf. *ruber*	Liberia	7.553	-8.492
DM 12620	KF551811					*Hipposideros* cf. *ruber*	Liberia	7.553	-8.492
IVB S119	EU934478					*Hipposideros* cf. *ruber*	Senegal	13.050	-13.083
IVB S132	HQ343242					*Hipposideros* cf. *ruber*	Senegal	14.071	-12.572
IVB S1374	EU934479					*Hipposideros* cf. *ruber*	Senegal	13.250	-13.217
IVB S8	HQ343240					*Hipposideros* cf. *ruber*	Senegal	12.884	-12.755
LSUMZ MT-4423	DQ054809					*Hipposideros cineraceus*	Malaysia	3.717	102.167
FMNH 190042	JQ915701					*Hipposideros coronatus*	Philippines	9.097	125.705
FMNH 202631	JQ915702					*Hipposideros coronatus*	Philippines	9.764	124.266
KU 166444		MT149672		MT149472	MT149373	*Hipposideros coronatus*	Philippines	11.813	125.278
	EF108148					*Hipposideros coxi*	Malaysia	1.378	110.120
	EF108147 redundant					*Hipposideros coxi*	Malaysia	1.378	110.120
UNIMAS 1424	EF108149					*Hipposideros diadema*	Malaysia	5.531	118.072
KU 164028	MT149816	MT149673	MT149569	MT149473	MT149374	*Hipposideros diadema*	Philippines	19.331	121.439
KU 164029	MT149817	MT149674	MT149570	MT149474	MT149375	*Hipposideros diadema*	Philippines	19.331	121.439
KU 164245	MT149818	MT149675	MT149571	MT149475		*Hipposideros diadema*	Philippines	13.796	120.159
	FJ460489					*Hipposideros doriae*	Malaysia	1.117	110.217
NHMOU.CHI MP4.2016	KY176014					*Hipposideros durgadasi*	India	23.317	78.414
UNIMAS 312	EF108150					*Hipposideros dyacorum*	Malaysia	4.401	117.889
UNIMAS 556	EF108151					*Hipposideros dyacorum*	Malaysia	3.316	113.125
	EU934468					*Hipposideros fuliginosus*	Guinea Bissau	11.117	-14.933
	EU934467					*Hipposideros fuliginosus*	Guinea Bissau	11.333	-13.900
	JX849198					*Hipposideros griffini*	Vietnam		
CVVD AG, 200700214	JN247005					*Hipposideros halophyllus*	Thailand		
NMP 91842	EU934471					*Hipposideros jonesi*	Benin	7.783	2.267
IVB S804	EU934472					*Hipposideros jonesi*	Senegal	12.350	-12.317
	EU934473					*Hipposideros jonesi*	Senegal	12.350	-12.317
EBD 23514	DQ054816					*Hipposideros khaokhouayensis*	Laos	18.433	102.950
	KF551824					*Hipposideros lamottei*	Guinea	7.570	-8.471

Voucher	cyt-b	ACOX2	COPS	ROGDI	STAT5	ScientificName	Country	Latitude	Longitude
	KF551823					*Hipposideros lamottei*	Guinea	7.570	-8.471
NHMOU.CHI MP15.2016	KY176015					*Hipposideros lankadiva*	India	23.317	78.414
LSUMZ MT-4478	MT149819	MT149676	MT149572	MT149476	MT149376	*Hipposideros larvatus*	Malaysia	1.970	103.500
LSUMZ MT-4479	redundant	MT149677	MT149573		MT149377	*Hipposideros larvatus*	Malaysia	1.970	103.500
LSUMZ MT-4488	MT149820	MT149678	MT149574	MT149477	MT149378	*Hipposideros larvatus*	Malaysia	1.970	103.500
UNIMAS 1485	EF108152 redundant					*Hipposideros larvatus*	Malaysia	1.717	110.467
UNIMAS 1501	EF108153					*Hipposideros larvatus*	Malaysia	1.717	110.467
FMNH 195507	JQ915904					*Hipposideros lekaguli*	Philippines	16.314	121.394
	KR908661					*Hipposideros lylei*	China	25.603	99.752
DM 12607	KF551825					*Hipposideros marisae*	Liberia	7.553	-8.492
FMNH 140601	JQ915906					*Hipposideros obscurus*	Philippines	13.767	124.350
KU 165040	redundant	MT149679	MT149575		MT149379	*Hipposideros obscurus*	Philippines	11.434	122.079
KU 165041	MT149821	MT149680	MT149576	MT149478	MT149380	*Hipposideros obscurus*	Philippines	11.434	122.079
KU 165226	MT149717		MT149577	MT149479	MT149381	*Hipposideros obscurus*	Philippines	13.447	120.426
PSUZC MM2006.129	JN247029					*Hipposideros pendelburyi*	Thailand	7.565	99.624
	DQ054810					*Hipposideros pomona*	Laos	18.250	104.517
	EU434952					*Hipposideros pratti*	China	27.729	115.734
FMNH 190070	JQ915992					*Hipposideros pygmaeus*	Philippines	9.097	125.705
KU 164542	MT149822	MT149681	MT149578	MT149480	MT149382	*Hipposideros pygmaeus*	Philippines	14.823	121.968
KU 164543	redundant	MT149682	MT149579	MT149481	MT149383	*Hipposideros pygmaeus*	Philippines	14.823	121.968
KU 164544	MT149716	MT149683	MT149580	MT149482	MT149384	*Hipposideros pygmaeus*	Philippines	14.823	121.968
LSUMZ MT-4425	MT149715	MT149684	MT149581	MT149483	MT149385	*Hipposideros ridleyi*	Malaysia	3.557	102.761
LSUMZ MT-4477	MT149823		MT149582	MT149484	MT149386	*Hipposideros ridleyi*	Malaysia	3.557	102.761
SMF 83828	DQ054811					*Hipposideros ridleyi*	Malaysia	3.717	102.167
	DQ054813					*Hipposideros rotalis*	Laos	18.250	104.517
	FJ347996					*Hipposideros ruber1*	Cameroon	3.150	13.000
	FJ347995					*Hipposideros ruber1*	Cameroon	4.451	11.571
	FJ347993					*Hipposideros ruber1*	Cameroon	3.564	13.408
	FJ347992					*Hipposideros ruber1*	Cameroon	3.564	13.408
	FJ347989					*Hipposideros ruber1*	Cameroon	5.385	11.688
FMNH 195085	MT149824	MT149685	MT149583	MT149485	MT149387	*Hipposideros ruber1*	D. R. Congo	-4.991	29.080
FMNH 215448	MT149826					*Hipposideros ruber1*	Kenya	1.036	34.753
FMNH 215449	MT149827					*Hipposideros ruber1*	Kenya	1.036	34.753

Voucher	cyt-b	ACOX2	COPS	ROGDI	STAT5	ScientificName	Country	Latitude	Longitude
FMNH 215450	redundant					*Hipposideros ruber1*	Kenya	1.036	34.753
FMNH 215451	redundant					*Hipposideros ruber1*	Kenya	1.036	34.753
FMNH 215452	redundant					*Hipposideros ruber1*	Kenya	1.036	34.753
FMNH 215453	redundant					*Hipposideros ruber1*	Kenya	1.036	34.753
FMNH 215476	MT149828					*Hipposideros ruber1*	Kenya	1.036	34.753
FMNH 215477	redundant					*Hipposideros ruber1*	Kenya	1.036	34.753
FMNH 215478	redundant					*Hipposideros ruber1*	Kenya	1.036	34.753
NMK 184904	MT149825	MT149686	MT149584	MT149486		*Hipposideros ruber1*	Kenya	0.212	34.899
NMK 184905	redundant					*Hipposideros ruber1*	Kenya	0.212	34.899
NMK 187407	redundant					*Hipposideros ruber1*	Kenya	1.036	34.753
NMK 187408	MT149829					*Hipposideros ruber1*	Kenya	1.036	34.753
NMK 187409	MT149830	MT149687	MT149585	MT149487	MT149388	*Hipposideros ruber1*	Kenya	1.036	34.753
NMK 187410	redundant					*Hipposideros ruber1*	Kenya	1.036	34.753
NMK 187412	MT149831					*Hipposideros ruber1*	Kenya	1.036	34.753
DM 12603	KF551819					*Hipposideros ruber1*	Liberia	7.553	-8.492
DM 13245	KF551815					*Hipposideros ruber1*	Liberia	7.553	-8.492
DM 13246	KF551820					*Hipposideros ruber1*	Liberia	7.553	-8.492
FMNH 225201	MT149832	MT149688	MT149586	MT149488	MT149389	*Hipposideros ruber1*	Rwanda	-2.485	29.199
FMNH 225202	MT149833					*Hipposideros ruber1*	Rwanda	-1.504	29.613
FMNH 225203	redundant					*Hipposideros ruber1*	Rwanda	-1.504	29.613
FMNH 225204	redundant					*Hipposideros ruber1*	Rwanda	-1.506	29.615
FMNH 225205	redundant					*Hipposideros ruber1*	Rwanda	-1.506	29.615
FMNH 225206	MT149834					*Hipposideros ruber1*	Rwanda	-1.506	29.615
FMNH 225207	redundant					*Hipposideros ruber1*	Rwanda	-1.506	29.615
FMNH 225208	MT149835	MT149689	MT149587	MT149489	MT149390	*Hipposideros ruber1*	Rwanda	-1.506	29.615
FMNH 225209	redundant					*Hipposideros ruber1*	Rwanda	-1.506	29.615
FMNH 192935	MT149836	MT149690	MT149588	MT149490	MT149391	*Hipposideros ruber1*	Tanzania	-1.094	31.515
FMNH 137629	FJ347987					*Hipposideros ruber1*	Uganda	32.283	-0.005
FMNH 160358	MT149837					*Hipposideros ruber1*	Uganda	-0.989	29.614
FMNH 160359	MT149838	MT149691	MT149589	MT149491	MT149392	*Hipposideros ruber1*	Uganda	-0.989	29.614
FMNH 160361	MT149839					*Hipposideros ruber1*	Uganda	-1.041	29.580
FMNH 161040	MT149840					*Hipposideros ruber1*	Uganda	-0.245	29.819
FMNH 223866	redundant	MT149692	MT149590	MT149492	MT149393	*Hipposideros ruber1*	Uganda	-0.342	31.966
FMNH 223867	MT149841					*Hipposideros ruber1*	Uganda	-0.342	31.966
FMNH 227415	MT149842					*Hipposideros ruber2*	Central African Republic	3.033	16.410

Voucher	cyt-b	ACOX2	COPS	ROGDI	STAT5	ScientificName	Country	Latitude	Longitude
FMNH 227416	MT149843					*Hipposideros ruber2*	Central African Republic	3.033	16.410
FMNH 227417	MT149844	MT149693	MT149591		MT149394	*Hipposideros ruber2*	Central African Republic	3.033	16.410
FMNH 149408	FJ347986	MT149694	MT149592	MT149493	MT149395	*Hipposideros ruber2*	D. R. Congo	-1.417	28.583
FMNH 149409	redundant					*Hipposideros ruber2*	D. R. Congo	-1.417	28.583
FMNH 149410	redundant	MT149695	MT149593	MT149494	MT149396	*Hipposideros ruber2*	D. R. Congo	-1.417	28.583
FMNH 149412	redundant					*Hipposideros ruber2*	D. R. Congo	-1.417	28.583
ROM 100546	FJ347978					*Hipposideros ruber2*	Ivory Coast	6.930	-7.217
FMNH 215479	redundant					*Hipposideros ruber2*	Kenya	0.244	34.907
FMNH 215480	MT149845					*Hipposideros ruber2*	Kenya	0.244	34.907
FMNH 215481	MT149846					*Hipposideros ruber2*	Kenya	0.244	34.907
FMNH 215482	redundant	MT149696	MT149594	MT149495	MT149397	*Hipposideros ruber2*	Kenya	0.244	34.907
FMNH 215483	redundant	MT149697	MT149595	MT149496	MT149398	*Hipposideros ruber2*	Kenya	0.244	34.907
NMK 184878	MT149847					*Hipposideros ruber2*	Kenya	0.248	34.906
NMK 184880	MT149848					*Hipposideros ruber2*	Kenya	0.248	34.906
NMK 184882	MT149849					*Hipposideros ruber2*	Kenya	0.248	34.906
NMK 184883	MT149850					*Hipposideros ruber2*	Kenya	0.248	34.906
NMK 184884	MT149851					*Hipposideros ruber2*	Kenya	0.248	34.906
NMK 187383	redundant					*Hipposideros ruber2*	Kenya	0.212	34.899
NMK 187384	MT149852					*Hipposideros ruber2*	Kenya	0.212	34.899
FMNH 165161	redundant					*Hipposideros ruber2*	Uganda	1.733	31.467
FMNH 165162	MT149853					*Hipposideros ruber2*	Uganda	1.683	31.533
FMNH 165163	redundant	MT149698	MT149596	MT149497	MT149399	*Hipposideros ruber2*	Uganda	1.683	31.533
FMNH 165164	MT149854					*Hipposideros ruber2*	Uganda	1.683	31.533
FMNH 165165	MT149855					*Hipposideros ruber2*	Uganda	1.683	31.533
FMNH 165166	redundant					*Hipposideros ruber2*	Uganda	1.750	31.583
FMNH 165167	redundant	MT149699	MT149597	MT149498	MT149400	*Hipposideros ruber2*	Uganda	1.733	31.467
FMNH 224069	redundant					*Hipposideros ruber2*	Uganda	0.501	30.426
FMNH 224071	redundant					*Hipposideros ruber2*	Uganda	0.501	30.426
FMNH 224074	MT149856					*Hipposideros ruber2*	Uganda	0.501	30.426
FMNH 224075	MT149857					*Hipposideros ruber2*	Uganda	0.501	30.426
	FJ347994					*Hipposideros ruber3*	Cameroon	3.564	13.408
	FJ347991					*Hipposideros ruber3*	Cameroon	2.941	9.911
	FJ347990					*Hipposideros ruber3*	Cameroon	2.941	9.911
	FJ347988					*Hipposideros ruber3*	Cameroon	4.913	9.241
EBD 18240	FJ347984					*Hipposideros ruber3*	Equatorial Guinea	1.889	9.793

Voucher	cyt-b	ACOX2	COPS	ROGDI	STAT5	ScientificName	Country	Latitude	Longitude
EBD 18266	FJ347985					*Hipposideros ruber3*	Equatorial Guinea	1.889	9.793
EBD 18511	FJ347983					*Hipposideros ruber3*	Equatorial Guinea	3.747	8.750
EBD 18942	FJ347981					*Hipposideros ruber3*	Principe	1.615	7.404
EBD 18926	FJ347982					*Hipposideros ruber3*	São Tomé	0.219	6.727
FMNH 219477	MT149858	MT149700	MT149598	MT149499	MT149401	*Hipposideros ruber4*	D. R. Congo	-5.290	14.871
FMNH 169707	KT583815					*Macronycteris commersoni*	Madagascar	-12.932	49.057
FMNH 175777	KT583822					*Macronycteris commersoni*	Madagascar	-16.380	45.345
FMNH 175966	KT583823					*Macronycteris commersoni*	Madagascar	-22.486	45.392
FMNH 175974	MT149859					*Macronycteris commersoni*	Madagascar	-22.317	45.293
FMNH 175975	MT149860					*Macronycteris commersoni*	Madagascar	-22.317	45.293
FMNH 176155	KT583824	MT149701	MT149599	MT149500	MT149402	*Macronycteris commersoni*	Madagascar	-22.778	43.523
FMNH 176158	MT149861					*Macronycteris commersoni*	Madagascar	-22.217	43.330
FMNH 176277	redundant					*Macronycteris commersoni*	Madagascar	-12.942	49.055
FMNH 177302	KT583825					*Macronycteris commersoni*	Madagascar	-16.315	46.810
FMNH 178803	redundant					*Macronycteris commersoni*	Madagascar	-12.712	49.474
FMNH 178806	KT583816					*Macronycteris commersoni*	Madagascar	-12.712	49.474
FMNH 178808	KT583817 redundant					*Macronycteris commersoni*	Madagascar	-12.712	49.474
FMNH 178809	KT583818					*Macronycteris commersoni*	Madagascar	-12.712	49.474
FMNH 178810	KT583819					*Macronycteris commersoni*	Madagascar	-12.712	49.474
FMNH 178811	KT583820					*Macronycteris commersoni*	Madagascar	-12.712	49.474
FMNH 178812	KT583826					*Macronycteris commersoni*	Madagascar	-12.712	49.474
FMNH 178815	KT583821 redundant					*Macronycteris commersoni*	Madagascar	-12.712	49.474
FMNH 179201	MT149862					*Macronycteris commersoni*	Madagascar	-17.280	49.420
FMNH 183934	KT583827					*Macronycteris commersoni*	Madagascar	-24.050	43.750
FMNH 183980	KT583813 redundant					*Macronycteris commersoni*	Madagascar	-12.337	49.385
FMNH 184030	KT583812					*Macronycteris commersoni*	Madagascar	-14.966	47.308
FMNH 184170	KT583828					*Macronycteris commersoni*	Madagascar	-24.650	43.963
FMNH 184887	MT149863					*Macronycteris commersoni*	Madagascar	-15.904	46.598
FMNH 209236	MT149864					*Macronycteris commersoni*	Madagascar	-18.063	44.541
FMNH 217940	KT583831 redundant					*Macronycteris commersoni*	Madagascar	-22.632	45.338
FMNH 221308	KT583829					*Macronycteris commersoni*	Madagascar	-12.932	49.057
FMNH 231862	MT149865	MT149702	MT149600	MT149501	MT149315	*Macronycteris commersoni*	Madagascar	-17.889	49.203
UADBA 32916	KT583830					*Macronycteris commersoni*	Madagascar	15.538	46.886
UADBA 32987	KT583814					*Macronycteris commersoni*	Madagascar	-13.932	49.057
UADBA 32989	KR606333					*Macronycteris commersoni*	Madagascar	-12.917	49.143

Voucher	cyt-b	ACOX2	COPS	ROGDI	STAT5	ScientificName	Country	Latitude	Longitude
FMNH 175970	MT149866	MT149703	MT149601	MT149502	MT149403	*Macronycteris cryptovalorona*	Madagascar	-22.317	45.293
FMNH 184173	MT149867	MT149704	MT149602	MT149503	MT149404	*Macronycteris cryptovalorona*	Madagascar	-24.650	43.963
AMNH 269871	KT583801					*Macronycteris gigas*	Central African Republic		
FMNH 219602	MT149868	MT149705	MT149603	MT149504	MT149405	*Macronycteris gigas*	D. R. Congo	0.241	20.883
FMNH 219682	MT149869	MT149706	MT149604	MT149415	MT149406	*Macronycteris gigas*	D. R. Congo	0.241	20.883
FMNH 220226	redundant	MT149707	MT149605	MT149505	MT149407	*Macronycteris gigas*	Kenya	-4.647	39.380
FMNH 220227	redundant	MT149708	MT149606	MT149506	MT149408	*Macronycteris gigas*	Kenya	-4.647	39.380
FMNH 220239	MT149870					*Macronycteris gigas*	Kenya	-4.215	39.451
DM 12602	KF551826					*Macronycteris gigas*	Liberia	7.553	-8.492
IVB S1032	EU934469					*Macronycteris gigas*	Senegal	12.350	-13.217
IVB S1044	EU934470					*Macronycteris gigas*	Senegal	12.350	-13.217
AMNH 269879	KT583802					*Macronycteris vittata*	Central African Republic	3.500	16.000
FMNH 215942	MT149871	MT149709	MT149607	MT149507	MT149409	*Macronycteris vittata*	Kenya	-3.300	39.995
FMNH 215943	redundant					*Macronycteris vittata*	Kenya	-3.300	39.995
FMNH 215944	redundant					*Macronycteris vittata*	Kenya	-3.300	39.995
FMNH 215945	redundant					*Macronycteris vittata*	Kenya	-3.300	39.995
FMNH 215946	MT149872					*Macronycteris vittata*	Kenya	-3.287	39.982
FMNH 215947	redundant					*Macronycteris vittata*	Kenya	-3.287	39.982
FMNH 215948	MT149873					*Macronycteris vittata*	Kenya	-3.287	39.982
FMNH 215949	redundant					*Macronycteris vittata*	Kenya	-3.287	39.982
FMNH 215950	MT149874					*Macronycteris vittata*	Kenya	-3.287	39.982
FMNH 215951	MT149875					*Macronycteris vittata*	Kenya	-3.282	39.971
FMNH 215952	MT149876					*Macronycteris vittata*	Kenya	-3.282	39.971
FMNH 215953	redundant	MT149710	MT149608		MT149410	*Macronycteris vittata*	Kenya	-3.282	39.971
FMNH 215954	MT149877					*Macronycteris vittata*	Kenya	-3.282	39.971
FMNH 215955	redundant					*Macronycteris vittata*	Kenya	-3.282	39.971
FMNH 215959	MT149878					*Macronycteris vittata*	Kenya	-3.309	40.018
FMNH 215960	MT149879					*Macronycteris vittata*	Kenya	-3.309	40.018
FMNH 215961	MT149880					*Macronycteris vittata*	Kenya	-3.309	40.018
FMNH 215962	MT149881					*Macronycteris vittata*	Kenya	-3.309	40.018
FMNH 215963	MT149882					*Macronycteris vittata*	Kenya	-3.309	40.018
FMNH 215967	MT149883					*Macronycteris vittata*	Kenya	-3.303	39.999
FMNH 215968	redundant					*Macronycteris vittata*	Kenya	-3.305	39.937
FMNH 215969	redundant					*Macronycteris vittata*	Kenya	-3.305	39.937
FMNH 220224	redundant					*Macronycteris vittata*	Kenya	-4.647	39.378

Voucher	cyt-b	ACOX2	COPS	ROGDI	STAT5	ScientificName	Country	Latitude	Longitude
FMNH 220225	MT149885					*Macronycteris vittata*	Kenya	-4.647	39.380
FMNH 220228	MT149886					*Macronycteris vittata*	Kenya	-4.647	39.380
FMNH 220229	MT149887	MT149711	MT149609	MT149508	MT149411	*Macronycteris vittata*	Kenya	-4.647	39.380
FMNH 220231	MT149888					*Macronycteris vittata*	Kenya	-4.614	39.354
FMNH 220232	MT149889					*Macronycteris vittata*	Kenya	-4.614	39.354
FMNH 220233	MT149890					*Macronycteris vittata*	Kenya	-4.614	39.354
FMNH 220234	redundant					*Macronycteris vittata*	Kenya	-4.614	39.354
FMNH 220235	MT149891	MT149712	MT149610	MT149509	MT149412	*Macronycteris vittata*	Kenya	-4.614	39.354
FMNH 220236	redundant					*Macronycteris vittata*	Kenya	-4.614	39.354
FMNH 220237	redundant					*Macronycteris vittata*	Kenya	-4.614	39.354
FMNH 220238	redundant					*Macronycteris vittata*	Kenya	-4.614	39.354
FMNH 220240	redundant					*Macronycteris vittata*	Kenya	-3.300	39.995
NMK 187219	redundant					*Macronycteris vittata*	Kenya	-3.335	40.031
NMK 187220	MT149884					*Macronycteris vittata*	Kenya	-3.335	40.031
NMK 187221	redundant					*Macronycteris vittata*	Kenya	-3.335	40.031
NMK 187222	redundant					*Macronycteris vittata*	Kenya	-3.335	40.031
DM 8645	KF551828 redundant					*Macronycteris vittata*	Mozambique	-18.565	32.220
DM 11510	KF551827					*Macronycteris vittata*	Mozambique	-18.978	34.176
FMNH 192800	redundant	MT149713	MT149611	MT149510	MT149413	*Macronycteris vittata*	Tanzania	-4.902	39.688
FMNH 192801	MT149892					*Macronycteris vittata*	Tanzania	-4.902	39.688
FMNH 192857	redundant	MT149714	MT149612	MT149511	MT149414	*Macronycteris vittata*	Tanzania	-4.902	39.688
FMNH 192858	redundant					*Macronycteris vittata*	Tanzania	-4.902	39.688
FMNH 192859	MT149893					*Macronycteris vittata*	Tanzania	-4.902	39.688
FMNH 192860	KT583807					*Macronycteris vittata*	Tanzania	-4.902	39.688
FMNH 192865	KT583808 redundant					*Macronycteris vittata*	Tanzania	-4.902	39.688
FMNH 192866	KT583809					*Macronycteris vittata*	Tanzania	-4.902	39.688
FMNH 220268		MT149614	MT149512	MT149417	MT149316	*Triaenops afer*	Kenya	-4.590	39.331

Supplementary material 1

Figure S1. Geographic distribution of voucher specimens used in this analysis

Authors: Bruce D. Patterson, Paul W. Webala, Tyrone H. Lavery, Bernard R. Agwanda, Steven M. Goodman, Julian C. Kerbis Peterhans, Terrence C. Demos

Data type: occurrence

Link: https://doi.org/10.3897/zookeys.929.50240.suppl1

Supplementary material 2

Figure S2. Phylogeny of Hipposideridae based on maximum likelihood analysis of cyt-b based on 452 individuals

Authors: Bruce D. Patterson, Paul W. Webala, Tyrone H. Lavery, Bernard R. Agwanda, Steven M. Goodman, Julian C. Kerbis Peterhans, Terrence C. Demos

Data type: phylogenetic tree

Link: https://doi.org/10.3897/zookeys.929.50240.suppl2

Supplementary material 3

Figure S3. Phylogeny of Hipposideridae based on Bayesian inference analysis of cyt-b based on 452 individuals

Authors: Bruce D. Patterson, Paul W. Webala, Tyrone H. Lavery, Bernard R. Agwanda, Steven M. Goodman, Julian C. Kerbis Peterhans, Terrence C. Demos

Data type: phylogenetic tree

Link: https://doi.org/10.3897/zookeys.929.50240.suppl3